

**A study of the role of presenilin (1)
in regulating synaptic function at
hippocampal synapses**

Lily Mae Yee Yu

July 2010

Thesis presented in partial fulfillment of the degree of
Doctor of Philosophy at University College London (UCL)

Department of Neuroscience, Physiology and Pharmacology, UCL
MRC Laboratory for Molecular and Cell Biology, UCL, London

I, Lily Yu confirm that the work presented in this thesis is my own. Where information has been derived from other sources, I confirm that this has been indicated in the thesis.

Abstract

Synapse dysfunction is emerging as a major factor in the pathogenesis of Alzheimer's disease (AD). Key insights into the pathological mechanisms have been provided through studies of familial AD (FAD) genes. Mutations in the *PSEN1* gene account for the vast majority of FAD cases, which are typified by the formation of amyloid plaques, neurofibrillary tangles and neuronal loss. The *PSEN1* gene encodes presenilin 1, a polytopic transmembrane protein, which is the catalytic core of a proteolytic enzyme complex known as γ -secretase. γ -secretase mediates the generation of amyloid- β (A β) peptides, key constituents of amyloid plaques, and hence it is central to AD pathology. γ -secretase has also been implicated in the proteolysis of a wide range of transmembrane proteins associated with different cellular signalling pathways and functions. However, the precise role that presenilins play in regulating synapse function is not clear. The aim of this thesis is to gain an understanding of the physiological role of presenilin 1 at hippocampal synapses in anticipation that this may provide a greater understanding of the mechanisms that underlie synaptic dysfunction during AD.

This study provides evidence that presenilin is implicated in modulating spontaneous excitatory synaptic transmission in hippocampal neurons in dissociated and slice cultures. Further experiments have revealed a role for presenilin in modulating synapse number but not neurotransmitter release probability, and calcium imaging suggests that γ -secretase activity is dispensable for regulation of cellular calcium homeostasis. In addition, experiments using pharmacological inhibitors of A β precursor protein processing and A β peptide generation have uncovered synaptic roles for γ -secretase that are potentially distinct from those of β -secretase. Together these findings suggest a role for presenilin in regulating basal glutamatergic synaptic transmission and synapse structure of hippocampal neurons.

Acknowledgements

Firstly, I would like to thank my supervisor, Dr Yuki Goda, for giving me the chance to work in her lab and for all the help, support and opportunities that she has provided to me during the course of my doctoral studies.

I would like to thank Dr Lorenzo Cingolani for his invaluable technical advice, time and assistance. I would also like to express my gratitude to all past and present members of the Goda lab for discussions and support.

Thank you to Dr Andrew Batchelor for sharing his practical knowledge and for many useful and inspiring conversations. Special thanks should be given to Professor Eddie Koo for providing me with valuable insights and encouragement throughout the course of this project. Thank you to Professor Sangram Sisodia and Dr Xulun Zhang for collaborative work and efforts. I would like to acknowledge the members of my PhD committee, Dr Antonella Riccio, Dr Sara Mole and Dr Joanne Taylor for guidance and reassurance.

I am very grateful to Eisai (London) Research Laboratories Ltd. for providing generous funding for my studies.

I owe much to my family and friends. Thank you for providing fun, laughter and solace when it was most needed. I am especially grateful to Billy, Lisa, David and Ray for everything that they have ever done for me. Thanks also to POTtery (yeah!). Finally, thank you so much to Simon for providing continuous support, encouragement, perspective and patience.

To 媽媽

Thank you for your love, guidance and for teaching me so much during our brief time together.

Abbreviations

μ	micron
a.a	amino acids
AD	Alzheimer's disease
AICD	APP intracellular domain
AMPA	α -amino-3-hydroxy-5-methyl-isoxazole-4-propionic acid
ANOVA	analysis of variance
AP5	(D/DL)-2-amino-5-phosphopentanoic acid
APH-1	anterior pharynx defective 1
APLP	amyloid precursor-like protein
ApoE	apolipoprotein E
ApoER2	apolipoprotein E receptor-2
APP	amyloid- β precursor protein
Asp2	aspartyl protease 2
A β	amyloid- β
BDNF	brain-derived neurotrophic factor
BME	Eagle's Basal Medium
bp	base pair
CA	cornu ammonis
CaMKII	calcium/calmodulin dependent protein kinase
cAMP	cyclic adenosine monophosphate
CBF1	C-promoter-binding factor 1
CCE	capacitative calcium entry
Cdk5	cyclin-dependent kinase 5
CHO	Chinese hamster ovary
CICD	cadherin intracellular domain
CICR	calcium induced calcium release
Cm	cell capacitance
CNQX	6-cyano-7-nitroquinoxaline-2,3-dione
CNS	central nervous system
Cre	cAMP responsive element
CSF-1R	colony-stimulating factor 1 receptor
CTF	C-terminal fragment
DAPT	N-[N-(3,5-di ⁻ uorophenacetyl)-l-alanyl]-S-phenylglycine t-butyl ester
DCC	deleted in colorectal cancer
DG	dentate gyrus
DIC	differential interference contrast
DIV	days <i>in vitro</i>
DMSO	dimethylsulphoxide
DNA	deoxyribonucleic acid
DNase	deoxyribonuclease
dNTP	deoxynucleotide tri-phosphate
E	embryonic
EDTA	ethylenediamine tetraacetic acid
EGTA	ethylene glycol tetraacetic acid
EPP	end-plate potential
EPSC	excitatory postsynaptic current

EPSP	excitatory postsynaptic potential
ER	endoplasmic reticulum
ERGIC	endoplasmic reticulum Golgi intermediate compartment
FCS	fetal calf serum
Fura-2 (AM)	fura-2 (acetoxymethyl ester)
G	Giga
GABA	gamma-aminobutyric acid
GFP	green fluorescent protein
GluA	glutamate receptor
GSK-3 β	glycogen synthase kinase 3 β
Hr(s)	hour(s)
HSG	human salivary gland epithelial
Hz	hertz
IP ₃	inositol-1,4,5-trisphosphate
IP ₃ R	inositol-1,4,5-trisphosphate receptors
kDa	kilodaltons
kHz	kilohertz
L	litre
L-685,458	(1S-Benzyl-4R-[1-(1S-carbamoyl-2-phenylethylcarbamoyl)-1S-3-methylbutylcarbamoyl]-2R-hydroxy-5-phenylpentyl)carbamic acid tert-butyl ester
LAR	leukocyte-common antigen related
LRP	low density lipoprotein receptor-related protein
LTD	long term depression
LTP	long term potentiation
m	meter
M	Molar / Mega
MAP2	microtubule associated protein 2
memapsin 2	membrane-anchored protease of the pepsin family
mEPSC	miniature excitatory postsynaptic current
min	minute
mIPSC	miniature inhibitory postsynaptic current
mV	millivolt
n	nano
NA	numerical aperture
NBQX	2,3-dihydroxy-6-nitro-7-sulfamoyl-benzo[f]quinoxaline-2,3-dione
NICD	notch intracellular domain
NMDA	N-methyl-D-aspartic acid
NMJ	neuromuscular junction
NR2(A/B)	NMDA receptor subunit 2 (A/B)
NRADD	neurotrophin receptor alike death domain protein
NRG-1	neuregulin-1
P	postnatal
p75 ^{NTR}	p75 neurotrophin receptor
pA	pico amp
PBS	phosphate buffered saline
PCR	polymerase chain reaction
PDL	poly-D-lysine
PEN-2	presenilin enhancer protein 2

PFA	paraformaldehyde
PKA	cyclic AMP-dependent protein kinase
PPR	paired-pulse ratio
Pr	release probability
PS	presenilin
PSD-95	postsynaptic density-95
PSGL-1	P-selectin glycoprotein ligand-1
R_{in}	input resistance
RIP	regulated intramembrane proteolysis
RRP	readily releasable pool
R_s	series resistance
RyR	ryanodine receptor
s.e.m	standard error of the mean
sAPP (α/β)	soluble amyloid- β precursor protein fragments (α/β)
SCN β 2	sodium channel subunit β 2
sec	second
SERCA	sarco/endoplasmic reticulum calcium ATPase
SPP	signal peptide peptidase
Su(H)	suppressor of hairless
TCF	T cell-specific transcription factor 1
TGN	trans Golgi network
TM	transmembrane domain(s)
TTX	tetrodotoxin
V	volt
VAChT	Vesicular Acetyl Choline Transporter
VGCC	voltage gated calcium channels
α	alpha
β	beta
γ	gamma
δ	delta
ϵ	epsilon
ζ	zeta
τ	tau

Table of Contents

Chapter 1: Introduction	19
1.1 Alzheimer's disease (AD)	20
1.1.1 Sporadic Alzheimer's disease (SAD)	21
1.1.2 Familial Alzheimer's disease (FAD)	22
1.1.3 Histopathological characteristics of AD	23
1.2 Biosynthesis of A β : APP processing	28
1.2.1 Amyloid-beta precursor protein (APP)	28
1.2.2 APP processing	29
The amyloidogenic pathway and generation of A β	30
The non-amyloidogenic/ constitutive pathway and generation of p3 fragments	31
1.3 Presenilin and γ -secretase	33
1.3.1 Presenilin: The catalytic core of γ -secretase	33
1.3.2 Nicastrin, APH-1 and PEN-2: The accessory proteins of γ -secretase	36
1.3.3 Formation and maturation of γ -secretase	39
1.3.4 Subcellular localisation of γ -secretase components	42
1.3.5 Subcellular location of γ -secretase activity	43
1.3.6 γ -secretase and regulated intramembraneous proteolysis of transmembrane substrates	46
1.4 Other cellular secretases	48
1.4.1 α -secretase	48
1.4.2 β -secretase	49
1.5 Cellular functions of γ -secretase	51
1.5.1 Nuclear signalling and developmental regulation by Notch/NICD and other γ -secretase associated transcriptional regulators	53
1.5.2 Cell signalling and cell adhesion through β -catenin and cadherins	55
1.5.3 γ -secretase independent forms of cellular regulation by presenilins	57
1.5.4 Presenilin and regulation of intracellular calcium	58
1.6 The role of presenilin at the synapse	61

1.6.1 The properties of a synapse.....	61
Synapse structure	61
Synaptic transmission	62
Synapse number	66
Synaptic plasticity and memory – focus on the hippocampus.....	68
1.6.2 Presenilin knock-out mice models	71
1.6.3 Presenilins, synaptic plasticity and learning and memory	74
1.6.4 Presenilins and synaptic transmission.....	77
1.6.5 Comparison of PS1 and PS2 associated γ -secretase functions	78
1.7 Concluding remarks	81
Aims	82
Chapter 2: Materials and Methods	83
2.1 Animals	83
2.1.1 Rat colonies.....	83
2.1.2 PS1 mice colonies and genotyping	84
2.2 Hippocampal cell culture (rat and mice).....	86
2.2.1 Materials.....	86
2.2.2 Methods.....	88
2.2.2.1 Preparation of glass coverslips.....	89
2.2.2.2 Preparation of astrocyte feeder layer.....	89
2.2.2.3 Preparation of rat hippocampal dissociated neurons.....	90
2.2.2.4 Preparation of mouse hippocampal dissociated neurons	90
2.2.2.5 Organotypic slice culture preparation	91
2.3 Drugs and Inhibitors.....	93
2.3.1 γ -secretase inhibitors.....	93
2.3.2 β -secretase inhibitors.....	94
2.4 Electrophysiology	96
2.4.1 Materials.....	96
2.4.2 Methods.....	98
2.4.2.1 Patch clamp recordings from hippocampal dissociated cells.....	98
Analysis.....	100
2.4.2.2 Electrophysiology from hippocampal organotypic slice cultures....	101

Analysis.....	103
2.5 FM Imaging.....	104
2.5.1 Materials.....	104
2.5.2 Methods.....	105
2.5.2.1 FM Styryl-dye labeling and imaging.....	105
Analysis.....	107
2.6 Calcium imaging.....	108
2.6.1 Materials.....	108
2.6.2 Methods.....	109
2.6.2.1 Live calcium imaging with Fura-2.....	109
2.6.2.2 Basal and KCl-stimulated calcium induced calcium release (KCl-stimulated CICR).	113
2.6.2.3 Estimating calcium concentration in hippocampal dissociated cultures	115
Analysis.....	117
2.7 Immunocytochemical fluorescence imaging.....	120
2.7.1 Materials.....	120
2.7.2 Methods.....	120
2.7.2.1 Immunocytochemical examination of pre and postsynaptic proteins	120
Antibody labelling of dissociated cultures.....	120
Confocal imaging.....	122
Analysis of pre and postsynaptic marker number	123
2.8 Organotypic spine analysis	125
2.8.1 Materials.....	125
2.8.2 Methods.....	125
2.8.2.1 Fluorescence labeling of spines of CA1 pyramidal cells in organotypic slices.....	125
Confocal imaging of spines of CA1 pyramidal cells in organotypic slices.....	126
Analysis.....	126
2.9 Statistics	127

Chapter 3: The role of presenilin in modulating spontaneous synaptic currents in hippocampal neurons	128
3.1 Introduction	128
3.2 Examination of the effect of γ -secretase activity inhibition on mEPSC properties in dissociated hippocampal neurons.....	130
3.3 Examination of mEPSC properties of hippocampal neurons from PS1 transgenic mice	136
3.4 Examination of the effect of γ -secretase activity inhibition on mEPSC properties in hippocampal organotypic slice cultures.....	142
3.5 Examination of the effect of γ -secretase activity inhibition on mIPSC properties in hippocampal organotypic slice cultures.....	146
3.6 Discussion	150
3.7 Conclusion	153
Chapter 4: The role of presenilin in modulating release probability in hippocampal neurons	154
4.1 Introduction.....	154
4.2 Estimating release probability using optical measurements of FM-dye destaining	155
4.2.1 Examination of release probability of PS1 +/+ and PS1 -/- neurons using FM dyes.....	156
4.2.2 Examination of release probability of γ -secretase inhibitor treated rat dissociated neurons using FM dyes	159
4.3 Examination of release probability of γ -secretase inhibitor treated organotypic slices by measuring paired-pulse ratio and the rate of MK801 blockade	162
4.4 Discussion	166
4.5 Conclusion	168
Chapter 5: The role of presenilin in modulating synapse number in hippocampal neurons	169
5.1 Introduction.....	169
5.2 Examination of synapse number in rat dissociated neurons treated with γ -secretase inhibitors	170
5.3 Examination of synapse number in PS1+/+ and PS1-/- mice neurons	174

5.4 Examination of spine number in rat organotypic slice cultures treated with γ -secretase inhibitors	176
5.5 Discussion	178
5.5.1 Limitations and points of further investigation.....	179
5.5.2 Potential mechanisms for γ -secretase associated regulation of synapse number	184
5.6 Conclusion	186
Chapter 6: The role of presenilin in modulating intracellular calcium in hippocampal neurons.....	187
6.1 Introduction	187
6.1.1 Evidence for calcium regulation of miniature frequency.....	187
6.1.2 The role of presenilins in regulating intracellular calcium	189
6.2 Investigating the effect of γ -secretase inhibition on basal intracellular calcium levels	192
6.3 Investigating the effect of γ -secretase inhibition on intracellular calcium levels during KCl-induced CICR	194
6.4 Investigating the effects of ryanodine receptor and SERCA blockade in γ -secretase inhibitor treated hippocampal neurons	198
6.5 Discussion	204
6.5.1 Calcium regulation and Familial Alzheimer's disease.....	209
6.6 Conclusion	209
Chapter 7: The role of β-secretase in modulating synapse function in hippocampal neurons.....	210
7.1 Introduction.....	210
7.2 Investigating the effects of β -secretase activity inhibition on mEPSC properties.....	214
7.3 Estimating release probability with styryl dyes in rat dissociated cells treated with β -secretase inhibitor	218
7.4 Investigating synapse number of rat dissociated cells treated with β -secretase inhibitor.....	220
7.5 Discussion	225
BACE-1 knock-out mice.....	226

Differences between γ -secretase and β -secretase inhibition on synapse function	228
7.6 Conclusion	234
Chapter 8: Overall summary and general discussions	235
8.1 Research summary	235
8.2 Possible γ -secretase dependent and γ -secretase independent action of presenilin at hippocampal synapses	243
8.3 Neuronal activity, A β peptides and synaptic transmission	244
8.4 Evaluating γ -secretase inhibitors as a possible therapeutic strategy for AD ..	245
8.5 Relation of current findings to AD.....	248
8.7 Final remarks.....	251
Appendix	252
Bibliography	253

Index of Figures and Tables

Figures

Figure 1.1 - A β plaque assembly.....	27
Figure 1.2 - APP processing by cellular secretases.....	32
Figure 1.3 - Structure of the γ -secretase complex.....	39
Figure 1.4 - Assembly of the γ -secretase complex.....	41
Figure 1.5 - Morphological differences between PS1 wild type (+/+) and constitutive PS1 knock-out (-/-) mice.....	72
Figure 2.1 - Hippocampal dissociated and organotypic slice cultures.....	93
Figure 2.2 - Molecular structure of γ -secretase and β -secretase inhibitors.....	95
Figure 2.3 - Properties of Fura-2 (AM).....	111
Figure 2.4 - Spontaneous calcium transients in hippocampal dissociated neurons.....	112
Figure 2.5 - Estimation of bath exchange rate during calcium imaging experiments.....	114
Figure 2.6 - Calculation of R _{min} in hippocampal neurons <i>in situ</i>	118
Figure 2.7 - Calculation of R _{max} in hippocampal neurons <i>in situ</i>	119
Figure 2.8 - Immunofluorescence analysis of synaptic marker puncta.....	124
Figure 3.1 - mEPSC frequency is modulated by chronic treatment with γ -secretase inhibitors.....	133
Figure 3.2 - Establishing timecourse of γ -secretase inhibitor treatment for mEPSC recordings.....	134
Figure 3.3 - Electrophysiological properties of rat dissociated neurons treated with γ -secretase inhibitors, DAPT and L-685,458.....	135
Figure 3.4 - mEPSC frequency is increased in presenilin-1 (PS1) knock-out mice.....	137
Figure 3.5 - Electrophysiological properties of dissociated neurons from PS1 +/+, PS1 +/- and PS1 -/- mice.....	138
Figure 3.6 – Examination of chronic γ -secretase treatment on miniature excitatory postsynaptic currents from PS1 +/+, PS1 +/- and PS1 -/- hippocampal cells.....	141
Figure 3.7 – Examination of mEPSC in rat hippocampal slice cultures treated with γ -secretase inhibitors, DAPT and L-685,458.....	144

Figure 3.8 – Electrophysiological properties of rat hippocampal organotypic slice neurons treated with DMSO mock control or γ -secretase inhibitor DAPT	145
Figure 3.9 – mEPSC frequency but not mIPSC frequency is modulated by chronic treatment with γ -secretase inhibitor, DAPT. (Configuration 1)	148
Figure 3.10 – mEPSC frequency but not mIPSC frequency is modulated by chronic treatment with γ -secretase inhibitor, DAPT. (Configuration 2)	149
Figure 4.1 – Stimulated FM dye uptake and destaining of hippocampal neurons ..	155
Figure 4.2 – Destaining kinetics of PS1 mice in different concentrations of extracellular calcium	157
Figure 4.3 – Destaining kinetics of PS1 mice cells following γ -secretase inhibitor treatment	158
Figure 4.4 – Destaining kinetics of rat dissociated neurons treated with γ -secretase inhibitors in different concentrations of extracellular calcium	160
Figure 4.5 – Estimation of readily releasable pool size in cells treated with γ -secretase inhibitors DAPT and L-685,458 and DMSO control	161
Figure 4.6 – Examining the effect of γ -secretase inhibition on paired pulse ratio ..	164
Figure 4.7 – Examining the effect of γ -secretase inhibition on rate of MK801 NMDA receptor block	165
Figure 5.1 – Immunofluorescence analysis of presynaptic synapsin and postsynaptic Homer markers of cells treated with γ -secretase inhibitors, DAPT or L-685,458 ..	172
Figure 5.2 – Immunofluorescence analysis of presynaptic synapsin and postsynaptic GluA1 of cells treated with γ -secretase inhibitors, DAPT or L-685,458	173
Figure 5.3 – Immunofluorescence analysis of synaptophysin in PS1 $+/+$ and PS1 $-/-$ cells	175
Figure 5.4 – Spine analysis of organotypic slices treated with γ -secretase inhibitors	177
Figure 6.1 - Measurement of basal calcium in hippocampal neurons	193
Figure 6.2 - Characterisation of KCl-stimulated calcium induced calcium release (CICR) in rat hippocampal dissociated neurons	196
Figure 6.3 - Measurement of peak calcium during KCl-stimulated CICR in hippocampal neurons	197
Figure 6.4 - The effects of ryanodine receptor inhibition on basal calcium levels in hippocampal neurons	200

Figure 6.5 - The effects of ryanodine receptor inhibition on peak calcium during KCl-stimulated CICR in hippocampal neurons.....	201
Figure 6.6 - The effects of thapsigargin on basal calcium levels in hippocampal neurons.....	202
Figure 6.7 - The effects of thapsigargin receptor inhibition on peak calcium during KCl-stimulated CICR in hippocampal neurons.....	203
Figure 7.1 – mEPSC frequency is modulated by chronic treatment with β -secretase inhibitor in rat dissociated hippocampal neurons.....	216
Figure 7.2 – mEPSC recordings of rat hippocampal organotypic slice cultures chronically treated with β -secretase inhibitor.....	217
Figure 7.3 – Destaining kinetics of β -secretase treated rat dissociated cultured neurons in different concentrations of extracellular calcium.....	219
Figure 7.4 – Immunofluorescence analysis of presynaptic synapsin and postsynaptic Homer markers of cells treated with β -secretase inhibitor IV.....	222
Figure 7.5 – Immunofluorescence analysis of presynaptic synapsin and postsynaptic GluA1 markers of cells treated with β -secretase inhibitor IV.....	223
Figure 7.6 – Spine analysis of organotypic slices treated with β -secretase inhibitor IV.....	224
Appendix I: Western blot of APP from rat dissociated neuronal cultures.....	252

Tables

Table 1.1: γ -secretase interacting proteins or substrates and proposed cellular functions of presenilin association.....	52
Table 2.1: Components for PS1 PCR reaction.....	85
Table 2.2: PS1 PCR reaction protocol.....	85
Table 2.3: Chemicals / Reagents / Products used for dissociated cell culture.....	86
Table 2.4: Buffers and Solutions, used for used for dissociated cell culture.....	87
Table 2.5: Chemicals / Reagents / Products used for organotypic slice culture.....	88
Table 2.6: Buffers and Solutions, used for organotypic cell culture.....	88
Table 2.7: Chemicals / Reagents / Products used for electrophysiology.....	96
Table 2.8: Buffers and Solutions, used for electrophysiology.....	97
Table 2.9: Chemicals / Reagents / Products used for FM imaging experiments.....	104
Table 2.10: Buffers and Solutions, used for FM imaging experiments.....	105
Table 2.11: Chemicals / Reagents / Products used for calcium imaging.....	108
Table 2.12: Buffers and Solutions, used for calcium imaging.....	108
Table 2.13: Buffers and Solutions, used for immunocytochemistry.....	120
Table 2.14: Chemicals / Reagents / Products used for visualization of spines in organotypic slices.....	125

Chapter 1 : Introduction

Synapses are specialised points of contacts which enable communication and transfer of neural information between a presynaptic neuron and postsynaptic neuron. The mechanisms of electrical information transfer across synapses differ depending on the type of synapse. Traditionally, synapses are classified into two groups, electrical synapses which enable bidirectional flow of electrical current through gap junction connections and chemical synapses where communication occurs through stochastic release of neurotransmitter from presynaptic vesicles in axonal boutons which cross the synaptic cleft to interact with postsynaptic receptors. Chemical synapses are highly plastic and can exhibit changes in pre and postsynaptic compartments including alterations in synaptic strength and structure during development and in response to activity. Understanding the molecular and cellular basis of synaptic transmission and function has been a key goal of modern neuroscience in past decades.

Recent synaptic studies have also started to focus on the mechanisms underlying synapse dysfunction and elimination, processes believed to be key early events associated with neurodegenerative diseases such as Alzheimer's disease (AD) (Selkoe, 2002). Changes in synapse function and neuronal homeostasis may potentially trigger processes that lead to synapse degeneration and loss, events which precede the pathological neuronal loss that is universally seen in AD patients (Dekosky and Scheff, 1990; Masliah et al., 1991; Terry et al., 1991). Therefore, for effective design of therapeutic strategies for AD, it is crucial to identify and understand the neuronal changes at the earliest possible stage. Understanding the physiological role of proteins involved in AD at the level of the synapse, may provide further insights into the cellular and molecular changes that occur during disease. One of the key molecules involved in AD is presenilin 1 (PS1). The vast majority of familial AD cases arise from missense mutations in the presenilin 1 gene, *PSENI*, which is inherited in an autosomal dominant manner. PS1 is highly

implicated in the pathobiology of AD as it is believed to be the catalytic subunit of γ -secretase, a cellular enzyme complex that generates amyloid-beta peptides ($A\beta$) by cleaving amyloid- β precursor protein (APP). These $A\beta$ peptides are the core constituents of one of the characteristic features of AD, the $A\beta$ plaques. In addition to its role in AD, studies have shown that PS1 is strongly implicated in regulating a wide range of different cellular functions. This chapter will provide an overview of our current knowledge of presenilin biology, discuss the role of presenilin in regulating physiological neuronal functions and provide a summary of the role of presenilins in AD pathogenesis.

1.1 Alzheimer's disease (AD)

Recent epidemiological estimates from the Alzheimer's disease international organization predict that in 2010, there will be approximately 35 million AD patients worldwide making it the most prevalent neurodegenerative disease (Prince and Jackson, 2009). Forecasts predict the number of cases will increase dramatically over the coming decades with 65.7 million estimated cases in 2030 and 115.4 million in 2050 (Prince and Jackson, 2009). AD is a devastatingly debilitating form of dementia associated with a progressively severe and irreversible decline in cognitive functions such as deterioration in learning and language abilities and gradual loss of memory. Behavioural disturbances such as aggression, agitation and apathy as well as psychological impairments like delusions, anxiety and depression have also been reported and can aid clinical diagnosis (Almkvist, 1996; Burns and Iliffe, 2009). However, clinical diagnosis of AD is often not straightforward as changes in cognitive ability or memory loss are also associated with a host of other dementias such as vascular dementia, frontotemporal dementia and dementia with Lewy bodies. Additionally, these symptomatic signs are often observed at a relatively advanced stage of AD and pathological changes to the brain may start to develop years before symptoms are fully recognized. Recent advances in functional imaging using compounds such as Pittsburgh compound-B (PIB) which label $A\beta$ plaques has aided clinical diagnosis and provided insights into early changes in brain activity (Klunk et al., 2004). However, the aim of current research efforts is to identify the earliest

stage when pathogenesis can be detected, ideally prior to the onset of symptoms. Targeting synaptic changes at the earliest stage may offer therapeutic strategies the greatest chance of success.

1.1.1 Sporadic Alzheimer's disease (SAD)

Current diagnostic procedures divide AD into two forms: sporadic AD (SAD) and familial AD (FAD). The risk factors associated with sporadic AD, which accounts for the vast majority of cases (90-95%) are not well understood. Aetiological studies investigating sociodemographic risk factors have shown a positive correlation between age and AD. Most cases of sporadic AD affect patients over the age of 65 and the age related risk doubles every 5 years over this age (Brouwers et al., 2008; LaFerla and Oddo, 2005). Other proposed secondary risk factors include family history, head injury, hypertension, high cholesterol levels, sedentary lifestyles, mental inactivity, cerebral vascular disease, gender (with increased risk in females), and environmental factors (Azad et al., 2007; Blennow et al., 2006; Burns and Iliffe, 2009; Prince and Jackson, 2009). However, follow up studies of these secondary factors will be required to assess their overall contribution and significance to SAD.

Recent studies have also identified that certain SAD cases may have a genetic basis. Unlike FAD which is primarily caused by genetic missense mutations, SAD is associated with an increase in the copy number of a susceptibility gene located on chromosome 19, *ApoE*. *ApoE* can be found as three major single nucleotide polymorphisms referred to as *ApoE 2*, *3* and *4*, each associated with a different level of risk. The most abundant form in the central nervous system (CNS) is *ApoE3* which is not linked to any change in risk whereas *ApoE2* leads to an advantageous decrease in risk. By contrast, the *ApoE4* allele leads to a significant increase in risk with approximately 70% of SAD patients having at least one copy of this high risk isoform (Corder et al., 1993; Corder et al., 1994; Corder et al., 1995; Holtzman, 2001; Kim et al., 2009a; Kim et al., 2009b; Saunders et al., 1993). The role of the protein encoded by the *ApoE* gene, Apolipoprotein E (ApoE) in the development of SAD is slowly being uncovered. ApoE is a glycoprotein which is implicated in the

receptor-mediated endocytosis of lipoprotein particles and cholesterol metabolism (Kim et al., 2009a; Pitas et al., 1987). Studies have shown that ApoE can sequester A β peptides and elimination of ApoE can cause a strong reduction in both extracellular and intracellular A β suggesting a role for ApoE in A β clearance (Holtzman et al., 2000a; Holtzman et al., 2000b; Jiang et al., 2008; Strittmatter et al., 1993). However, overall the molecular mechanisms associated with SAD remain to be fully elucidated.

1.1.2 Familial Alzheimer's disease (FAD)

In addition to sporadic forms of AD, there are autosomal dominant forms of early onset familial Alzheimer's disease (FAD) which typically affects individuals that are 65 years and below (Fraser et al., 2000; Goedert and Spillantini, 2006; Tandon and Fraser, 2002). FAD cases only account for approximately 5-10% of total AD cases and apart from an accelerated age of onset and a shorter time period required for exhibition of pathological features, the general pathophysiological features of AD such as the expression of plaques and tangles are similar between FAD and SAD cases (Lantos et al., 1992; Vetrivel et al., 2006).

Studies of families with FAD have provided great insight into the general molecular mechanisms involved in AD. FAD is associated with mutations in three genes: *APP* gene (on chromosome 21) encoding amyloid-beta precursor protein (APP) (Goate et al., 1991), *PSEN1* (on chromosome 14) encoding presenilin 1 (PS1) (Sherrington et al., 1995) and *PSEN2* (on chromosome 1) encoding presenilin 2 (PS2) (Levy-Lahad et al., 1995). Currently over 200 mutations have been reported in these genes, with the majority being located within *PSEN1* (179 for *PSEN1*, 14 for *PSEN2* and 32 for *APP*; see Alzheimer disease and frontotemporal dementia database website or www.alzforum.org for up to date reports, Marambaud and Robakis, 2005; Tanzi and Bertram, 2001). Most mutations are missense mutations which lead to single amino acid shifts, though deletion, insertion and splice mutations have been reported (De Strooper, 2007). Interestingly, mutations are found distributed throughout the presenilin protein rather than being concentrated within a particular domain/ exon

(Bergmans and De Strooper, 2010; Fraser et al., 2000). On the whole, *PSEN1* mutations are considered more aggressive than *PSEN2* and *APP* mutations and typically lead to an earlier age of onset (Brouwers et al., 2008; Tandon and Fraser, 2002).

Studies of FAD patients and transgenic mice models of FAD mutations have revealed that most clinical mutations are associated with neuronal loss and an overproduction of A β within the CNS. More specifically, most studies have indicated that these mutations lead to an elevated production of the neurotoxic aggregation prone form of A β peptide, A β ₄₂ (Borchelt et al., 1996; Citron et al., 1992; Citron et al., 1997; Duff et al., 1996; Haass et al., 1994; Haass and Selkoe, 2007; Hardy and Selkoe, 2002; Scheuner et al., 1996). However, an alternative theory has been suggested by recent reports which showed using different FAD mice models that it is the ratio of A β ₄₀ to A β ₄₂ that determines AD pathogenesis rather than absolute levels of A β ₄₂ production (Bentahir et al., 2006; Kumar-Singh et al., 2006). However, some mutations can lead to reduced A β production, which brings into question whether clinical mutations lead to a toxic gain-of-function or loss-of-function of presenilin (Bentahir et al., 2006). Taken together, these mutations suggest that A β production is a pivotal event in the molecular pathway underlying FAD.

1.1.3 Histopathological characteristics of AD

The first reported case of AD was made in 1901 by Alois Alzheimer after conducting post-mortem examinations on a patient referred to as Auguste D who was suffering from senile dementia prior to her death (see Fortini, 2003 for review). Through histological analysis using Bielschowsky silver staining of brain tissue, Alzheimer discovered the two hallmark characteristics used to clinically confirm the disease, the presence of extracellular A β plaques and intracellular neurofibrillary tangles (Goedert and Spillantini, 2006).

The neurofibrillary tangles observed in AD patients mainly consist of a protein called tau. Tau is a primarily neuronal specific microtubule associated protein which under basal physiological conditions aids the stabilisation of microtubules especially in axonal processes (Querfurth and LaFerla, 2010). During AD it has been proposed that tau undergoes abnormal proteolytic processing and becomes hyperphosphorylated at proline-directed serine/threonine residues which results in the generation of non-membrane associated paired helical filamentous structures which then aggregate to give rise to neurofibrillary tangles (Buee et al., 2000; Grundke-Iqbal et al., 1986a; Grundke-Iqbal et al., 1986b; Kidd, 1963; Paudel et al., 1993). Neurofibrillary tangles are often found within the intracellular regions of neurons with particularly strong aggregation in the cell soma and apical dendrites. However, the abnormal accumulation of tau is not exclusively confined to AD as other neurodegenerative diseases including Amyotrophic Lateral Sclerosis (ALS), Pick's disease, corticobasal degeneration, frontal temporal dementia with parkinsonism linked to chromosome 17 and tangle only dementia all exhibit tau filaments (Skovronsky et al., 2006). These conditions come under the collective umbrella of neurodegenerative tauopathies (for review see Buee et al., 2000; Lee et al., 2001).

Extensive light and electron microscopy studies have shown that extracellular plaques that accumulate in AD are mainly composed of a peptide known as A β (Allsop et al., 1983). A β is a product of the proteolytic cleavage of APP. APP is processed by a series of different catalytic reactions to give rise to a range of A β peptides of multiple lengths. A β peptides can be found in several different states of aggregation within the brain. A β peptides are initially formed as single unit monomers and progressive self-aggregation leads to formation of dimers, oligomers, protofibrils, fibrils and finally A β plaques (Figure 1.1, Bitan et al., 2003; Caughey and Lansbury, 2003). A β neuritic plaques mainly consist of A β fibrils containing the longer, more neurotoxic aggregation prone A β_{42} peptide isoform arranged into insoluble β -sheet structures (Glenner et al., 1984; Glenner and Wong, 1984a; Glenner and Wong, 1984b; Iwatsubo et al., 1994; Selkoe and Wolfe, 2007). These neuritic plaques are often found in close association with the axons and dendrites of neurons as well as glia and blood vessels (Georgakopoulos et al., 1999; Glenner et al., 1984; Hardy, 1997; Ribaut-Barassin et al., 2000; Selkoe and Schenk, 2003).

Furthermore studies have shown that neuronal processes in contact with plaques may exhibit dystrophic morphology, hyperactivity, and dysregulation of calcium homeostasis suggesting that these extracellular plaques are influencing the structure and health of closely associated neurons (Busche et al., 2008; Garcia-Alloza et al., 2009; Kuchibhotla et al., 2008; Meyer-Luehmann et al., 2008; Spires et al., 2005; Spires-Jones et al., 2007; Wu et al., 2010). However, there is growing evidence that suggests that early cellular changes observed during AD are more tightly associated with smaller A β species, in particularly oligomers, rather than fibrils and plaques (Haass and Selkoe, 2007; Walsh et al., 2005; Walsh and Selkoe, 2007).

Since Alzheimer's original observations, the pathological phenotype of plaques and tangles have been reported in many regions of the CNS including the hippocampus, entorhinal cortex, amygdala and neocortex, key regions of the brain associated with different forms of learning and memory (Braak and Braak, 1991a; Braak and Braak, 1991b; Gomez-Isla et al., 1996). The temporal appearance of A β plaques and neurofibrillary tangle deposition in the AD brain is different. Studies in transgenic mice models carrying mutations in presenilin, APP and tau genes have shown that amyloid pathology occurs prior to tau accumulation suggesting that the amyloid pathway is engaged before tau dysregulation (McGowan et al., 2006; Oddo et al., 2003a; Oddo et al., 2003b). There is also some evidence from transgenic mice that A β fibrils could stimulate tangle formation (Gotz et al., 2001). Primary cell culture studies also showed that A β peptide aggregates could trigger tau hyperphosphorylation in somatodendritic compartments of rat septal neurons (Zheng et al., 2002). Additionally, neuronal loss is another key characteristic of AD which often accompanies the pathohistological appearance of A β deposits and tau neurofibrillary tangles. Neuronal loss is typically measured as a decrease in brain weight and increase in ventricular areas as a result of temporal lobe atrophy, especially in the hippocampus.

However, whilst the presence of A β plaques and neurofibrillary tangles are used to confirm the presence of AD, there is still great debate over the pathological involvement of these protein aggregates. Indeed past studies have shown that plaque and tau accumulations are often poorly correlated with the extent of memory loss. Furthermore, these features can be found in elderly patients who do not experience

dementia (Arriagada et al., 1992; Delaere et al., 1990; Kazee and Johnson, 1998). This suggests that A β plaques and neurofibrillary tangles are possibly not the pathological species involved in early stages of AD when cognitive defects start to occur. The current consensus is that the best correlate to early memory impairments is the extent of synapse loss and neuronal dysregulation which precludes neuronal loss (Braak and Braak, 1997; Dekosky and Scheff, 1990; Selkoe, 2002; Terry et al., 1991; Terry, 2000). Hence extensive research efforts have concentrated on gaining a better understanding of the cellular and molecular events which lead to synapse dysfunction and degeneration.

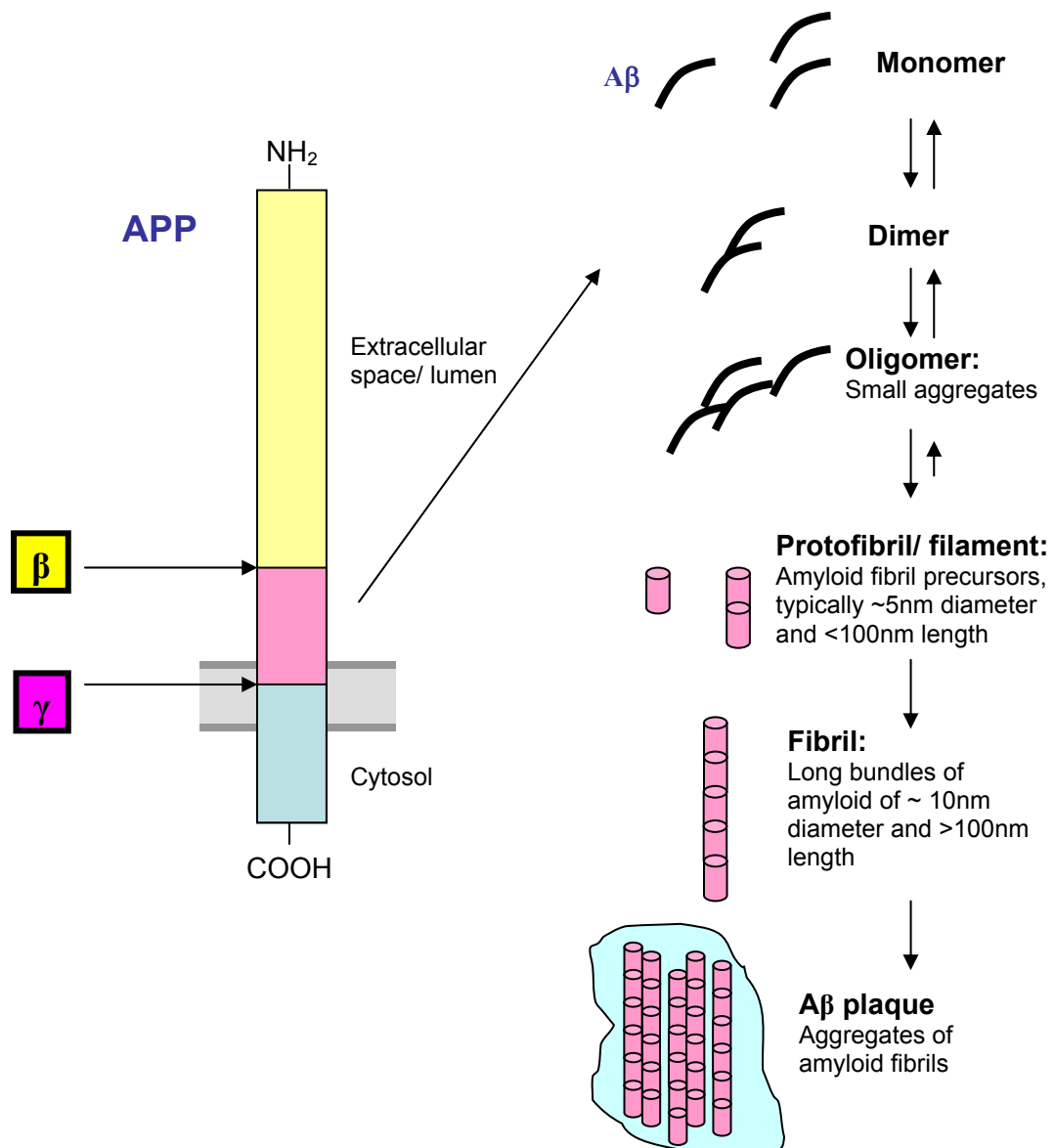


Figure 1.1 - Aβ plaque assembly.

The assembly of Aβ plaques occurs through a series of aggregation steps. The key constituent of Aβ plaques are Aβ peptides, which are generated through sequential cleavage of APP by β-secretase and γ-secretase. Newly biosynthesised soluble monomeric peptides are mostly released into the extracellular milieu and can form largely unstructured dimers and oligomers. These steps are reversible. Protofibrils are usually generated from Aβ oligomers and dimers that aggregate to form β-sheet and α-helical secondary structures. Maturation and aggregation of protofibrils give rise to fibrils which can aggregate to form insoluble Aβ plaques.

1.2 Biosynthesis of A β : APP processing

1.2.1 Amyloid-beta precursor protein (APP)

The *APP* gene encodes for APP, a type I integral single transmembrane helical glycoprotein with a large luminal N-terminus domain containing a signal peptide, and a short cytoplasmic tail (Kang et al., 1987; Robakis et al., 1987a; Robakis et al., 1987b; Sisodia et al., 1993; Turner et al., 2003). In mammals, APP belongs to the same protein family as APP like protein 1 (APLP1) (Wasco et al., 1992) and 2 (APLP2) (Wasco et al., 1993). However, APP is the only member of the group that can be processed to generate A β peptides (Zheng and Koo, 2006). APP also shares homology with APPL in the fruit fly *Drosophila* (Rosen et al., 1989) and APL-1 in the nematode *Caenorhabditis elegans* (*C. elegans*) (Daigle and Li, 1993). APP is ubiquitously expressed throughout the CNS and alternative mRNA splicing of exon 7 and 8 gives rise to three main isoforms composed of either 695 (APP695), 751 (APP751) or 770 (APP770) amino acids (Suh and Checler, 2002; Thinakaran and Koo, 2008; Turner et al., 2003). APP695 is predominately expressed in neurons whilst APP751 and APP770 are found in glia and non-neuronal cells.

Structural studies on APP have revealed different domains that may be important for different cellular functions. The extracellular N-terminus ectodomain of APP contains a wide range of sequences that modulate protein-protein interactions. These include the E1 domain which enables interaction with copper and zinc, the E2 domain which contains the RERMS sequence and interacts with extracellular matrix proteins and the kunitz protease inhibitor (KPI) region located on the extracellular N-terminus ectodomain of APP770 and APP751 (but not APP695) has been shown to regulate cell adhesion through the interaction to heparin and collagen (Mattson, 1997; Turner et al., 2003; Wolfe and Guenette, 2007; Zheng and Koo, 2006). The extracellular domain of APP has also been proposed to act as a cell surface receptor for different ligands including A β peptides, F-spondin and Nogo-66 (see Zheng and Koo, 2006 for review). Located on the cytoplasmic domain of the C-terminal tail is a YENPTY motif which enables internalisation of APP and also interaction with

many different intracellular proteins with phosphotyrosine-binding domains (Thinakaran and Koo, 2008; Turner et al., 2003; Zheng and Koo, 2006). One example is Fe65, a nuclear adaptor protein which can regulate synapse structure and growth cone activity (Sabo et al., 2003). Recent studies also showed that AICD, the intracellular fragment generated from γ -secretase cleavage of β -CTF can form a complex with Fe65 to modulate nuclear signalling and transcription regulation by binding to Tip60, a histone acetyltransferase (Cao and Sudhof, 2001; Cao and Sudhof, 2004). Other cellular functions of APP or γ -secretase cleavage products include cell migration, cell adhesion, synapse remodelling, axonal transport, apoptosis and protein phosphorylation (see for review: Thinakaran and Koo, 2008; Zheng and Koo, 2006). Studies conducted on APP knockout mice show that these animals were viable and exhibited a mild phenotype which included lower mass, decreased locomotion and impaired long-term potentiation (Dawson et al., 1999; Zheng et al., 1995).

1.2.2 APP processing

The biology of APP is complex as many different cellular roles have been reported not only for the full length protein but also for the different fragments (e.g. AICD, A β) generated from the cleavage of APP by cellular proteases (see for review: Marcello et al., 2008; Mattson, 1997; Rowan et al., 2005; Thinakaran and Koo, 2008; Turner et al., 2003; Venkitaramani et al., 2007; Zheng and Koo, 2006). Under basal conditions, full length APP holoprotein is constitutively trafficked to the plasma membrane. During its journey to the cell surface, APP can be post-translationally modified by tyrosine sulphation, N and O glycosylation or phosphorylation by different kinases including GSK-3 β , SAPK1b/ JNK3, Cdc2, and Cdk5 (Brouwers et al., 2008; Buxbaum et al., 1990; De Strooper and Annaert, 2000; Georgopoulou et al., 2001; Lee et al., 2003).

Once at the cell surface, full length APP can be processed through two separate pathways referred to as the amyloidogenic pathway, which ultimately leads to the generation of A β peptides, and the non-amyloidogenic or constitutive pathway which

leads to production of p3, a small peptide not believed to play a role in AD pathology (Brouwers et al., 2008). Surface antibody feeding assays have shown that APP can undergo internalisation and reinsertion back in the plasma membrane (Koo et al., 1996; Koo and Squazzo, 1994). The subcellular site of APP processing and cleavage is still widely debated (see for review: Thinakaran and Koo, 2008).

The amyloidogenic pathway and generation of A β

Firstly it is important to note that the generation of A β not only occurs during AD pathogenesis but also during normal basal physiological states (Haass et al., 1992; Seubert et al., 1992; Shoji et al., 1992). In order to generate A β , APP is sequentially cleaved by two enzyme complexes (See Figure 1.2). The first proteolytic event takes place either between residues Met 671 and Asp 672 (known as the +1 site) or between residues 682 and 683 (referred to as the +11 site) on the extracellular N-terminus of APP by β -secretase (BACE-1) which gives rise to two fragments, a soluble APP beta peptide (sAPP- β) that gets released into the extracellular space and a membrane associated fragment, β -carboxyl C-terminal fragment (β -CTF, also known as C99 (which refers to the number of amino acids) or β -stub) (Selkoe, 2001; Sisodia and George-Hyslop, 2002). β -CTF is subsequently cleaved by γ -secretase at γ , ϵ and ζ sites to generate a range of A β species ranging from 37-49 amino acids in length and APP intracellular domain (AICD) (also known as γ -CTF or C59) (Brouwers et al., 2008; Dries and Yu, 2008). A β is predominantly secreted into the extracellular space, whilst AICD is released into the intracellular space.

Under basal physiological states, the more soluble A β_{40} peptide accounts for approximately 90% of the total A β produced, whilst the more fibrillogenic A β_{42} peptide is produced at less than 10% of the total amount (Brouwers et al., 2008; Hardy and Mullan, 1992). However in AD, this trend is altered with patients and FAD transgenic mutant mice models showing a tendency towards an increase in A β_{42} production, A β aggregation and/or plaque deposition (Iwatsubo et al., 1994; Jarrett et al., 1993; Mori et al., 1992; Saido et al., 1995; Scheuner et al., 1996; Selkoe and Wolfe, 2007; Steiner et al., 2001).

The non-amyloidogenic/ constitutive pathway and generation of p3 fragments

Past studies have revealed that the main product of APP processing is not A β through the amyloidogenic pathway but p3 through the constitutive pathway (Anderson et al., 1991; Esch et al., 1990; Seubert et al., 1993; Sisodia et al., 1990). The generation of p3 fragments, like A β fragments, requires two subsequent cleavage events on APP to occur (see figure 1.2). The first event involves the cleavage of N-terminus APP at residues Lys 687 and Leu 688 by α -secretase to generate two peptides, a soluble APP alpha fragment (sAPP- α) and a membrane bound, α -carboxyl C-terminal fragment (α -CTF, also known as C83 or α -stub). α -secretase processing of APP prevents the formation of A β peptides and therefore precludes amyloidogenesis. Cleavage by α -secretase occurs within the A β region between amino acids lysine 16 and leucine 17 amino acids (with residue numbers being relative to the start of A β which is designated residue 1)(Dominguez et al., 2004; Sisodia and George-Hyslop, 2002). Like sAPP- β , newly generated sAPP- α fragments are released into the extracellular space. α -CTF is then cleaved within the transmembrane region by γ -secretase to generate p3 and AICD. As with A β fragments, a range of differently sized p3 fragments can be generated depending on the precise location of γ -secretase cleavage of α -CTF. The exact cellular role of p3 is not clearly understood, but enhancing the production of p3 may be an attractive therapeutic option. It has been proposed that generation of p3 may be neuroprotective purely by decreasing the amount of A β produced (Esch et al., 1990; Skovronsky et al., 2000). As α -secretase and β -secretase processing of APP are mutually exclusive to each other, increasing the amount of APP that is processed through the constitutive (α -secretase) pathway means less APP is made available for processing through the amyloidogenic (β -secretase) pathway and therefore less A β is generated (Skovronsky et al., 2000). However, other studies have shown that increasing α -secretase activity has no effect on decreasing A β generation suggesting A β generation may be tightly controlled by other regulatory processes (Rossner et al., 2000).

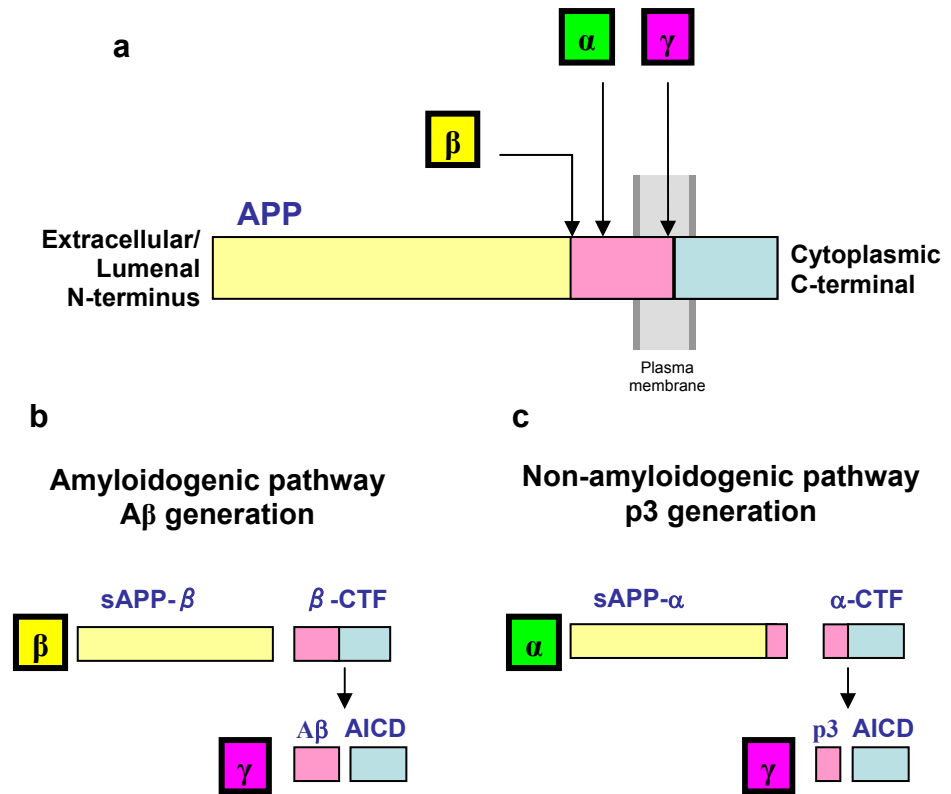


Figure 1.2 - APP processing by cellular secretases.

(a) APP is a transmembrane protein with a large extracellular N-terminus domain and shorter cytoplasmic C-terminal tail. APP can be processed by two pathways, either the amyloidogenic pathway or the non-amyloidogenic pathway.

(b) The amyloidogenic pathway leads to A β generation. Firstly β -secretase cleavage of APP gives rise to soluble β -APP fragments (sAPP- β) and β -CTF (also known as C99 or β -stub). Subsequent cleavage of γ -CTF by γ -secretase, generates two further peptide fragments: A β and AICD (also known as C59 or γ -CTF). Different cleavage sites on β -CTF can give rise to different peptide fragments. AICD is generated by γ -secretase cleavage at the ϵ -site of β -CTF.

Whilst γ -secretase cleavage at the γ -site of β -CTF leads to A β generation.

(c) The non amyloidogenic pathway leads to p3 generation. Firstly, α -secretase cleavage of APP generates soluble α -APP fragments (sAPP- α) and α -CTF (also C89 or α -stub). This pathway precludes A β formation as α -secretase cleavage occurs within the A β peptide. Subsequent cleavage of α -CTF by γ -secretase, gives rise to p3 and also AICD.

1.3 Presenilin and γ -secretase

As already mentioned, most FAD mutations are associated with an overproduction of A β peptides and neuronal loss. Most of these mutations occur within the *PSEN1* gene, identifying PS1 as an important component in the pathogenesis of AD. Determining the cellular role of PS1 may provide insights into the mechanisms which underlie AD pathology. PS1 is a protein that acts as part of a larger enzyme complex known as the γ -secretase. γ -secretase is an important protease involved in the processing of a range of cellular proteins and regulation of multiple cellular processes (see table 1.1). Early biochemical studies showed that γ -secretase exists as a high molecular weight complex but the composition of the enzyme complex has been an issue of intense debate. Current evidence from biochemical purification and activity reconstitution studies shows that γ -secretase activity is derived from a multi subunit complex composed of four integral components: PS (1 or 2), nicastrin, anterior pharynx defective 1 (APH-1), and presenilin enhancer protein 2 (PEN-2) (Edbauer et al., 2003; Fraering et al., 2004b; Hebert et al., 2004; Kimberly et al., 2003; Sato et al., 2007; Takasugi et al., 2003) (see Figure 1.3).

1.3.1 Presenilin: The catalytic core of γ -secretase

The presenilins were first isolated through positional cloning and two homologs were found, PS1 (Sherrington et al., 1995) and PS2 (Levy-Lahad et al., 1995) which share 67% sequence similarity (Kovacs et al., 1996). Homologs of presenilins have been reported in different model systems including *Xenopus*, *Drosophila* and *C. elegans* suggesting that presenilin function is evolutionarily conserved (Tandon and Fraser, 2002). The presenilins are polytopic membrane proteins, where PS1 is 467 amino acids long and PS2 is 448 amino acids (Dries and Yu, 2008). Despite some differences in function (discussed below), the similarities in structure between PS1 and PS2 have meant that most of the studies investigating presenilin topology have focused on PS1. The following information referring to the structure of presenilin

will be based around our current understanding of PS1 data but should also be largely applicable to PS2.

Topological modelling studies have proposed many possible arrangements of PS1 but the current accepted structure indicates 9 transmembrane domains (TM), a large hydrophilic intracellular loop between TM 6 and 7, a N-terminus which projects into the cytoplasm and a C-terminal tail located within the lumen/ extracellular space (Laudon et al., 2005; Oh and Turner, 2005a; Oh and Turner, 2005b; Spasic et al., 2006) (See Figure 1.3). Current evidence strongly suggests that PS1 is the catalytic subunit of γ -secretase (Fortini, 2002; Nyabi et al., 2003; Sisodia and George-Hyslop, 2002; De Strooper and Annaert, 2001; Wolfe et al., 1999b). PS1 is an aspartyl protease with two highly conserved catalytic aspartate residues at amino acid position 257 (in TM 6) and 385 (in TM7) which are both found within the active site of the γ -secretase enzyme complex (Spasic and Annaert, 2008; Wolfe et al., 1999b). Additionally two conserved motifs have been identified: a YD motif in TM 6 (hydrophobic region 6) and a GxGD catalytic motif in TM 7 (hydrophobic region 8) (Beel and Sanders, 2008; Haass and Steiner, 2002; Sato et al., 2006; Steiner and Haass, 2000). These motifs are crucial for peptidase function and are also found in bacterial type 4 prepilin peptidase (TFPP), signal peptide peptidase (SPP) and SPP-like (SPPL) proteases (Friedmann et al., 2004; Kaether et al., 2006a; Weihofen et al., 2002; Weihofen and Martoglio, 2003). A recent study also indicated that residue Tyr389 within the active zone may be important for catalytic action of γ -secretase (Tolia et al., 2006).

Convincing evidence that the aspartate residues are essential for γ -secretase activity was demonstrated through mutagenesis studies. Site directed mutagenesis of either aspartate residues led to a significant decrease in the production of A β from APP, indicating that these residues are crucial for γ -secretase activity (Kimberly et al., 2000; Wolfe et al., 1999b; Yu et al., 2000a). Additionally, biochemical studies showed that application of aspartyl protease transition state analogs designed against the active site of γ -secretase could block the formation of A β and led to an accumulation of α -CTF and β -CTF fragments (substrates for γ -secretase which are generated by α and β secretase cleavage of APP), providing further evidence that the aspartate residues are necessary for γ -secretase activity (Esler et al., 2000; Li et al.,

2000). The aspartate residues also seem to be evolutionarily conserved as mutagenesis of an equivalent aspartate residue within PS2 also led to a decrease in γ -secretase processing of APP and Notch (Kimberly et al., 2000; Steiner et al., 1999a).

Further evidence that presenilin is involved in γ -secretase activity was provided by knock-out mice studies. Cultured cortical neurons from PS1 knock-out animals exhibited an accumulation of APP C-terminal fragments and a greatly reduced production of A β , indicative of a major reduction in γ -secretase activity (De Strooper et al., 1998; Naruse et al., 1998). These results were mirrored by *in vivo* studies of conditional PS1 knock-out mice where the PS1 gene was deleted in the adult animal. A near absent production of A β_{40} and A β_{42} peptides was observed in animals generated by crossing conditional PS1 mice and APP transgenic mice, a AD model which normally develops amyloid pathology (Saura et al., 2005). The presence of amyloid plaques in 6 month old APP transgenic mice was almost completely absent in APP transgenic and conditional PS1 knock-out crossed animals, suggesting that γ -secretase activity of PS1 is also required for plaque deposition (Saura et al., 2005). These studies show that A β peptide and plaque generation is predominantly produced by PS1 containing γ -secretase complexes rather than PS2 containing complexes. Studies from embryonic stem cells lacking both PS1 and PS2 showed that A β generation was totally abolished (Herreman et al., 2000; Zhang et al., 2000). Together these knock-out studies show that the presenilins are essential for γ -secretase activity associated with APP processing.

In addition to being the catalytic component of γ -secretase, presenilin was also shown to undergo endoproteolysis. PS1 is initially synthesised as an approximately 43-48 kDa holoprotein but rapidly undergoes regulated endoproteolysis at residues 292 and 293 within the intracellular loop (between TM 6 and 7) to generate a ~ 27-30 kDa N-terminus fragment and a ~16-18 kDa C-terminal fragment (Fortini, 2002; Marambaud and Robakis, 2005; Podlisny et al., 1997; Thinakaran et al., 1996). Once endoproteolysis occurs, the N and C terminal fragments come together to form a non-covalently linked heterodimer in a 1:1 conformation (Campbell et al., 2003; Thinakaran et al., 1998). It is now generally accepted that it is the heterodimeric form of PS1 rather than the intact holoprotein that provides the enzymatic activity for the γ -secretase complex (Levitan et al., 2001; Thinakaran et al., 1996). Site

directed mutagenesis of either of the conserved aspartyl residues was shown to not only significantly decrease γ -secretase activity but also prevented generation of the PS1 heterodimer, leading to accumulation of the holoprotein form of PS1 (Wolfe et al., 1999a; Wolfe et al., 1999b; Yu et al., 2000a). Together, this data indicate two points; that presenilin undergoes auto-endoproteolysis and that endoproteolysis is an important process for maturation of the γ -secretase complex and activity. However, PS1 mutants that are unable to undergo endoproteolysis are still able to assemble into γ -secretase complexes, suggesting that endoproteolysis is not strictly required for γ -secretase function (Steiner et al., 1999b). Studies also revealed that inhibitors of γ -secretase could specifically crosslink the “active” N and C terminal heterodimeric fragments of presenilin (Esler et al., 2000; Li et al., 2000; Seiffert et al., 2000). No interaction between the inhibitors and the holoprotein/ full length form of PS1 was detected (Li et al., 2000). This indicates that γ -secretase inhibitors could selectively block γ -secretase dependent functions of PS1, whilst leaving the PS1 holoprotein function or γ -secretase independent functions of presenilin unchanged. γ -secretase inhibitors were also shown to have a similar effect on γ -secretase processing as PS1 knock-out manipulations (De Strooper et al., 1999).

1.3.2 Nicastrin, APH-1 and PEN-2: The accessory proteins of γ -secretase

As discussed in the previous section, presenilin is responsible for providing the enzymatic activity of γ -secretase. However, overexpression studies highlighted that presenilin alone may not be sufficient for γ -secretase activity. Thinakaran and colleagues (1997) found that overexpression of human PS1 could replace endogenous presenilin in both neuroblastoma cell lines and neuronal cultures and the amount of PS1 N and C terminal heterodimeric fragments was not increased despite the overexpression of PS1 protein (Thinakaran et al., 1997). Together these results indicate that there are certain limiting elements that prevent excess γ -secretase complex generation. Experimental evidence showed that nicastrin, APH-1 and PEN-2 could interact with presenilin and the interaction was important for γ -secretase processing of substrates, Notch and APP (Edbauer et al., 2002; Francis et al., 2002;

Goutte et al., 2002; Yu et al., 2000b). These results have strongly suggested that presenilin, nicastrin, APH-1 and PEN-2 are the core components of γ -secretase. Reconstitution experiments in yeast, *Saccharomyces cerevisiae*, provided confirmation of this hypothesis. *Saccharomyces cerevisiae* is deficient in endogenous γ -secretase activity but overexpression of exogenous presenilin, nicastrin, APH-1 and PEN-2 together are sufficient for the generation of γ -secretase activity (Edbauer et al., 2003). This study also confirmed the results of Thinakaran and colleagues by showing that γ -secretase activity could not be reconstituted by overexpression of wild type presenilin alone. Indeed, co-expression of any three components proved insufficient to generate γ -secretase activity (Edbauer et al., 2003). Other studies from Chinese hamster ovary (CHO) cells (Kimberly et al., 2003) and *Drosophila* S2 cells (Takasugi et al., 2003) confirmed that overexpression of presenilin-1, nicastrin, APH-1 and PEN-2 could reconstitute γ -secretase activity in mammalian cells. This data shows that nicastrin, APH-1 and PEN-2 act as accessory proteins to the catalytic core of presenilin and all four components are necessary and sufficient to generate cellular γ -secretase activity.

Nicastrin is a 130kDa glycosylated type 1 single transmembrane protein involved in the recognition of γ -secretase substrates and maturation of the γ -secretase complex (Chavez-Gutierrez et al., 2008; Morais et al., 2003; Shah et al., 2005; Yu et al., 2000b). APH-1 is a seven transmembrane domain protein which provides scaffold support and stabilisation for the complex and is necessary for transport of nicastrin to the cell surface (De Strooper, 2003; Francis et al., 2002; Goutte et al., 2002; Lee et al., 2002; Niimura et al., 2005; Takasugi et al., 2003). There are three isoforms in humans; APH-1a-short, APH-1a-long and APH-1b. An additional isoform is found in rodents, APH-1c, which is duplicated from the APH-1b gene (Hebert et al., 2004). PEN-2 is a small (approximately 10-12 kDa) hairpin like protein with two transmembrane domains and proposed to play a role in the initiation of presenilin endoproteolysis and maturation of the enzyme complex (Crystal et al., 2003; Francis et al., 2002; Prokop et al., 2005; Steiner et al., 2002; Takasugi et al., 2003).

The identification of the different isoforms of presenilin and APH-1 suggest that theoretically there are several possible combinations of γ -secretase complexes that can be generated. Biochemical analysis reveals that different isoforms of presenilin

and APH-1 do not co-exist in the same γ -secretase complex suggesting that only one presenilin, APH-1, PEN-2 and nicastrin are present in each complex (Sato et al., 2007; Shirotani et al., 2004b). Currently it is unclear whether there is a preferential formation of complexes with a particular combination of presenilin or APH-1 subunits. It is also not known if different complexes are located within different subcellular compartments or if they process different substrates. Furthermore, it remains to be established if there are different complexes preferentially involved in AD pathology or normal cellular substrate processing. Interestingly, recent *in vitro* and *in vivo* studies have shown that γ -secretase complexes consisting of PS2 rather than PS1 lead to a decreased processing of APP and reduced generation of A β (Lai et al., 2003; Mastrangelo et al., 2005). This suggests that γ -secretase complexes containing PS1 may act as more potent cellular proteases than complexes containing PS2. However, most studies investigating the role of different γ -secretase components have focused on overexpression analysis in cell lines which may not reflect the levels of γ -secretase activity *in vivo*.

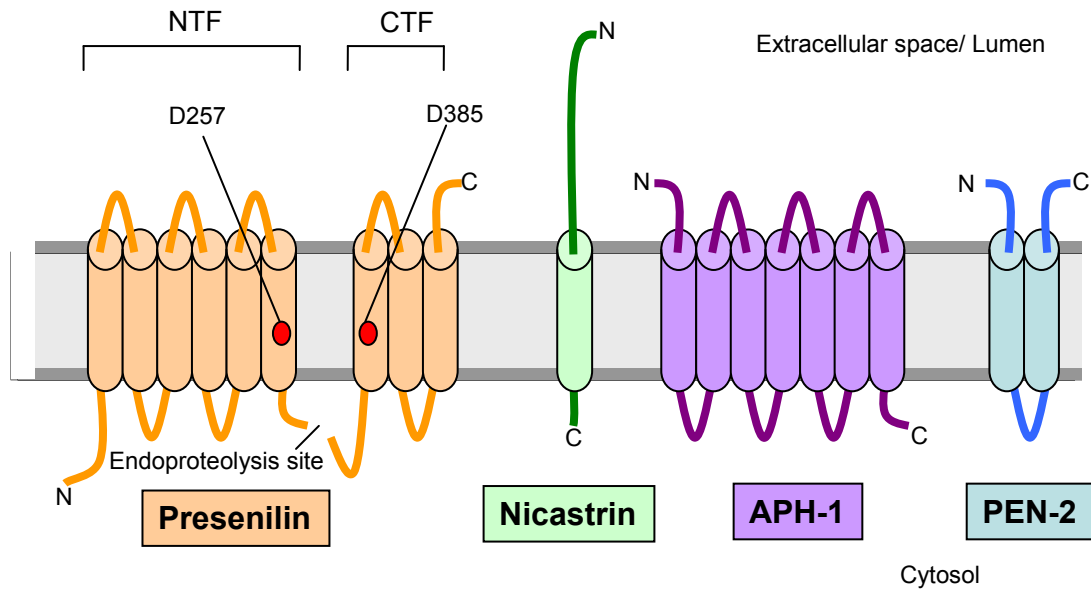


Figure 1.3 - Structure of the γ -secretase complex

The γ -secretase enzyme complex consists of four integral transmembrane proteins: presenilin, nicastrin, APH-1 and PEN-2. Presenilin (orange) is the catalytic component of the complex. The active site of presenilin is located with transmembrane regions 6 and 7 which contain two catalytic aspartate residues at sites 257 and 385. A mature (catalytically active) complex is formed upon assembly of all four components and the generation of NTF and CTF fragments by endoproteolysis of presenilin. Endoproteolysis occurs within the intracellular loop between transmembrane domains 6 and 7.

1.3.3 Formation and maturation of γ -secretase

Biochemical studies originally identified γ -secretase as components within high molecular weight protein complexes, ranging from a few hundred to over 2000 kDa (Capell et al., 1998; De Strooper et al., 1997; Gu et al., 2004; Yu et al., 1998). More recent studies from detergent purified γ -secretase complexes have indicated that the stoichiometry of the active complex, containing presenilin, nicastrin, APH-1 and PEN-2 in a 1:1:1:1 ratio with a molecular weight of 200 – 250 kDa (Li et al., 2009; Osenkowski et al., 2009; Sato et al., 2007). Formation of γ -secretase complex occurs in a highly regulated manner within the endoplasmic reticulum (ER). Current models propose that the interaction between nicastrin and APH-1 occurs first, which

is then followed by the binding of full length presenilin to this dimeric structure (Capell et al., 2003; LaVoie et al., 2003; Lee et al., 2002; Niimura et al., 2005; Shirotani et al., 2004a; Takasugi et al., 2003). The C-terminal tail of presenilin binds directly with nicastrin to form a stable trimeric complex (Kaether et al., 2004). The subsequent binding of PEN-2 to the trimeric complex stimulates endoproteolysis of presenilin to generate the active γ -secretase complex (Fraering et al., 2004a; Kim and Sisodia, 2005; Luo et al., 2003; Steiner et al., 2002; Takasugi et al., 2003; Watanabe et al., 2005). Once fully assembled, γ -secretase can leave the ER and translocate to different subcellular compartments including the endoplasmic reticulum-Golgi intermediate compartment (ERGIC), cis-Golgi, trans-Golgi, endosomes and lysosomes en route to the plasma membrane. The interaction between TM4 of presenilin (1) and TM1 of PEN-2 masks the ER-retention signals of these proteins and enables exit of the complex from the ER (Fassler et al., 2010). Any presenilin that is not incorporated into active γ -secretase complexes (the majority of presenilin is not) is eventually degraded by the proteasome (Kim et al., 1997; Kopan and Ilagan, 2004; Lai et al., 2003; Thinakaran et al., 1996; Thinakaran et al., 1997). Mature γ -secretase complexes have a half life of several days whilst unincorporated proteins have a half life of ~1-6 hrs (Dries and Yu, 2008). Figure 1.4 shows a proposed model of the steps involved in γ -secretase assembly.

A recent study has also shown that other cellular proteins are implicated in regulating the subcellular location of γ -secretase. The protein, retention in endoplasmic reticulum 1 (Rer1p) was shown to interact with the first domain of PEN-2 to maintain ER localisation of γ -secretase complex (Kaether et al., 2007). Other reports have also revealed that other factors including transmembrane trafficking protein 21 (TMP21), β -adrenergic receptor, CD147, calsenilin, pigment epithelial derived factor (PEDF) may act as modulators of γ -secretase cleavage, maturation and trafficking (Chen et al., 2006; McCarthy et al., 2009; Pardossi-Piquard et al., 2009; Spasic et al., 2007; Zhou et al., 2005). Further studies will be required to determine if other regulators of γ -secretase location exist.

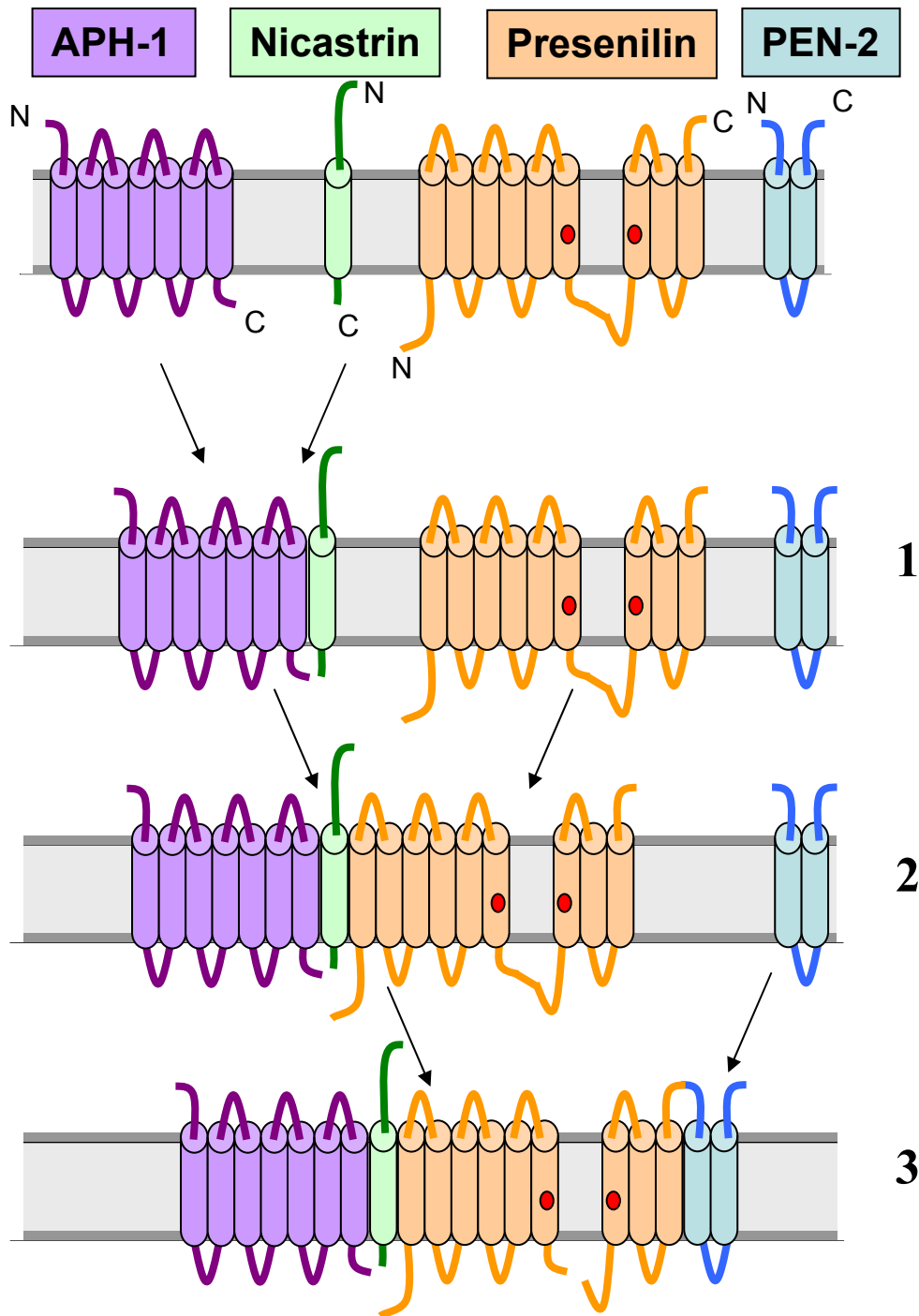


Figure 1.4 - Assembly of the γ -secretase complex

Assembly of the γ -secretase enzyme complex occurs in a stepwise manner in the ER. The first step involves APH-1 and nicastrin coming together to form a subcomplex (1). Presenilin, in its immature holoprotein form, then interacts with the APH-1 and nicastrin subcomplex to generate a trimeric complex (2). Finally PEN-2 binds to the presenilin, nicastrin and APH-1 complex to generate the fully assembled γ -secretase complex (3). Endoproteolysis of the large intracellular loop (between transmembrane 6 and 7) of presenilin generates the N and C-terminal fragments of presenilin, which gives rise to the mature, catalytically active form of γ -secretase.

1.3.4 Subcellular localisation of γ -secretase components

The subcellular localisation of γ -secretase has been under intense study over the last two decades. PS1 and PS2, nicastrin, APH-1, and PEN-2 were all initially reported to be predominately located within the ER and Golgi, but also in lysosomes, and endosomes (Annaert et al., 1999; Kim et al., 2000; Kovacs et al., 1996; Lah and Levey, 2000; Lee et al., 1996; Rechards et al., 2003). However, other studies using surface biotinylation, immunofluorescence and immunoelectron techniques showed that small quantities of PS1, nicastrin, APH-1 and PEN-2 could be located near/ at the plasma membrane (Chyung et al., 2005; Hansson et al., 2005; Kaether et al., 2002; Lah et al., 1997; Ray et al., 1999). These findings are consistent with an ultrastructural immunogold electron microscopy study which showed that PS1 could be associated to the plasma membrane, ER, endosomes, nuclear membrane, Golgi and post-Golgi membranes (Rechards et al., 2003).

These studies indicate that γ -secretase can be found throughout the secretory pathway and in many subcellular compartments but with the majority being located within the ER. Zhang et al., (1998) found using subcellular fractionation methods that exogenously transfected presenilin holoprotein was localised in the ER whilst PS NTF and CTF fragments were localised to the Golgi (Zhang et al., 1998a). Annaert et al., (1999) analysed PS1 wild type neurons and showed that endogenous uncleaved PS holoproteins were associated with the nuclear envelope whilst PS NTF and CTF fragments were associated with post ER membranes and the intermediate compartment but not downstream of the cis-Golgi (Annaert et al., 1999). These studies are in line with the notion that export from the ER involves the endoproteolysis of presenilin holoprotein, probably at the ER, to generate the catalytically active NTF and CTF fragments of presenilin which can then exit the ER. The localisation of γ -secretase can also be altered throughout development. The majority of γ -secretase components are found outside lipid rafts during embryonic stages which then translocate to lipid raft rich regions during postnatal stages (Vetrivel et al., 2005; Vetrivel et al., 2004). It is not clear if this switch is a regulatory mechanism that enables different substrates to be cleaved by γ -secretase during different stages in development.

PS1 and PS2 are found in CNS neurons and glial cells as well as in other tissue including muscle, lung and spleen (Lah et al., 1997; Lee et al., 1996). Hippocampal and cortical pyramidal neurons have particularly high expression levels of PS1 (Page et al., 1996). Recent immunofluorescence study has shown that PS1 exhibits good co-localisation to Homer and Bassoon suggesting that it is found at mature synapses in rat dissociated culture systems (Inoue et al., 2009). In mature mouse hippocampal neurons immunofluorescence labelling has shown strong co-localisation between PS1 and MAP2 indicating its presence in dendritic regions. Moreover, the PS1 signal is also strong in the cell body and axons, where the staining pattern is similar to presynaptic puncta labelling (Cook et al., 1996; Fraser et al., 2000; Lah et al., 1997). A study using immunolabelling methods for electron microscopy showed that PS1 is located at the postsynaptic density of spines and also some synaptic vesicles in the presynaptic bouton of neurons (Lah et al., 1997). Other reports have also found that PS1 is associated with synaptic vesicles, dense core vesicles, somatodendritic clathrin-coated vesicles, synaptic adhesion sites and neuronal growth cones (Behr et al., 1999; Efthimiopoulos et al., 1998; Frykman et al., 2010; Thinakaran and Parent, 2004). However, a separate study showed no colocalisation between PS1 and the synaptic vesicle marker synaptobrevin, and also a lack of punctate staining in hippocampal axons (Annaert et al., 1999).

1.3.5 Subcellular location of γ -secretase activity

Despite the high levels of γ -secretase components in the ER, it is not clear if this subcellular compartment is the main site of γ -secretase processing in the cell. Processing of certain substrates including APP and Notch by γ -secretase is understood to take place in compartments located downstream of the ER, most probably at or near the cell surface (Cupers et al., 2001; Koo and Squazzo, 1994; Sisodia et al., 2001). However, the majority of the studies examining the location of presenilin has focused mainly on the site of protein expression and assume that its expression is correlated with γ -secretase activity. One issue with this assumption is that only a limited amount of synthesised PS is incorporated into active γ -secretase complexes suggesting that expression may not be a good indicator of activity (Dries

and Yu, 2008; Lai et al., 2003; McCarthy et al., 2009). More recent biochemical studies using biotin surface labelling have shown that γ -secretase activity is found on the plasma membrane of HeLa and CHO cells suggesting that active γ -secretase complexes can reside at the cell surface. Quantitative western blot analysis indicated that approximately 6% of γ -secretase protein (PS1 NTF) is found on the cell surface (Chyung et al., 2005). Furthermore, γ -secretase cleavage assays also showed that the surface population of γ -secretase accounts for 6.1% of the total cellular γ -secretase activity (Chyung et al., 2005). This study suggests that a small but significant amount of active γ -secretase can be isolated from the cell membrane, consistent with the role of PS1 in cleaving cell surface proteins such as APP, Notch, and cadherins. It is currently unclear which intracellular compartments may provide the majority of the cellular γ -secretase activity.

An elegant study by Kaether and colleagues (2006) tried to tackle this question by engineering a green fluorescent protein (GFP) tagged version of the γ -secretase substrate β -CTF (GFP- β -CTF) (the membrane associated fragment that remains after β -secretase cleavage of APP), which upon cleavage by γ -secretase, gives rise to two protein fragments, A β peptide and GFP tagged AICD (GFP-AICD) (Kaether et al., 2006a; Kaether et al., 2006b). GFP-AICD fragments are not membrane associated and diffuse within the intracellular milieu upon generation. Visualisation of diffuse cytoplasmic GFP signal is a positive sign of GFP-AICD production by γ -secretase cleavage of GFP- β -CTF. However blocking GFP- β -CTF processing using a specific γ -secretase inhibitor, DAPT causes the GFP component to remain associated with the intracellular membrane compartment. Hence the GFP signal between γ -secretase processed (diffuse) and γ -secretase unprocessed (membrane associated) β -CTF can be readily distinguished. By inhibiting the traffic of GFP- β -CTF through different subcellular compartments in the secretory pathway, the sites of γ -secretase activity can be assessed. If γ -secretase activity is present in a subcellular compartment where transport has been blocked, then the GFP signal would be cytoplasmic and diffuse. On the other hand if γ -secretase activity is not present at a particular subcellular compartment then the GFP signal would be membrane associated and highlight the intracellular compartment where γ -secretase cleavage is absent. Inhibition of transport from the ER (using Brefeldin A), Trans Golgi Network (TGN) (using a 20°C temperature block) and Golgi (using monensin) resulted in membrane

associated GFP- β -CTF signal suggesting that there is no γ -secretase activity in these subcellular compartments. The only cellular region where diffuse GFP signal was observed was at the plasma membrane. This study shows that the ER, TGN and Golgi are not sites of γ -secretase cleavage whereas the plasma membrane is a site of γ -secretase activity (Kaether et al., 2006b). This study highlights the discrepancy between subcellular location of γ -secretase components and the site of γ -secretase activity. Other subcellular compartments where γ -secretase activity had been previously reported such as endosomes and lysosomes were not tested in this study (Chen et al., 2000; Koo and Squazzo, 1994; Vetrivel et al., 2004). Recent subcellular fractionation studies showed that γ -secretase activity can be found in synaptic membrane, synaptic vesicle and endosomal fractions (Frykman et al., 2010). Further studies will be required to determine if there are other intracellular sites of γ -secretase activity. Additionally, it will be important to identify whether different substrates are cleaved at different subcellular sites within neurons.

γ -secretase inhibitors have also been shown to influence presenilin localisation. Application of cell permeable inhibitors L-685,458 (also known as inhibitor X) or compound E, led to an elevation of cell surface PS1 and PEN-2 by enhancing the translocation step from the Golgi and TGN to the plasma membrane (Wang et al., 2004). This result suggests that inhibition of γ -secretase activity may modulate expression of γ -secretase components at the plasma membrane. Interestingly a cell impermeable γ -secretase inhibitor, MRL631, that could block Notch processing (presumably at the cell surface) by γ -secretase, did not alter expression of surface presenilin 1 suggesting that intracellular but not extracellular γ -secretase activity was required for the trafficking of PS1 to the cell surface (Wang et al., 2004).

1.3.6 γ -secretase and regulated intramembrane proteolysis of transmembrane substrates

γ -secretase is a unique protease, not only because it is a multi component complex but because the proteolytic cleavage occurs within the transmembrane region of its substrates, a process termed regulated intramembrane proteolysis (RIP). Because of this property, γ -secretase is classified as a member of the intramembrane cleaving protease (I-Clip) family which includes serine protease rhomboid, signal peptide peptidase (SPP) and metalloprotease S2P (Beel and Sanders, 2008; Kopan and Ilagan, 2004; Steiner and Haass, 2000; Wolfe and Kopan, 2004). Transition state inhibitors have shown that substrates interact with presenilin rather than with other γ -secretase components (Kornilova et al., 2005), however it has remained unclear how presenilin could hydrolyse the peptide-bonds of substrates within the hydrophobic lipid environment of membranes. Annaert and colleagues indicate that presenilin maintains a ring like structure that enables substrates to interact with the active zone of presenilin (Annaert et al., 2001). Recent reports using negative stain and cryo electron microscopy have revealed greater insights into the structure of presenilin. Using protein obtained from cultured cells, presenilin was found to have a spherical structure of approximately 10 nm in diameter with an internal compartment which enabled water molecules to enter and aid intramembrane proteolysis (Lazarov et al., 2006; Ogura et al., 2006; Osenkowski et al., 2009). The water cavity was located within TM 6 and 7, which contains the active zone region and the aspartate residues required for γ -secretase activity (Sato et al., 2006; Tolia et al., 2006). Hence this cavity contains the necessary elements for RIP.

Nearly all substrates of γ -secretase are type 1 transmembrane proteins with an extracellular region comprised of less than 300 amino acids (Annaert and De Strooper, 2002; Struhl and Adachi, 2000). The truncated extracellular region is generated by pre-processing of the extracellular domain by other cellular proteases such as α and β secretase to induce the release of the ectodomain. Truncated substrates initially bind to the γ -secretase complex at a site near the presenilin active zone prior to undergoing RIP (Kornilova et al., 2005). Surprisingly the substrates do

not appear to have any shared sequence motif (Annaert and De Strooper, 2002; Struhl and Adachi, 2000).

γ -secretase can perform RIP at three different sites within the transmembrane region of substrates, known as the γ , ζ and ϵ -sites. The ϵ -site is located closest to the intracellular C-terminal region of the membrane. Cleavage at this site gives rise to intracellular fragments such as AICD and NICD from APP and Notch respectively (see Ebinu and Yankner, 2002; Gu et al., 2001; McCarthy et al., 2009; Weidemann et al., 2002; Wolfe and Guenette, 2007). The ζ -site is located 3 amino acids closer to the N-terminus from the ϵ -site and the γ site is located 3 amino acids up from the ζ -site and closest to the N-terminus/ extracellular region (see Steiner et al., 2008). For APP, it is cleavage at the γ -site that is necessary for generating $A\beta_{40}$ and $A\beta_{42}$, the major $A\beta$ peptides released during physiological conditions and AD pathogenesis, respectively (Brouwers et al., 2008). The presence of three different sites for RIP explains the heterogeneity of peptide fragments generated by γ -secretase cleavage, and why a range of different $A\beta$ fragment sizes are generated from APP. It is currently unclear if all substrates are cleaved at all three sites like in the case of APP or if there is preferential cleavage at a particular site (s).

Understanding the mechanisms and components involved in the regulation of γ -secretase activity will hopefully provide insights and enable the design of effective therapeutic strategies for treatment of AD. One recent report showed that siRNA knock down of the accessory cargo protein TMP21 could selectively enhance cleavage at γ -sites whilst leaving ϵ -cleavage sites undisturbed. This means that TMP21 could selectively modulate $A\beta$ production whilst leaving NICD and AICD generation (and associated nuclear signalling pathways) from Notch and APP respectively intact (Chen et al., 2006). Further research is required to determine if there are other regulators of γ -secretase cleavage at specific sites.

1.4 Other cellular secretases

In addition to γ -secretase, the roles of two other cellular secretases have also been heavily investigated in recent years. The main reason for the interest in α and β secretase, like γ -secretase, comes from their well documented involvement in the cleavage of APP and the generation of A β (Lammich et al., 1999; Vassar et al., 1999). As already discussed, both α and β secretase process APP prior to γ -secretase cleavage, to generate APP C-terminal fragments which act as substrates for γ -secretase. Cleavage of APP by α and β secretase, gives rise to the N-terminus of p3 and A β , respectively. The next section provides a brief overview of the properties of α and β secretase.

1.4.1 α -secretase

The molecular identity of the component(s) which underlies α -secretase cleavage of APP remains to be fully resolved. Studies suggest that the enzymatic activity is attributed to several different candidates including members of a disintegrin and metalloprotease family (ADAM) such as ADAM 10, ADAM 9, ADAM 19, ADAM 17 (also known as tumour necrosis factor- α converting enzyme (TACE)) (Allinson et al., 2003; Asai et al., 2003; Buxbaum et al., 1998b; Kojro and Fahrenholz, 2005; Lammich et al., 1999; Parvathy et al., 1998). Many members of the ADAM family of proteins contain a cysteine-rich disintegrin domain, a pro-domain, a transmembrane domain, a cytoplasmic tail, and a metalloproteinase domain which contains the HEXGHXXGXXHD consensus sequence (Endres and Fahrenholz, 2010; Parkin et al., 2004). The catalytic activity of ADAM proteins derives from the metalloproteinase domain whilst the pro-domain is important for maintaining the correct structural organisation. As suggested by the name, the disintegrin domain is important for interaction with extracellular matrix proteins, integrins, and the cysteine residues may be required for interactions with other substrates (Parkin et al., 2004). Currently it is not known what contribution each of these proteins provides to

total cellular α -secretase activity. However as multiple proteins are potentially implicated, designing specific inhibitors has been particularly challenging. Studies have shown that cleavage of APP by α -secretase takes place at the plasma membrane of neurons (Parvathy et al., 1999). In addition to processing of APP, other α -secretase substrates have also been identified and include prion protein PrP, ephrins, N-cadherin, Notch, tumour necrosis factor- α , transforming growth factor- α and APLP2 (see Endres and Fahrenholz, 2010; Pruessmeyer and Ludwig, 2009). Like substrates of γ -secretase, there is also a lack of sequence homology amongst α -secretase substrates. The main similarity between different α -secretase substrates is the presence of a α -helix structure close to enzymatic cleavage site, which is approximately 12-16 amino acids from the plasma membrane (Sahasrabudhe et al., 1993; Sisodia, 1992).

1.4.2 β -secretase

The identity of β -secretase is better understood than that of α -secretase. Over a decade ago, multiple labs independently reported using different techniques the cloning of the enzyme underlying β -secretase activity, beta site APP-cleaving enzyme 1 (BACE-1) (but also known as aspartyl protease 2 (Asp2) and membrane-anchored protease of the pepsin family (memapsin 2) (Cai et al., 2001; Hussain et al., 1999; Lin et al., 2000; Sinha et al., 1999; Vassar et al., 1999; Yan et al., 1999). BACE1 is a type 1 transmembrane aspartyl protease of 501 amino acids in length and contains a N-terminus signal peptide (amino acids residues (a.a) 1-12), a preprotein domain (a.a 22-45), a catalytic domain (a.a 45-459), 2 conserved aspartic protease motifs (DTGS at residues 93-96 and DSGT at a.a 289-292) and a C-terminal extension with a transmembrane domain (a.a. 460-477) and a cytoplasmic tail (Selkoe and Schenk, 2003). BACE1 is predominately expressed in neurons and whilst its subcellular localisation is still under debate, reports have shown that BACE1 is located in early endosomes and the trans-Golgi network, cellular compartments that provide the more acidic environment proposed to be required for optimal β -secretase activity (Laird et al., 2005; Vassar, 2004). Knock-out mice studies have shown that β -secretase cleavage is involved in APP processing.

Crossing BACE-1 knockout animals with mutant transgenic mice overexpressing APP lead to an absence of A β generation, providing unequivocal evidence that BACE-1 is necessary for A β production (Luo et al., 2001). Unlike γ -secretase knock-out mice, BACE1 knock-out mice are viable and exhibit normal behaviour (Cai et al., 2001; Luo et al., 2001; Roberds et al., 2001). BACE-1 is also implicated in the cleavage of a wide range of membrane associated proteins including neuregulin-1 (NRG-1), neuregulin-3 (NRG-3), voltage-gated sodium channel β 2 subunit (SCN β 2), P-selectin glycoprotein ligand-1 (PSGL-1) and sialyl transferase ST6Gal (see for review: De Strooper et al., 2010). Genetic screens have also identified a homologue of BACE-1, BACE-2 which shares 68% sequence similarity (Bennett et al., 2000; Solans et al., 2000; Yan et al., 1999). Expression of BACE-2 in the CNS is low and may not provide a major contribution to β -secretase activity in the brain (Bennett et al., 2000; Solans et al., 2000; Yan et al., 2001).

1.5 Cellular functions of γ -secretase

In addition to presenilins role in AD, studies have also shown that presenilins and associated γ -secretase activity is important for modulating different cellular functions. γ -secretase is a promiscuous cellular protease which can cleave a wide range of substrates associated with many different cellular processes including trafficking, signal transduction, cell adhesion, calcium homeostasis, apoptosis and synapse function (Beel and Sanders, 2008; Hass et al., 2009; McCarthy et al., 2009; Parks and Curtis, 2007; Vetrivel et al., 2006; Wakabayashi and De Strooper., 2008). Table 1.1 shows a summary of substrates and protein interactors of γ -secretase and proposed signalling processes. Additionally, not only can γ -secretase cleavage of substrates directly alter signalling pathways, but intracellular domain fragments such as NICD from Notch, AICD from APP and CICD from cadherins may also play a role in membrane to nuclear signalling pathways (see McCarthy et al., 2009). With the wide range of substrates and the presence of multiple γ -secretase cleavage sites, understanding the biology of presenilin and γ -secretase seems complex. Many of the substrates listed were identified using *in vitro* biochemical methods and the functional physiological significance of most of these interactions in neuronal systems remains to be shown. The following section will discuss the role of a few selected γ -secretase substrates and their proposed cellular functions.

Table 1.1: γ -secretase interacting proteins or substrates and proposed cellular functions of presenilin association

	Cell adhesion, synaptic connections	Synaptogenesis, neurite outgrowth, differentiation	Calcium regulation	Trafficking/ transport	Cell signalling/ development/ Gene transcription	Plasticity/ synaptic transmission	Receptor tyrosine kinase	Other functions
APLP-1 + 2	X	X			X			
ApoER2					X			Lipoprotein receptor
APP	X	X		X	X	X		
β -catenin	X	X			X	X		
Cadherin (E+N)	X				X	X		
Calsenilin			X					
CD43 + 44	X				X			
CSF-1R		X					X	
DCC		X			X			Netrin-1 receptor
Delta		X			X			Notch pathway ligand
Ephrin-B1, B2		X						Eph receptor ligands
ErbB4					X		X	Apoptosis
γ -protocadherins	X				X			
GluA3						X		Glutamate receptor subunit
Insulin receptor					X		X	
Jagged		X			X			Notch pathway ligand
LAR	X	X						Receptor protein tyrosine phosphatase
LRP1					X			Endocytosis
Megalin/ LRP2					X			LDL receptor
Nectin-1 α	X	X						Notch pathway ligand
Notch					X			Notch receptor
NRADD								Apoptosis
NRG-1		X			X			CNS development
p75 ^{NTR}		X			X			Neurotrophin receptor
SCN β 2	X							Migration regulator
SorLA, Sortilin				X	X			Sorting receptors
Sorcin			X					
Syntaxin 1A + 5				X				

The table was adapted from information from the following reviews: McCarthy et al., 2009; Parks and Curtis, 2007; Vetrivel et al., 2006; Wakabayashi and De Strooper., 2008. See reviews for original references. Abbreviations: APLP, amyloid precursor-like protein; ApoER2, apolipoprotein E receptor-2; APP, amyloid precursor protein; CSF-1R, colony-stimulating factor 1 receptor; DCC, deleted in colorectal cancer; GluA3, glutamate receptor subunit 3; LAR, leukocyte-common antigen related; LRP, low density lipoprotein receptor-related protein; NRADD, neurotrophin receptor alike death domain protein; NRG-1, neuregulin-1; p75^{NTR}, p75 neurotrophin receptor; SCN β 2, sodium channel subunit β 2.

1.5.1 Nuclear signalling and developmental regulation by Notch/NICD and other γ -secretase associated transcriptional regulators

Numerous studies have established that PS1 is implicated in the proteolytic cleavage of Notch. Notch is a type 1 integral transmembrane protein with an N-terminus domain which contains extracellular calcium binding Notch/ Lin12 regions and epidermal growth factor (EGF) repeats. The C-terminal intracellular tail contains tandem ankyrin domains and a PEST domain (Fortini, 2002).

Notch is predominantly located on the cell surface following its initial production in the ER and transport to the plasma membrane. During the passage to the cell surface, Notch is processed in the trans-Golgi region by a member of the furin family to produce two closely associated fragments, which is the mature form of Notch. Once at the cell surface, Notch interacts with Notch ligands, members of the Delta/Serrate/Lag-2 family including Delta and Jagged which are located on adjacent cells. Ligand binding to Notch acts as a trigger for two subsequent proteolysis reactions. Firstly, α -secretase cleavage by a disintegrin and metalloprotease domain family protein gives rise to an intramembrane and an ectodomain fragment. Secondly, whilst the ectodomain fragment gets released extracellularly, the intramembrane domain undergoes γ -secretase processing to generate a cytoplasmic protein, Notch intracellular domain (NICD). Upon generation, NICD traffics to the nucleus to interact with the Rel-family transcription factor, C-promoter-binding factor (CBF1 in mammals; *Drosophila* equivalent is Suppressor of hairless (Su-H));

C. elegans equivalent is LAG-1) and activate gene transcription (Chan and Jan, 1999; Louvi and Artavanis-Tsakonas, 2006; Schroeter et al., 1998). NICD is believed to play a role in a range of cell functions including regulating nuclear signal transduction, cell fate and development (Bray, 2006; De Strooper et al., 1999; Fortini, 2002; Mumm et al., 2000; Mumm and Kopan, 2000; Struhl and Greenwald, 1999; Ye et al., 1999).

Strong evidence that the presenilins were involved in Notch signalling came from knock-out mice studies. Western blot analysis and pulse chase experiments showed that NICD production was essentially absent from PS1 knock-out neurons (De Strooper et al., 1999). Furthermore the lack of NICD production observed in PS1 knock-out cells could be mimicked by application of several γ -secretase inhibitors to wild type cells, indicating that γ -secretase activity of PS1 was specifically required for generation of NICD (De Strooper et al., 1999). Morphological analysis showed that constitutive PS1 knock-out mice (on PS2 background) exhibited severe developmental defects during late embryonic ages including disturbed somitogenesis and segmentation and impairment in axial skeletal development (De Strooper et al., 1998; Shen et al., 1997; Wong et al., 1997) which was very similar to the phenotype observed in Notch knock-out mice (Conlon et al., 1995; Swiatek et al., 1994). Interestingly, Wong et al., (1997) also showed that PS1 levels may directly influence expression levels of Notch1 and Dll1 (Notch1 ligand) mRNA which were decreased in PS1^{-/-} mice compared to control animals (Wong et al., 1997). This data suggests that the defects in embryonic development observed in PS1 mice are due to PS1 processing of Notch.

Studies in other model systems showed similar findings regarding γ -secretase processing of Notch. In *Drosophila*, when the presenilin homolog gene was inactivated, such mutants exhibited a Notch knock-out phenotype with impaired Notch nuclear signalling and morphological defects during development (Selkoe, 2000). Studies of mutant Sel-12 in *C.elegans*, which shares 50% homology with human PS1 also has defects in Notch signalling which affects oviposition (Jarriault and Greenwald, 2002). Together, these studies show that the regulation of Notch signalling by presenilins is highly conserved.

As Notch signalling is involved in regulating nuclear transcription and certain signalling cascades, blocking γ -secretase processing of Notch may generate many undesired effects and this is the main reason why γ -secretase is deemed an unsuitable pharmacological target for AD therapeutics. However, one study showed that in adult PS1 conditional knock-out brain, the expression of Notch effector genes *Hes1*, *Hes5*, and *Dll1* are no different to wild type (Yu et al., 2001). This is in contrast to studies using constitutive PS1 knock-out animals and shows Dll1 levels are reduced in the embryo (Wong et al., 1997). This suggests that potentially different regulatory mechanisms may be used in adult and embryonic development with adult Notch processing potentially not requiring PS1 activity. If so then use of γ -secretase inhibitors in adult animals may bypass the deleterious developmental effects of eliminating PS1/ γ -secretase activity in the embryo. Further studies will be required to investigate the cellular effects of differential developmental processing of Notch by γ -secretase.

Studies have also shown that ErbB4, a transmembrane receptor tyrosine kinase implicated in cell growth, proliferation and differentiation can be sequentially processed by α -secretase and γ -secretase to generate B4-ICD which can translocate to the nucleus and potentially regulate transcriptional processes (Ni et al., 2001; Sisodia and George-Hyslop, 2002; Wong et al., 1997).

1.5.2 Cell signalling and cell adhesion through β -catenin and cadherins

β -catenin is implicated in modulating a range of different cellular processes through its association with Wnt intracellular signalling cascades (De Ferrari and Inestrosa, 2000; Fraser et al., 2000). Wnts are secreted glycoprotein growth factors involved in regulating many different neuronal processes including axon guidance and regulation of neuronal and synapse morphology (Salinas and Zou, 2008). Upon binding its receptor Frizzled at the cell surface, Wnt can activate a signalling cascade which blocks glycogen-synthase-kinase-3 β (GSK-3 β) activity and limits the phosphorylation of β -catenin. This process stabilises cellular β -catenin by

preventing its degradation. Unphosphorylated β -catenin can translocate to the cell nucleus and interact with the LEF/TCF (T cell-specific transcription factor 1) transcriptional regulators which trigger activation of cyclin D1, metalloproteases and other Wnt target genes.

However, in the absence of Wnt, a separate signalling cascade is stimulated. In this instance, cytoplasmic β -catenin can be phosphorylated by GSK-3 β which promotes its interaction with Axin, adenomatous polyposis coli and β -transducing repeat-containing protein, and initiates the process of β -catenin proteasomal degradation. This process prevents β -catenin from activating Wnt target genes and subsequent nuclear signalling.

Biochemical studies have revealed that the cytoplasmic loop of presenilins can interact with β -catenin as well as other armadillo-repeat proteins including δ -catenin (Levesque et al., 1999; Murayama et al., 1998; Yu et al., 1998; Zhou et al., 1997). However, different studies have indicated that presenilin can stabilise, destabilise or have no effect on β -catenin cellular levels; calling into question the functional significance of the interaction between these two proteins on Wnt associated nuclear signalling (Hass et al., 2009; Nishimura et al., 1999; Zhang et al., 1998b). Presenilin can also interact with GSK-3 β , leading to the phosphorylation of PS1 at amino acid residues 353 and 357 which reduces the interaction between PS1 and β -catenin (Kirschenbaum et al., 2001).

Another proposed role for β -catenin is in regulating cell-cell interactions by acting as a linker molecule between cadherins, cell adhesion molecules located at the cell surface and α -catenin, an intracellular protein which interacts with the actin cytoskeleton (Goda, 2002; Okuda et al., 2007). Some evidence suggests that presenilins can be found at the plasma membrane in a complex with β -catenin and N- (neuronal, in neuronal cells) and E- (epithelial, in non-neuronal cells) cadherins (Baki et al., 2001; Georgakopoulos et al., 1999; Marambaud et al., 2002; Marambaud et al., 2003; Uemura et al., 2003). Marambaud and colleagues find that γ -secretase cleavage of E-cadherin disrupts cadherin- β -catenin interactions and initiate disassembly of the adherens junctions of fibroblasts. γ -secretase inhibitors could prevent the calcium (ionomycin) stimulated disruption of cell-cell adhesion

(Marambaud et al., 2002). This study suggests that γ -secretase may act as a negative regulator of cell adhesion through its interactions with cadherins. However, another study proposes that PS1 interaction with N-cadherin causes dissociation of p120-catenin and β -catenin from N-cadherin and enhances the interaction between N-cadherin and γ -catenin to promote synapse stabilisation and maturation in chick ciliary neurons (Rubio et al., 2005). It remains to be determined whether N-cadherin, β -catenin and PS1 interactions can modulate central synapse formation and stabilisation.

Presenilin is also involved in the processing of SCN β 2, a member of the IgCAM superfamily which may act as a cell adhesion molecule. Block of γ -secretase activity using selective γ -secretase inhibitor DAPT resulted in impaired cell-cell adhesion in Chinese hamster ovary cells overexpressing SCN β 2. This result suggests that γ -secretase processing of SCN β 2 is also important for regulation of cell-cell contacts (Kim et al., 2005).

1.5.3 γ -secretase independent forms of cellular regulation by presenilins

Recent studies have revealed that presenilins can modulate different cellular functions in a manner that is independent of its catalytic γ -secretase activity. Most studies tend to associate γ -secretase independent functions of presenilin with the “inactive” holoprotein form of presenilin (as opposed to the “active” N and C terminal fragments that occur after presenilin endoproteolysis). It is currently unclear what proportion of cellular presenilin may act in this way, but this feature of presenilins may provide a function for the population of presenilin proteins that is not incorporated in the γ -secretase complex. The role of presenilins as ER calcium leak channels is discussed below. Other γ -secretase independent actions of presenilins are extensively discussed in the following reviews (Hass et al., 2009; Selkoe and Wolfe, 2007).

1.5.4 Presenilin and regulation of intracellular calcium

Much attention has surrounded the hypothesis that changes in intracellular calcium may be an underlying factor for neuronal loss in AD (Bezprozvanny and Mattson, 2008; Green and LaFerla, 2008; Khachaturian, 1989; LaFerla, 2002; Mattson, 2010). Many FAD mutations in PS1 and PS2 have been associated not only with A β deposition but also dysregulation of intracellular calcium homeostasis (LaFerla, 2002). Indeed there are reports that show that these two factors are linked. Some studies indicate that A β peptides can elevate intracellular calcium in cultured cells, providing experimental evidence that calcium overload may be a potential mechanism for AD pathogenesis (Demuro et al., 2005; Guo et al., 1999; Mattson, 1992; Mattson et al., 1993). However, intracellular calcium is also required for a wide range of cellular processes in neurons (see for review: Berridge et al., 1999; Berridge et al., 2000; Berridge et al., 2003).

Maintenance of intracellular calcium concentration is achieved by balancing the amount of calcium entering and leaving the cell through the plasma membrane and the amount being sequestered and released from intracellular ER stores. Calcium from the extracellular milieu can enter the cell through voltage-gated calcium channels and voltage-gated ligand channels such as NMDA receptors, GluA2-lacking AMPA receptors and acetylcholine receptors located on the plasma membrane (Berridge et al., 2003; LaFerla, 2002). Conversely, calcium ATPases such as the plasma membrane calcium ATPase and sodium calcium exchanger are responsible for transporting calcium from cytoplasmic regions to the extracellular space (Strehler and Zacharias, 2001). Intracellular calcium buffers such as calretinin, calbindin and parvalbumin also help maintain basal calcium concentrations within a range of a few ten - hundreds nM (Baimbridge et al., 1992). Internal ER calcium stores actively transports calcium from the cytoplasm into the lumen of the ER through the sarco/endoplasmic reticulum calcium ATPase (SERCA) pump. Conversely, calcium is released from ER stores into the cytoplasm through inositol-1,4,5-trisphosphate receptors (IP₃R) and ryanodine receptors (RyR) located on the ER membrane. Calcium release from ER stores is important for modulating IP₃ signalling, calcium-induced calcium release (CICR) and capacitative

calcium entry (CCE), which involves opening of plasma membrane store-operated calcium channels to enable calcium influx to replenish ER calcium stores (Bojarski et al., 2008; Verkhratsky, 2002).

Existing evidence has shown that presenilins are implicated in modulating intracellular calcium homeostasis under physiological conditions and in AD (Bezprozvanny and Mattson, 2008; Bojarski et al., 2008; Green and LaFerla, 2008; Thinakaran and Parent, 2004). Transgenic mice studies have shown that presenilins can modulate calcium stores either by regulating the SERCA pump (Green et al., 2008), IP₃R (Cheung et al., 2008; Cheung et al., 2010; Stutzmann et al., 2004), RyR (Chakroborty et al., 2009; Chan et al., 2000; Lee et al., 2005; Stutzmann et al., 2007; Zhang et al., 2009), sorcin (a ryanodine binding protein) (Pack-Chung et al., 2000), calsenilin (a calcium binding protein) (Buxbaum et al., 1998a; Leissring et al., 2000) and also by acting as a passive calcium leak channel in the ER (Nelson et al., 2007; Tu et al., 2006).

By making single channel recordings from reconstituted bilayers expressing PS1 proteins, Tu et al., (2006) propose that wild type PS1 holoprotein can act directly as a low conductance calcium leak channels in the ER and thus play a role in the regulation of intracellular calcium stores (Tu et al., 2006). Overexpression of a PS1 D257A mutant lacking both γ -secretase activity and the ability to undergo endoproteolysis was still able to form a functional leak channel, providing evidence that the holoprotein form of PS1 was specifically involved (Tu et al., 2006). Leak channels could also be formed in APH-1 null cells which are deficient in active γ -secretase complexes. This report provides an insight into the role of PS1 in the ER but further experiments will be required to determine if endogenous PS1 may play a similar role in neuronal systems. Tu and colleagues (2006) also showed that FAD mutant presenilin constructs, PS1-M146V and PS2-N141I, did not have the ability to form functional leak channels leading to calcium accumulation and overload in the ER. Studies of other PS1 mutants also show similar disruptions in intracellular calcium signalling (Green et al., 2008; Lee et al., 2005). This suggests that either a dysregulation of intracellular calcium levels or calcium signalling may be a potential pathogenic mechanism in AD (LaFerla, 2002).

One recent study showed using live calcium imaging that intracellular calcium was reduced in presenilin double knock-out cells (Zhang et al., 2009). The authors found that the effect on calcium signalling could be mimicked by application of ryanodine to wild type neurons suggesting that presenilins are involved in modulating calcium release from intracellular stores. Interestingly these double knock-out animals also had impaired short and long term plasticity (paired-pulse facilitation and LTP) when presenilin 1 and 2 was eliminated from the presynaptic CA3 cell at hippocampal CA3-CA1 synapses. Together this result suggests that presenilins may modulate intracellular calcium concentration through interaction with RyR which in turn may affect synaptic plasticity. However, it is unclear whether the mechanism by which presenilin regulates intracellular calcium through RyR is dependent or independent of γ -secretase activity of presenilins, and this point will need to be addressed.

Presenilins can also regulate CCE. CCE enables depleted intracellular ER stores to be replenished by calcium influx through store-operated channels in the plasma membrane (Herms et al., 2003; LaFerla, 2002; Ris et al., 2003; Yoo et al., 2000). Studies have shown that CCE is depressed in several FAD mutations and associated with an increase in ER calcium (Smith et al., 2002; Yoo et al., 2000). Presenilin associated regulation of CCE was shown to involve both γ -secretase dependent and γ -secretase independent actions (Akbari et al., 2004). These experiments demonstrate that presenilin may modulate intracellular calcium through a wide range of possible signalling mechanisms and emphasises the need to gain a greater understanding the role of presenilin in maintaining calcium homeostasis.

1.6 The role of presenilin at the synapse

Insights into the potential role of presenilins in modulating synapse dysfunction and degeneration during AD may be gained by understanding the role of presenilins in modulating normal synapse function. Although some studies have started to investigate the functional role of presenilin during physiological states, currently there are still a lot of unknowns. This section will describe some of the main properties of synapses and provide a summary of past studies to date that have focussed on the role of presenilins in modulating synapse function.

1.6.1 The properties of a synapse

Synapse structure

The term *synapse* was originally coined by Charles Sherrington in the late 19th century (Sherrington, 1897). This term is used to describe the specialised functional intercellular connection from a presynaptic neuron onto a postsynaptic target, which in the CNS is usually another neuron. The synapse is the site at which information transfer occurs through a process known as synaptic transmission. Electron microscopy studies from the 1950's revealed the key properties that define the morphology of chemical synapses in the CNS (Cowan et al., 2001; De Robertis and Bennett, 1955; Palay, 1956; Palay and Palade, 1955). The presynaptic axonal bouton contains 10-100's of small (approximately 20-50nm diameter) vesicles containing neurotransmitter which accumulate within a region of the bouton referred to as the active zone (Harris and Sultan, 1995; Schikorski and Stevens, 1997). Studies of single release sites revealed that the number of docked vesicles, which are primed and ready for release, are variable. This typically ranges from 2-16 vesicles and is largely correlated to the size of the presynaptic bouton (Harris and Sultan, 1995). It is this pool of docked vesicles which is thought to morphologically represent the readily releasable pool (Schikorski and Stevens, 2001; Ziv and Garner, 2004).

Opposite the presynaptic bouton is the postsynaptic compartment of a synapse. The postsynaptic compartment of an excitatory synapse is easily recognised by the electron dense thickening of membrane which is often associated with an actin rich spine-like protrusion (Cowan et al., 2001). The postsynaptic compartment of an inhibitory synapse is located on the dendritic shaft and is less distinctive at the ultrastructural level as the postsynaptic thickening is often absent (Sheng and Hoogenraad, 2007). The postsynaptic membrane contains postsynaptic receptors involved in neurotransmitter reception and signal propagation. Together the intracellular actin cytoskeleton and associated scaffold proteins help maintain the structure of the postsynaptic compartment and a host of other proteins such as kinases, phosphatases and other molecules are implicated in intracellular signalling pathways (Scannevin and Huganir, 2000; Sheng and Hoogenraad, 2007).

Separating the pre and the postsynaptic compartments is the synaptic cleft. The synaptic cleft is approximately 20-24 nm in width and contains a dense matrix of proteins such as the extracellular domains of synaptic surface proteins emanating from pre and postsynaptic cells and cell adhesion molecules (Lucic et al., 2005; Zuber et al., 2005). Cell adhesion molecules are involved in formation of synapses during development and maintenance of synapse structure in mature neuronal systems (Garner et al., 2002; Scheiffele, 2003). Cell adhesion molecules can also co-ordinate structural changes in the pre and postsynaptic compartments of the synapse in response to different types of neuronal activity, hence playing a key role in modulating structural plasticity of the synapse. The proteins within the cleft also help limit the diffusion of neurotransmitter away from the cleft, enabling a higher concentration of neurotransmitter to reach the postsynaptic site (Chua et al., 2010).

Synaptic transmission

Synaptic transmission is a process that enables information transfer and communication between cells in neural networks. For fast (~100 μ s) synaptic transmission, a series of co-ordinated events must occur. Arrival of an action potential causes the membrane of the presynaptic bouton to become depolarised, leading to an influx of calcium through the opening of voltage gated calcium

channels (VGCC) located at the active zone. There are two main classes of pharmacologically definable calcium channels involved in modulating presynaptic calcium influx, P/Q ($Ca_{v2.1}$) and N ($Ca_{v2.2}$) type calcium channels relevant to fast synaptic transmission. These channels are closed at resting membrane potentials and rapidly activate upon depolarisation of the membrane. The calcium influx through VGCC causes a transient rise in local intracellular calcium in the bouton. The calcium binds to synaptotagmin I, the main calcium sensor on synaptic vesicles (Geppert et al., 1994; Xu et al., 2009) and initiates the fusion of docked vesicles to the presynaptic membrane leading to vesicle exocytosis and neurotransmitter release. The neurotransmitter diffuses across the synaptic cleft and binds receptors on the postsynaptic neuron.

There are two main classes of postsynaptic receptors; ionotropic and metabotropic receptors. As implied by the name, ionotropic receptors are ion channels. Glutamatergic ionotropic receptors are non selective cation channels which enable conductance of potassium, sodium, and calcium ions, leading to cell depolarisation. GABAergic ionotropic receptors are ion channels that enable the passage of chloride ions and causes cell hyperpolarisation. Metabotropic receptors are ligand activated G-protein coupled receptors which can indirectly associate with certain ion channels through intracellular second messenger signalling pathways. It is generally accepted that the major excitatory neurotransmitter in the hippocampus is glutamic acid (glutamate) and the major inhibitory neurotransmitter is gamma-aminobutyric acid (GABA) (Sheng and Hoogenraad, 2007).

Normal synaptic release of glutamate from excitatory boutons typically activates the α -amino-3-hydroxy-5-methyl-isoxazole-4-propionic acid (AMPA) and N-methyl-D-aspartic acid (NMDA) ionotropic glutamate receptors (Andersen et al., 2007). Whereas stronger, high frequency stimuli is required for activation of metabotropic glutamate (1) receptors which are perisynaptically located (Batchelor and Garthwaite, 1997; Baude et al., 1993). Under certain situations, glutamate can also spill-over and activate receptors on adjacent synapses (Kullmann and Asztely, 1998) or act on presynaptic autoreceptors.

AMPA receptors are homo or hetero oligomers composed of GluA1-4 subunits (Hollmann et al., 1989; Hollmann and Heinemann, 1994; Madden, 2002). GluA1-2 and GluA2-3 subunit arrangements are believed to be the most common combinations of AMPA receptors in the hippocampus (Wenthold et al., 1996). The binding of glutamate to AMPA receptor subunits leads to activation of the ion channel and the generation of an inward excitatory postsynaptic current (EPSC). The kinetics of channel opening is very quick which gives rise to an EPSC with a fast rise time (a few hundred μ sec). The EPSC depolarises the postsynaptic membrane. An action potential can be generated if a large EPSP is formed or if multiple EPSPs summate to depolarise the cell beyond the threshold for action potential generation. Synaptic transmission during resting conditions mainly involves the AMPA receptor. However, membrane depolarisation, for example by activation of AMPA receptors, can aid activation of the NMDA receptor (Andersen et al., 2007).

NMDA receptors are heteromeric complexes consisting of NR1 and NR2A-D subunits (Cull-Candy et al., 2001; McBain and Mayer, 1994). The NMDA receptor is unique in that it requires two agonists for ligand associated receptor activation. NR2 subunits contain the glutamate binding site and the co-agonist glycine or D-serine binds to NR1 subunits. NMDA receptors are activated by a slightly different mechanism to AMPA receptors. For activation not only do both ligand binding sites on the NR1 and NR2 subunits need to be occupied but membrane depolarisation is also required, meaning these receptors are also voltage activated.

The pore of NMDA receptors is blocked by a magnesium ion at resting membrane potentials (Nowak et al., 1984). It is this magnesium block that prevents the entry of ions through the NMDA receptor ion channel during basal conditions, such that the NMDA receptor does not significantly contribute to the postsynaptic current at resting membrane potentials. However, depolarisation of the membrane by either activation of AMPA receptors or back propagating actions potentials enables the magnesium block to be released from the pore, allowing the influx of calcium ions and generation of a cation current. The current generated through the NMDA receptor is much slower than that of AMPA currents, lasting up to a few hundred milliseconds. This is because glutamate dissociates from the NR2 subunit fairly slowly and the receptor is therefore in the activated state for a relatively long period

of time. NMDA receptors are also considered coincidence detectors as both presynaptic release and postsynaptic membrane depolarisation are needed for their activation. NMDA receptors are highly permeable to calcium and provide a means for calcium entry in the cell. Postsynaptic calcium influx is a necessary step in the activation of many different calcium dependent signalling cascades such as activation of calcium/calmodulin dependent protein kinase (CaMKII), a serine/threonine protein kinase implicated in the induction of a form of synaptic plasticity known as long term potentiation (LTP) (Silva et al., 1992). Studies showed that it is the NR2B containing NMDA receptors that are important for LTP, as this subunit binds to α -CaMKII with higher affinity than NR2A subunit (Barria and Malinow, 2005). This was further clarified through genetic inhibition of NR2B which led to impairment in LTP and contextual fear conditioning (Zhao et al., 2005).

GABA_A receptors are heteropentameric assemblies composed of a combination of subunits (which include α , β , γ , δ , ϵ , θ and π) arranged to form a chloride permeable ion channel (though some bicarbonate ions can also pass) (Mohler et al., 2005). In the adult hippocampus, GABA_A receptors are predominately found postsynaptically. Ligand-activation of GABA_A receptors leads to an increase in chloride conductance, which gives rise to an inhibitory postsynaptic current and contributes to cell hyperpolarisation. Hyperpolarisation of the cell has an inhibitory effect on cell excitability by setting the membrane potential further from the action potential generation threshold.

Studies from Bernard Katz and colleagues identified the quantal nature of synaptic transmission from experiments conducted at the frog neuromuscular junction (NMJ) where the presynaptic terminal of a motoneuron contacts a postsynaptic muscle cell. Through intracellular recordings from the muscle endplate, Katz and colleagues revealed that end plate potentials (EPPs) can be evoked by stimulation of the presynaptic motoneuron. However, a second population of end plate potentials was also observed in the absence of stimulation and termed miniature depolarising EPPs (mEPPs). mEPPs were similar in waveform to evoked EPPs but smaller and more uniform in amplitude. These mEPPs corresponded to the postsynaptic response to the stochastic release of a single “packet” (vesicle) of neurotransmitter called quantum from the presynaptic terminal in an action potential/ stimuli independent

manner (Del Castillo and Katz, 1954a; Del Castillo J. and Katz, 1954b; Fatt and Katz, 1952). This result indicates that neurotransmitter release not only occurs in a synchronous manner with action potential stimulation but also in a spontaneous manner in the absence of action potentials. Quantal analysis revealed that the size of evoked/stimulated postsynaptic responses can vary from trial to trail and these fluctuations are associated with the number of quanta released. This proposes that a mEPP is the postsynaptic response to the smallest unit of neurotransmitter release, a quantum, and the size of evoked EPP is linked to the number of quanta released (Andersen et al., 2007). Hence it is possible to examine the efficacy of a synaptic connection by examining the quantal parameters: the number of active release sites (n), the release probability of a connection (pr) and the quantal size (amplitude of the postsynaptic response following release of neurotransmitter from a single synaptic vesicle) (q) (Branco and Staras, 2009; Cowan et al., 2001; Kerchner and Nicoll, 2008). By studying these quantal parameters it may be possible to get an understanding of the relative changes in pre and postsynaptic function. An alteration in n and/or pr is associated with a change in presynaptic quantal release and q being associated with the number and quality of postsynaptic receptors. By examining these parameters it is possible to locate the pre and/ or postsynaptic factors that contribute to the change in synaptic efficacy. Later studies also found that quantal synaptic transmission could also occur in the CNS with largely similar properties to the NMJ (Auger and Marty, 2000; Lisman et al., 2007).

Synapse number

The number of synaptic contacts on a neuron is controlled by the dynamic formation and elimination of synapses. Both processes can occur not only during development but also in mature systems to help refine neural networks. Synapse structure and number can also be regulated by neuronal activity (Goda and Davis, 2003). CNS neurons often extend long axons which make multiple *en passant* synapses onto postsynaptic dendrites. Molecular components of the presynaptic release machinery such as syntaxin and SNAP25 are ideally positioned along the length of the axonal process to enable recruitment to synapses during formation of new boutons (Ziv and

Garner, 2004). Current models suggest that the formation of new contacts at central synapses can be initiated by the release of secreted factors, including Wnts and neurotrophins such as brain-derived neurotrophic factor (BDNF) (Goda and Davis, 2003). Contact between processes/ filopodia from the postsynaptic dendrite with the presynaptic axon can lead to establishment of new synapses (Garner et al., 2002; Goda and Davis, 2003; Ziv and Garner, 2004). Studies have indicated that pre and postsynaptic compartments can assemble simultaneously to form a synaptic contact (Okabe et al., 2001). The presence of low numbers of synaptic vesicles in an ill-defined presynaptic bouton which often lacks mitochondria are signs of an early or immature synapse (Ziv and Garner, 2004). Whereas a more established synapse is more readily recognised by the presence of docked vesicles, a large reserve pool of presynaptic vesicles in a structurally well defined bouton on the presynaptic axon. Maturation of the postsynaptic compartment is associated with the presence of postsynaptic receptors such as NMDA and AMPA receptors and postsynaptic density (PSD)-95 and scaffold proteins.

To decrease synapse number, processes relating to synapse disassembly (where single contacts between two neurons are eliminated) and input elimination (where all contacts between two neurons are eliminated) are involved (Goda and Davis, 2003). The mechanisms regarding synapse elimination are poorly defined but are believed to be driven by the postsynaptic cell. Live imaging studies have revealed that spine morphological changes and retraction may indicate early stages of synapse elimination. These morphological changes in postsynaptic structure are associated with changes in the actin cytoskeleton which can be regulated by activity and different intracellular signalling pathways (see Goda and Davis, 2003 for extensive discussion). Overall, the dynamic regulation of synapse formation and elimination is necessary for the maintenance of synapse number.

Recent studies have also indicated that presynaptic vesicles are highly mobile and can split from existing mature synapses and traffic in anterograde and retrograde directions to other boutons along the same axon. These mobile vesicles can functionally incorporate into existing synapses and undergo stimulated synaptic release (Darcy et al., 2006; Staras et al., 2010). Interestingly, studies have also indicated that these mobile vesicles can form orphan release sites where synaptic

release occurs in the absence of a postsynaptic target (Krueger et al., 2003; Staras et al., 2010). These studies suggest that mobile vesicles may be involved in maintaining the presynaptic vesicle pools of existing synapses but may also be implicated in the formation of new synapses in mature neuronal networks. Though not yet tested, the loss of synaptic vesicles from presynaptic terminals could potentially be an early marker of synapse elimination. Therefore, conceptually, synapse vesicle movement may be implicated in both synapse formation and elimination.

However, the molecular mechanisms that regulate synapse number, including synapse stabilisation are still poorly understood. Also on a technical level, establishing the time point when a synapse can be defined as “formed” or “lost” is not trivial. The morphology of an immature/ dissembled synapse is often variable and difficult to assess purely by examining still fluorescence images. Time lapse imaging provides a more convincing read out of synapse formation or loss but ultimately the connection needs to be assessed on a functional level before it can be established as a synapse. As synapse loss is a key early event in AD pathogenesis understanding the mechanisms that regulate synapse number will be important to understand the structural changes that occur during AD.

Synaptic plasticity and memory – focus on the hippocampus

As already mentioned, memory loss is one of the key symptoms used by clinicians to aid the diagnosis of AD and other dementias. The hippocampus is a key structure involved in memory storage and is one of the first and most severely affected regions of the brain by A β plaque deposits. The hippocampus (or hippocampal formation) is a curved cylindrical structure positioned within the medial lateral ventricle and part of the limbic system. The hippocampal formation is a group of cortical regions which can be divided into the dentate gyrus (DG), the hippocampus (proper), the subicular complex and the entorhinal cortex (EC). The subicular complex can be further subdivided into the subiculum, presubiculum and parasubiculum. The hippocampus (proper) can be subdivided into three areas termed cornu ammonis

(CA) 1, CA2 and CA3. The main excitatory cells of the hippocampus are the pyramidal cells. Different subsections of the pyramidal cell can occupy different anatomically defined layers (or laminae) of the hippocampus. The stratum oriens contains the basal dendrites, stratum pyramidale contains the cell soma, and the stratum radiatum and stratum lacunosum moleculare contain the apical dendrites of pyramidal cells. A widely studied excitatory circuit within the hippocampal formation is the “trisynaptic circuit” which consists of synapses made from EC to DG, DG to CA3 and CA3 to CA1. This circuit has been extensively used for synaptic studies of the hippocampus because the connections and projections are well characterised and defined and the gross cytoarchitecture and circuitry is well maintained after slice preparation.

Studies from the 1950’s provided the first major source of evidence that the hippocampal formation may be important for learning and memory formation. Milner and colleagues examined a patient named HM who had lost the ability to form new memories following surgical bilateral medial temporal lobe resection (Scoville and Milner, 1957). This work indicated that the medial temporal lobe and the hippocampus were important for declarative memory. In addition, human and animal studies have also shown that the hippocampus is also important for spatial learning (Eichenbaum, 2000; Maguire et al., 1997; Morris et al., 1982; Squire, 1992). These and many other studies have demonstrated that the hippocampus is important for different types of learning and memory (Eichenbaum, 2000; Squire, 1992).

However understanding the cellular changes underlying mechanisms of learning and memory in the hippocampus has been challenging. Past studies have shown that activity or experience can bidirectionally alter the strength of synaptic connections. The plastic nature of synapses has been proposed as a property that enables the brain to integrate cognitive information and form new memories (Lynch, 2004; Martin and Morris, 2002; Morris et al., 2003). A form of long term plasticity termed long term potentiation (LTP), has been proposed as a potential cellular correlate for learning and memory where either chemical or electrical stimulation can lead to an activity-dependent strengthening of synaptic connections (Bashir and Collingridge, 1992; Bliss and Collingridge, 1993; Bliss and Lomo, 1973). Further studies have shown that impairing LTP induction by either genetic or pharmacological methods can lead

to defects in the ability of animals to perform hippocampal-dependent spatial memory tasks providing strong evidence that LTP and learning and memory may be closely associated (Barnes et al., 1994; Bejar et al., 2002; Castro et al., 1989; Giese et al., 1998; Jones et al., 2001a; Jones et al., 2001b; McNaughton et al., 1986; Morris et al., 1986; Moser et al., 1998).

Studies have also identified several key characteristics that make LTP a good candidate mechanism for learning and memory (Bliss and Collingridge, 1993; Malenka and Nicoll, 1998; Malenka and Nicoll, 1999). As memories can often last a lifetime, one important consideration for the proposal that LTP is the cellular correlate for learning and memory is the fact that it can be persistent and long lasting with demonstrations of *in vitro* and *in vivo* potentiation lasting from hours to weeks to years (Bliss and Collingridge, 1993; Malenka and Nicoll, 1999). Input specificity which refers to the increase in synaptic strength only at active stimulated synapses and not at unstimulated cells is another factor (Engert and Bonhoeffer, 1997; Engert and Bonhoeffer, 1999). Studies have also shown that LTP is associative. This refers to the ability of activity at one synapse to influence the plasticity of another nearby synapse. The final property is cooperativity which refers to the temporally matched onset of pre and postsynaptic activity. The properties of input-specificity, associativity and cooperativity can be supplied by the known characteristics and actions of the NMDA receptor. The induction of LTP is dependent on NMDA receptor activation. Strong evidence for the involvement of NMDA receptors came from pharmacological experiments where blockade of NMDA receptors using selective antagonist, D-AP5 could inhibit induction of hippocampal LTP (Collingridge et al., 1983). D-AP5 had no effect on the expression of LTP or on basal synaptic transmission, which means NMDA receptors were crucial for LTP induction but dispensable for other forms of synaptic activity. The importance of NMDA receptor activation during LTP induction was further highlighted using genetic NMDA receptor knock-out animals or site directed mutagenesis of the C-terminal tail which also showed that LTP could not be induced in the absence of functional NMDA receptors (Sprengel et al., 1998; Tsien et al., 1996b). The ligand and voltage dependent activation, high permeability to calcium ions and the requirement for temporally associated pre and postsynaptic activity are the major molecular properties of the NMDA receptor that make it a key factor in the induction

of LTP. For this reason many AD transgenic models have used LTP paradigms and hippocampal-dependent spatial tasks (such as Morris water maze) to assess any changes in learning and memory.

1.6.2 Presenilin knock-out mice models

Several types of presenilin knockout mice models have been generated. The first series of presenilin transgenic animals were constitutive presenilin 1 knock-out mice which identified the key role of PS1 in embryonic development. As already mentioned, PS1 knock-out embryos have severe developmental abnormalities including an impaired axial skeletal development, disturbed somitogenesis, respiratory problems and cerebral haemorrhaging due to deficiencies in Notch signalling (De Strooper et al., 1998; Shen et al., 1997; Wong et al., 1997) (Figure 1.5). Like Notch knock-out animals, PS1 constitutive knock-out mice did not survive beyond embryonic ages (Conlon et al., 1995; Swiatek et al., 1994). It was found that the developmental impairments in the embryo were associated more with PS1 null animals than PS2 null animals. In fact, PS2 constitutive knock-out animals were viable and survived till late postnatal ages (Herreman et al., 1999). The only phenotypic difference between PS2 knock-out and wild type mice was the development of mild pulmonary fibrosis and haemorrhages in adult animals at approximately 6 months of age (Herreman et al., 1999). However, a constitutive PS1 and PS2 double knock-out mice showed a phenotype that mimicked the Notch knock-out mice, with lethality being observed at ~E8.5-11.5 (Donoviel et al., 1999; Herreman et al., 1999). This shows that PS1 and PS2 double knockout mice exhibit a more severe phenotype than knocking out PS1 alone, demonstrating that a deficiency in PS2 enhances the effect of PS1 elimination on embryonic development but elimination of PS2 alone has little effect on embryonic development

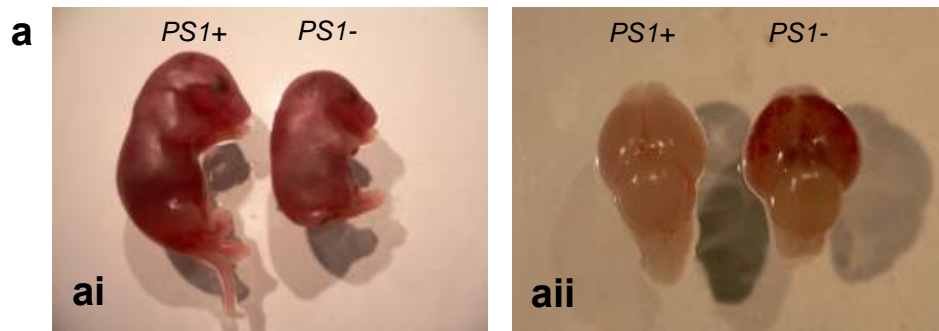


Figure 1.5 - Morphological differences between PS1 wild type (+/+) and constitutive PS1 knock-out (-/-) mice

(ai) Image of PS1 +/+ (left) and PS1 -/- animal (right). **(aii)** Excised brain from PS1 +/+ (left) and PS1 -/- (right) animal. In general, PS1 -/- are smaller in size than PS1 +/+ . Heterozygous (+/-) animals exhibit similar morphology to wild type animals (data not shown). PS1 -/- animals also show varying degrees of haemorrhaging in the brain which is not commonly observed in PS1 +/+ and PS1 +/- .

One major problem with constitutive PS1 knock-out animals was that embryonic lethality precluded the study of PS1 during postnatal ages. To overcome this issue, more recent knock-out animals of presenilins have been generated using Cre/LoxP mediated deletion methods (Tsien et al., 1996a; Tsien et al., 1996b). The Cre/LoxP system has been extensively used to produce animals where the targeted gene can be temporally inactivated by Cre-recombinase, a type I bacterial topoisomerase that catalyses site-specific recombination of DNA. The gene of interest can be engineered to have LoxP DNA motifs at both ends of the gene (termed a floxed gene) which are then used by Cre-recombinase as excision recognitions sites to enable conditional elimination of the floxed gene. In addition, different promoters can be used to generate tissue/ cell type specific knock-out animals.

Dewachter et al., (2002) generated conditional knock-out mice where PS1 expression was controlled by a Thy-1 promoter which led to PS1 gene elimination in post mitotic cells, and therefore was mainly neuron specific (Dewachter et al., 2008). Conditional PS1 knock-out mice were also generated with α -CaMKII promoter which led to PS1 gene elimination in forebrain excitatory neurons starting from juvenile ages (Feng et al., 2001; Yu et al., 2001). To eliminate the PS1 gene in mice, floxed PS1 mice were crossed with α -CaMKII-Cre mice and progressive knock-out was observed from 3-4 weeks after birth (Tsien et al., 1996a; Tsien et al., 1996b; Yu et al., 2001). This approach enables the impact of presenilin elimination to be

assessed in adult animals and circumvents the developmental issues observed with constitutive knock-out animals. PS1 could also be eliminated in floxed cultured cells by infection or transfection of Cre viruses or cDNA respectively.

The α -CaMKII promoter was also used to generate forebrain specific double PS1 and PS2 knock-out animals (Saura et al., 2004). In line with constitutive PS1 knock-out studies where minimal A β production was observed (De Strooper et al., 1998; Naruse et al., 1998), adult conditional forebrain specific PS1 and PS2 knock-out animals did not exhibit any amyloid plaque deposits indicating that neuronal presenilin is required for A β and plaque generation in embryonic and adult stages of development. PS1 and PS2 conditional double knock-out animals also exhibited signs of AD pathobiology at 6 months of age, with the accumulation of glial fibrillary acidic protein, neurofibrillary tangles and hyperphosphorylated tau. Inflammation and neurodegeneration was observed in the cortex and hippocampus in a progressive and age-dependent manner (Saura et al., 2004). Furthermore, functional changes in neurons occurred before noticeable neurodegeneration. Neurons also had reduced dendritic complexity and spine loss by 6 months. This suggests a loss of presenilin function can eventually lead to an AD phenotype. However, an electron microscopy study which used the same PS1 and PS2 conditional knock-out animals as Saura and colleagues (2004) showed that at 2 months of age, a significant increase in spine density of CA1 pyramidal neurons of the hippocampus could be observed (Aoki et al., 2009). Closer examination using quantitative HRP DAB labelling revealed a significant (28%) increase in NR2A subunits in spines and an increase (31%) in postsynaptic density measurements (Aoki et al., 2009). Together the studies of Saura et al., (2004) and Aoki et al., (2009) provide evidence that elimination of presenilin initially leads to an increase in spine density which is then followed by a subsequent decrease in spine density with age.

An important point to note with presenilin knock-out mice studies is that both γ -secretase dependent and γ -secretase independent forms of presenilin activity are eliminated. This means that it is not possible to identify whether a change in cell function is attributed to a loss of γ -secretase dependent activity of presenilin or loss of γ -secretase independent activity of presenilin, or both. This factor makes the

identification of molecular mechanisms potentially more complicated in knock-out studies.

1.6.3 Presenilins, synaptic plasticity and learning and memory

Conditional presenilin knock-out mice models have been extensively used in experiments that have examined aspects of learning and memory. The following studies mainly investigated the role of presenilin in LTP experiments and behavioural tests such as the Morris water maze.

LTP is often proposed as a cellular correlate of learning and memory and induced by either strong electrical stimulation (e.g application of high frequency trains of stimuli, see Bliss et al., 1986) or chemical stimulation (see for example: Otmakhov et al., 2004) which leads to a long lasting enhancement of postsynaptic strength. Studies from forebrain specific PS1 conditional knock-out animals showed no change in LTP induction or expression/ maintenance in the CA1 region (Yu et al., 2001) or dentate gyrus (Feng et al., 2001). Additionally knock-out of PS1 in forebrain neurons in adult animals did not lead to any impairment in paired-pulse facilitation, a form of presynaptic short term plasticity (Yu et al., 2001). In conflict with these reports, a study from PS1 neuronal specific knock-out mice reported impairment in the induction/ initial phase of CA1 LTP (Dewachter et al., 2008). Interestingly, despite a reduced response during the initial phase of LTP, the expression/ maintenance phases of LTP were no different to wild type control animals. It is unclear why only the initial phase is impaired. The authors also observed a corresponding decrease in NMDA receptor field EPSP response and reduced expression of activated α -CaMKII, NR1 and NR2B subunits, suggesting that PS1 may regulate cellular proteins required for LTP induction. These PS1 neuronal specific knock-out mice also exhibited a smaller number of synaptic vesicles (total population and docked vesicles) and a reduction in paired-pulse ratio, suggesting that PS1 is involved in regulating presynaptic vesicle pools and release probability (Dewachter et al., 2008).

The reason for the difference in LTP between the conditional forebrain specific PS1 knock-out animals and the neuron specific PS1 knock-out mice are currently unclear. The main difference between these two knock-out models is the use of different promoters. However, the α -CaMKII promoter used in forebrain specific PS1 knock-out mice (Feng et al., 2001; Yu et al., 2001) and the thy-1 promoter used in neuronal knock-out mutants (Dewachter et al., 2008) should exhibit similar effects as both promoters should essentially cause specific elimination of PS1 from neurons, which means the differences may arise from other subtle differences between the two mice models. Further studies will be required to understand the reason for the discrepancy in LTP between different conditional PS1 knock-out mice.

Studies from forebrain specific (α -CaMKII promoter) conditional presenilin double knock-out animals revealed that eliminating both PS1 and PS2 led to a reduction in LTP and paired-pulse facilitation (at inter-event intervals of 20-100ms). Examination of synaptoneurosomes also revealed a reduction in NR1, NR2A subunits and CaMKII suggesting a decrease in certain synaptic proteins (Saura et al., 2004). Interestingly no change in NR1, NR2A and CaMKII was seen in total lysates. The forebrain specific double presenilin knock-out animals (Saura et al., 2004) seem to be phenotypically more similar to neuron specific PS1 knock-out animals (Dewachter et al., 2008) than forebrain specific PS1 knock-outs (Feng et al., 2001; Yu et al., 2001).

A recent study at CA3-CA1 synapses in the hippocampus found that LTP and synaptic facilitation were impaired only when PS1 and PS2 were both eliminated from the presynaptic cell. No change in LTP was observed upon PS1 and PS2 elimination from the postsynaptic neuron (Zhang et al., 2009). This suggests that presynaptic presenilins rather than postsynaptic presenilins are involved in modulating LTP (Zhang et al., 2009). However, this result is at odds with an earlier report which showed that presenilin associated impairments in LTP was mainly postsynaptically expressed (Saura et al., 2004). Zhang et al., (2009) also shows that short term facilitation is only impaired when both PS1 and PS2 are presynaptically eliminated as presynaptic elimination of PS1 on its own does not lead to any impairment in paired-pulse ratio. Taken together, there seems to be a considerable

amount of variability in long and short term plasticity between different presenilin mice models. The reasons behind these differences are not entirely clear at present.

Behavioural studies also revealed some discrepancies between different conditional presenilin knock-out mice. Most studies examined the performance of different animals on the Morris water maze, a test of spatial memory. One study showed that forebrain specific PS1 knock-out mice which exhibited no changes in hippocampal LTP did show a mild behavioural impairment in spatial memory task with an extended period of time required to locate the platform and a subsequent decrease in the number of crossings (Yu et al., 2001). This indicates that PS1 is not required for long term plasticity but it is for spatial memory. However, this finding was not confirmed by Feng and colleagues who performed virtually identical experiments using a forebrain specific PS1 knock-out animal (Feng et al., 2001). Feng and colleagues found normal learning and retention in the Morris water maze and normal contextual fear conditioning (Feng et al., 2001). The differences between these studies are currently not well understood.

Dewachter et al., (2008) showed that neuron specific PS1 knock-out animals showed no difference in Morris water maze performance (spatial navigation task), no change in novel object recognition task, no change in amygdala dependent cued conditioning but a decreased freezing in hippocampal and amygdala dependent contextual fear conditioning (Dewachter et al., 2008). This study suggests that neuronal presenilin is not required for most hippocampal dependent tasks including spatial navigation tasks but is involved in a hippocampal and amygdala dependent behavioural task.

Conditional double knock-out mice also showed an impaired performance on the Morris water maze and contextual fear conditioning tasks suggesting elimination of both PS1 and PS2 can lead to defects in hippocampal dependent forms of learning and memory (Saura et al., 2004). Presenilin double knock-out animals had impaired LTP and spatial and associative memory at 2 months of age but in the absence of any changes in neuron number. By 6 months, an extreme impairment in the performance of the Morris water maze was observed together with neurodegeneration. This suggests that functional changes may precede the noticeable loss of neurons. However, the molecular mechanisms underlying the

behavioural changes observed in presenilin knock-out mice remains poorly understood. Interestingly, pharmacological intrahippocampal infusion of a γ -secretase inhibitor after training led to an enhanced spatial memory performance suggesting that γ -secretase acts as a negative regulator of long-term memory (Dash et al., 2005). This study also indicates that γ -secretase inhibitor treatment may not generate the same results as presenilin knock-out mice in behavioural tests. It is not clear if the differences arise from a non-specific action of the inhibitors or if there are compensatory mechanisms present in the knock-out animals or another unidentified possibility.

1.6.4 Presenilins and synaptic transmission

As constitutive PS1 knock-out mice do not survive beyond late embryonic stages, the role of PS1 in these animals could not be analysed in postnatal/ adult ages. Due to this developmental defect, all synaptic studies investigating the role of PS1 from these animals involved generating neuronal cultures from tissue obtained from embryonic mice. A recent electrophysiological study examines the role of PS1 in modulating basal synaptic transmission. Dissociated cortical neurons from constitutive PS1 null mice showed an increase in miniature excitatory postsynaptic current (mEPSC) frequency without a change in mEPSC amplitude (Parent et al., 2005). One interpretation of this result is that PS1 null neurons exhibit a change in presynaptic function, in the absence of a change in postsynaptic activity. Intriguingly, immunofluorescence data reports a lack of change in presynaptic active zone marker, bassoon, but an increase in postsynaptic density staining, and an overall increase in colocalised PSD-95 and bassoon signal. An increase in spine number was also observed. This result suggests that PS1 may modulate synapse number in cortical cultures. Taken together, these results show that PS1 may play a role in modulating synaptic transmission and synapse number in cortical neurons.

Additionally, Parent and colleagues found that the PS1 null phenotype could be mimicked by chronic application of a potent γ -secretase inhibitor suggesting that γ -secretase activity of presenilin was required for regulation of synapse function of

cortical cells (Parent et al., 2005). Separate studies also showed that pharmacological inhibition of γ -secretase activity could lead to an increase in mEPSC frequency in hippocampal neurons (Kamenetz et al., 2003; Priller et al., 2006).

Parent and colleagues also showed that a membrane-tethered protein fragment named α -deleted in colorectal cancer C-terminal fragment (α -DCC CTF) could accumulate within the membrane compartments of PS1 knock-out neurons or after block of γ -secretase cleavage in wild type cells (Parent et al., 2005). The authors proposed that accumulation of α -DCC CTF could increase cAMP/ PKA signalling and enhanced neurite development in neuroblastoma cells and potentially provide a mechanistic explanation for the increase in miniature frequency and number of synaptic contacts in cortical neurons (Parent et al., 2005). Together this study proposes that γ -secretase activity is involved in regulating cortical synaptic transmission and further studies will be required to determine if cAMP/PKA/ α -DCC signalling plays a major role in modulating synaptic transmission at other synapses.

1.6.5 Comparison of PS1 and PS2 associated γ -secretase functions

Despite the similarities in sequence homology, it is unclear whether PS1 and PS2 share parallel functional roles. Intriguingly, the vast majority of FAD mutations have been found in PSEN1 gene (>170) with only a handful of cases being reported in PSEN2 gene (~10). Additionally PSEN1 mutations tend to be more aggressive than mutations in PSEN2, as shown by the onset of symptoms at an earlier age (Bertram and Tanzi, 2004; Tandon and Fraser, 2002). These genetic differences are suggestive that PS1 and PS2 may not have the same function in FAD pathology.

Past studies have indicated that PS1 is the major isoform transcribed in the brain with PS2 being more highly expressed in peripheral tissues (Beel and Sanders, 2008; Tandon and Fraser, 2002). However other in situ hybridisation experiments have shown that both PS1 and PS2 transcripts can be found in the hippocampus, cortex

and other CNS regions (Kovacs et al., 1996; Lee et al., 1996). The subcellular localisation of PS1 and PS2 remains to be fully determined. A study undertaken on mammalian cell lines showed using biochemical cell fractionation techniques that PS1 and PS2 were found in intermediate buoyant density fractions, which contained markers for the ER, Golgi, TGN, endosomal vesicles and lysosomal vesicles (Kim et al., 2000). However PS1 but not PS2 is also found in a low buoyant density fraction, which corresponds to non-identified subcellular region(s) that excluded the organellar markers associated with the intermediate fraction (Kim et al., 2000). This study suggests a potential difference in PS1 and PS2 subcellular distribution.

Phenotypic differences between PS1 knock-out and PS2 knock-out mice suggest that these proteins may potentially play dissimilar roles in Notch signalling. As already mentioned, PS1 constitutive knock-out animals exhibit severe impairments in embryonic developments (De Strooper et al., 1998; Shen et al., 1997; Wong et al., 1997) whilst PS2 knock-out animals do not have any noticeable embryonic defects (Herreman et al., 1999). Only at later stages of adult development did PS2 knock-out animals display differences to wild type animals, suggesting PS2 activity does not seem to be required for Notch signalling in the embryo and that PS1 and PS2 have differential roles in development. However a more severe impairment in embryonic development was observed in PS 1 and 2 double knock-out animals when compared to PS1 animals suggesting that loss of both genes exaggerates the effect of loss of PS1 (Donoviel et al., 1999; Herreman et al., 1999). These results suggest that there may be some functional overlap between PS1 and 2 but it seems that PS1 is the main homologue implicated in Notch signalling during embryonic development. The proposed minor role of PS2 may be compensated for by the presence of PS1 allele in PS2 knock-out animals (Herreman et al., 1999). However, the opposite situation does not apply, presence of PS2 does not rescue/ compensate for the lack of PS1 implying a dominant role for PS1 in embryonic development (De Strooper et al., 1998; Shen et al., 1997; Wong et al., 1997)

Analysis of A β generation also showed that PS1 and PS2 may have differential roles in APP processing. It was also shown that only very low amounts of A β were generated in PS1 constitutive knock-out animals (De Strooper et al., 1998; Naruse et al., 1998) suggesting that PS1 plays a significant role in A β generation. The presence of some remaining residual A β suggests that a small component of γ -secretase is

derived (presumably) from PS2 in cultured neurons. However, the amount of A β generated by PS2 knock-out animals is highly comparable to control animals providing evidence that APP processing can be completely rescued by PS1 in PS2 knock-out cells (Herreman et al., 1999). Another study shows that the amount of APP-CTFs found in PS1 wild type mice after treatment with γ -secretase inhibitors is comparable to the amount of APP-CTFs found in PS1 knock-out mice suggesting that similar deficiencies in APP processing are seen upon either blocking γ -secretase activity pharmacologically or eliminating the PS1 gene (Parent et al., 2005). These studies indicate that PS1 is the main presenilin isoform involved in APP processing and γ -secretase complexes composed of PS2 may play a limited role in APP proteolysis. This finding has been confirmed with *in vivo* studies showing that APP cleavage is less efficient with PS2 containing complexes than PS1 containing γ -secretase complexes (Mastrangelo et al., 2005).

γ -secretase inhibitors were also used to determine the relative contributions of PS1 and PS2 to cellular γ -secretase activity. Drug binding studies conducted on blastocyst cell membranes showed that the K_i values of γ -secretase inhibitors on PS1+/+ PS2+/+ membranes were more closely matched to PS1+/- PS2-/- than to PS1-/-PS2+/+ cell membranes (Lai et al., 2003). This result suggests that most endogenous γ -secretase activity is supplied by PS1 rather than PS2. It was also shown that PS1 and PS2 are not associated within the same high molecular weight protein complex which supports the notion that each γ -secretase complex contains only one PS protein (Lai et al., 2003).

However, other studies using blastocyte pluripotent stem cell lines have indicated that PS2 can contribute to a greater percentage of the cellular γ -secretase activity than originally shown. PS1-/- blastocytes only showed ~ 40 – 50% reduction in γ -secretase activity (Herreman et al., 2000; Zhang et al., 2000). This indicates that the contribution of PS1 and PS2 to total γ -secretase activity may vary between cell types. Overall, these studies support the notion that PS1 and PS2 associated γ -secretase complexes have differential cellular functions with PS1 being the major source of cellular γ -secretase activity.

1.7 Concluding remarks

Studies of FAD patients have revealed the crucial role of presenilin (1) in AD pathogenesis. In line with this observation, presenilin mutant mice often develop the characteristic hallmarks of AD; amyloid plaques, neurofibrillary tangles and neuronal loss. Presenilin knock-out mice studies have also outlined potential roles for presenilin in regulating certain forms of plasticity, learning and memory. However, whether presenilin plays a major role in regulating synapse function in hippocampal neurons remains to be fully determined. Investigations into the role of presenilin in modulating different synaptic functions may provide further insights into the pathogenic mechanisms that occur during AD progression. The subsequent chapters of this thesis examine the impact of the loss of γ -secretase activity or presenilin 1 expression on different aspects of synaptic function in hippocampal neurons.

Aims

The aim of this thesis is to examine the role of presenilin (1) in regulating synaptic transmission and neuronal function in hippocampal neurons. Presenilin function is investigated by two separate approaches. A constitutive PS1 knock-out mouse model is used to examine the γ -secretase dependent and γ -secretase independent roles of presenilin 1 and specific γ -secretase inhibitors are used to examine the synaptic effects of selective block of γ -secretase activity of presenilin.

The roles of presenilin in regulating the following aspects of synapse function are investigated:

- Excitatory and inhibitory spontaneous synaptic transmission using whole-cell recordings in dissociated and organotypic cultures
- Release probability using optical (FM styryl dye destaining kinetics) and electrophysiological (PPR and rate of MK801 block of NMDA receptor current) methods
- Synapse number using immunocytochemical methods
- Intracellular calcium concentration using live calcium imaging

The synaptic effects of β -secretase inhibition are also examined. This series of experiments have been performed to further investigate whether loss of A β production has any effects on synapse function. These experiments may also provide some insight into the potential synaptic effects that may arise with therapeutic treatment with γ -secretase and β -secretase inhibitors.

Chapter 2: Materials and Methods

The experiments outlined in this thesis were performed on hippocampal primary dissociated cultures and organotypic slice cultures. Both of these well characterised model systems have been widely used for the study of synapse function and plasticity. Primary dissociated cultures comprise of simple neuronal networks with extensive synaptic connections arranged on a monolayer. These cultures are well adapted for use with a range of techniques including electrophysiology, immunocytochemistry and live cell imaging. Organotypic slice cultures enable the study of synapse function in a system whereby the gross cytoarchitecture of a hippocampal slice is largely maintained during development *in vitro* and provide an advantageous system for conducting long term whole-cell recordings and neuropharmacological characterisations. All experiments were performed at room temperature and with a minimum of three separate culture preparations unless otherwise mentioned. All chemicals and reagents used aside from those listed below were purchased from Sigma-Aldrich.

2.1 Animals

All animal procedures were carried out in accordance with ‘The Animals (Scientific Procedures) Act 1986’.

2.1.1 Rat colonies

Sprague-Dawley rats were obtained in-house from UCL Biological Services Unit. Animals were collected and used on the day of dissection and preparation.

2.1.2 PS1 mice colonies and genotyping

PS1 mice were kindly provided by Professor S. Sisodia (University of Chicago, USA). Detailed descriptions of the method used for generating PS1 $-/-$ mice can be found in (Wong et al., 1997). Briefly, PS1 $-/-$ animals were generated by using a PS1 targeting vector to replace the second coding exon (exon 4, amino acids 30-113) and neighbouring sequences with a neomycin-resistance gene and HSV thymidine gene by homologous recombination. PS1 $+/-$ animals were backcrossed with matched background wild type mice strains (C57Bl/6J) and heterozygote offsprings were used for mating.

Analysis of mouse genotype was performed using polymerase chain reaction methods (PCR). DNA was extracted from PS1 tail biopsies and brain tissue samples using a QIAGEN [®] DNeasy Blood and Tissue kit according to manufacturers' instructions. For genotyping, three specifically designed primers (sequence supplied and designed by Sisodia lab) against the neomycin cassette and the PS1 gene were used in a PCR to determine the presence of targeted PS1 null and/or endogenous PS1 alleles, generating a 370 base pair (bp) and a 500 bp PCR fragment for the respective alleles. The primer sequences are outlined below:

Neomycin	CCA TTG CTC AGC GGT GCTG
mPS1 forward	AGC CAA GAA CGG CAG CAG CAG CAT GAC AGG CAG AG
mPS1 reverse	CTT CCA TGA GCC ATT TGC TAA GTGC

PCR products were separated by agarose gel electrophoresis (0.7% agarose in 1x TAE buffer containing 0.5 μ g/ml ethidium bromide), visualised by UV illumination and examined for 370 bp and 500 bp bands against a 100 bp DNA molecular weight ladder. Genotyping procedures were performed by D. Elliott. Only animals that yielded duplicate positive genotyping results (obtained from two different tissue samples) were included in the final data set. For PS1 mice experiments, embryonic littermates were used for comparison.

Table 2.1 shows the components used for PCR amplification of PS1 DNA. A total volume of 25 μL was used for each PCR tube.

Table 2.1: Components for PS1 PCR reaction.

Compound	Concentration	Volume	Final Conc.
PCR buffer	10x	2.5 μL	1x
dNTPs (Contains ATP, GTP, CTP, TTP)	10 mM	1.0 μL	100 μM / dNTP
MgCl ₂	50 mM	0.75 μL	1.5 mM
Primers: Neo mPS1 forward mPS1 reverse	50 μM	0.25 μL each	0.5 μM /Primer
Taq Polymerase (Add last)	5 U/ μL	0.25 μL	0.05 U/ μL
Mouse DNA	N/A	1.0-2.0 μL	(1.0-2.0 μL)

Table 2.2 shows the protocol used for PCR amplification of PS1 mice DNA.

Table 2.2: PS1 PCR reaction protocol.

Step	Temperature ($^{\circ}\text{C}$)	time (min)
1	94.0	5
2	94.0	1
3	60.0	1
4	72.0	2
5	Repeat 35 times to Step 2	
6	72.0	10
7	4.0	24
8	END	

2.2 Hippocampal cell culture (rat and mice)

2.2.1 Materials

Table 2.3: Chemicals / Reagents / Products used for dissociated cell culture

Product	Company	Location
12 mm glass coverslips	Assistent	Sondheim, Germany
Acetic acid	Sigma - Aldrich	Dorset, UK
Aztek atomiser	Sylmasta Ltd	Sussex, UK
B27 supplement	Invitrogen	Paisley, UK
DNase I	Merck chemicals	Darmstadt, Germany
Eagle's Basal medium (BME)	Invitrogen	Paisley, UK
Fetal calf serum (FCS) (batch tested)	Sigma – Aldrich Invitrogen	Dorset, UK Paisley, UK
Glutamax	Invitrogen	Paisley, UK
Hank's balanced salt solution (HBSS)	Invitrogen	Paisley, UK
Mito™ serum extender	BD bioscience	New Jersey, US
Neurobasal medium	Invitrogen	Paisley, UK
Papain	Lorne laboratories Ltd	Reading, UK
Poly-D-lysine (PDL)	Sigma - Aldrich	Dorset, UK
Sterile plastic for tissue culture (Nunc)	VWR international	Lutterworth, UK
Rat tail collagen	(personal stocks extracted from Sprague- Dawley rat tails)	London, UK
Trypsin	(MRC LMCB in house stocks)	London, UK
Trypan blue	Invitrogen	Paisley, UK

Table 2.4: Buffers and Solutions, used for used for dissociated cell culture

Buffer / Solution	Contents	Storage	Sterilisation
Astrocyte medium	BME, 6 mg/ml glucose, 10 mM HEPES, 1 mM sodium pyruvate, 100 units/ml penicillin, 0.1 mg/ml streptomycin, 10 mM HEPES, 10% FCS	4°C	0.2 µM filter
Dissection solution	HBSS with 10 mM HEPES	4°C	0.2 µM filter
Neuronal medium	Neurobasal, 6 mg/ml glucose, 0.1% Mito™ serum extender, 2.5% B27 supplement, 100 units/ml penicillin, 0.1 mg/ml streptomycin, 2 mM glutamax	4°C	0.2 µM filter
Papain digestion solution	Dissection solution containing 1.5 µM calcium choride, 2 mg/ml L-cysteine, 0.1 µm/ml DNase I, 0.5 mM EDTA, 30 units papain	4°C	0.2 µM filter
PDL-collagen solution	Acetic acid (0.025%), 1:7 dilution rat tail collagen, 5 µm/ml PDL in HPLC grade water	Room temp	0.2 µM filter

Table 2.5: Chemicals / Reagents / Products used for organotypic slice culture

Product	Company	Location
Ceramic blades	Campden Instruments	Loughborough, UK
Cyanoacrylate	RS components	Northants, UK
Earle's balanced salt solution (EBSS)	Invitrogen	Paisley, UK
Horse serum	Invitrogen	Paisley, UK
Minimum essential medium with Glutamax-1(MEM)	Invitrogen	Paisley, UK
Millicell™ membrane inserts	Millipore	Watford, UK
Sterile 6 well plate for tissue culture (Nunc)	VWR international	Lutterworth, UK
Vibrating microtome	Campden Instruments	Loughborough, UK

Table 2.6: Buffers and Solutions, used for organotypic cell culture

Buffer / Solution	Contents	Storage	Sterilisation
Organotypic culture medium	50% MEM, 25% horse serum, 23% EBSS, 36 mM glucose, 100 units/ml penicillin, 0.1 mg/ml streptomycin	4°C	0.2 µM filter
Organotypic slicing medium	EBSS with 25 mM HEPES	4°C	0.2 µM filter

2.2.2 Methods

Cell culture procedures were performed under sterile conditions in laminar flow cabinets. Cell culture media was warmed to 37°C and equilibrated within humidified 5% CO₂ incubator prior to use. All cultures were maintained at 37°C with humidified 5% CO₂ to maintain pH balance.

2.2.2.1 Preparation of glass coverslips

All dissociated cultures were plated on pre-cleaned glass coverslips which have been treated for 12-18 hrs with 100% fuming nitric acid, then thoroughly rinsed with deionised water for 3-4 hrs and maintained in 100% ethanol till use. When needed, coverslips were placed into a sterile Petri dish inside a flow cabinet and left at room temperature for 30-40 min or until the ethanol had fully evaporated. 12 dry coverslips were inserted into the middle two rows of a 24 well plate. (The surrounding outer two rows were filled with 700 µl water at the time of glial cell plating (see below) to minimise medium evaporation). A light mist-like layer of PDL-collagen mix was applied to the coverslips using a fine atomiser powered by a positive pressure pump. Coated coverslips were left to dry at room temperature before sterilisation by UV illumination for 15-18 min. Plates were then packaged and sealed using plastic vacuum wrap and stored for a maximum of 4 weeks.

2.2.2.2 Preparation of astrocyte feeder layer

To enhance neuronal survival and development, neurons were grown on top of a monolayer of astrocytes. Astrocytes were obtained by taking excess cells from a hippocampal dissection and plating them in T25 sterile flasks in astrocyte growth medium. After 4-6 days incubation, the astrocytes formed a 65-95% confluent monolayer and were ready for plating onto glass coverslips. For this, astrocytes were first rinsed twice with 1x PBS (lacking calcium and magnesium ions), followed by a rapid application (and subsequent aspiration) of trypsin to aid detachment of the cells from the flask. Once detached, cells were gently triturated with a flame polished sterile plugged Pasteur pipette for 5-10 passages to breakdown any clusters of astrocytes. Cells were plated onto poly D-lysine-collagen coated coverslips at 2,500 – 3,500 cells per well in 500 µl of astrocyte growth medium and maintained in a 37°C incubator supplied with 5% CO₂ for 3-5 days until 60-80% confluency was achieved.

2.2.2.3 Preparation of rat hippocampal dissociated neurons

Dissociated neuronal cultures were prepared from hippocampal tissue, containing the dentate gyrus and regions CA1-3 of P0-1 rat pups. Following decapitation, the brain was rapidly removed from the animal's skull by performing a sagittal cut from the medial occipital region to the frontal lobe area firstly of the skin followed by that of the skull. Hemispheres were separated down the midline with a sharpened spatula and submerged in ice cold dissection solution. The hippocampus was visible once the meninges and midbrain regions were excised using sharp forceps under a stereomicroscope. The hippocampus was removed from the brain using a sharpened spatula and cut into 3-4 equally sized pieces using a sterile no. 10 blade. The tissue pieces were rinsed once with dissection solution and then transferred into a falcon tube containing papain digestion solution and incubated at 37°C for 20-28 min. After this time, the papain solution was aspirated and the tissue rinsed 3x with pre-warmed neuronal culture medium. To dissociate the digested hippocampal pieces, a sterile flame polished plugged Pasteur pipette was used to gently triturate the tissue 3 times. In order to estimate the number of viable cells, 5 µl of trypan blue was added to 50 µl of the triturated cell mixture and then live cells that excluded the dye were counted using a hemacytometer. Cells were seeded in 500 µl neuronal culture medium at 12,500 – 17,500 cells per well. After 24–48 hrs, 100 µl of neuronal culture medium containing the anti-mitotic agent, cytosine arabinoside (4 µM final concentration) was added to each well to minimise further astrocyte growth. An example of a dissociated neuron cultured for 12 days *in vitro* (DIV) is shown in Figure 2.1 a.

2.2.2.4 Preparation of mouse hippocampal dissociated neurons

Previous characterization of PS1^{-/-} mice (Wong et al., 1997) have shown no surviving animals beyond postnatal ages suggesting that knock-out of the PS1 gene results in late embryonic (E) lethality. Consistent with this, genotyping postnatal animals after weaning (at P21) did not yield the PS1^{-/-} genotype. For this reason, embryonic pups were used to prepare PS1 mice dissociated cultures. 3-11 month old

female PS1 +/- mice were mated with male PS1 +/- mice to generate litters which should contain a combination of PS1 +/-, PS1 +/+ and PS1 -/- pups. E15-17 mice were obtained from pregnant female PS1 +/- mice. All pups from a given litter were individually dissected and hippocampi were removed. Cortical brain samples and tail biopsies (approximately 2 mm) were also collected from each pup and placed in individual eppendorf tubes for genotyping. Samples were maintained on ice or stored at -20°C until genotyping. All mice were genotyped by D. Elliott using PCR (see section 2.1.2).

Hippocampi from individual pups were digested, triturated, counted and plated separately to prevent mixing of different genotypes. Mice neurons were plated at 19,000 – 22,500 cells per well onto coverslips with rat astrocyte feeder layer. Initial experiments where mice neurons were plated at the same (low) density as that used for rat cultures resulted in poor cell health, assessed by excess cell debris in the culture media after plating and morphological abnormalities such as sunken somas.

2.2.2.5 Organotypic slice culture preparation

Organotypic slices were cultured using a modified interface method (De Simoni et al., 2003; De Simoni and Yu, 2006; Stoppini et al., 1991). This is a simple and adaptable procedure that enables the culture of static slices at the air-medium interface, enabling them to be studied over a wide developmental period. 1 ml of pre-warmed organotypic culture medium was put into each well of a 6 well plate, followed by a semi permeable membrane insert (Millipore). 3 smaller pieces of semi permeable membrane, termed confetti, were placed onto the surface of each insert, and a hippocampal slice was placed on top of each confetti piece. From past experience, slices in culture flatten and strongly adhere to any membranous material over time. Thus, these smaller pieces of confetti allow for the easy manoeuvre and access of organotypic slices whilst minimising stress and damage to the slice when transferring from the culture insert to the experimental set up. Culture plates and organotypic culture and slicing media were freshly prepared on the day of slicing.

Plates were maintained at 37°C whilst organotypic slicing medium was maintained on ice.

Parasagittal hippocampal slices were prepared from P6-8 male Sprague-Dawley rats. The brain was removed from the skull using the method outlined in section 2.2.2.3, and immersed in ice cold organotypic slicing medium. A midline cut was made using a no. 22 blade to separate the two hemispheres. A wide ended spatula was used to manoeuvre each hemisphere onto the stage of the slicing chamber. Each hemisphere was glued along the midline cut using cyanoacrylate, and 300 µM thick slices were cut in ice-cold slicing solution using a vibrating microtome (vibraslice, Campden Instruments, Ltd) with either a ceramic blade or a stainless steel blade. The cut slices were transferred to a Petri dish containing ice cold slicing solution, and the hippocampus was isolated under a dissecting microscope. Dissected hippocampal slices were quickly rinsed in 10 ml ice cold organotypic culture medium and carefully plated onto the small confetti pieces using a wide end sterile plastic or glass Pasteur pipette. Excess culture medium was removed from the surface of the membrane insert using a flame polished glass Pasteur pipette, and the plate was returned to the incubator. Organotypic culture medium was replaced every 2-3 days by aspirating 900 µl and replacing with 1 ml pre-warmed medium. Figure 2.2 b shows a typical hippocampal slice soon after slicing (top) and after 14 days *in vitro* (bottom).

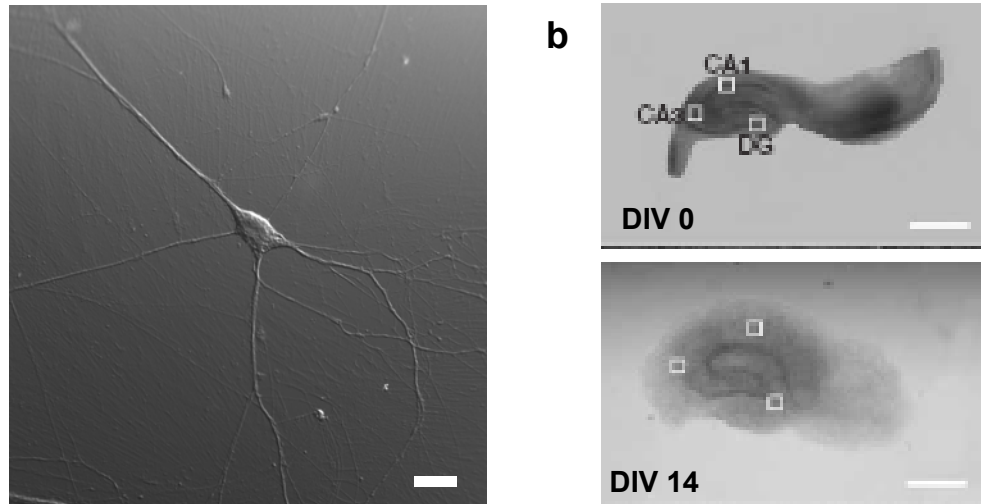


Figure 2.1 - Hippocampal dissociated and organotypic slice cultures

(a) Low magnification DIC image of a rat dissociated neuron grown in culture at DIV 12. These low density cultures are used for most of the experiments discussed in this thesis. Scale bar, 20 μm .

(b) Image of sample organotypic slice cultures made from the hippocampal formation at DIV 0 (top) and DIV 14 (bottom). Note the broadening and thinning of the slice with time whilst gross cytoarchitecture and slice shape is largely maintained. Scale bar, 1 mm. Image adapted from De Simoni and Yu, 2006.

2.3 Drugs and Inhibitors

2.3.1 γ -secretase inhibitors

PS1 mice, rat dissociated and organotypic cultures were used for pharmacological experiments to examine the effects of γ -secretase inhibitors on synapse function. The following two γ -secretase inhibitors were used for most experiments:

N-[N-(3,5-di⁻uorophenacetyl)-l-alanyl]-S-phenylglycine t-butyl ester (DAPT) is a dipeptidic compound which interacts with the C-terminal fragment of presenilin (Morohashi et al., 2006) and shown to reduce A β production in human neuronal cultures (Dovey et al., 2001) and rat cortical cultures (Hoey et al., 2009). DAPT was used at a final concentration of 10 μ M (Chyung et al., 2005; Yang et al., 2008). Figure 2.2 a (top, red) shows the molecular structure for DAPT.

(1S-Benzyl-4R-[1-(1S-carbamoyl-2-phenylethylcarbamoyl)-1S-3-methylbutylcarbamoyl]-2R-hydroxy- 5-phenylpentyl)carbamic acid tert-butyl ester (L-685,458) is a transition state analogue and shown by previous studies to bind to the active zone region of presenilins to inhibit its enzymatic activity (Li et al., 2000; Shearman et al., 2000), and blocks A β production in a range of APP overexpressing cell lines (Shearman et al., 2000). L-685,458 was used at a final concentration of 1 μ M (Kamenetz et al., 2003). Figure 2.2 a (bottom, blue) shows the molecular structure for L-685,458.

2.3.2 β -secretase inhibitors

In chapter 7, the effects of β -secretase inhibitor treatment on dissociated and organotypic hippocampal cultures were examined. β -secretase IV is an inhibitor which acts at the active site of β -secretase and was used at a final concentration of 1 μ M (Wen et al., 2008). Figure 2.2 b (green) shows the molecular structure for β -secretase IV.

The drugs listed above were purchased from Merck Biosciences, made up in dimethyl sulfoxide (DMSO) and stored according to manufacturer's recommendations. 0.1% DMSO was used as a mock vehicle control for all experiments (Sigma).

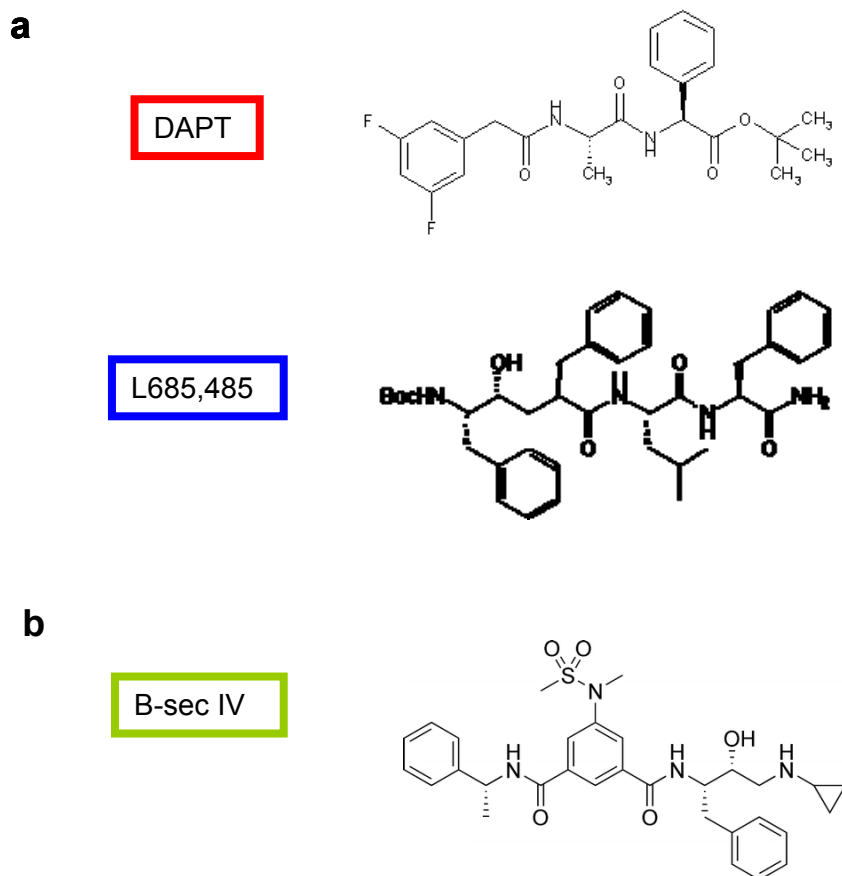


Figure 2.2 - Molecular structure of γ -secretase and β -secretase inhibitors

(a) Molecular structure of γ -secretase inhibitors DAPT (red, top) and L-685,485 (blue, bottom). These inhibitors are used throughout this thesis to pharmacologically block γ -secretase dependent actions of presenilin in both dissociated and organotypic slice cultures. (Adapted from Tomita and Iwatsubo, 2004).

(b) Molecular structure of β -secretase inhibitor IV (β -sec IV) (green). This drug was used to inhibit β -secretase activity in dissociated and organotypic slice cultures. (Adapted from Stachel et al., 2004).

2.4 Electrophysiology

2.4.1 Materials

Table 2.7: Chemicals / Reagents / Products used for electrophysiology

Product	Company	Location
2-chloroadenosine	Sigma - Aldrich	Dorset, UK
ATP dipotassium salt	Sigma - Aldrich	Dorset, UK
Axon pclamp 10.2	Molecular devices	Berkshire, UK
Borosilicate glass capillaries (150F- 7.5)	Harvard Apparatus	Edenbridge, UK
CNQX	Tocris Bioscience	Bristol, UK
Creatine phosphate dipotassium salt	Merck chemicals	Darmstadt, Germany
DB2 micropipette holders	G23 instruments	London, UK
DL-AP5	Tocris Bioscience	Bristol, UK
GTP sodium salt	Sigma - Aldrich	Dorset, UK
MK801 maleate	Tocris Bioscience	Bristol, UK
NBQX	Tocris Bioscience	Bristol, UK
Picrotoxin	Sigma - Aldrich	Dorset, UK
Tetrodotoxin citrate (TTX)	Tocris Bioscience	Bristol, UK

Table 2.8: Buffers and Solutions, used for electrophysiology

Buffer / Solution	Contents	Storage	Sterilisation
External solution for dissociated cultures	130 mM NaCl, 2.5 mM KCl, 2.2 mM CaCl ₂ , 1.5 mM MgCl ₂ , 10 mM HEPES, 10 mM D-glucose	4°C	0.2 µM filter
External solution for organotypic slice cultures	120 mM NaCl, 2.5 mM KCl, 2.2 mM CaCl ₂ , 1.5 mM MgCl ₂ , 1.25 mM NaH ₂ PO ₄ , 26 mM NaHCO ₃ , 11 mM D-glucose	4°C	0.2 µM filter
Internal solution for dissociated cultures and organotypic – mEPSC	100 mM K gluconate, 17 mM KCl, 5 mM NaCl, 10 mM HEPES–KOH, 0.5 mM EGTA–KOH, 4 mM MgCl ₂ , 20 mM K ₂ creatine phosphate, 4 mM K ₂ -ATP, 0.5 mM Na ₃ -GTP.	-20°C	0.2 µM filter
Internal solution for organotypic – mEPSC and mIPSC (low Cl internal)	105 mM K gluconate, 3 mM KCl, 2 mM NaCl, 10 mM HEPES–KOH, 0.5 mM EGTA–KOH, 20 mM K ₂ creatine phosphate, 4 mM K ₂ -ATP, 0.5 mM Na ₃ -GTP.	-20°C	0.2 µM filter
Internal solution for organotypic slices – paired-pulse and MK801 experiments	115 mM Cs methanosulfonate, 20 mM CsCl, 10 mM Cs-HEPES, 4 mM NaCl ₂ , 4 mM Mg-ATP, 0.5 mM Na ₃ -GTP, 10 mM K ₂ creatine phosphate, 0.5 mM EGTA–Cs.	-20°C	0.2 µM filter

Abbreviations: mEPSC – miniature excitatory postsynaptic current; mIPSC – miniature inhibitory postsynaptic current

2.4.2 Methods

Electrophysiology methods were used to study the electrical properties of neurons. For this thesis, recordings were made from visualised neurons in whole-cell configuration in voltage clamp mode. PS1 mice dissociated cultures were used between 10-16 DIV whilst rat dissociated culture recordings were performed on 10-17 DIV neurons. Organotypic slices were used at two different ages, from DIV 6-8 for paired-pulse ratio and MK801 block experiments and DIV 9-15 for miniature EPSC and IPSC recordings.

2.4.2.1 Patch clamp recordings from hippocampal dissociated cells

Coverslips were transferred from the incubator to the glass bottomed chamber of an Olympus IX70 inverted microscope. The microscope was fixed on a vibration isolation air-table (Technical manufacturing corporation, Massachusetts, US) and all connections and wires were grounded to the air table to minimise electrical noise. The amplifier was an Axopatch 200B linked to an Intel Celeron CPU (2.53 Hz) via a National instruments BNC-2090 board. Data was acquired using a custom programme written in house by Dr. D. Hagler (called Acquire). An Axon CV203BU headstage was attached to a XYZ stainless steel stage with actuators motorized from Newport which was securely attached to the microscope and remotely controlled using a Soma Instruments touch pad controller (MC300). Glass pipettes were pulled from thick walled filamented borosilicate capillaries (GC150F-7.5) using either a Narishige 2 stage vertical puller (Model PP830) or a Sutter Instruments Flaming/Brown horizontal puller (Model P97) using a 5 step program. Pipettes used for whole cell recordings were neither fire polished nor coated with sylgard. Pipettes were of 2.5-5.8 M Ω resistance when filled with potassium-gluconate internal solution using a plastic/fused silica micropipette (Microfil, World Precision Instruments, Florida, USA) attached to a 1ml syringe. The internal solution was filtered through a 0.4 μ m syringe filter prior to pipette filling to remove any dust (Nalgene, Hereford, UK). Glass pipettes were placed in a DB2 holder (G23 instruments, London, UK) which contained an Ag/AgCl wire (AgCl layer generated

using electrophoresis) and electrically connected to the headstage via a gold pin. An additional ground electrode, made from silver wire either coated with an AgCl layer or attached to a small AgCl pellet was submerged in extracellular solution in the bath chamber and connected to the headstage using insulated wire.

Positive and negative pressure could be applied to the recording electrode through a mouthpiece connected to the pipette holder by a length of silicone tubing to aid in achieving a giga-ohm seal. To obtain a recording, a recording electrode was placed in the bath chamber and the pipette offset was adjusted to zero using manual controls on the amplifier to eliminate the potential difference between the ground electrode and the recording pipette. The recording electrode was positioned above visually selected neurons using a 10x phase contrast objective (0.30 NA) and patched under differential interference contrast (DIC) optics with 40x magnification objective (0.85 NA). Pipette resistance and seal formation was monitored by applying a 5 mV (100 ms duration) test pulse in voltage-clamp mode. Positive pressure was applied to the patch pipette during the approach to the soma to prevent blockage of the pipette tip. Upon visualisation of a small dimple on the cell soma and an increase in electrode resistance, positive pressure was stopped and gentle suction was applied to the mouth piece to aid seal formation. When the seal increased to 100 M Ω , holding current was injected (voltage command -40 mV) to promote formation of a high resistance seal (>1G Ω (cell-attached)). When cell-attached configuration was obtained, pipette capacitance transients were manually cancelled on the amplifier and the cell was set to a holding potential of -70 mV. To achieve the whole-cell configuration, short bursts of negative suction were applied to the pipette until the membrane at the tip of the patch pipette broke. Series resistance was uncompensated and input resistance and access resistance were monitored throughout the recording and recordings terminated if an increase of over 20% was observed. Holding current and resting membrane potential was also monitored at the start and end of recordings.

Dissociated cells were voltage clamped at -70 mV and recordings were filtered online at 2 kHz (4 pole Bessel filter) and digitized at 10 kHz using Acquire software. mEPSCs were continually recorded in the presence of 0.5 μ M TTX and 100 μ M picrotoxin. For a subset of neurons, CNQX (20 μ M) or NBQX (20 μ M) and DL-

AP5 (50 μM) was applied at the end of the mEPSC recording period to block glutamatergic currents to show that the events recorded, corresponded to excitatory currents. Recordings were carried out at room temperature and in external solution for dissociated cultures (see Table 2.8). For γ or β -secretase inhibitors experiments, drugs were also included in the bath solution during the recordings and coverslips were discarded 30-45 mins after removal from the incubator.

Analysis

Peak amplitude and frequency values were measured with Analyse software (written by D. Hagler) and input resistance, series resistance, cell capacitance, rise time and decay time were calculated in Igor 6.0.3.1 using custom scripts written by Dr. L.A. Cingolani in the lab. Cells with an access resistance of $<30 \text{ M}\Omega$ and resting membrane potential less than -45 mV were used for analysis. mEPSCs were identified offline using Analyse software. mEPSCs were scored based on the criteria that the decay time was slower than the rise time and amplitudes were at least double the baseline noise, using a threshold crossing principle. Raw traces were visually examined and false events were not counted. Analysis of dissociated cells was performed on a 100 sec time window at the beginning of each continuous recording. Cells with large baseline fluctuations which did not permit an accurate measure of baseline values were not analysed.

To estimate the rise and decay times, the baseline of each single event was taken as the average value from -2.5 ms to -12.5 ms before the peak mEPSC amplitude. The time to reach from 10 to 90% of the peak amplitude was taken as the rise time value.

For the decay time, the following formula was used:

$$\text{Decay } \tau = \frac{\int_{t_p}^{t_b} I(t) dt}{I_p}$$

where the area between 10 to 90% of the decay slope (peak amplitude to downstream baseline) was divided by the peak amplitude.

Series resistance (R_s), input resistance (R_{in}) and cell capacitance (C_m) was calculated from a 5 mV (100ms duration) test pulse from each cell, using the following equations:

$$R_s = \Delta V / I_i$$

where ΔV was 5 mV, and I_i was the instantaneous current;

$$R_{in} = \Delta V / I_{ss}$$

where ΔV was 5 mV, and I_{ss} was the steady state current;

$$C_m = \tau / R_s$$

where τ was estimated using a double exponential fit of the decay phase of the instantaneous current, and R_s was series resistance.

2.4.2.2 Electrophysiology from hippocampal organotypic slice cultures

The procedure for electrophysiological recordings in organotypic slice cultures was the same as that outlined for dissociated cultures (see section 2.4.2.1) except for the following modifications. Hippocampal slice cultures were transferred to the glass bottomed chamber of an Olympus BX50WI upright microscope and held in place using 5 parallel dental floss fibres attached to a U shaped flattened platinum wire. An Axopatch 200B amplifier was connected to an Intel Pentium 4 CPU (2.8 Hz) via an Axon instruments digidata 1440A. Slice recordings were made using either Acquire software or Clampex 10.2 (Axon instruments). An Axon CV203BU headstage was attached to a Luigs and Neumann motorized micromanipulator which was mounted to the vibration isolation table and moved independently from the microscope. The slice was continuously perfused with organotypic extracellular

solution (bubbled with 95% O₂ and 5% CO₂) at a flow rate of 1.0-1.5 ml/min delivered using either a gravity flow perfusion system linked to a Capex L2C (Charles Austen) vacuum pump or a peristaltic pump (Ismatec) where the inflow rate was equalized to the outflow rate. 10x (0.30 NA) and 40x (0.80 NA) water immersion objectives were used with DIC optics to visually identify CA1 pyramidal cells in the hippocampal slice. In some slices, a mild positive pressure was applied for a short period to the surface of the slice to remove excess debris from the cell soma (Edwards et al., 1989). The pipette was then withdrawn from the bath and replaced with a new pipette to attempt to patch cells in the cleaned region.

For mEPSC recordings in organotypic slices, the same conditions as that used for dissociated neurons were applied (see section 2.4.2.1). To record both mEPSCs and mIPSCs in organotypic slices, a low Cl internal was used (see Table 2.8). For these experiments cells were either held at -50 mV where both inward mEPSC and outward mIPSCs were observed simultaneously or cells were first held at -70 mV to detect inward mEPSC currents and then held at 0 mV to record outward mIPSCs. For experiments where evoked AMPA and NMDA EPSCs were examined, a cesium methanesulfonate based internal solution was used. For evoked current experiments, a single cut was also made between the CA3 and CA1 regions of the slice using a no. 10 blade to minimize recurrent activity. To evoke EPSCs, the Schaeffer collateral axons of the stratum radiatum were stimulated with a concentric bipolar electrode placed onto the superficial regions of the slice and at least 200 μ M from the cell soma to minimize the chances of stimulating the cell directly. For AMPA currents, cells were voltage clamped at -70 mV and Schaffer collaterals were stimulated to achieve an amplitude of approximately 30 pA. For NMDA currents, cells were voltage clamped at -40 mV, and stimulation was set to obtain a 50-80 pA current.

Paired-pulse ratio (PPR) and rate of NMDA current block using a non-competitive NMDA receptor antagonist, MK801, were used as two separate estimates of release probability. For paired-pulse experiments, neurons were voltage clamped at -70 mV and two identical afferent stimuli separated by 50 ms interval were used to evoke sequential excitatory postsynaptic currents. Each pair of stimuli was given at a frequency of 0.2 Hz and up to 80 sweeps were recorded. NBQX (10 μ M) was applied at the end of PPR experiments and blocked both EPSCs, confirming that the

currents were glutamatergic. NBQX was also perfused continuously to isolate the NMDA receptor current for MK801 experiments. The rate of NMDA current block by use-dependent antagonist MK801 was determined at a holding potential of -40 mV, which relieved the magnesium block of NMDA receptors to generate an inward NMDA current upon synaptic stimulation (Huang and Stevens, 1997). In this configuration, the presence of MK801 leads to a progressive reduction in NMDA receptor current amplitude due to block of open NMDA receptors (Huang and Stevens, 1997). After obtaining a stable baseline, a single current stimulus was applied to the Schaeffer collaterals to get a synaptic NMDA current. Stimulation was then stopped and MK801 (40 μ M) was bath applied for 9-10 min to ensure the slice was saturated with the inhibitor. After this period, MK801 was continuously perfused, and changes in the EPSC amplitude were monitored in response to stimulation at 0.125 Hz. Recordings were terminated after 150 sweeps. γ -secretase inhibitors, β -secretase inhibitors or 0.1% DMSO vehicle control was included in the perfusate when testing slices that had been chronically treated with these drugs.

Analysis

For mEPSC recordings made using Acquire, frequency and amplitude were determined in Analyse, whereas for data obtained using clampex 10.2, frequency and amplitude measurements were made in clampfit 10.2. Criteria for miniature event detection were the same as that described for dissociated cells. For rise time and decay time measurements the same method as that used for dissociated cells was applied except the baseline of each single event was taken as the average value from -7 to -17 ms before the peak mEPSC amplitude. Analysis was performed on 5 min continuous recordings. Paired-pulse ratio and MK801 block experiments were analysed in Clampfit 10.2. Initial experiments estimating paired-pulse ratio were performed in the presence of 2-chloroadenosine, an agonist of presynaptic A1 receptors that reduces polysynaptic excitation (Futai et al., 2007)(data not shown). Other reports (Scanziani et al., 1992) have shown that 2-chloroadenosine could have a strong influence on presynaptic release probability, and thus experiments were repeated in the absence of 2-chloroadenosine. All experiments presented in this thesis were from the latter group. Due to the lack of 2-chloroadenosine, occasional bursting activity was observed in a minority of organotypic slices. Sweeps containing bursting activity were eliminated from analysis. The baseline of each

sweep was calculated by taking the average over a 20 ms period up to 3.5 ms before the first stimulation. To obtain the paired-pulse ratio of a cell, the mean peak amplitude of the 2nd EPSC was divided by the mean peak amplitude of the 1st EPSC (A_2/A_1). Approximately 68 – 80 sweeps were averaged and analysed. To measure the rate of MK801 block, the peak amplitude of each EPSC was plotted against time and a mono-exponential decay curve fit was used to obtain the time constant (τ) of MK801 block for each cell. The NMDA current amplitude generated by the first stimuli in the presence of MK801 was set to one and all subsequent NMDA current responses were normalised to the amplitude of the first stimuli.

2.5 FM Imaging

2.5.1 Materials

Table 2.9: Chemicals / Reagents / Products used for FM imaging experiments

Product	Company	Location
Advasep - 7	Biotium	Hayward, CA, US
CNQX	Tocris biosciences	Bristol, UK
DL – AP5	Tocris biosciences	Bristol, UK
Field stimulation chamber	Custom made in house	London, UK
FM 1-43	Invitrogen	Paisley, UK
Metamorph software	Molecular devices	Berkshire, UK
Stimulator	Grass technologies	Slough, UK

Table 2.10: Buffers and Solutions, used for FM imaging experiments

Buffer / Solution	Contents	Storage	Sterilisation
External solution for dissociated cultures - 2.2 mM (normal) calcium	130 mM NaCl, 2.5 mM KCl, 2.2 mM CaCl ₂ , 1.5 mM MgCl ₂ , 10 mM HEPES, 10 mM D-glucose, 10 µM CNQX, 50 µM DL-AP5, 100 µM picrotoxin	4°C	0.2 µM filter
External solution for dissociated cultures - 1 mM (low) calcium	130 mM NaCl, 2.5 mM KCl, 1 mM CaCl ₂ , 2 mM MgCl ₂ , 10 mM HEPES, 10 mM D-glucose, 10 µM CNQX, 50 µM DL-AP5, 100 µM picrotoxin	4°C	0.2 µM filter
External solution for dissociated cultures - 5 mM (high) calcium	130 mM NaCl, 2.5 mM KCl, 5 mM CaCl ₂ , 0.6 mM MgCl ₂ , 10 mM HEPES, 10 mM D-glucose, 10 µM CNQX, 50 µM DL-AP5, 100 µM picrotoxin	4°C	0.2 µM filter
External solution for dissociated cultures - 0.5 mM calcium (used for washes and removal of FM dye)	130 mM NaCl, 2.5 mM KCl, 0.5 mM CaCl ₂ , 10 mM MgCl ₂ , 10 mM HEPES, 10 mM D-glucose, 10 µM CNQX, 50 µM DL-AP5, 100 µM picrotoxin	4°C	0.2 µM filter

2.5.2 Methods

2.5.2.1 FM Styryl-dye labeling and imaging

FM-dye labelling and visualisation of neurons was conducted on an Olympus BX50WI upright epifluorescence microscope setup. Dissociated cells loaded with FM1-43 were viewed through a 40x (0.80 NA) water immersion objective using a

475/40 nm excitation filter, 505LP dichroic and a 535/45 nm emission filter with light supplied by a Prior Lumen 200 illumination system. Metamorph 7.1.0.0 imaging software running on an Intel Celeron CPU (2.53 GHz) was used to control a Princeton Instruments 1392 x 1040 cooled-CCD camera and a Uniblitz VMM-D1 shutter driver to enable time lapse acquisition of 12-bit images. A gravity flow perfusion system (1-2 ml/min) with suction supplied by a Capex vacuum pump was used for washing away excess extracellular dye.

A glass bottomed, custom built slotted field stimulation chamber assembled with two parallel platinum wires set 1 cm apart, was used to induce stimulated uptake of styryl dye, FM1-43 dye into synaptic vesicles. Extracellular field stimulation consisted of a 2 ms 22 V square pulses applied via a stimulator (Grass, Astro-Med, USA) connected to the platinum wires. To selectively load the recycling vesicle pool, 600 stimuli at 10 Hz was applied to the cells in the presence of FM1-43 (10 μ M) in the extracellular solution for dissociated neurons. After stimulation, neurons remained in solution containing the dye for a further 30 sec for vesicle endocytosis to complete (Murthy et al., 1997; Tokuoka and Goda, 2008). Cells were then rinsed 1x for 30 sec using 0.5 mM calcium solution, followed by a 1 min wash with a fluorescent quenching agent Advasep-7 (1 mM, Biotium) in 0.5 mM calcium solution. Advasep-7 was then removed from the solution and a 7-8 min wash in low calcium solution was applied to remove excess dye from the extracellular space and plasma membranes. Low 0.5 mM calcium solution also helped to reduce unloading of the dye by spontaneous spikes.

An estimate of release probability at single synapses was obtained by examining the rate of vesicle exocytosis (destaining) of the recycling pool (Branco et al., 2008). For this, neurons were returned to normal calcium (2.2 mM) dissociated solution and stimulated using 900 stimuli at 5 Hz (Murthy et al., 1997) to cause vesicle release which can be visualized by a gradual decrease in FM fluorescence intensity at presynaptic puncta. Field stimulation applied to induce synaptic vesicle exocytosis also helped differentiate actively recycling vesicles (which lost fluorescence when stimulated) from non-specific tissue staining or unhealthy neurons (which did not respond to stimulation). For all exocytosis stimulations, timelapse images were acquired every 10 sec for 5 mins (700 ms exposure time), and a 60 sec baseline (zero

stimulation) period was made prior to initiating stimulation to monitor any possible photobleaching.

An estimate of the readily releasable pool size (RRP) at presynaptic terminals was performed by stimulating FM dye uptake using 30 stimuli at 1 Hz field stimulation (Tokuoka and Goda, 2008; Waters and Smith, 2000). Following an 8 min wash period in 0.5 mM calcium, cells were stimulated using 600 stimuli at 20 Hz repeated 3 times with a 15 sec interval between each train to induce destaining of dye from the RRP. Dissociated cells of DIV 13-17 were used for FM experiments. All FM imaging experiments were performed at room temperature in the presence of 10 μ M CNQX and 50 μ M DL-AP5 to prevent recurrent activity, and 100 μ M picrotoxin to block GABA_A currents. *n* refers to the number of coverslips used and an average of 50 boutons were imaged for each coverslip.

Analysis

Image analysis of FM experiments was performed in metamorph 7.1.0.0. For both recycling pool and RRP experiments, FM loaded puncta were selected by placing a size 5 ellipse around fluorescent regions located along a neuronal process. For estimates of local background levels in recycling pool destaining experiments, a size 5 ellipse was placed on non fluorescent (and non neuronal) regions located adjacent to the FM loaded bouton. For each frame, background region measurements were averaged and this value was subtracted from each FM loaded region at the same time point. All data points were normalized to the fluorescence of the first frame and fluorescence pixel measurements were plotted against time. A plateau followed by a monotonic decay curve (least squares fit) was fitted to estimate the decay constant for FM destaining in Prism (version 5.0.1, Graphpad).

Background subtraction for the readily releasable pool experiments was obtained by taking the remaining fluorescence at the end of the destaining protocol from the fluorescence obtained prior to destaining. Fluorescence values (post background subtraction) for the RRP were determined by taking an average of the first five frames prior to destaining. The fluorescence values of γ -secretase inhibitor treated cells were normalized to the fluorescence values of DMSO control cells from the same preparation.

2.6 Calcium imaging

2.6.1 Materials

Table 2.11: Chemicals / Reagents / Products used for calcium imaging

Product	Company	Location
EGTA AM	Invitrogen	Paisley, UK
Fluorescein	Sigma	Dorset, UK
Fura-2 AM	Invitrogen	Paisley, UK
Image pro plus	Media cybernetics	Bethesda, MD, US
Ionomycin	Sigma	Dorset, UK
Ryanodine	Tocris Bioscience	Bristol, UK
Thapsigargin	Tocris Bioscience	Bristol, UK

Table 2.12: Buffers and Solutions, used for calcium imaging

Buffer / solution	Contents	Storage	Sterilisation
External solution for basal calcium measurements	130 mM NaCl, 2.5 mM KCl, 2.2 mM CaCl ₂ , 1.5 mM MgCl ₂ , 10 mM HEPES, 10 mM D-glucose, 100 µM picrotoxin	4°C	0.2 µM filter
External solution for KCl based depolarisation	72.5 mM NaCl, 60 mM KCl, 2.2 mM CaCl ₂ , 1.5 mM MgCl ₂ , 10 mM HEPES, 10 mM D-glucose, 100 µM picrotoxin	4°C	0.2 µM filter
External solution for measurement of R min (zero CaCl ₂)	130 mM NaCl, 2.5 mM KCl, , 1.5 mM MgCl ₂ , 10 mM HEPES, 10 mM D-glucose,	4°C	0.2 µM filter

	100 μ M picrotoxin, 4 mM EGTA-AM		
External solution for KCl induced depolarisation during measurement of R min (zero CaCl_2)	72.5 mM NaCl, 60 mM KCl, 1.5 mM MgCl_2 , 10 mM HEPES, 10 mM D-glucose, 100 μ M picrotoxin, 4 mM EGTA-AM	4°C	0.2 μ M filter

2.6.2 Methods

2.6.2.1 Live calcium imaging with Fura-2

Fura-2 is a polyamino carboxylic acid which is capable of binding free calcium ions in cells. Upon binding calcium, the fluorescence excitation wavelength maximum shifts from 363 nm (calcium free) to 335 nm (calcium bound) (Figure 2.3 a). This property of Fura-2 enables ratiometric estimates of intracellular calcium concentrations by monitoring the fluorescence at wavelengths of 340 nm (increases in signal upon binding calcium) and 380 nm (decreases in signal upon binding calcium). Such ratiometric dyes were preferred over single wavelength dyes as measurements should be independent of variations in dye loading, intracellular dye concentration and differences in neuronal structure. A non-fluorescent, membrane permeable (uncharged) form of Fura-2, Fura-2-acetoxymethyl ester (Fura-2-AM) was used to deliver the dye into cells. When applied to the bath, Fura-2-AM can pass from the extracellular space into the intracellular compartment of cells where endogenous intracellular esterases can cleave the AM groups to generate the charged, less membrane permeable, and fluorescent molecule known as Fura-2 (Figure 2.3 b).

Fura-2 imaging of neurons was conducted on a Zeiss Axiovert 135 TV inverted microscope setup. This microscope set up was kindly provided by Professor John Garthwaite and Dr Andrew Batchelor at UCL. Dissociated cells containing Fura-2 were viewed through a 10x fluar (0.5 NA) air objective using a 340/15 nm and

380/15 nm excitation filter, 430 LP dichroic and a 510/40 nm emission filter with light supplied by a Prior Lumen 200 illumination system. Image Pro 6.3 Software (Media cybernetics Inc, Bethesda, USA) was used to control a Qimaging Rolera XR Camera and paired 340 and 380 nm wavelengths 12 bit monochrome images were acquired using a filter wheel switching mechanism inside the Prior Lumen 200 lamp housing. Cells were continuously perfused with extracellular dissociated solution containing picrotoxin (100 μ M) at 1.5- 2 ml/min using a peristaltic pump (Ismatec). Tetrodotoxin (TTX, 0.5 μ M) was used to block calcium signals resulting from spontaneous network activity. DMSO mock, γ -secretase inhibitors or intracellular store drugs (ryanodine or thapsigargin) were also maintained in the extracellular solution following a chronic drug treatment. Dissociated cultures from DIV 13-15 were used.

Cells were loaded by preincubating coverslips in Fura-2 AM (1 μ M) dissolved in dissociated culture media for 25 min at 37°C/ 5% CO₂ incubator. After this period, coverslips were briefly rinsed in extracellular dissociated cell solution and placed onto the microscope chamber. A DIC image was taken to aid neuronal identification. For background subtraction, 340 nm and 380 nm fluorescence images were acquired from a region within the microscope chamber that was not associated with the coverslip i.e. a non cellular region. For data collection, a region of the coverslip containing small networks of healthy neurons was selected and paired timelapse images were captured by rapid sequential switching from 340 nm (600 ms exposure) to 380 nm (60 ms exposure) wavelengths. Paired 340 and 380 nm images were captured every 2.18 sec and the ratio for each frame was obtained by dividing fluorescence values excited by 340 nm and 380 nm wavelengths.

Initial experiments were performed to determine the overall spontaneous network activity of dissociated neuronal cultures. Preliminary observations showed that the number of spontaneous calcium transients was variable from preparation to preparation but also from coverslip to coverslip (see Figure 2.4 for examples). Spontaneous calcium transients were usually highly temporally synchronized across cells (as shown in Figure 2.4) and could be blocked with sodium channel inhibitor, TTX (Figure 2.4 b). For all experiments presented in chapter 6, TTX was present throughout the course of the experiment. The maintenance of cells in TTX for the

duration of the experiment provided conditions similar to those used during mEPSC recordings.

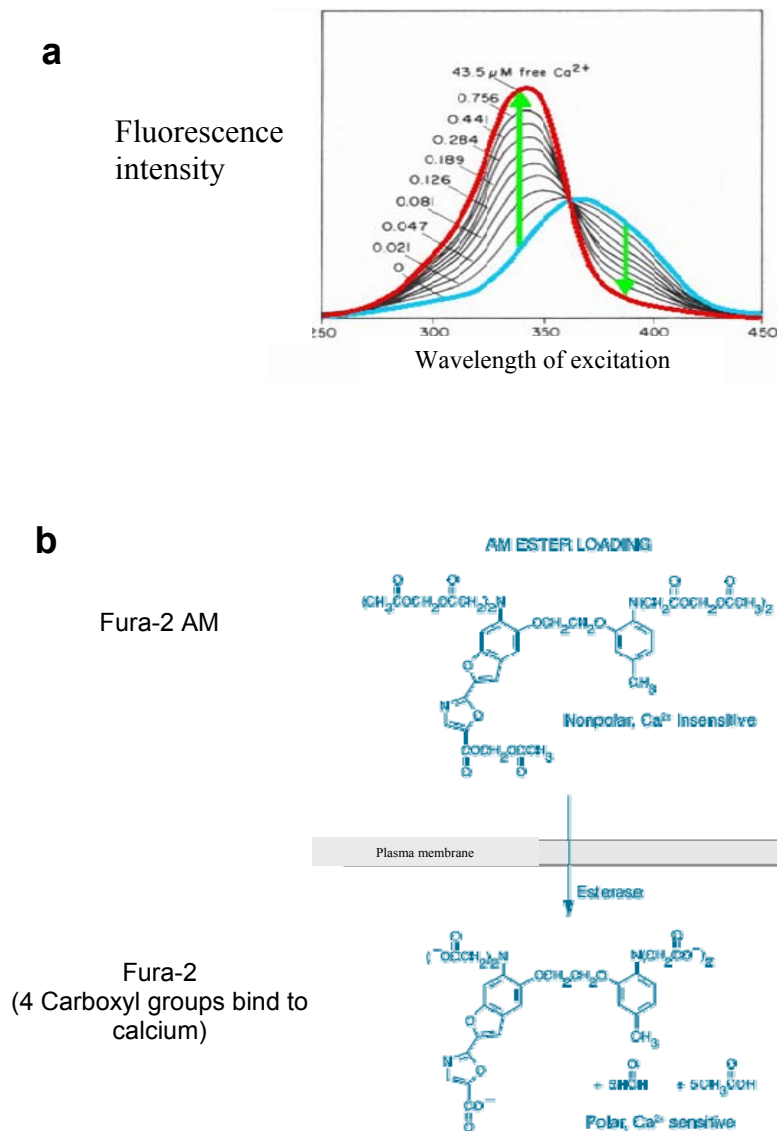


Figure 2.3 - Properties of Fura-2 (AM)

(a) Ratiometric properties of Fura-2 are displayed. Binding of calcium to Fura-2 causes a spectral shift of the fluorescence excitation maximum from 363 nm (calcium free) to 335 nm (calcium bound). By imaging at 340 and 380 wavelengths, the intracellular calcium ratio and concentrations can be estimated. Adapted from www.bphys.uni-linz.ac.at

(b) Fura-2 AM contains acetoxymethyl (AM) ester groups which generate an uncharged molecule which can permeate plasma membranes. Once inside the cell, intracellular endogenous esterases cleave the AM ester groups to give rise to a Fura-2, a charged and less membrane permeable form of the calcium dye. Fura-2 form is fluorescent and binds intracellular free calcium. Adapted from www.biotek.com

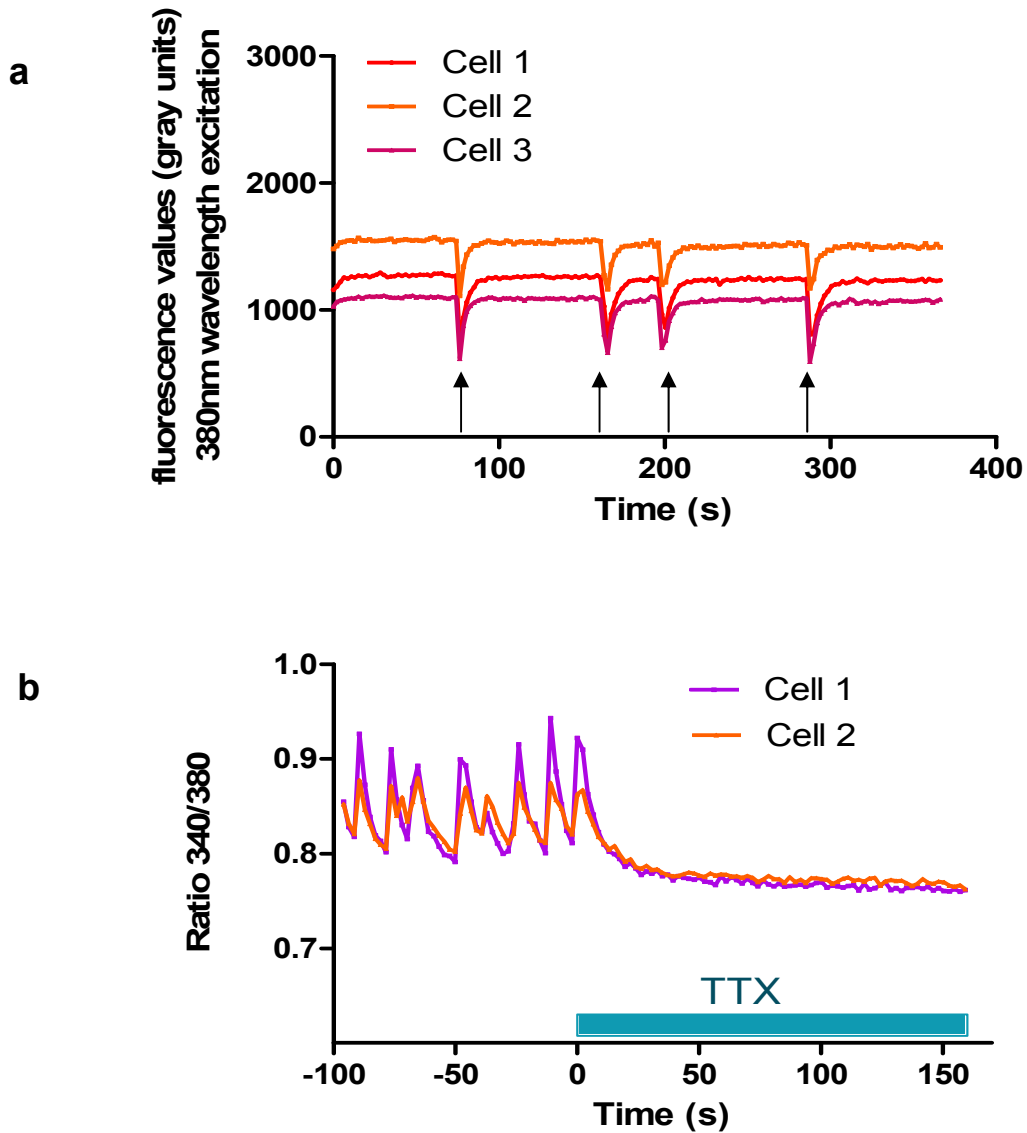


Figure 2.4 - Spontaneous calcium transients in hippocampal dissociated neurons

(a) The presence of highly temporally synchronised calcium transients in 3 different neurons in a hippocampal dissociated culture at DIV 14. Calcium transients were measured using 380 nm wavelength and are represented as downward deflections (see arrows) from baseline basal calcium.

(b) Spontaneous calcium transients are presented as the ratio between 340 nm and 380 nm wavelengths and seen as upward deflections. Application of 500 nM TTX at time 0 eliminates all calcium transients suggesting these calcium signals result purely from spontaneous action potential generation within the neuronal network.

2.6.2.2 Basal and KCl-stimulated calcium induced calcium release (KCl-stimulated CICR).

Basal and KCl-stimulated CICR calcium was measured in the same cells. Basal calcium was taken as the calcium measurements in the absence of exogenous stimulation. KCl-stimulated CICR was stimulated using 30 sec bath application of 60 mM KCl in extracellular bath solution. KCl equiosmolarly replaced NaCl to maintain osmotic balance at 285-290 mOsm.

To examine the period that KCl remains in the bath and evaluate the time taken for solutions to enter and exchange in the microscope chamber, the same protocol used for KCl application during CICR experiments was re-run after data had been collected but with KCl being replaced with a fluorescein solution (50-200 μ M). Figure 2.5 shows the fluorescence signal from a cell loaded with Fura-2 and excited using 340 nm wavelengths. The fluorescence of the cell before, during and after KCl application (application shown by black and white checkered bar) is represented as a solid red line. Note how the cellular fluorescence signal increases in response to KCl application and then decays back to baseline levels. This same protocol was administered once again but with 30 sec fluorescein application instead of KCl. The timecourse for fluorescein application is represented by a dashed red line and is superimposed onto the timecourse of KCl application. The fluorescence signal observed during fluorescein application is much stronger than the signal seen during KCl application (and effectively saturates the pixels of the camera) but provides an estimate of the time taken for solutions to exchange in the microscope chamber. The superimposed KCl and fluorescein applications also show that the cellular change in fluorescence in response to KCl is temporally matched to the amount of time KCl is in the microscope chamber.

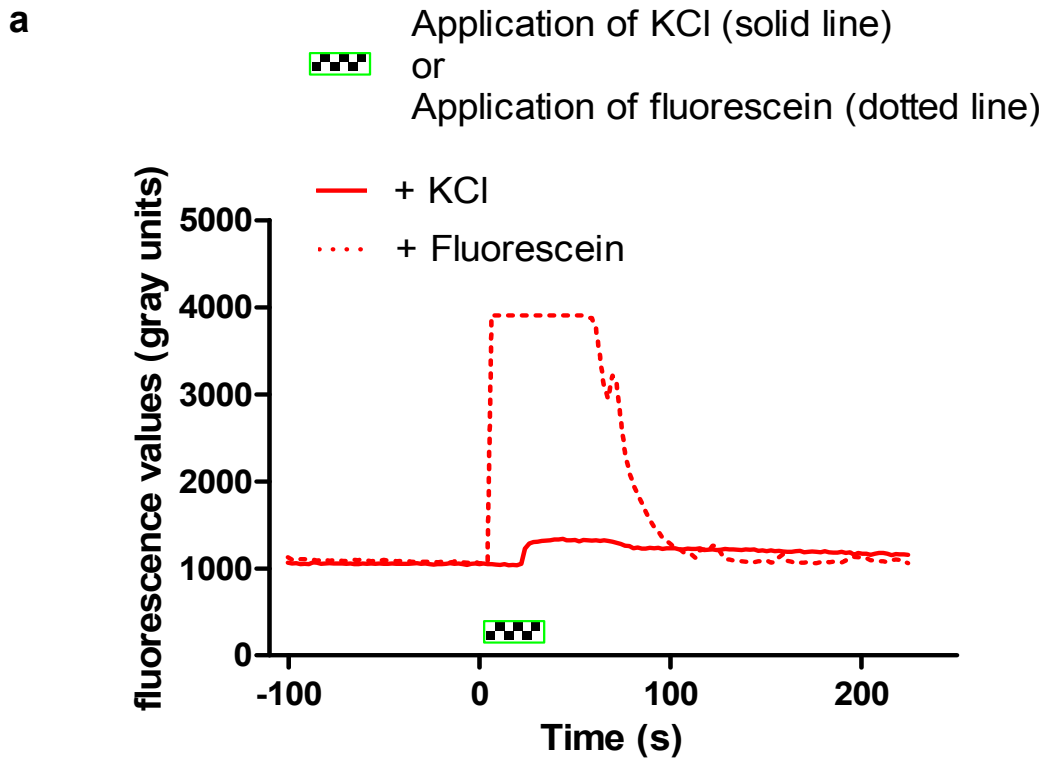


Figure 2.5 - Estimation of bath exchange rate during calcium imaging experiments

(a) The solid red line shows the 340 nm wavelength fluorescence response of a neuron loaded with fura-2 before, during and after 60 mM KCl application. KCl was applied at time 0 for 30 sec, indicated by checked box. KCl application is represented by the black and white checked box. Note the modest increase in fluorescence values during KCl application.

The dotted red line shows a subsequent fluorescein (100 μ M) application (using the same protocol as that used for KCl, but with KCl being replaced by fluorescein) onto the same cell. Note the rapid and dramatic increase in fluorescence values upon fluorescein application (application represented by black and white checked box). The plateau phase represents saturation of the camera. Note how the fluorescence values come back to baseline by \sim 100-120 sec after application. This suggests that the bath exchange time is approximately 100-120 sec.

2.6.2.3 Estimating calcium concentration in hippocampal dissociated cultures

In addition to the direct comparison of ratio values, these values can also be used to estimate intracellular calcium concentrations ($[Ca^{2+}]_i$) according to standard procedures first described by Grynkiewicz et al., (1985) using the following equation:

$$[Ca^{2+}]_i = K_d (Sf2/Sb2) (R - R_{min} / R_{max} - R)$$

In this equation, K_d is the dissociation constant of fura-2 for calcium at room temperature, and it is set at 135 nM (Grynkiewicz et al., 1985; Koch and Barish, 1994). $Sf2$, $Sb2$, R_{min} and R_{max} values were calculated *in situ* from hippocampal neuronal cultures. $Sf2$ refers to the amount of free calcium and $Sb2$ is the amount of bound calcium measured using 380 nm excitation wavelength. $Sf2$ was determined by taking the 380 nm fluorescence in zero calcium and $Sb2$ was taken as the 380 nm fluorescence in 2.2 mM external calcium. The $Sf2/Sb2$ ratio was calculated to be 7.7 by taking the mean 340/380 nm values from 4 separate coverslips.

R_{min} is the estimated 340/380 fluorescence ratio obtained in the absence of calcium. To obtain *in situ* measurements of this ratio value, the ionophore, ionomycin (10-20 μ M) (Erdahl et al., 1995; Wang et al., 1998) with 4 mM EGTA and 0 mM extracellular calcium was bath applied to hippocampal cultures to reduce free calcium as much as possible (Brenowitz and Regehr, 2003) (Figure 2.6, solid red bar shows ionomycin, EGTA, 0mM calcium extracellular solution application). After several minutes upon application, a minor but stable drop in ratio values (Figure 2.6, red line) was observed, relative to the baseline ratio measured in 2.2 mM calcium extracellular solution (Figure 2.6 green line represents cellular response at 2.2 mM calcium). R_{min} was taken as the minimum value during the plateau in the presence of ionomycin and EGTA in 0 mM calcium and was 0.68 (n=4 coverslips).

R_{max} is the estimated 340/380 fluorescence ratio obtained in the presence of saturating concentrations of calcium. For this, ionomycin (10-20 μ M) was bath applied in 2.2 mM calcium extracellular solution (Figure 2.7, solid blue bar shows ionomycin application). After several minutes of application, ratio values gradually

increased, indicating an increase in intracellular calcium, which was followed by a plateau phase corresponding to the saturation of fura-2 (Figure 2.7, blue line). The plateau value gave an R_{max} value of 14.05 (n=4 coverslips).

As R_{min} and R_{max} values were applied to all subsequent ratio values to estimate intracellular calcium levels, it was important to show that the range of fluorescence observed during basal conditions and high KCl-stimulated CICR (discussed later) is within the range set by *in situ* measurements of R_{min} and R_{max} . To test this, ratio values for both basal and KCl-stimulated CICR conditions were obtained prior to measurement of R_{min} or R_{max} in hippocampal cells. The green line on Figure 2.6 and Figure 2.7 shows ratio values for basal calcium and during KCl application (black and white checked bar). This result shows that basal and peak CICR ratio values obtained in the same cells as that used to measure R_{min} and R_{max} were within the range of R_{min} and R_{max} measurements. Additionally basal and CICR ratio values obtained in cells where either R_{min} or R_{max} measurements were also measured were similar to the ratio values obtained for subsequent experiments where R_{min} and R_{max} were not calculated (see chapter 6). Due to this outcome, I justified that R_{min} and R_{max} values could be applied to all ratio measurements.

As a further control to show that the increase in ratio obtained during KCl-stimulated CICR was associated in part with extracellular calcium concentration, KCl was applied in the presence of 0 mM calcium extracellular solution during the plateau phase of R_{min} measurements where cellular calcium concentrations was assumed to be at its lowest point. The purple line on Figure 2.6 shows the basal and CICR ratio values in 0 mM calcium and KCl application is indicated by the checked box. As expected, no changes in fluorescence ratio were observed during KCl application in the absence of calcium; this strongly indicated that KCl-stimulated CICR requires calcium influx from the extracellular solution (Figure 2.6.).

Analysis

Fura-2 images were analysed in Image J (NIH, US). To make results comparable to an earlier published study (Zhang et al., 2009), analysis was performed on somatic regions (see also Basarsky et al., 1994; Koch and Barish, 1994). Neuronal somas were traced on DIC images and the template was overlaid onto 340 nm and 380 nm fluorescence images. Fluorescence values for each frame were noted for both wavelengths and the ratio for each frame was calculated by dividing 340 nm values by 380 nm values (340/380). Regions of interest were also superimposed onto background images and the mean fluorescence from these regions was subtracted from both 340 and 380 nm images at matched timepoints.

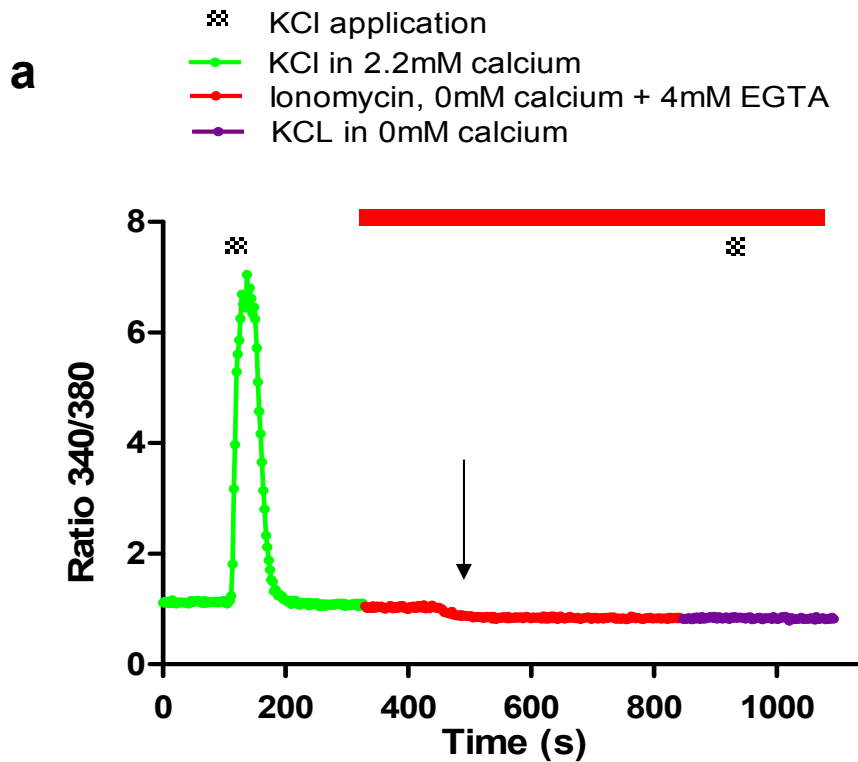


Figure 2.6 - Calculation of R_{min} in hippocampal neurons *in situ*

(a) The cellular response of a neuron during basal conditions and during KCl-stimulated CICR in the presence of 2.2 mM calcium extracellular solution (light green line). The black and white checked bar shows KCl application period (30 sec). This pattern reflects a typical cellular response to KCl application. To calculate R_{min} in hippocampal cells, ionomycin (20 μ M) and 4 mM EGTA in 0 mM calcium extracellular solution was applied to the bath. The red line shows the cellular response and the solid red bar represents ionomycin/EGTA application period. Note the drop in ratio values approximately 2 min into application of ionomycin solution, indicated by black arrow. The plateau phase following the ratio drop is considered the time point where Fura-2 is minimally bound by calcium (calcium free) and represents R_{min} . The purple line shows the cellular response to a further application of KCl (second black and white checked bar) whilst in the presence of 0 mM extracellular calcium. Note how there is no increase in ratio values during this second KCl application, in the absence of extracellular calcium. This result shows that KCl-stimulated CICR occurs only in the presence of calcium.

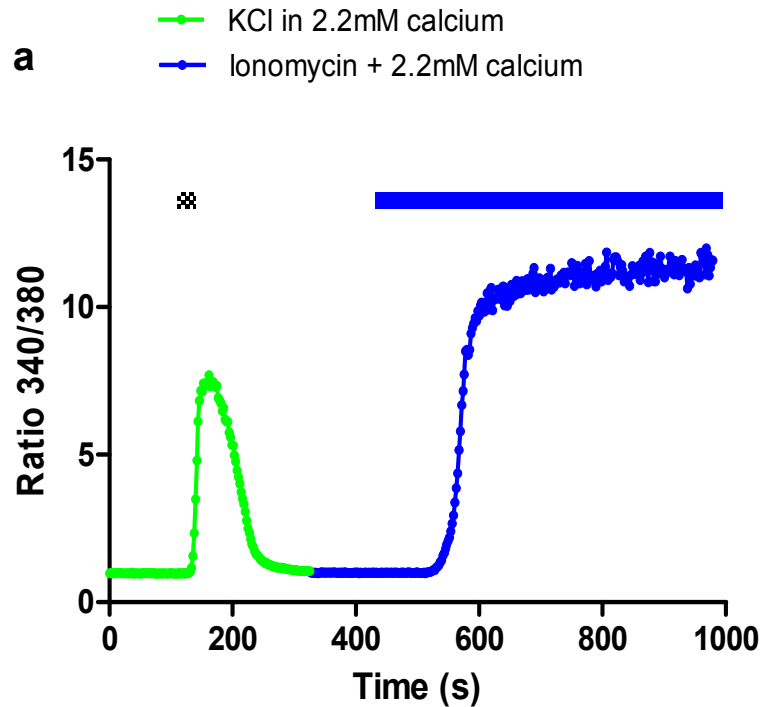


Figure 2.7 - Calculation of Rmax in hippocampal neurons *in situ*

(a) The cellular response of a neuron during basal conditions and during KCL-stimulated CICR in the presence of 2.2 mM calcium extracellular solution (light green line). The black and white checked bar shows KCl application period (30 sec). This pattern reflects a typical cellular response to KCl application.

To calculate Rmax in hippocampal cells, ionomycin (20 μ M) in 2.2 mM calcium extracellular solution was applied to the bath. The blue line shows the cellular response and the solid blue bar represents ionomycin application period. Note the increase in ratio values approximately 2-3 min into the application of ionomycin. The plateau phase following the increase in ratio is considered the time point where Fura-2 is maximally bound by calcium (dye is saturated) and represents Rmax. Note that Rmax ratio values are higher than values obtained during KCl application suggesting that calcium influx upon KCl application does not saturate the calcium dye.

2.7 Immunocytochemical fluorescence imaging

2.7.1 Materials

Table 2.13: Buffers and Solutions, used for immunocytochemistry

Buffer/solution	Contents	Storage
Phosphate buffered saline (PBS) 1x	137 mM NaCl, 27 mM KCl, 10 mM Na ₂ HPO ₄ , 1.8 mM KH ₂ PO ₄ , pH 7.3-4	Room temperature
Fixative solution	4% (v/v) paraformaldehyde (PFA), 4% (w/v) sucrose in 1x PBS. pH 7.3-4	Room temperature
Permeabilisation solution	0.3% (v/v) Triton X-100, 10% (v/v) goat serum in 1x PBS	Room temperature
Blocking solution	10% (v/v) goat serum in 1x PBS	Room temperature

2.7.2 Methods

2.7.2.1 Immunocytochemical examination of pre and postsynaptic proteins

Antibody labelling of dissociated cultures

Immunofluorescence labeling against synaptic proteins is an established method for identifying synaptic connections in primary culture systems. Primary neuronal cultures are an ideal system for this technique as the extracellular matrix is fairly low compared to brain tissue and thus background staining is minimal, which aids reliable identification of synapses. To identify synapses, primary antibodies against presynaptic vesicle markers, synapsin (1:800 dilution, anti-mouse or rabbit, synaptic systems, Germany) or synaptophysin (1:300, anti-rabbit, synaptic systems) and postsynaptic markers, Homer (1:1500, anti-rabbit, synaptic systems) or glutamate receptor subunit GluA1 (1:20 dilution, anti-rabbit, Calbiochem) were used.

Additionally, an antibody against microtubule associated protein 2 (MAP2, 1:800, anti-chicken, Abcam) was applied to all coverslips to label neuronal processes.

For rat dissociated neurons treated with γ -secretase inhibitors and β -secretase inhibitor IV, both postsynaptic GluA1 and Homer staining was performed with synapsin as a presynaptic marker. For PS1 mice cultures, only synaptophysin staining was performed.

As the epitope for the GluA1 antibody was located on the N-terminus extracellular domain, labelling was performed on live cultures. Thus, with a restricted period of incubation (16 min), this antibody should presumably label a large proportion of the surface population of GluA1 receptors and a minimal amount of the intracellular pool due to the slow rate of endocytosis (Adesnik et al., 2005; Cingolani et al., 2008; Passafaro et al., 2001). For Homer, synapsin and synaptophysin where the protein is largely located within the intracellular compartment, antibodies were applied after fixation.

The procedure below outlines the steps for double pre and postsynaptic marker labelling. For cells where GluA1 was co-labelled with synapsin, all points in the procedure apply. For cells that were either co-labelled with synapsin and Homer or labelled with synaptophysin alone all steps prior to fixation were omitted. GluA1 primary antibodies were applied directly to culture media. All other primary and secondary antibodies were applied in PBS solution containing 10% (v/v) goat serum.

GluA1 antibody was diluted in conditioned culture medium (1:20 dilution) and applied to coverslips. Coverslips were maintained in a 5% CO₂ incubator at 37°C for 16 min. After this period, cells were rinsed with 37°C PBS 3-4 times and then fixed with 4% PFA/4% sucrose fixative solution (pH 7.25-7.35) at room temperature for 15 min. This fixative makes covalent cross-links between proteins to enable good preservation of cell structure (Cingolani et al., 2008; Passafaro et al., 2001; St-Laurent et al., 2006).

After fixation, cells were rinsed 3 times with PBS and subsequently permeabilised with 0.3% (v/v) Triton X-100 for 10 min. Coverslips were rinsed 2x with PBS and then incubated in a solution containing 10% (v/v) goat serum for 0.5-1 hr to block

non-specific sites. Next, primary antibodies (against Homer, synapsin, synaptophysin or MAP2) were applied for 1 hr at room temperature. After this period, cells were washed 4x with PBS, with each wash lasting 10 minutes. Cy-2 or Cy-3 conjugated secondary antibodies (1:300 dilution, anti-rabbit or mouse, Jackson Immunoresearch) were applied to label either pre or postsynaptic proteins. Secondary antibodies were species matched with primary antibodies, for example, presynaptic synapsin was labelled with an anti-mouse monoclonal primary antibody and a mouse secondary antibody was used to fluorescently conjugate the primary antibody. In this case, the postsynaptic marker was labelled with an antibody from a different species to the presynaptic antibody, for example, a polyclonal rabbit primary antibody would be used to label GluA1 and an anti-rabbit secondary antibody of a different colour to the presynaptic antibody was used. An AMCA secondary antibody (1:200 dilution, anti-chicken, Jackson Immunoresearch) was used to label MAP2. All secondary antibodies were applied for 1 hour at room temperature. Cells were washed 4x with PBS, with each wash lasting 10 mins to remove excess unbound secondary antibody. One final wash in 0.1% PBS was made prior to mounting using antifade solution (Sigma) onto glass slides. Coverslips were left overnight at room temperature and then sealed with nail varnish before acquiring images on a confocal microscope.

Confocal imaging

Confocal images were obtained using a Leica SPE confocal microscope, mounted on a Leica DM2500 inverted microscope using a 40x oil objective (1.15 NA). AMCA fluorophore was excited with a 405 nm solid state laser and emission fluorescence between 412-469 nm wavelengths was collected with a spectrophotometer detector. The 405 nm excitation laser was used with a 405/532 nm dichroic mirror. Cy2 fluorophore was excited with a 488 nm solid state laser and emission fluorescence between 500-530 nm wavelengths was collected. The 488 nm solid state laser was used with a 488/635 nm dichroic mirror. Cy3 fluorophore was excited by a 532 solid state laser; with a 405/532 nm dichroic mirror and emission fluorescence between 570-723 nm wavelengths was collected. Confocal Z-stacks were acquired using a sequential line-scan mode, with 3x scan averaging, 1x accumulation, and 0.3 μm between optical planes. The pinhole diameter was set to 1 Airy units, and 1024

x 1024 pixel, 8 bit images were captured using Leica LASAF software. Images for test and control groups were acquired within the same imaging session where the same laser power, gain and offset settings were used for all groups.

Analysis of pre and postsynaptic marker number

All drug treatment groups were processed, imaged and analysed together with DMSO mock control groups. Images were either acquired or analysed (or both) blind to treatment. Analysis was performed on z-series projections made from all images that were in focus. All images were processed with a smoothing function prior to generating of the z-series projection. For synapse density measurements, somatic regions were excluded from analysis. For this, the perimeter of the soma was manually traced and a zero value was applied to all pixels within the traced region. Only presynaptic (synapsin and synaptophysin) and postsynaptic (GluA1 and Homer) markers that co-localised with MAP2 signal were used for analysis in order to exclude background staining with synaptic markers. Practically, a MAP2 mask was generated by thresholding the MAP2 signal to the sum of the mode and standard deviation of the signal in the MAP2 channel. This mask was then applied to both pre and post synaptic marker images to create a template for synaptic marker analysis. All synaptic marker counts were processed using semi-automated non-subjective procedures in Image J to eliminate any potential bias. A rolling ball radius was applied to all masked images to subtract and level dendritic shaft background fluorescence. Images were subsequently thresholded to 10x the standard deviation of the image to isolate distinct puncta. A watershed procedure was applied to images to bisect any closely overlapping structures into individual components. Individual puncta was then automatically counted for each marker. To fulfill the criteria of a synapse, pre and postsynaptic markers were overlaid and co-localisation was automatically assessed and counted. Neurite length measurements were made using Neuron J (Meijering et al., 2004) or neurite tracer (Pool et al., 2008) plugin modules within Image J.

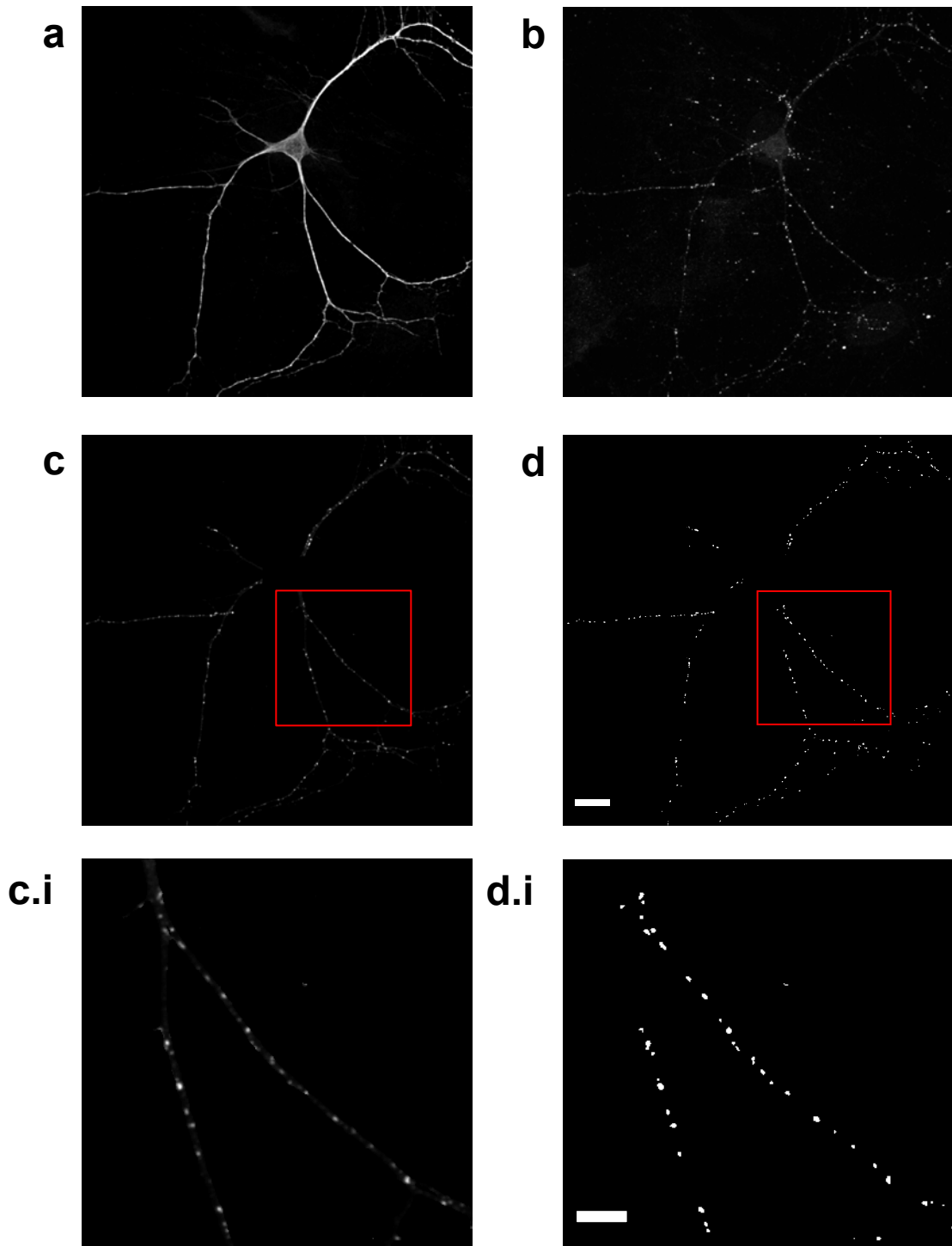


Figure 2.8 - Immunofluorescence analysis of synaptic marker puncta

Sample image of a typical neuron immunolabelled against MAP2 (a) and synaptic marker Homer (b). Panel (c) shows the same synaptic marker image as in (b) after processing with a MAP2 mask (extracted from a) and with somatic regions subtracted. Panel (d) shows the same image as in (c) but after rolling ball subtraction, thresholding and watershed processing. Panel (c.i) and (d.i) show magnified images of the red region shown in panel (3) and (4) respectively. Scale bar for panels a – d is 20 μm . Scale bar for panels c.i and d.i is 40 μm .

2.8 Organotypic spine analysis

2.8.1 Materials

Table 2.14: Chemicals / Reagents / Products used for visualization of spines in organotypic slices

Product	Company	Location
Alexa 488 hydrazide	Invitrogen	Paisley, UK
Antifade	Sigma - Aldrich	Dorset, UK
Coverglass	Assistent	Sondheim, Germany
Glass slides	Fisher - scientific	Loughborough, UK

2.8.2 Methods

2.8.2.1 Fluorescence labeling of spines of CA1 pyramidal cells in organotypic slices

The number of spines on a dendritic process can provide an estimate of synapse number in organotypic slice cultures. For this, CA1 pyramidal cells were visualized by addition of a green shifted fluorescently conjugated hydrazide, Alexa 488 (100-300 μM) to the intracellular solution and filled by patching cells in whole-cell configuration. Cells were filled for 15-20 mins before slow withdrawal of the patch pipette from the soma. Cells where the somatic membranes resealed quickly with minimal dye loss were retained for confocal imaging and analysis. Slices were rinsed twice using PBS and then fixed with 4% PFA/ 4% sucrose in PBS overnight. Following this, slices were mounted and sealed with antifade solution onto glass slides and maintained at 4°C until imaging.

Confocal imaging of spines of CA1 pyramidal cells in organotypic slices

Alexa Fluor – 488 hydrazide was excited with a 488 nm laser, 488/635 nm dichroic mirror and fluorescence collected between 500-530 nm wavelengths. Low magnification organotypic spine Z-stacks were acquired using a 40x oil objective with the same settings as that used for dissociated cultures but with 0.5 μm step between planes. High magnification Z-stack images of secondary or tertiary branches from basal and apical dendrites were acquired as low magnification images but with the following adjustments: 63x oil objective, 5x zoom and 0.4 μm step between optical sections. Images were acquired at 512 x 512 pixels at 8 bit. Images for drug treated test and control groups were acquired within the same imaging session where the same laser power, gain and offset settings were used for all groups.

Analysis

Spine analysis was performed on Z-stack projections of Alexa-488 filled apical and basal dendrites. Spine number was estimated by manually counting the number of spine-like protrusions emanating from the dendritic shaft. Protrusions were counted if they fit any of the following criteria (As De Simoni et al., 2003, based on Harris et al., 1992; Peters and Kaiserman-Abramof, 1969):-

- Mushroom spine: head diameter $>$ 2-fold greater than neck diameter
- Stubby spine: neck length is similar to neck diameter
- Thin spine: head and neck diameter is similar but length is greater than neck diameter
- Filopodial process: as thin spine but head diameter can be smaller than neck diameter.

Process length was measured by tracing a line along the dendritic shaft using either Leica LASAF software or Neuron J plugin within Image J processing suite.

2.9 Statistics

Data was assessed with unpaired two-tailed Student's t-test for comparison of control and drug treatment groups. Non-parametric Mann-Whitney test was performed for data that was not normally distributed. For comparison of three or more groups, a one-way analysis of variance (ANOVA) test followed with a Tukeys post hoc test was used. Power calculations were also performed for data sets where low samples sizes were obtained to help determine the statistical power of the results. Statistical significance in figures is represented by $p < 0.05^*$, $p < 0.01^{**}$, and $p < 0.001^{***}$. All data values are presented as mean \pm standard error of the mean (s.e.m).

Chapter 3: The role of presenilin in modulating spontaneous synaptic currents in hippocampal neurons

3.1 Introduction

The key role of presenilin in the generation of A β peptides has prompted many studies to try and gain a better understanding of the biology of presenilin. Studies have primarily focused on the hippocampus as it is a region of the CNS that is heavily afflicted with amyloid accumulations during AD. Additionally, impairments in neuronal and synaptic activity in the hippocampus have been widely associated with the learning and memory deficits commonly observed in AD patients. Moreover, the progressive impairment in cognitive functions observed during AD is highly associated with the extent of synapse loss (Dekosky and Scheff, 1990; Scheff and Price, 2003; Sze et al., 1997; Terry et al., 1991). Hence understanding the role of presenilins in modulating synaptic activity and function may provide valuable insights into the mechanisms that may contribute to the synapse loss, neurodegeneration and memory deficits associated with AD.

Studies investigating the role of presenilin in spatial learning paradigms and long term synaptic plasticity such as LTP have been extensively examined in a wide range of transgenic mice models (see introduction). However the role of presenilins in regulating basal synaptic transmission remains to be fully elucidated. A recent study performed on dissociated cortical cultures reported that PS1^{-/-} cells exhibit a higher mEPSC frequency rate than PS1^{+/+} and PS1^{+/-} cells but with no change in mEPSC amplitude (Parent et al., 2005). This effect on mEPSC frequency of PS1^{-/-} mice

could be mimicked by γ -secretase treatment of PS1^{+/+} cells indicating that γ -secretase activity is required for modulation of spontaneous synaptic transmission in cortical cultures. Additionally, PS1^{-/-} cells showed an increase in spine density and synapse number when compared to PS1^{+/+} cells which may be correlated with the increase in mEPSC frequency. Other studies revealed that γ -secretase inhibitor treatment of hippocampal neurons also showed similar enhancements in mEPSC frequency in the absence of a change in mEPSC amplitude, suggesting that γ -secretase activity is important for modulation of hippocampal synaptic transmission (Kamenetz et al., 2003; Priller et al., 2006). At the start of this project, no reports had examined spontaneous currents in hippocampal neurons from PS1^{-/-} mice. The role that presenilins and γ -secretase activity plays in modulating synaptic function in the hippocampus remains to be fully understood.

The aim of this chapter was to perform an extensive investigation into the role of presenilin in modulating basal synaptic spontaneous currents in two different model systems of the hippocampus: dissociated cultured neurons and organotypic slice cultures. These currents represent the random spontaneous stochastic release of neurotransmitter from the presynaptic terminal and subsequent activation of postsynaptic ionotropic receptors in an action potential independent manner (Cowan et al., 2001; Frerking et al., 1997; Wall and Usowicz, 1998). These events can be detected by performing patch clamp recordings from the postsynaptic neuron. Whole-cell recordings provide information about the total activity of synaptic connections made onto the postsynaptic cell. Examining release events can provide insights into the loci of modulation with presynaptic changes being often associated with an alteration in frequency and postsynaptic modifications being linked with a change in amplitude (Cowan et al., 2001; Del Castillo and Katz, 1954b; Kerchner and Nicoll, 2008; Prange and Murphy, 1999). As mentioned in the introduction, the two main factors which influence the frequency of spontaneous events are the number of functionally active synaptic connections being made onto a neuron (n) and the release probability (Pr) of a synapse, whereas spontaneous synaptic current amplitude on the other hand is linked with changes in the postsynaptic receptor number and conductance (q) (Cowan et al., 2001; Kerchner and Nicoll, 2008). By examining spontaneous synaptic currents, one can start to determine if there may be any alterations in presynaptic and/or postsynaptic function. The electrophysiology

experiments presented in this chapter mainly focus on spontaneous excitatory synaptic currents and were performed in the presence of GABA_A receptor blocker, picrotoxin to enable selective examination of excitatory responses (Figure 3.1 – 3.9). However preliminary recordings were also made in organotypic slices to examine inhibitory synaptic currents (Figure 3.10 – 3.11). For recordings of inhibitory currents, picrotoxin was omitted from the extracellular solution and AMPA and NMDA receptor antagonist, NBQX and DL-AP5 were used to inhibit glutamatergic currents. All spontaneous events were recorded in the presence of TTX (0.5 μ M) to block sodium channels and the generation of action potentials and will be referred to as miniature excitatory or inhibitory postsynaptic currents (mEPSC, mIPSC) from hereon.

3.2 Examination of the effect of γ -secretase activity inhibition on mEPSC properties in dissociated hippocampal neurons.

The first experiment of this chapter examined the effects of γ -secretase inhibitor treatment on mEPSC properties in hippocampal rat dissociated neuronal cultures. Whilst the effects of γ -secretase inhibition on A β production in rat dissociated neuron has been studied before (Hoey et al., 2009), the impact of γ -secretase inhibition on mEPSCs have not been investigated in rat dissociated cultures prior to this study. γ -secretase inhibitors have been extensively used to show that γ -secretase activity is required for regulated intramembraneous proteolysis of APP to generate A β (De Strooper et al., 1998). To examine whether γ -secretase activity is required for the regulation of mEPSC in hippocampal cultures, two structurally different, cell permeable and potent γ -secretase inhibitors, DAPT and L-685,458 were chosen.

Previous studies have used DAPT and L-685,458 in many different cell preparations, at a wide range of concentrations and for an assortment of treatment times (from hours to weeks) (see for example, Kamenetz et al., 2003; Parent et al., 2005; Priller

et al., 2006). Due to the lack of consensus in treatment times, initial studies were performed in dissociated neurons to determine whether there were any differences in mEPSC frequency and amplitude following different application periods. Neurons were pre-incubated with either DAPT (10 μ M) or L-685,458 (1 μ M) for 1 hr, 3 hrs, 24 hrs and 48 hrs.

A significant increase in mEPSC frequency was observed following 48 hr pre-treatment of hippocampal dissociated cells with either DAPT or L-685,458 when compared to DMSO mock control cells (Figure 3.1 left; DMSO: $n = 21$, 2.50 ± 0.45 Hz; DAPT: $n = 15$, 9.35 ± 1.97 Hz; L-685,458: $n = 14$, 7.56 ± 1.70 Hz. Student's t-test: DMSO versus DAPT, $p = 0.0004$ ***; DMSO versus L-685,458, $p = 0.0017$ **). However, no significant changes in amplitude were observed after 48 hr treatment with DMSO mock, DAPT or L-685,458 (Figure 3.1 right; DMSO: 26.86 ± 3.33 pA; DAPT: 27.62 ± 2.73 pA; L-685,458: 23.60 ± 2.11 pA. Student's t-test: DMSO versus DAPT, $p = 0.87$; DMSO versus L-685,458, $p = 0.47$). Figure 3.2 summarises the mEPSC frequency and amplitude results for the other treatment times. Treatment with DAPT for 24 hr showed a significant increase in mEPSC frequency but not with L-685,458 for the same duration, relative to DMSO mock control (Figure: 3.2a iii left; DMSO: $n = 10$, 2.63 ± 0.68 Hz; DAPT: $n = 7$, 9.39 ± 1.39 Hz; L-685,458: $n = 6$, 6.89 ± 2.44 Hz. Student's t-test: DMSO versus DAPT, $p = 0.0002$ ***; DMSO versus L-685,458, $p = 0.056$). No significant differences in mEPSC amplitude were observed following 24 hr treatment with DAPT or L-685,458 when compared to DMSO control (Figure 3.2 a iii right; DMSO: 22.57 ± 4.07 pA; DAPT: 22.41 ± 2.27 pA; L-685,458: 23.47 ± 5.04 pA. Student's t-test: DMSO versus DAPT, $p = 0.98$; DMSO versus L-685,458, $p = 0.89$). Treatment with DAPT or L-685,458 for 3 hrs did not show any differences in mEPSC frequency when compared to DMSO control (Figure 3.2 a ii left; DMSO: $n = 6$, 4.85 ± 1.64 Hz; DAPT: $n = 6$, 11.51 ± 3.08 Hz; L-685,458: $n = 6$, 5.93 ± 1.74 Hz. Student's t-test: DMSO versus DAPT, $p = 0.08$; DMSO versus L-685,458, $p = 0.66$). This same treatment also did not show any differences in mEPSC amplitude (Figure 3.2 a ii right, DMSO: 37.19 ± 8.99 pA; DAPT: 32.70 ± 2.85 pA, L-685,458: 31.14 ± 4.91 pA, Student's t-test: DMSO versus DAPT, $p = 0.64$; DMSO versus L-685,458, $p = 0.57$). Treatment of cells for 1 hr with DAPT, L-685,458 or DMSO did not show any significant differences in mEPSC frequency (Figure 3.2 a i left; DMSO: $n = 6$,

4.38 ± 1.64 Hz; DAPT: n = 9, 4.23 ± 0.88 Hz; L-685,458: n = 6, 6.31 ± 2.09 Hz. Student's t-test: DMSO versus DAPT, p = 0.91; DMSO versus L-685,458, p = 0.47) or amplitude (Figure 3.2 a i right; DMSO: 23.59 ± 3.75pA; DAPT: 28.23 ± 2.37pA; L-685,458: 32.61 ± 5.47pA. Student's t-test: DMSO versus DAPT, p = 0.29; DMSO versus L-685,458, p = 0.23).

Together these results suggest that 48 hr treatment with DAPT or L-685,458 is sufficient for a significant effect on mEPSC frequency. However mEPSC amplitude does not seem to change with acute or chronic γ -secretase inhibition as there were no significant changes in event size with 1 hr, 3 hr or 24 hr DAPT or L-685,458 pre-incubation when compared to DMSO mock control of the equivalent time point. This result shows γ -secretase activity is involved in the modulation of mEPSC frequency but not mEPSC amplitude at hippocampal synapses. Additionally, this result also shows that chronic treatment rather than acute treatment with γ -secretase inhibitors is required for an effect on mEPSC frequency. For this reason, all subsequent drug treatments were performed with chronic pre-incubation for 36-48 hrs and in line with other studies in neuronal culture systems where chronic pharmacological treatments were used (Kamenetz et al., 2003; Priller et al., 2007).

Further kinetic analysis of mEPSC waveform was also conducted on data obtained from dissociated cultures. Figure 3.3a shows that 10-90% rise time (left) and decay time (right) of mEPSCs following DAPT or L-685,458 treatments were not significantly different to DMSO mock control cells. There were also no significant differences in resting membrane potential, input resistance and cell capacitance between rat cultures treated with DMSO, DAPT or L-685,458 cells, suggesting that passive membrane properties are not altered upon chronic inhibition of γ -secretase activity (Figure 3.3b). In summary, chronic treatment of rat dissociated neurons with γ -secretase inhibitors results in a higher mean mEPSC frequency rate when compared to DMSO mock control cells. This indicates that γ -secretase activity is involved in the modulation of mEPSC frequency in wild type rat hippocampal dissociated cultures.

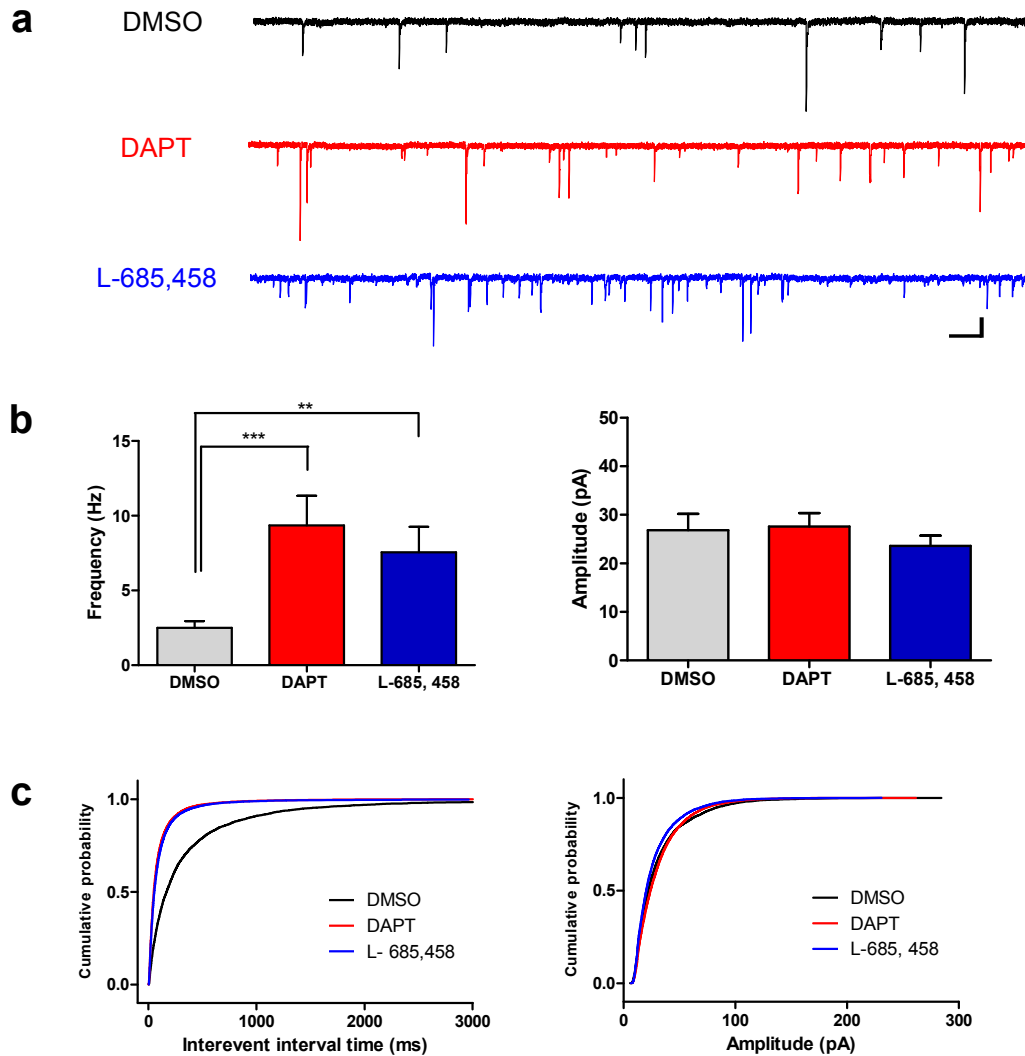


Figure 3.1 - mEPSC frequency is modulated by chronic treatment with γ -secretase inhibitors

(a) Sample traces of mEPSC recordings from hippocampal rat dissociated neurons chronically treated for 48 hr with DMSO mock control (black) or γ -secretase inhibitor DAPT (red) or L-685,458 (blue). Scale bar, 25 pA, 200 ms. (b) Summary of mEPSC frequency (left) and amplitude (right) for DMSO (grey, $n = 21$, frequency mean: 2.50 ± 0.45 Hz, amplitude mean: 26.86 ± 3.33 pA), DAPT (red, $n = 15$, frequency mean: 9.35 ± 1.97 Hz, amplitude mean: 27.62 ± 2.73 pA), and L-685,458 (blue, $n = 14$, frequency mean 7.56 ± 1.70 Hz, amplitude mean: 23.60 ± 2.11 pA). Statistical analysis was performed using student's t-test (bar graphs; $p < 0.01$ **, $p < 0.001$ ***). Chronic treatment with γ -secretase inhibitors significantly increased mean mEPSC frequency compared to DMSO mock control but did not change mEPSC amplitude. (c) Cumulative distribution plots of interevent interval time (left) and mEPSC amplitude (right) for data shown in (b).

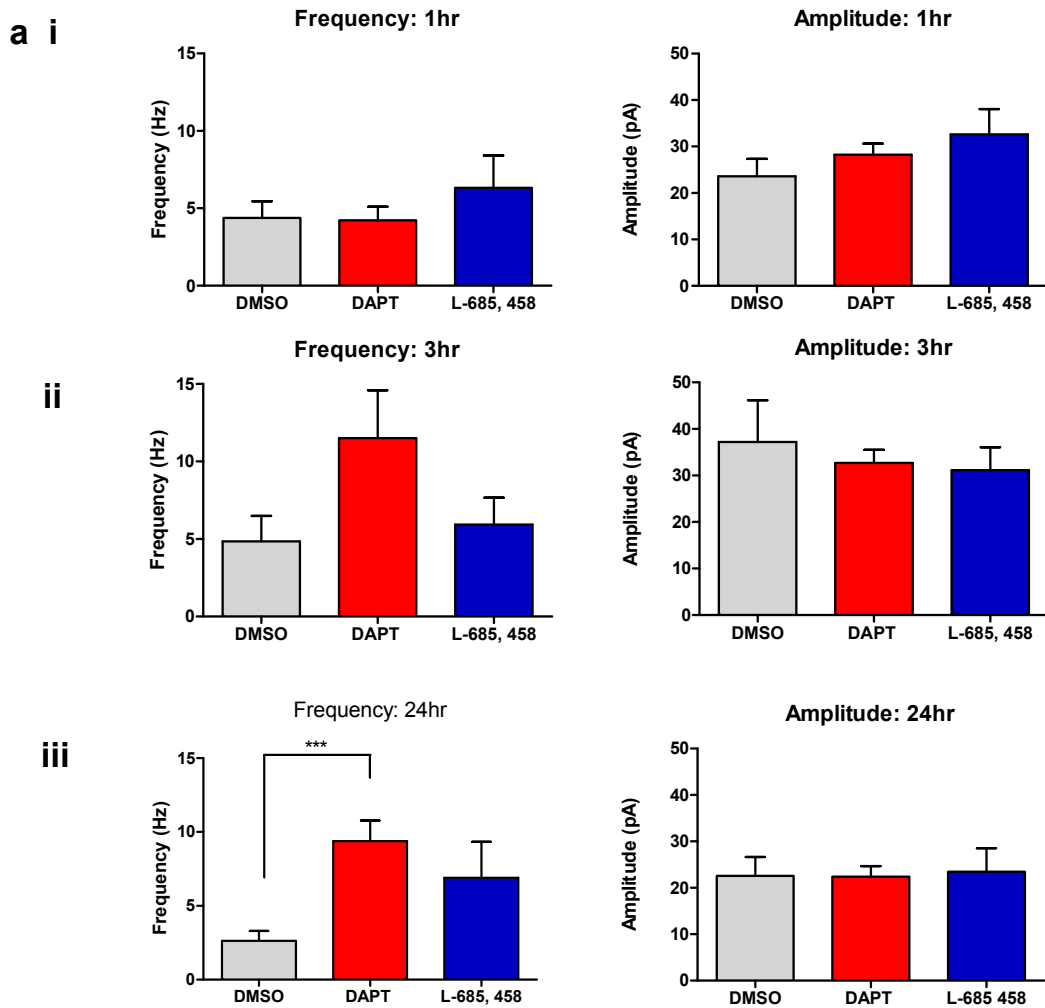


Figure 3.2 - Establishing timecourse of γ -secretase inhibitor treatment for mEPSC recordings.

(a) mEPSC frequency and amplitude in rat dissociated cultures was analysed following 1 hr (i), 3 hr(ii) and 24 hr (iii) pretreatment with γ -secretase inhibitor, DAPT (red) or L-685,458 (blue) or with DMSO mock control (grey). Statistical analysis was performed using student's t-test. Treatment with DAPT (10 μ M) for 24 hrs (and 48 hrs – see Figure 3.1) lead to a significant increase in mEPSC frequency compared to DMSO mock control cells. L-685,458 application (1 μ M) for 24 hrs also exhibited a higher mEPSC rate but not at a statistically significant level (24 hr; DMSO: 2.63 ± 0.68 Hz [n = 10]; DAPT: 9.39 ± 1.39 Hz [n = 7], L-685,458: 6.89 ± 2.44 Hz [n = 6], student's t-test: DMSO versus DAPT: $p = 0.0002$ ***, DMSO versus L-685,458, $p = 0.056$). 24 hr treatment with either DAPT or L-685,458 did not significantly influence mEPSC amplitude (24 hr; DMSO: 22.57 ± 4.07 pA [n = 10]; DAPT, 22.41 ± 2.27 pA [n = 7], L-685,458, 23.47 ± 5.04 pA [n = 6]). Treatment with DAPT or L-685,458 for 3hrs did not significantly alter mEPSC frequency (3 hr; DMSO: 4.85 ± 1.64 Hz [n = 6]; DAPT: 11.51 ± 3.08 Hz [n = 6]; L-685,458: 5.93 ± 1.74 Hz [n = 6]). Treatment with DAPT or L-685,458 for 3 hr also had no effect on mEPSC amplitude (3 hr; DMSO: 37.19 ± 8.99 pA [n = 6]; DAPT, 32.70 ± 2.85 pA[n = 6], L-685,458, 31.14 ± 4.91 pA [n = 6]). Treatment with DAPT or L-685,458 for 1 hr did not significantly alter mEPSC frequency compared to DMSO control (1 hr; DMSO: 4.38 ± 1.64 Hz [n = 6]; DAPT, 4.23 ± 0.88 Hz [n = 9], L-685,458, 6.31 ± 2.09 , [n = 8]). mEPSC amplitude was also not significantly altered following 1 hr treatment with DAPT or L-685,458 (DMSO: 23.59 ± 3.75 pA [n = 6]; DAPT, 28.23 ± 2.37 pA [n = 9], L-685,458, 32.61 ± 5.47 pA [n = 8]). No changes in mEPSC amplitude were observed between DAPT or L-685,458 treatments relative to mock control DMSO at any of the tested timepoints. This data suggests mEPSC frequency, but not amplitude can be modulated by chronic but not acute block of γ -secretase activity using inhibitors, DAPT and L-685, 458.

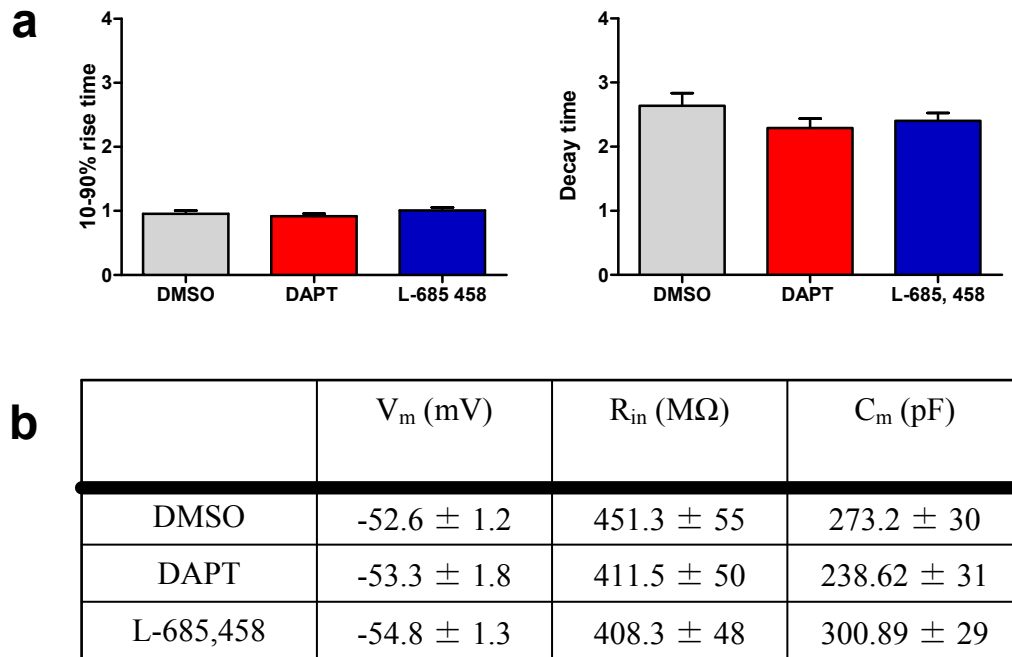


Figure 3.3 - Electrophysiological properties of rat dissociated neurons treated with γ -secretase inhibitors, DAPT and L-685,458.

(a) Measurements of 10-90% rise time (left) and decay time constant (right) of mEPSCs from rat dissociated neurons chronically treated with either DMSO control (grey, $n = 21$) or γ -secretase inhibitors; DAPT (red, $n = 15$), or L-685,458 (blue, $n = 14$). Statistical analysis was performed using student's t-test. Neither rise time nor decay time were significantly altered between γ -secretase inhibitors DAPT and L-685,458 when compared to DMSO mock control.

(b) Table featuring resting membrane potential (V_m), input resistance (R_{in}) and membrane capacitance (C_m) of cells chronically treated with DMSO mock control, DAPT and L-685,458.

3.3 Examination of mEPSC properties of hippocampal neurons from PS1 transgenic mice

The role of PS1 in modulating hippocampal mEPSC frequency and amplitude had not been examined in PS1 mutant mice prior to this study. The next experiment in this chapter was to investigate whether there were any differences in mEPSC properties between PS1^{+/+}, PS1^{+/-} and PS1^{-/-} hippocampal neurons. In addition, the effects of γ -secretase inhibitor treatment on PS1^{+/+}, PS1^{+/-} and PS1^{-/-} hippocampal neurons was also examined. The PS1^{-/-} mice were generated on a PS2^{+/+} background (Wong et al., 1997). However the role of PS1 and PS2 in regulating hippocampal mEPSC properties was unknown. The examination of PS1^{-/-} animals where *PSEN1* gene function had been eliminated should lack all PS1 associated γ -secretase activity in addition to the loss of PS1 γ -secretase independent functions. The use of γ -secretase inhibitors on the other hand should block both PS1 and PS2 associated γ -secretase complexes but should not influence γ -secretase independent functions of presenilins (see introduction). Examining the effects of γ -secretase inhibition on PS1^{-/-} cells will provide a way to examine whether there is a major contribution of PS2 associated γ -secretase complexes in the regulation of mEPSC properties.

Recordings showed that PS1^{-/-} neurons exhibit a higher mean mEPSC frequency than PS1^{+/+} and PS1^{+/-} mice (Figure 3.4 b left; PS1^{-/-}: 6.18 ± 1.14 Hz; PS1^{+/+} mean: 3.04 ± 0.53 Hz; PS1^{+/-} mean: 2.81 ± 0.44 Hz. One-way ANOVA followed by a Tukey's post hoc test: PS1^{+/+} versus PS1^{+/-}: $p > 0.05$, PS1^{+/+} versus PS1^{-/-}: $p < 0.05$ *; PS1^{+/-} versus PS1^{-/-}: $p < 0.05$ *). No significant differences in mEPSC amplitude were observed between PS1^{+/+}, PS1^{+/-} or PS1^{-/-} mice (Figure 3.4 b right; PS1^{+/+}: 21.46 ± 1.92 pA, PS1^{+/-} mean: 20.84 ± 2.97 pA, PS1^{-/-}: 20.41 ± 1.68 pA. One-way ANOVA: $p = 0.94$). This result suggests that the PS1 gene is required for modulating mEPSC frequency but not mEPSC amplitude. This result is consistent with the study by Parent et al., (2005) which showed that PS1^{-/-} cortical

cells also exhibit a higher mEPSC frequency rate than PS1^{+/+} cells. Figure 3.5 shows the 10-90% rise time and decay time of mEPSC from PS1^{+/+}, PS1^{+/-} and PS1^{-/-} cells. There were no significant differences between the three genotypes. There were also no significant differences in resting membrane potential, input resistance and cell capacitance between PS1^{+/+} and PS1^{+/-} compared to PS1^{-/-} cells (Figure 3.5 b).

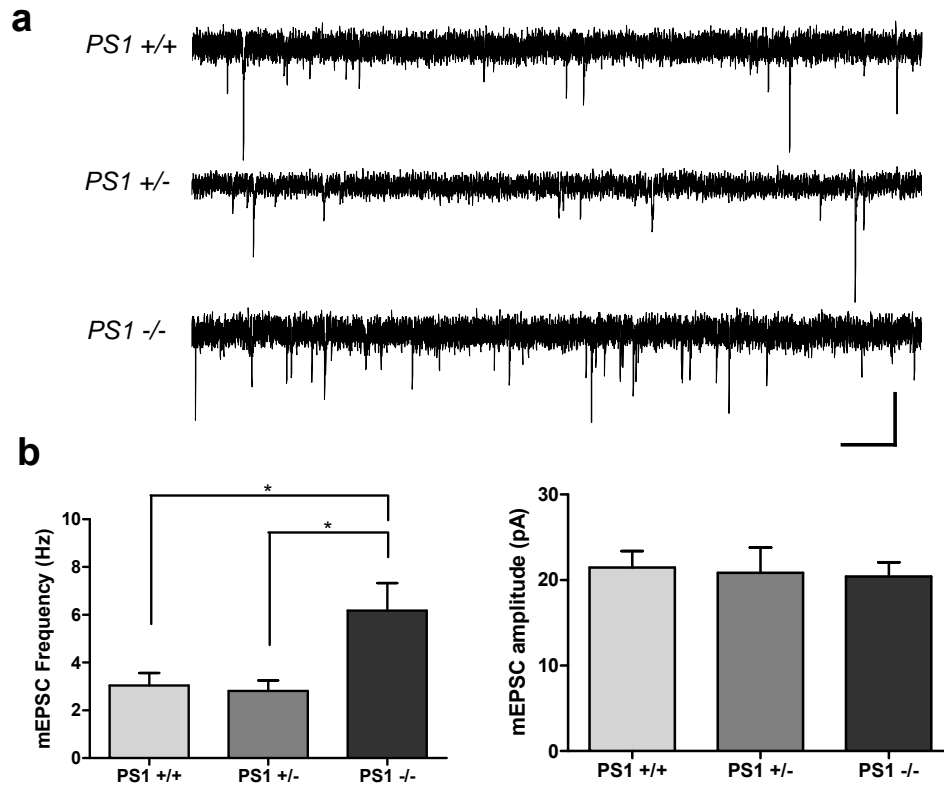


Figure 3.4 - mEPSC frequency is increased in presenilin-1 (PS1) knock-out mice.

(a) Sample traces of mEPSC recordings from hippocampal PS1^{+/+} (top), PS1^{+/-} (middle) and PS1^{-/-} (bottom) mice neurons. Scale bar, 20 pA, 200 ms. (b) Summary of mEPSC frequency (left) and amplitude (right) for PS1^{+/+} (light grey, n = 22), PS1^{+/-} (mid grey, n = 18) and PS1^{-/-} (dark grey, n = 21) neurons. Statistical analysis was performed using ANOVA followed by a Tukey post test (bar graphs; $p < 0.05$ *). PS1^{-/-} animals exhibit a significantly higher mEPSC frequency (mean: 6.18 ± 1.14 Hz) than PS1^{+/+} (mean: 3.04 ± 0.53 Hz) or PS1^{+/-} (mean: 2.81 ± 0.44 Hz) animals. mEPSC amplitude is not significantly altered across genotypes (PS1^{+/+}: 21.46 ± 1.92 pA, PS1^{+/-}: 20.84 ± 2.97 pA, PS1^{-/-}: 20.41 ± 1.68 pA). There was no significant differences between PS1^{+/+} and PS1^{+/-} animals in mEPSC frequency or amplitude. This data shows that elimination of PS1 leads to an increase in mEPSC frequency.

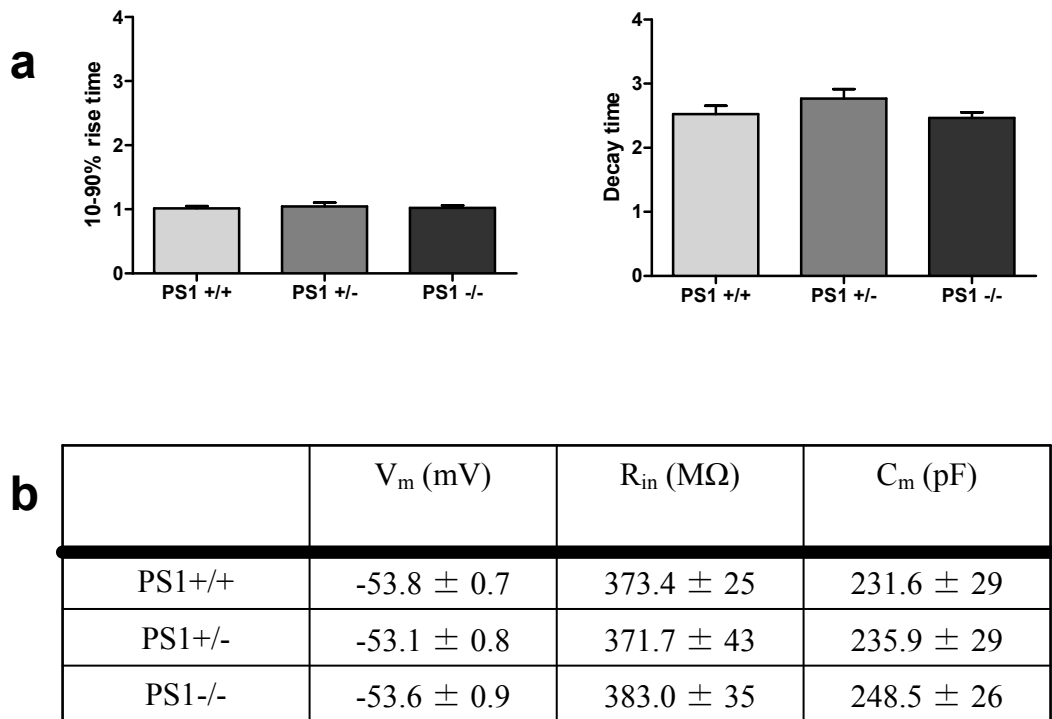


Figure 3.5 - Electrophysiological properties of dissociated neurons from PS1 +/+, PS1 +/- and PS1 -/- mice.

(a) Measurements of 10-90% rise time (left) and decay time constant (right) of mEPSCs from PS1 +/+ (light grey, $n = 22$), PS1 +/- (mid grey, $n = 18$) and PS1 -/- (dark grey, $n = 21$) neurons. Statistical analysis was performed using ANOVA followed by a Tukey post test. Rise time and decay time was not significantly different between the genotypes. (b) Table featuring resting membrane potential (V_m), input resistance (R_{in}) and membrane capacitance (C_m) of hippocampal dissociated cells from PS1 +/+, PS1 +/- and PS1 -/- mice.

Next, I examined whether γ -secretase inhibitors had any effect on PS1+/+, PS1 +/- and PS1 -/- cells (Figure 3.6). Chronic treatment of PS1+/+ cells with DAPT or L-685,458, led to a significant increase in mean mEPSC frequency when compared to PS1+/+ cells treated with DMSO mock control (Figure 3.6 a i middle; PS1 +/+ DMSO, $n = 12$, 3.75 ± 0.82 Hz; PS1 +/+ DAPT, $n = 7$, 10.43 ± 3.47 Hz; PS1 +/+ L-685,458, $n = 5$, 6.95 ± 1.05 Hz. Student's t-test: DMSO versus DAPT, $p = 0.03^*$; DMSO versus L-685,458, $p = 0.04^*$). There were no significant effects on mean mEPSC amplitude following γ -secretase inhibitor treatment of PS1 +/+ cells (Figure

3.6 a i right; PS1 $+/+$ DMSO, 23.44 ± 3.27 pA; PS1 $+/+$ DAPT, 28.26 ± 6.36 pA; PS1 $+/+$ L-685,458, 22.26 ± 3.95 pA. Student's t-test: DMSO versus DAPT, $p = 0.46$; DMSO versus L-685,458, $p = 0.84$). PS1 $+/-$ cells treated with γ -secretase inhibitors DAPT and L-685,458 both led to significant increases in mean mEPSC frequency (Figure 3.6 a ii middle; PS1 $+/-$ DMSO, $n = 12$, 3.51 ± 0.50 Hz; PS1 $+/-$ DAPT, $n = 9$, 9.84 ± 1.74 Hz; PS1 $+/-$ L-685,458, $n = 6$, 11.6 ± 2.20 Hz. Student's t-test: DMSO versus DAPT, $p = 0.0009^{***}$; DMSO versus L-685,458, $p = 0.0002^{***}$). There were no significant effects on mEPSC amplitude following γ -secretase inhibitor treatment of PS1 $+/-$ cells (Figure 3.6 a ii right; PS1 $+/-$ DMSO, 23.04 ± 4.31 pA; PS1 $+/-$ DAPT, 32.01 ± 4.95 pA; PS1 $+/-$ L-685,458, 31.70 ± 5.78 pA. Student's t-test: DMSO versus DAPT, $p = 0.19$; DMSO versus L-685,458, $p = 0.26$). Finally the effects of γ -secretase inhibitors on PS1 $-/-$ cells were examined. PS1 $-/-$ showed an increase in mEPSC frequency when compared to PS1 $+/-$ and PS1 $+/+$ cells under basal conditions (without drugs, Figure 3.4 b, left). Treatment of PS1 $-/-$ cells for 48 hr with DAPT and L-685,458 did not lead to any significant changes in mEPSC frequency when compared to PS1 $-/-$ cells treated with DMSO mock control (Figure 3.6a iii middle; PS1 $-/-$ DMSO, $n = 12$, 8.16 ± 1.58 Hz; PS1 $-/-$ DAPT, $n = 14$, 6.98 ± 1.29 Hz; PS1 $-/-$ L-685,458, $n = 11$, 7.57 ± 1.22 Hz. Student's t-test: DMSO versus DAPT, $p = 0.57$; DMSO versus L-685,458, $p = 0.77$). There were also no significant effects on mEPSC amplitude following γ -secretase inhibitor treatment of PS1 $-/-$ cells (Figure 3.6 a iii right; PS1 $-/-$ DMSO, 22.66 ± 2.55 pA; PS1 $-/-$ DAPT, 21.79 ± 1.77 pA; PS1 $-/-$ L-685,458, 19.78 ± 1.74 pA. Student's t-test: DMSO versus DAPT, $p = 0.78$; DMSO versus L-685,458, $p = 0.37$).

Overall this data suggests that PS1 $-/-$ mice exhibit a higher mEPSC frequency rate under basal conditions and treatment of PS1 $+/+$ and PS1 $+/-$ cells with γ -secretase inhibitors leads to an elevation in mEPSC frequency rate that is comparable to that observed with PS1 $-/-$ cells. The lack of effect of γ -secretase inhibitors on PS1 $-/-$ animals suggests that most γ -secretase activity that is associated with modulating mEPSC frequency in hippocampal neurons occurs through PS1 rather than PS2. Examination of mEPSC amplitude showed that there were no significant differences between drug treated neurons and DMSO mock controls in all three genotypes suggesting neither γ -secretase dependent or independent activity of presenilins is required for regulation of mEPSC size. As both γ -secretase dependent and γ -

secretase independent forms of PS1 activity are eliminated in PS1^{-/-} mice, it is not possible to determine which is more important for modulating mEPSC frequency using this single approach. However taking this result and the finding that increased mEPSC frequency rate is observed upon γ -secretase treatment of PS1^{+/+} and PS1^{+/-} mice suggests that PS1 associated γ -secretase dependent activity rather than PS1 γ -secretase independent activity is required for modulation of mEPSC. This result provides evidence that PS1 plays a role in modulating mEPSC frequency in mice hippocampal cultures and is consistent with observations of PS1 activity on cortical neurons (Parent et al., 2005).

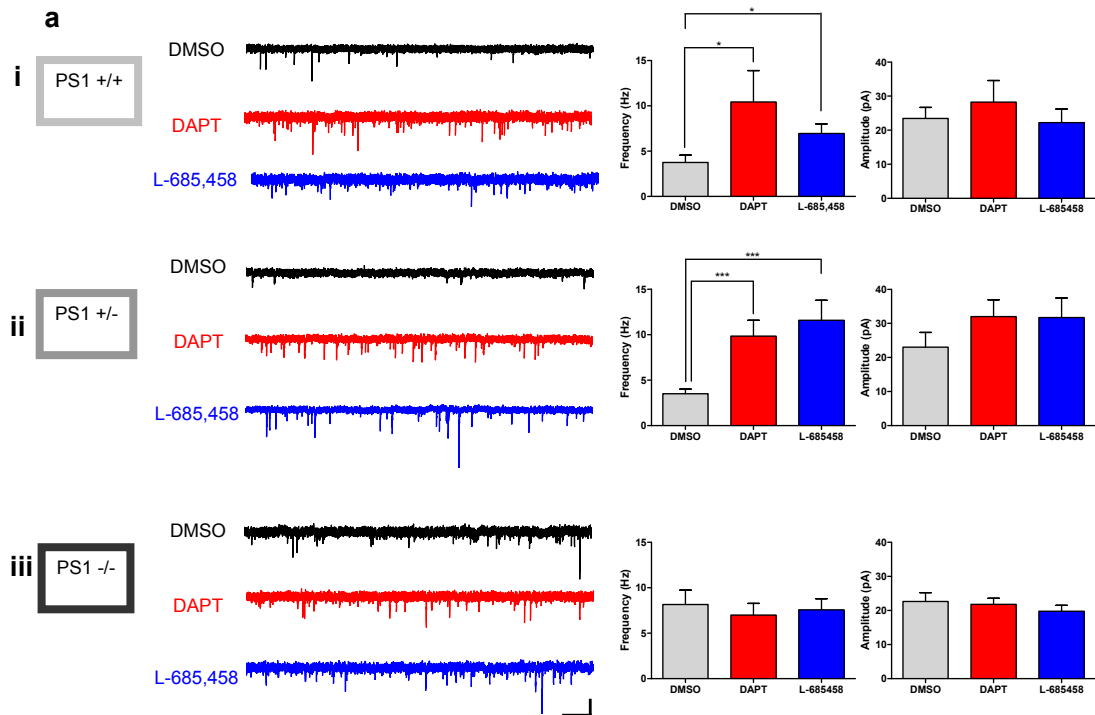


Figure 3.6 – Examination of chronic γ -secretase treatment on miniature excitatory postsynaptic currents from PS1 +/+, PS1 +/- and PS1 -/- hippocampal cells.

(a) Left, Sample traces from PS1 +/+ (light grey, i), PS1 +/- (mid grey, ii) and PS1 -/- (dark grey, iii) mice, treated with DMSO mock control (black), or γ -secretase inhibitor; DAPT (red) or L-685,458 (blue). Scale bar, 20 pA, 200 ms. Middle and right, Summary of mEPSC frequency and amplitude data for PS1 +/+ (i), PS1 +/- (ii) and PS1 -/- (iii) neurons, respectively. For each genotype, γ -secretase inhibitor (DAPT (red) or L-685,458 (blue)) treatment was compared to DMSO mock control (grey). Statistical analysis was performed using student's t-test (bar graphs; $p < 0.05$ *, $p < 0.01$ **, $p < 0.001$ ***). (i) Application of γ -secretase inhibitor, DAPT to PS1 +/+ cells (red, $n = 7$, frequency mean: 10.43 ± 3.47 Hz, amplitude mean: 28.26 ± 6.36 pA) increased mEPSC frequency significantly when compared to DMSO control (grey, $n = 12$, frequency mean: 3.75 ± 0.82 Hz, amplitude mean: 23.44 ± 3.27 pA) (DMSO versus DAPT, $p = 0.03$ *). Application of L-685,458 to PS1 +/+ cells (blue, $n = 5$, frequency mean: 6.95 ± 1.05 Hz, amplitude mean: 22.26 ± 3.95 pA) also caused an increase in mean frequency relative to DMSO control (DMSO versus L-685,458, $p = 0.04$ *). (ii) Application of DAPT (red, $n = 9$, frequency mean: 9.844 ± 1.74 Hz, amplitude mean: 32.01 ± 4.95 pA) or L-685,458 (blue, $n = 6$, frequency mean: 11.6 ± 2.20 Hz, amplitude mean: 31.70 ± 5.78 pA) to PS1 +/- cells significantly raised mEPSC frequency with respect to DMSO mock (grey, $n = 12$, frequency mean: 3.51 ± 0.50 Hz, amplitude mean: 23.04 ± 4.31 pA). (mEPSC frequency DMSO versus DAPT; $p = 0.0009$ ***; DMSO versus L-685,458; $p = 0.0002$ ***). mEPSC amplitude was not significantly altered in PS1 +/- cells treated with DAPT or L-685,458. (iii) PS1 -/- cells were treated with DMSO mock control (grey, $n = 12$, frequency mean: 8.16 ± 1.58 Hz, amplitude mean: 22.66 ± 2.55 pA), DAPT (red, $n = 14$, frequency mean: 6.98 ± 1.29 Hz, amplitude mean: 21.79 ± 1.77 pA), or L-685,458 (blue, $n = 11$, frequency mean: 7.57 ± 1.22 Hz, amplitude mean: 19.78 ± 1.74 pA). No changes in mEPSC frequency were observed in PS1 -/- animals following treatment with DAPT or L-685,458. There were no significant changes in mean mEPSC amplitude following drug treatment in PS1+/, PS1 +/- or PS1 -/- mice. Together this data suggests inhibition of γ -secretase activity in PS1 +/+ or PS1 +/- animals leads to an increase in mEPSC frequency but not in PS1 -/- animals.

3.4 Examination of the effect of γ -secretase activity inhibition on mEPSC properties in hippocampal organotypic slice cultures.

The experiments discussed so far, examined either the impact of γ -secretase activity block or PS1 gene elimination (or both) on mEPSC properties in hippocampal dissociated cultures made from rat and mice. Next, to understand whether the increase in mEPSC frequency following γ -secretase activity inhibition can also occur in a more intact hippocampal model, organotypic hippocampal parasagittal slices were treated with DAPT or L-685,458 and mEPSC recordings were made. Organotypic cultures were selected over acute slices as prolonged (48 hr) treatment of γ -secretase inhibitors was required for a robust effect on mEPSC rate in dissociated cultures (Figure 3.1). One key benefit of this well characterised system over primary dissociated culture is that the extracellular environment is more similar to that found *in vivo* and the gross cytoarchitecture and connectivity is largely maintained. Unfortunately due to the propensity for PS1^{-/-} animals to die during late embryonic developmental stages, the production of slices from these mice was not an available option. The main problem being embryonic hippocampal tissue tended to be much softer and smaller than postnatal tissue which made generation of a suitable number of consistent slices much more challenging. A general observation about organotypic slice cultures is that the mean mEPSC frequency was much lower than dissociated cultures. This warranted longer recording times to get a more comparable estimate of the mEPSC population.

As observed in dissociated cultures, γ -secretase treatment of organotypic slices also led to an increase in mean mEPSC frequency in slices (Figure 3.7) with DAPT showing a highly significant increase and L-685,458 a lesser yet still significant increase compared to DMSO control (Figure 3.7 b left, DMSO: n = 20, 0.36 ± 0.06 Hz; DAPT: n = 17, 1.35 ± 0.27 Hz; L-685,458: n = 16, 0.75 ± 0.18 Hz. Student's t-

test: DMSO versus DAPT, $p = 0.0004$ ***; DMSO versus L-685,458, $p = 0.032$ *). In common with dissociated neurons, there was no significant difference in mean mEPSC amplitude in organotypic slices treated with DMSO (mock), DAPT or L-685,458 (Figure 3.7 b right; DMSO: 17.40 ± 0.60 pA; DAPT: 18.23 ± 2.31 pA; L-685,458: 19.43 ± 1.08 pA. Student's t-test: DMSO versus DAPT, $p = 0.71$; DMSO versus L-685,458, $p = 0.09$).

This result is largely in agreement with a previous report which showed that 24 hr pre-treatment with 1 μ M L-685,458 could lead to an increase in mEPSC frequency but not amplitude in hippocampal rat organotypic cultures (Kamenetz et al., 2003). Figure 3.8 a shows the 10-90% rise time (left) and decay time (right) of mEPSC from organotypic slices treated with DMSO (mock control), DAPT or L-685,458. There was no significant difference in rise time or decay time between the three conditions. There were also no significant differences in resting membrane potential, input resistance and cell capacitance between DMSO, DAPT and L-685,458 treated slices (Figure 3.8 b). Together these results show that γ -secretase activity block can influence the presynaptic function of neurons in intact slice preparations as well as in dissociated cells.

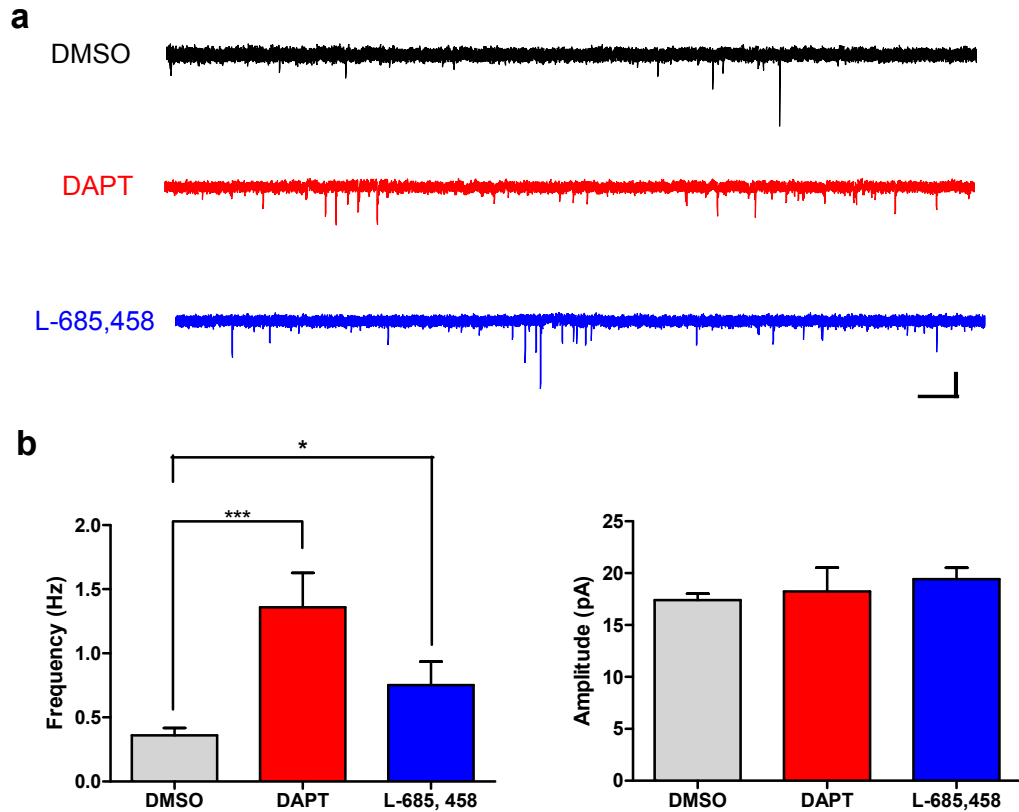


Figure 3.7 – Examination of mEPSC in rat hippocampal slice cultures treated with γ -secretase inhibitors, DAPT and L-685,458.

(a) Sample traces of mEPSC recordings from hippocampal rat organotypic slices treated for 48 hr with DMSO mock control (black) or γ -secretase inhibitors, DAPT (red) or L-685,458 (blue). Scale bar, 20 pA, 1000 ms. **(b)** Summary of mEPSC frequency (left) and amplitude (right) for DMSO (grey, $n = 20$, frequency mean: 0.36 ± 0.06 Hz, amplitude mean: 17.40 ± 0.60 pA), DAPT (red, $n = 17$, frequency mean: 1.35 ± 0.27 Hz, amplitude mean: 18.23 ± 2.31 pA) and L-685,458 (blue, $n = 16$, frequency mean: 0.75 ± 0.18 Hz, amplitude mean: 19.43 ± 1.08 pA) recordings. Slices treated with γ -secretase inhibitor; DAPT or L-685,458 were compared to DMSO mock control slices. Statistical analysis was performed using student's t-test. Slices chronically treated with γ -secretase inhibitor DAPT or L-685,458 exhibited a significant increase in mean mEPSC frequency when compared to DMSO mock control (DMSO versus DAPT, $p = 0.0004$ ***; DMSO versus L-685,458, $p = 0.032$ *). mEPSC amplitude was not significantly altered between DMSO and γ -secretase inhibitor treated slices.

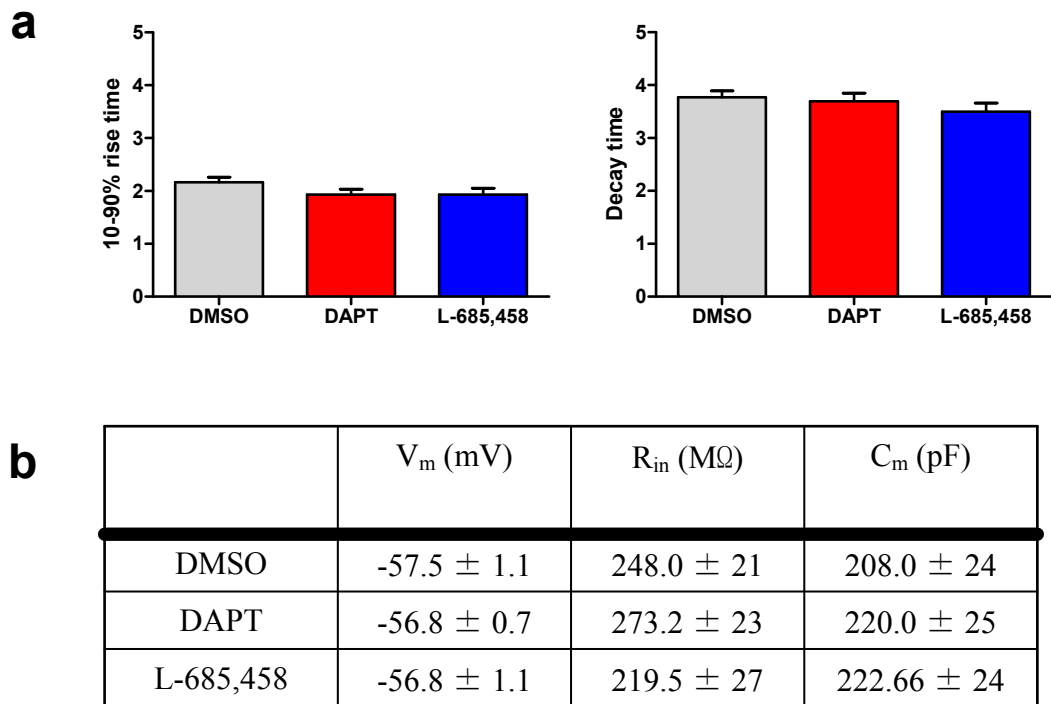


Figure 3.8 – Electrophysiological properties of rat hippocampal organotypic slice neurons treated with DMSO mock control or γ -secretase inhibitor DAPT.

(a) Measurements of 10-90% rise time (left) and decay time constant (right) of mEPSCs from neurons of rat organotypic slices chronically treated with either DMSO (mock control) or γ -secretase inhibitor, DAPT or L-685,458. Slices treated with DAPT or L-685,458 were compared to DMSO mock control slices. Statistical analysis was performed using student's t-test. Neither rise time or decay time were significantly altered between the DAPT nor L-685,458 treated slices and DMSO mock control slices.

(b) Table featuring resting membrane potential (V_m), input resistance (R_{in}) and membrane capacitance (C_m) of organotypic slice neurons chronically treated with DMSO (mock control), DAPT and L-685,458.

3.5 Examination of the effect of γ -secretase activity inhibition on mIPSC properties in hippocampal organotypic slice cultures.

As already demonstrated above, pharmacological blockade of γ -secretase activity using DAPT and L-685,458 in rat and mice dissociated cultures and rat organotypic slice cultures, led to an increase in mEPSC frequency when compared to DMSO mock control cells. Next, I wanted to investigate whether there was any effect of γ -secretase inhibition on mIPSCs. This experiment was conducted in organotypic slice cultures using a low chloride based internal, in the absence of picrotoxin and measured using two configurations. Configuration 1 involved holding the cell at -50 mV and recording both mEPSC and mIPSC simultaneously. Configuration 2 involved firstly holding the cell at -70 mV to record mEPSC and then holding the cell at 0 mV (close to the reversal for cations) to measure mIPSCs. For the latter, NBQX (20 μ M) and DL-AP5 (50 μ M) were applied to specifically isolate inhibitory currents when holding the cell at 0 mV.

Recordings where mEPSC and mIPSCs were recorded simultaneously (Figure 3.9), showed an increase in mean mEPSC frequency in cells treated with γ -secretase inhibitor DAPT when compared to DMSO controls, consistent with previous observations (see Figure 3.1) (Figure 3.9 b i left, DMSO: $n = 7$, 0.18 ± 0.03 Hz; DAPT: $n = 6$, 0.56 ± 0.14 Hz. Student's t-test: DMSO versus DAPT frequency, $p = 0.016$ *). No significant effects on mean mEPSC amplitude was observed between DMSO mock and DAPT treated slices (Figure 3.9 b i right, DMSO: $n = 7$, 17.56 ± 1.15 pA; DAPT: $n = 6$, 17.77 ± 1.399 pA. Student's t-test: DMSO versus DAPT amplitude, $p = 0.91$). Examination of mIPSC showed no significant effects on mean frequency or mean amplitude between DMSO mock and DAPT treated slices (Figure 3.9 b ii, DMSO: 0.25 ± 0.07 Hz, 15.21 ± 1.00 pA; DAPT: 0.24 ± 0.07 Hz, 14.21 ± 0.54 pA. Student's t-test: DMSO versus DAPT frequency, $p = 0.94$; DMSO versus

DAPT amplitude, $p = 0.42$). This result suggests that γ -secretase blockade selectively increases excitatory transmission whilst leaving inhibitory currents unaltered. However as the number of mIPSC observed under this configuration was relatively low, an alternative approach was used to determine if this effect was still seen. For this configuration 2 was used. Recording mEPSC at -70 mV showed similar effects to previous observations, with an increase in mEPSC frequency but not amplitude in slices treated with DAPT when compared to DMSO control slices (Figure 3.10 b i, DMSO: $n = 7$, 0.27 ± 0.03 Hz, 15.65 ± 0.50 pA; DAPT: $n = 5$, 0.84 ± 0.27 Hz, 15.03 ± 1.05 pA. DMSO versus DAPT frequency, $p = 0.033$ *, DMSO versus DAPT amplitude, $p = 0.57$). For recordings of mIPSC at 0 mV, no difference was seen in mIPSC frequency or amplitude between DMSO and DAPT treated samples (Figure 3.10 b ii, DMSO: $n = 7$, 1.52 ± 0.30 Hz, 27.07 ± 1.08 pA; DAPT: $n = 5$, 1.61 ± 0.28 Hz, 29.41 ± 1.31 pA. DMSO versus DAPT mIPSC frequency, $p = 0.83$; DMSO versus DAPT mIPSC amplitude, $p = 0.20$). Together these results indicate that γ -secretase activity is involved in the modulation of miniature excitatory currents but not inhibitory currents.

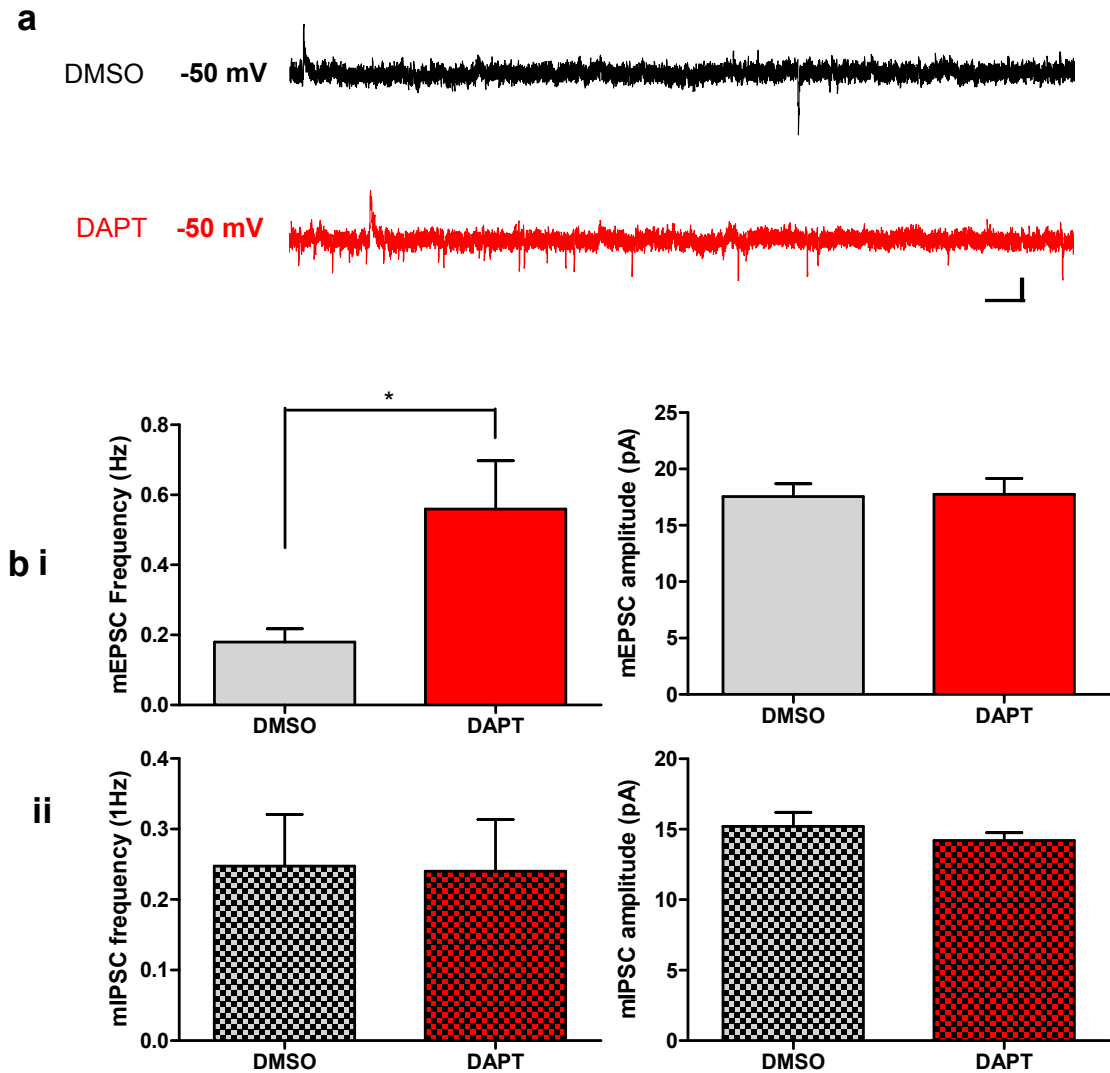


Figure 3.9 – mEPSC frequency but not mIPSC frequency is modulated by chronic treatment with γ -secretase inhibitor, DAPT. (Configuration 1).

(a) Sample traces of mEPSC and mIPSC recordings from hippocampal organotypic slices treated with DAPT (red) or DMSO mock (grey). Cells were patched using a low Cl Kgluconate based internal and voltage clamped at -50 mV. mEPSC were visualised as fast inward currents whilst mIPSC were seen as slower outward currents. mEPSC and mIPSC were recorded simultaneously from the same cell. Scale bar, 20 pA, 1000 ms. (b i) Summary of mEPSC frequency (left) and mEPSC amplitude (right). Statistical analysis was performed using student's t-test. Slices treated with DAPT (red, n = 6, frequency mean: 0.56 ± 0.14 Hz, amplitude mean: 17.77 ± 1.399 pA) displayed an significant increase in mEPSC frequency when compared to DMSO mock control slices (grey, n = 7, frequency mean: 0.18 ± 0.03 Hz, amplitude mean: 17.56 ± 1.15 pA). (DMSO versus DAPT frequency, $p = 0.016$ *). mEPSC amplitude was not significantly altered between DMSO and DAPT groups. (b ii) Summary of mIPSC frequency (left, checked) and mIPSC amplitude (right, checked). Slices treated with DAPT (red, n = 6, frequency mean: 0.24 ± 0.07 Hz, amplitude mean: 14.21 ± 0.54 pA) displayed no difference in mIPSC frequency or amplitude when compared to DMSO mock control slices (grey, n = 7, frequency mean: 0.25 ± 0.07 Hz, amplitude mean: 15.21 ± 1.00 pA). This result indicates that treatment with γ -secretase inhibitor, DAPT leads to an increase in mEPSC frequency but with no significant change in mIPSC frequency. Neither mEPSC or mIPSC amplitude is altered been DMSO or DAPT treated slices.

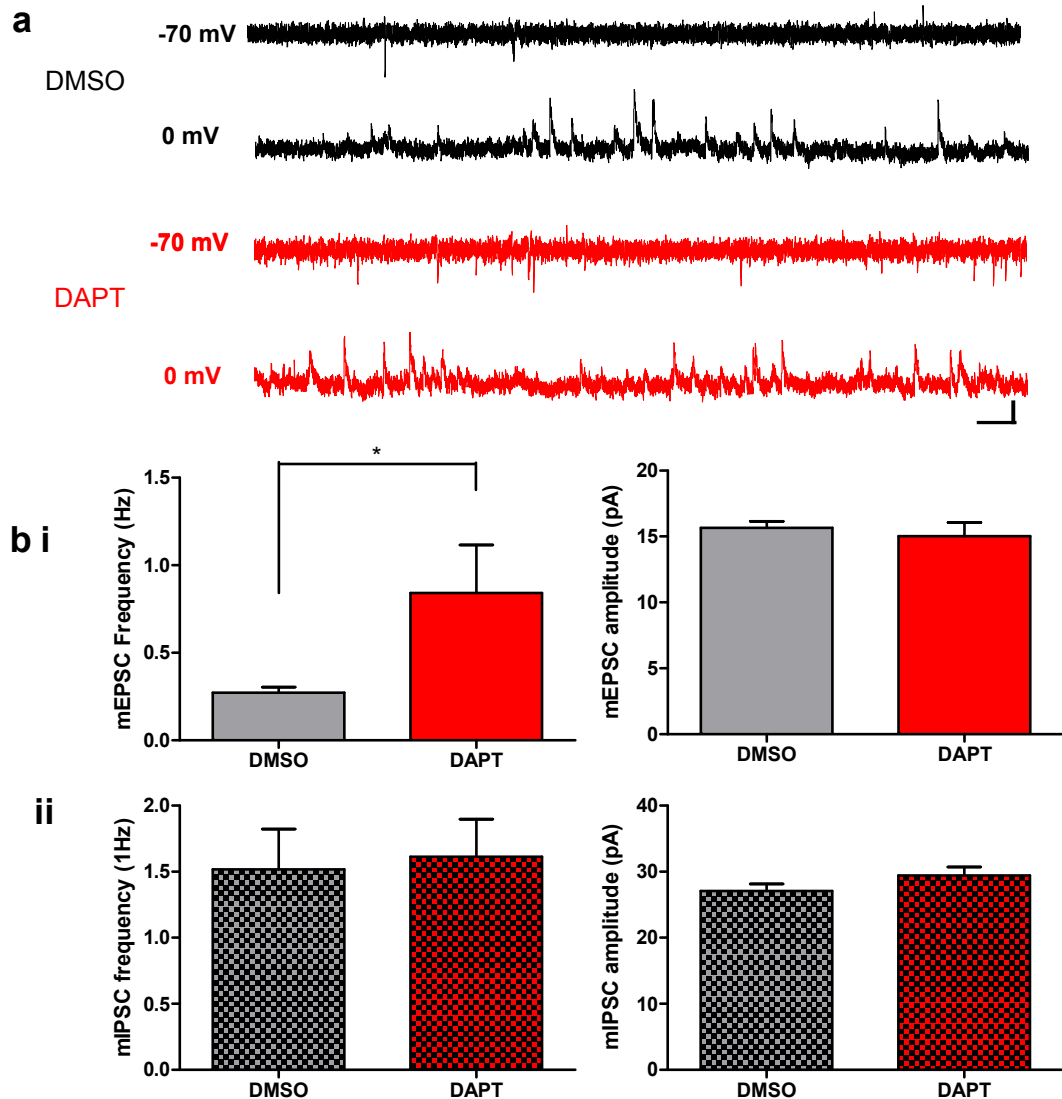


Figure 3.10 – mEPSC frequency but not mIPSC frequency is modulated by chronic treatment with γ -secretase inhibitor, DAPT. (Configuration 2).

(a) Sample traces of mEPSC and mIPSC recordings from hippocampal organotypic slices treated with DAPT (red) or DMSO mock (grey). Cells were patched using a low Cl Kgluconate based internal solution and firstly voltage clamped at -70 mV to visualised fast inward mEPSCs and then 0 mV to visualise slower outward mIPSCs. Scale bar, 20 pA, 1000 ms. (b i) Summary of mEPSC frequency (left) and mEPSC amplitude (right). Statistical analysis was performed using student's t-test. Slices treated with DAPT (red, $n = 5$, frequency mean: 0.84 ± 0.27 Hz, amplitude mean: 15.03 ± 1.05 pA) displayed an significant increase in mEPSC frequency when compared to DMSO mock control slices (grey, $n = 7$, frequency mean: 0.27 ± 0.03 Hz, amplitude mean: 15.65 ± 0.50 pA). (DMSO versus DAPT frequency, $p = 0.033$ *). mEPSC amplitude was not significantly altered between DMSO and DAPT groups. (b ii) Summary of mIPSC frequency (left, checked) and mIPSC amplitude (right, checked). Slices treated with DAPT (red, $n = 5$, frequency mean: 1.61 ± 0.28 Hz, amplitude mean: 29.41 ± 1.31 pA) displayed no difference in mIPSC frequency or amplitude when compared to DMSO mock control slices (grey, $n = 7$, frequency mean: 1.52 ± 0.30 Hz, amplitude mean: 27.07 ± 1.08 pA). This result indicates that treatment with γ -secretase inhibitor, DAPT leads to an increase in mEPSC frequency but with no significant change in mIPSC frequency. As with mEPSC, mIPSC amplitude is not altered between DMSO or DAPT treated slices. This result complements the result obtained in Fig 3.10.

3.6 Discussion

The aim of this chapter was to gain a general understanding of the role of presenilins in modulating mEPSC and mIPSC in hippocampal neurons. The results presented outline a role for the γ -secretase associated activity of presenilins in regulating mEPSC frequency but not amplitude. The effect on mEPSC frequency was robustly observed following 48 hr pre-incubation with either DAPT or L-685,458 in dissociated rat and mice wild type neurons as well as organotypic slices. Interestingly, γ -secretase inhibitor application for shorter durations did not reveal statistically significant results. However the results obtained for shorter treatments also seemed to be more variable which may be linked with the smaller sample sizes currently obtained for certain experiments (see Figure 3.2). One example where a large but statistically insignificant result was observed is with 3 hr pre-treatment with DAPT when compared to DMSO mock control cells (Figure 3.2 ii). For this experiment, a sample size of 6 was acquired for both control and test treatments with an average frequency standard deviation of 5.78 Hz. Application of this value to power calculations showed that a sample size of 14-16 cells may generate a statistically significant result with a power of 80%. Therefore, the low sample size obtained for this experiment may not be adequate to detect a statistically significant outcome and further experiments are warranted to provide a better estimate of the effect of 3 hr DAPT treatment on mEPSC frequency. Power calculations for cells treated with L-685,458 for 24 hrs also suggests that a larger sample size ($n = 16-18$ as opposed to $n = 6-10$) may provide a more reliable estimate of statistical significance. However, current interpretations of the results obtained in this chapter generally suggest that presenilin function may target synaptic processes that occur over a longer (rather than shorter) time frame.

This effect on mEPSC frequency is in agreement with previous studies reporting of the impact of pharmacological block of γ -secretase activity on mEPSC properties. Parent et al., (2005) showed using cortical dissociated neurons that PS1^{-/-} mice exhibited a higher mEPSC frequency rate than PS1^{+/+} mice. 4-24 hr treatment of PS1^{+/+} cells with γ -secretase inhibitors L-685,458 (1 μ M) or compound E (10 nM) also led to an increase in mEPSC frequency. Kamenetz et al., (2003) showed that 24

hr treatment with L-685,458 (1 μ M) elevated mEPSC frequency rate in rat hippocampal organotypic slice cultures. In agreement with experiments presented in Figure 3.2, Kamenetz et al., (2003) also showed that 1 hr pre-treatment of L-685,458 did not cause any changes in mEPSC frequency or amplitude. Priller et al., (2006) showed that with extended (18-20 day) treatment with DAPT (1 μ M), mEPSC frequency was increased in hippocampal autaptic culture preparations. Taken together with the observations reported in this chapter, there is good evidence that γ -secretase activity is implicated in modulating mEPSC frequency in cortical and hippocampal cultured mice and rat neurons.

Results from PS1^{-/-} mice also indicated that the γ -secretase activity involved in modulating mEPSC frequency is associated with PS1 rather than PS2. Application of γ -secretase inhibitors to PS1^{-/-} neurons showed no major additional effects on mEPSC frequency or amplitude (Figure 3.6), suggesting that PS2 does not contribute to γ -secretase activity modulation of mEPSC frequency in hippocampal neurons. This conclusion is in line with previous studies showing that γ -secretase activity in neuronal cultures is primarily derived from PS1 (De Strooper et al., 1998; Naruse et al., 1998; Parent et al., 2005). However, from the experiments performed so far, one cannot rule out any other possible effects of PS2 associated γ -secretase activity on cellular functions that are independent of presenilin 1 associated γ -secretase activity modulation of mEPSC. Whilst the levels of PS2 expression were not directly tested in our hippocampal culture system, an earlier study using a conditional PS1^{-/-} mouse model showed that elimination of PS1 does not alter PS2 protein expression, suggesting that PS2 levels are not up or down regulated in PS1^{-/-} animals (Yu et al., 2001). One important point to note is that immunolabelling or examining protein expression of PS1 and PS2 may not provide the most reliable correlate for cellular γ -secretase activity and could be potentially misleading as only a small proportion of cellular presenilins (in “active” N and C terminal derivative form) is incorporated into active γ -secretase complexes through a tightly regulated albeit not entirely understood process (Dries and Yu, 2008; Lai et al., 2003; Thinakaran et al., 1997). In light of this, investigating the γ -secretase activity of PS2 and PS1 complexes separately in hippocampal synapses may provide insights into potential differential roles in modulating unique synaptic functions. One possible approach is to selectively knock-down endogenous PS1 or PS2 using siRNA techniques and

determine if there are any differential changes in miniature current properties. Alternatively, constitutive PS2 knock-out animals (Herreman et al., 1999) may provide insights into the role of PS2 in synaptic transmission.

One recent report has indicated that mEPSC frequency and amplitude recorded in hippocampal CA1 neurons are not significantly altered in acute slices from conditional CA3 region-specific PS1 and PS2 double knockout mice (Zhang et al., 2009). The reason for the discrepancy between the findings of Zhang et al., (2009), which utilised presenilin double knock-out animals, and others using constitutive PS1^{-/-} mice (Parent et al., 2005 and Figure 3.5 -3.7) and γ -secretase inhibitor treated cells (Kamenetz et al., 2003; Parent et al., 2005; Priller et al., 2006) and Figure 3.1-3, 3.6-10) is currently not fully understood. Potentially the difference may be related to the preparation (acute slices versus dissociated and organotypic slices) or the selective presynaptic knockout of presenilin (as opposed to global effects of interfering with PS, as is the situation in PS1^{-/-} cells and γ -secretase inhibitors).

The effect of γ -secretase activity inhibition on spontaneous inhibitory currents had not been investigated prior to this study. Interestingly, preliminary experiments indicate that block of γ -secretase does not alter mIPSC properties suggesting a selective effect on excitatory synapses. It is currently unknown if γ -secretase selectively translocates to excitatory synapses or if the effect on mEPSC frequency is linked with selective processing of a substrate that modulates spontaneous currents at excitatory synapses but not at inhibitory synapses. It has recently been shown that overexpression of APP can lead to a reduction in excitatory AMPA and NMDA current amplitude but with no change in inhibitory GABA current amplitude (Kamenetz et al., 2003). This may indicate that γ -secretase processing of APP may lead to changes in excitatory but not inhibitory synaptic transmission. Further studies will be required to determine how the loss of γ -secretase activity and APP processing alters excitatory synapse function. Interestingly, a study showed that mEPSC frequency is increased in APP knock-out mice suggesting loss of APP (and loss of γ -secretase processing of APP) can lead to the opposite effect of APP overexpression. This provides an interesting mechanism where γ -secretase processing of APP may act to bidirectionally regulate synaptic transmission (Priller et al., 2006). mIPSC properties are yet to be determined in APP knock-out mice.

3.7 Conclusion

This chapter showed that γ -secretase activity of presenilin (1) is implicated in regulation of mEPSC frequency at hippocampal excitatory synapses. This result suggests that presenilins are potentially involved in regulating presynaptic properties. However, it is currently unclear how γ -secretase activity may lead to a change in presynaptic function. As changes in presynaptic function are commonly associated with either an alteration in release probability or synapse number, the next two chapters will address these two points in turn.

Chapter 4: The role of presenilin in modulating release probability in hippocampal neurons

4.1 Introduction

The data presented in chapter 3 provides evidence that pharmacological inhibition of γ -secretase activity and PS1 deficiency can lead to an increase in mEPSC frequency suggestive of a change in presynaptic function. One factor that may contribute to a change in presynaptic function is a change in release probability. The release probability (Pr) at synapses in the CNS can be highly variable (Allen and Stevens, 1994; Branco et al., 2008; Branco and Staras, 2009; Dobrunz and Stevens, 1997; Murthy et al., 1997). This variability is observed at multiple levels, from synapses between different brain regions, synapses being made between different classes of neurons, synapses from different axons onto the same postsynaptic cell and synapses from the same axon onto the same postsynaptic cell (Branco et al., 2008; Branco and Staras, 2009; Dobrunz, 2002; Dobrunz and Stevens, 1997). Release probability has also been shown to be closely associated with the size of the readily releasable pool (RRP) at single synapses (Branco et al., 2009; Dobrunz, 2002; Rosenmund and Stevens, 1996). To examine if release probability was altered following γ -secretase activity inhibition using pharmacological agents or elimination of PS1 gene, an electrophysiological estimate was used in organotypic slice cultures whilst live cell imaging of single synapses was adopted for dissociated cultures.

4.2 Estimating release probability using optical measurements of FM-dye destaining

An estimate of release probability of a synapse can be measured directly by examining the rate of FM dye de-staining from single presynaptic terminals as a measure of synaptic vesicle exocytosis (Figure 4.1). The expectation is that synapses with a high release probability will display a faster rate of de-staining and synapses with lower release probabilities will exhibit a slower rate of de-staining upon successive stimulation (Branco et al., 2008; Zakharenko et al., 2001). FM dye de-staining was measured by applying 900 stimuli at 5 Hz and the rate of fluorescence loss was observed by acquiring images at 0.1 Hz. Experiments were performed in the presence of CNQX (20 μ M) and DL-AP5 (50 μ M) to block postsynaptic glutamatergic receptors and recurrent activity and picrotoxin (100 μ M) to block postsynaptic GABA_A receptors.

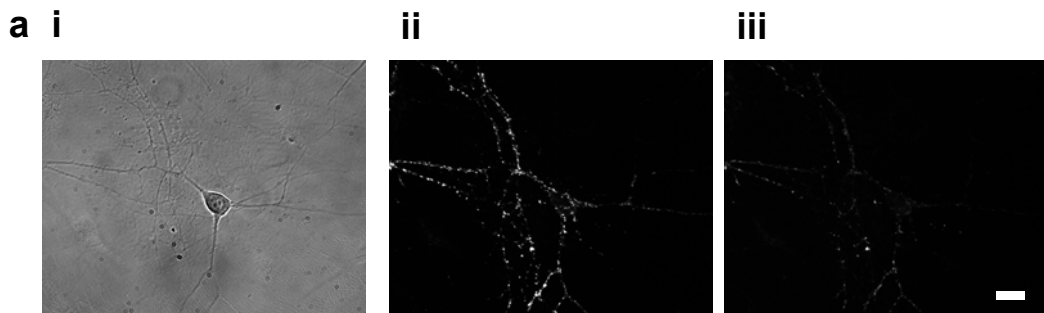


Figure 4.1 – Stimulated FM dye uptake and destaining of hippocampal neurons

(a) (i) 40x magnification DIC image of a rat dissociated neuron at DIV 14. (ii) A fluorescent image of the same neuron as in (i) but after stimulated uptake (and subsequent exchange of the extracellular solution) of FM 1-43 dye using 600 stimuli at 10 Hz field stimulation. Note the dotted pattern along neuronal processes. This fluorescent signal mostly corresponds to FM dye loading into active presynaptic terminals. Applying a further field stimulation of 900 stimuli at 5 Hz leads to exocytosis and subsequent destaining of the FM dye from the presynaptic boutons (iii). Note how most of the FM signal disappears following this stimulation. The remaining regions stained with FM-dye most likely correlate with non-specific signal where dye has associated with the membrane of the cell or presynaptic boutons that have not destained. Scale bar, 20 μ m

4.2.1 Examination of release probability of PS1 +/+ and PS1 -/- neurons using FM dyes

The rate of FM dye destaining from PS1 +/+ and PS1 -/- dissociated neurons was performed in low (1 mM calcium, Figure 4.2 a i), normal (2.2 mM calcium, Figure 4.2 a ii) and high calcium concentrations (5 mM calcium, Figure 4.2 a iii). Analysis revealed that the rate of dye destaining in PS1 +/+ and PS1 -/- cultures at a given calcium concentration did not show any significant differences, thus suggesting a lack of change in release probability between these genotypes (Figure 4.2 b i-iii). The rate of destaining for both genotypes increased with increasing concentrations of calcium as expected of calcium dependence of neurotransmitter release (Dodge, Jr. and Rahamimoff, 1967). This result shows that the release machinery in both genotypes can respond adequately to changes in calcium. This result indicates that the difference in mEPSC frequency observed between PS1 +/+ and PS1 -/- neurons may not be associated with a change in release probability. To further investigate this point, both genotypes were treated with γ -secretase inhibitor DAPT to determine if γ -secretase inhibition causes any alteration of Pr at single synapses. Quantification of destaining kinetics in normal calcium concentrations showed that chronic pre-treatment with DAPT did not alter the rate of destaining of either PS1 +/+ or PS1 -/- cells (Figure 4.3). This result provides further evidence that release probability in mice is not altered by the loss of PS1 gene or presenilin associated γ -secretase activity and the difference in mEPSC frequency is not related to changes in release probability.

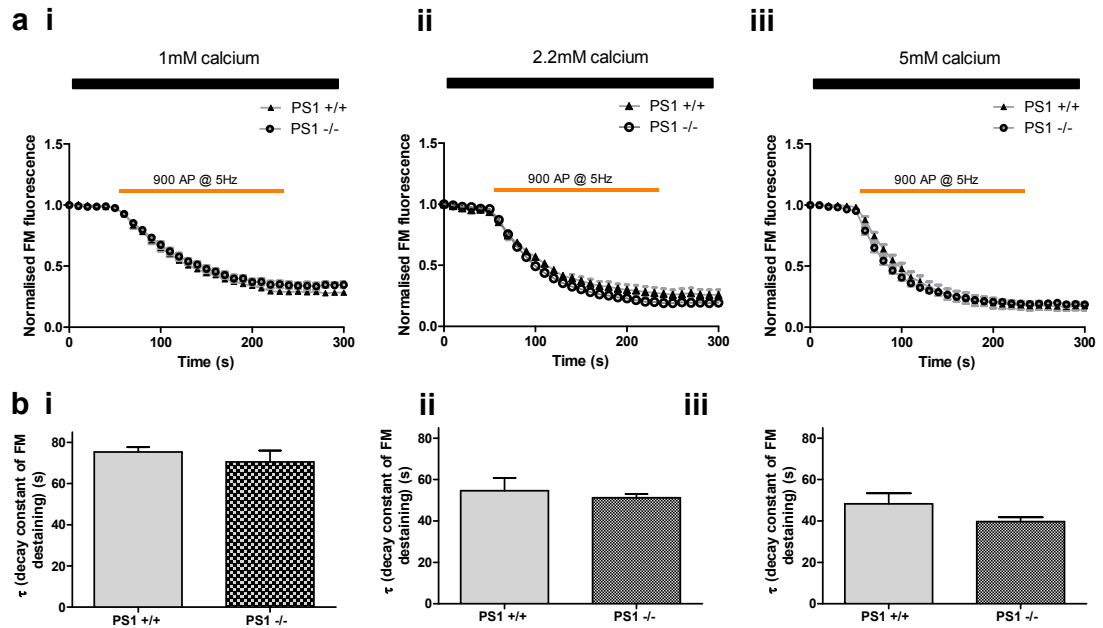


Figure 4.2 – Destaining kinetics of PS1 mice in different concentrations of extracellular calcium.

(a) Average destaining timecourse of PS1 +/+ mice (black triangle) and PS1 -/- mice (open circle) in low (1 mM) calcium (i), normal (2.2 mM) calcium (ii) and high (5 mM) calcium (iii) in extracellular bath solution. Orange bar shows timecourse of field stimulation (900 stimuli at 5 Hz) used to elicit FM dye destaining from neuronal boutons. (b) Summary of decay constants (τ) obtained from experiments shown in (a). PS1 +/+ (light grey) and PS1 -/- (checked grey) respond similarly at a given extracellular calcium concentrations. However, note that the decay constant of FM dye destaining is altered in response to changing extracellular calcium concentrations irrespective of PS1 genotype. (b, i) Mean response in 1 mM calcium extracellular calcium shows PS1 +/+ ($\tau = 75.39 \pm 2.30$, $n = 3$) and PS1 -/- ($\tau = 70.56 \pm 5.48$, $n = 5$) destaining kinetics are similar (student's t-tests, PS1+/+ versus PS1-/-, $p = 0.54$). (b, ii) A similar lack of significant difference is observed in 2.2 mM extracellular solution between PS1 +/+ ($\tau = 54.67 \pm 6.13$, $n = 5$) and PS1 -/- ($\tau = 51.24 \pm 1.77$, $n = 5$) (student's t-tests, PS1+/+ versus PS1-/-, $p = 0.60$). (b, iii) With 5 mM extracellular calcium the decay constant between PS1 +/+ ($\tau = 48.26 \pm 5.11$, $n = 5$) and PS1 -/- ($\tau = 39.71 \pm 2.08$) is also not significantly altered (Student's t-tests, PS1+/+ versus PS1-/-, $p = 0.11$). This data suggests that elimination of PS1 gene does not lead to a change in synaptic vesicle destaining dynamics from hippocampal boutons. n corresponds to the number of coverslips.

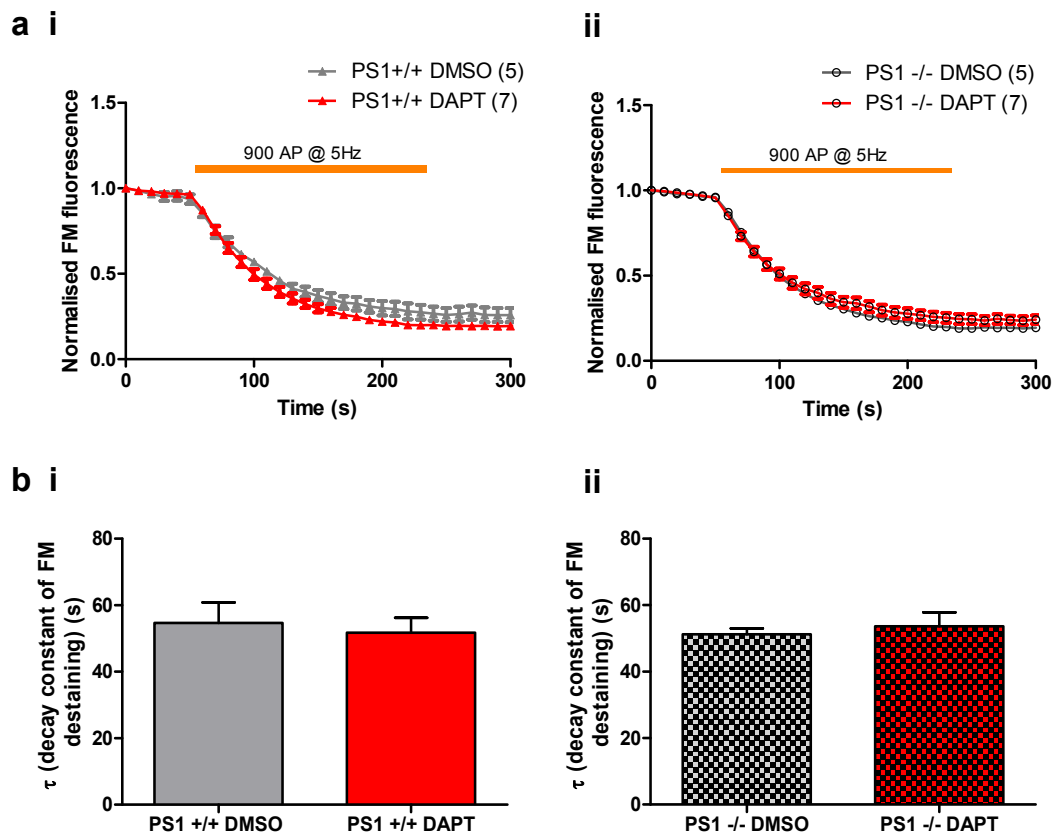


Figure 4.3 – Destaining kinetics of PS1 mice cells following γ -secretase inhibitor treatment.

(a) Average destaining timecourse of PS1 +/+ mice (i, triangles) and PS1 -/- mice (ii, open circles) in normal (2.2 mM) calcium concentrations. Cells for each genotype were treated with either DMSO mock control (grey) or γ -secretase inhibitor, DAPT (red). Orange bar shows timecourse of field stimulation (900 stimuli at 5 Hz) used to elicit FM dye destaining from neuronal boutons. (b) Summary of decay constants (τ) obtained from experiments shown in (a). PS1 +/+ cells treated with DMSO or DAPT destained with similar kinetics (b i, PS1 +/+ DMSO, (light grey), $n = 5$, $\tau = 54.67 \pm 6.13$; PS1 +/+ DAPT (red), $n = 7$, $\tau = 51.78 \pm 4.44$. Student's t-test: PS1 +/+ DMSO versus DAPT, $p = 0.70$). PS1 -/- cells treated with DMSO or DAPT also destained with similar kinetics (b ii, PS1 -/- DMSO (light grey checked squares), $n = 5$, $\tau = 51.24 \pm 1.77$; PS1 -/- DAPT (red checked squares), $n = 7$, $\tau = 53.61 \pm 4.26$. Student's t-test: PS1 -/- DMSO versus DAPT, $p = 0.67$). This data indicates that γ -secretase inhibition does not alter synaptic vesicle destaining kinetics in either PS1 +/+ or PS1 -/- cells.

4.2.2 Examination of release probability of γ -secretase inhibitor treated rat dissociated neurons using FM dyes

As shown in chapter 3, block of γ -secretase activity in rat dissociated hippocampal cultures using two specific inhibitors, DAPT and L-685,458 was sufficient to cause an increase in mEPSC frequency. To determine whether this electrophysiological change was due to a change in release probability, FM dye destaining properties were examined in rat dissociated cultures treated with DAPT and L-685,458. As performed for electrophysiological recordings, rat cells were treated with DAPT or L-685,458 for 48 hrs prior to experiments to block γ -secretase activity. Analysis of drug treated and DMSO mock control cells showed no significant effect on synaptic vesicle exocytosis (Figure 4.4). This data is in line with observations made in dissociated PS1 mice neurons where no differences between PS +/+ and PS1 -/- was seen (Figure 4.2 and 4.3). Together this data suggests that γ -secretase activity of presenilins is not essential for regulating release probability at single synapses of dissociated neurons.

I next examined the readily releasable pool (RRP), which correlates to the population of vesicles that are primed and ready to undergo release and hence influence release probability (Tokuoka and Goda, 2008; Waters and Smith, 2000). To estimate RRP, 30 action potentials were applied at 1 Hz in the presence of FM dye in the extracellular solution. Cells treated with DMSO mock or γ -secretase inhibitors, DAPT and L-685,458 did not reveal any significant differences in fluorescence following loading of the RRP (Figure 4.5). This result suggests γ -secretase activity is not involved in the regulation of presynaptic RRP size.

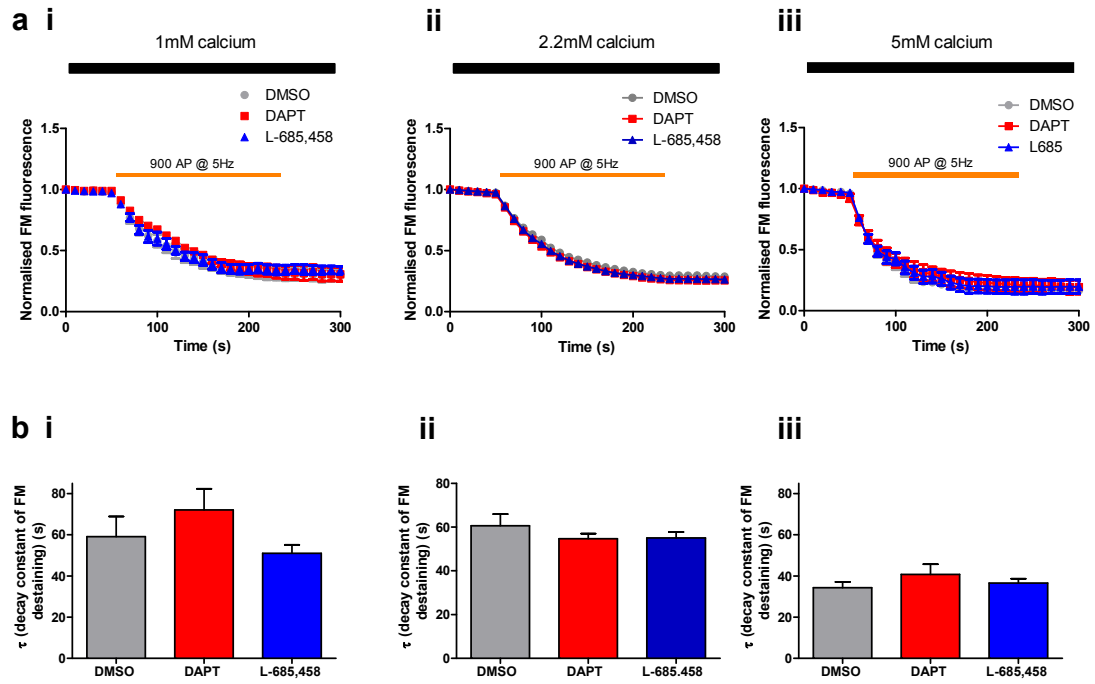


Figure 4.4 – Destaining kinetics of rat dissociated neurons treated with γ -secretase inhibitors in different concentrations of extracellular calcium.

(a) Average destaining timecourse of neurons treated with DMSO mock (grey), DAPT (red) and L-685,458 (blue) in 1 mM calcium (i), 2.2 mM calcium (ii) and 5 mM calcium (iii) in extracellular bath solution. Orange bar shows timecourse of field stimulation (900 stimuli at 5 Hz) used to elicit FM dye destaining from neuronal boutons. (b) Summary of decay constants (τ) obtained from experiments shown in (a). There was no significant differences in destaining kinetics between DAPT and L-685,458 treated cells compared to DMSO mock control cells in (low) 1 mM calcium (b i, DMSO: $n = 6$, $\tau = 59.13 \pm 9.77$; DAPT: $n = 6$, $\tau = 72.07 \pm 10.29$; L-685,458: $n = 5$, $\tau = 51.02 \pm 9.20$. Student's t-test, DMSO versus DAPT, $p = 0.38$; DMSO versus L-685,458, $p = 0.50$). There was also no significant differences in destaining kinetics between DAPT and L-685,458 treated cells compared to DMSO mock control cells in (normal) 2.2 mM calcium (b ii, DMSO: $n = 19$, $\tau = 60.63 \pm 5.33$; DAPT: $n = 16$, $\tau = 54.72 \pm 2.30$; L-685,458: $n = 18$, $\tau = 55.06 \pm 2.70$. Student's t-test, DMSO versus DAPT, $p = 0.35$; DMSO versus L-685,458, $p = 0.37$). This same pattern was also seen between DAPT and L-685,458 treated cells compared to DMSO mock control cells in (high) 5 mM calcium (b iii, DMSO: $n = 7$, $\tau = 34.30 \pm 2.86$; DAPT: $n = 5$, $\tau = 40.74 \pm 4.96$; L-685,458: $n = 7$, $\tau = 36.61 \pm 2.13$. Student's t-test, DMSO versus DAPT, $p = 0.26$; DMSO versus L-685,458, $p = 0.53$). This result shows that γ -secretase inhibition has minimal effect on FM dye destaining kinetics in rat dissociated neuronal cultures. This suggests that γ -secretase activity is not involved in the modulation of synaptic vesicle dynamics.

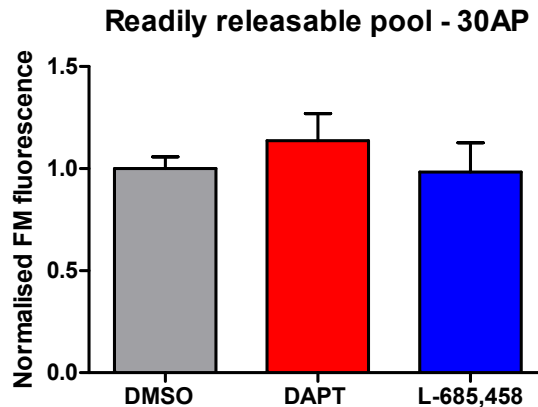
a

Figure 4.5 – Estimation of readily releasable pool size in cells treated with γ -secretase inhibitors DAPT and L-685,458 and DMSO control.

(a) Quantification of readily releasable pool size of cells treated with DMSO mock (grey), DAPT (red) and L-685,458 (blue). Values for γ -secretase treated cells were normalised to DMSO controls for a given culture. There was no significant changes in readily releasable pool size (measured as fluorescence obtained with 30 action potentials (and after background subtraction) – see methods) between DMSO mock, DAPT and L-685,458 treated cells. (DMSO: $n = 15$, $\tau = 1.00 \pm 0.06$; DAPT: $n = 13$, $\tau = 1.14 \pm 0.13$; L-685,458: $n = 8$, $\tau = 0.98 \pm 0.14$. Student's t-test, DMSO versus DAPT, $p = 0.33$; DMSO versus L-685,458, $p = 0.90$). This results shows γ -secretase activity is not involved in the regulation of readily releasable pool size.

4.3 Examination of release probability of γ -secretase inhibitor treated organotypic slices by measuring paired-pulse ratio and the rate of MK801 blockade

FM-destaining experiments outlined above show that Pr was not altered at single synapses in dissociated neurons treated with γ -secretase inhibitors suggesting that the increase in mEPSC frequency observed following γ -secretase inhibition is not due to changes in Pr. To examine whether this conclusion is also applicable to organotypic slices which have been treated with γ -secretase inhibitors, an electrophysiological approach was used. A widely used method for measuring release probability in slices is examination of the paired-pulse ratio (PPR). Paired-pulse facilitation is a form of presynaptic plasticity that has been linked with low release probability synapses and can be largely explained by the presence of residual calcium in presynaptic terminals (Katz and Miledi, 1968). Arrival of an action potential at a synapse leads to a transient elevation of local calcium in the presynaptic terminal. If a second action potential arrives within a few ten - hundreds of milliseconds, the residual calcium leads to a greater increase in the neurotransmitter released due to an increase in release probability and/or number of docked presynaptic vesicles (Cowan et al., 2001; Wu and Saggau, 1994; Zucker and Regehr, 2002). Conversely if a synaptic connection has a high release probability, the number of vesicles being exocytosed is higher during the first pulse that then depletes the number of vesicles available for release during the second pulse. Therefore, PPR is generally considered to be inversely correlated to release probability, with low probability synapses showing high PPR and high probability synapses exhibiting low PPR (Dobrunz and Stevens, 1997). Analysis of PPR showed that there were no significant differences between slices treated with γ -secretase inhibitor DAPT and DMSO mock control slices (Figure 4.6).

To further characterise release probability in organotypic slice cultures, another popular method was utilised, the rate of NMDA receptor mediated blockade by open

channel blocker MK801. MK801 was first used to estimate release probabilities in hippocampal acute brain slices by Hessler and colleagues (Hessler et al., 1993) and by Rosenmund and colleagues in autaptic dissociated hippocampal cultures (Rosenmund et al., 1993). More recently, MK801 was also used to characterise release probability in organotypic slice cultures (Futai et al., 2007). MK801 is a specific blocker of active (open state) NMDA receptors and the rate of progressive irreversible block of synaptic NMDA receptor currents is directly correlated with release probability, with an increased rate of block reflecting an increase in presynaptic release probability.

These experiments were conducted in slices with CA3-CA1 cut to prevent recurrent excitation and continuously maintained in extracellular bath solution (EBS) with picrotoxin. Additionally NBQX (20 μ m) was added to the EBS to block AMPA receptors and enable isolation of NMDA currents. Cells were held at -40 mV to depolarise cells and aid relief of the voltage dependent magnesium block of the NMDA receptor. Slices were perfused with MK801 for approximately 10 mins in the absence of stimulation to enable complete exchange of the recording chamber (Huang and Stevens, 1997). Following this, the Schaeffer collaterals were stimulated at 0.125 Hz and rate of NMDA receptor current block with MK801 was measured. No differences in the rate of synaptic NMDA current block were observed in slices treated with DAPT or L-685,458 when compared to DMSO mock control slices (Figure 4.7). This result shows that γ -secretase activity is dispensable for the regulation of release probability in hippocampal organotypic slices.

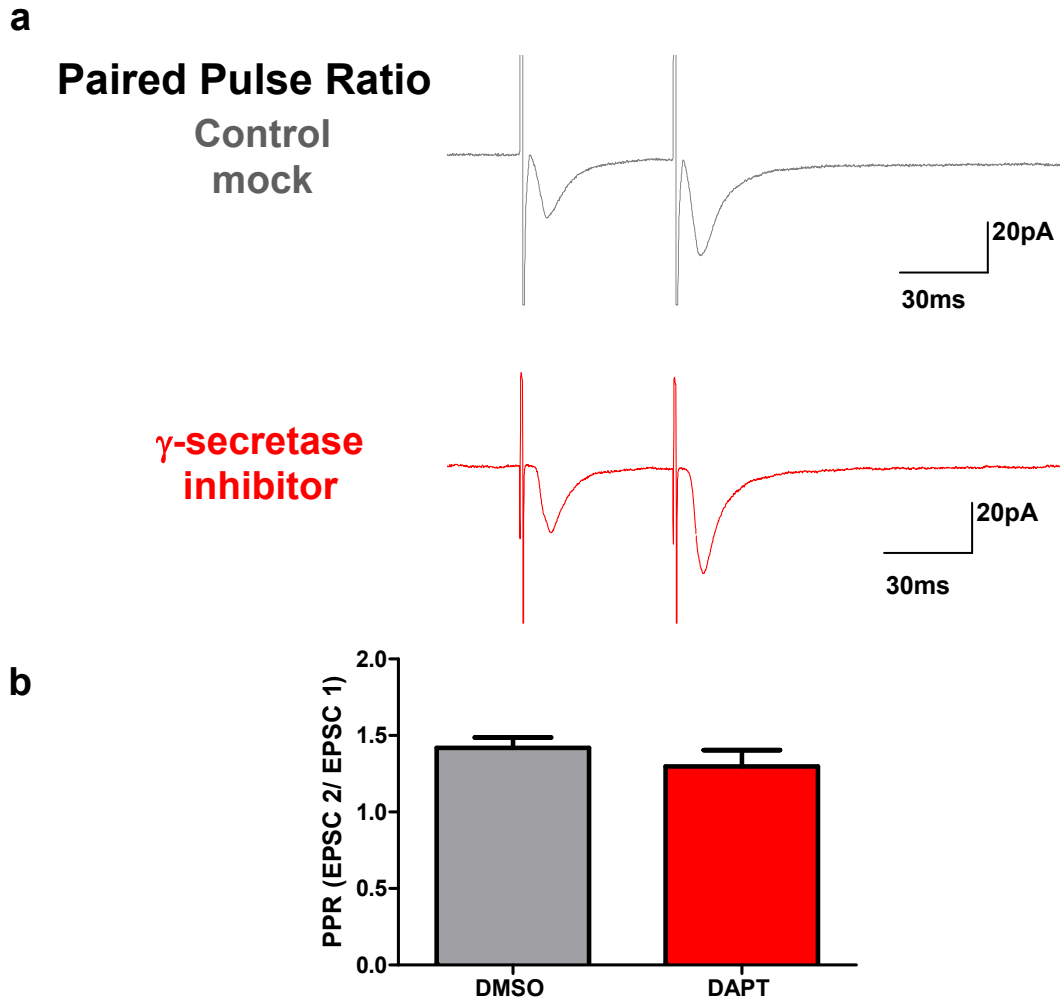


Figure 4.6 – Examining the effect of γ -secretase inhibition on paired pulse ratio.

(a) Sample averaged traces from a cell treated with DMSO mock (grey, top) and γ -secretase inhibitor, DAPT (red, bottom). **(b)** Quantification of paired pulse ratio (PPR) of DMSO control (grey) and DAPT drug (red). No significant changes in PPR were observed between DMSO and DAPT treated slices (DMSO: $n = 8$, mean PPR: 1.419 ± 0.07 ; DAPT: $n = 12$, mean PPR = 1.30 ± 0.37 . Student's t-test, DMSO versus DAPT, $p = 0.41$). This results indicates that γ -secretase activity is not involved in the regulation of PPR, suggesting that γ -secretase activity is not required for regulating release probability.

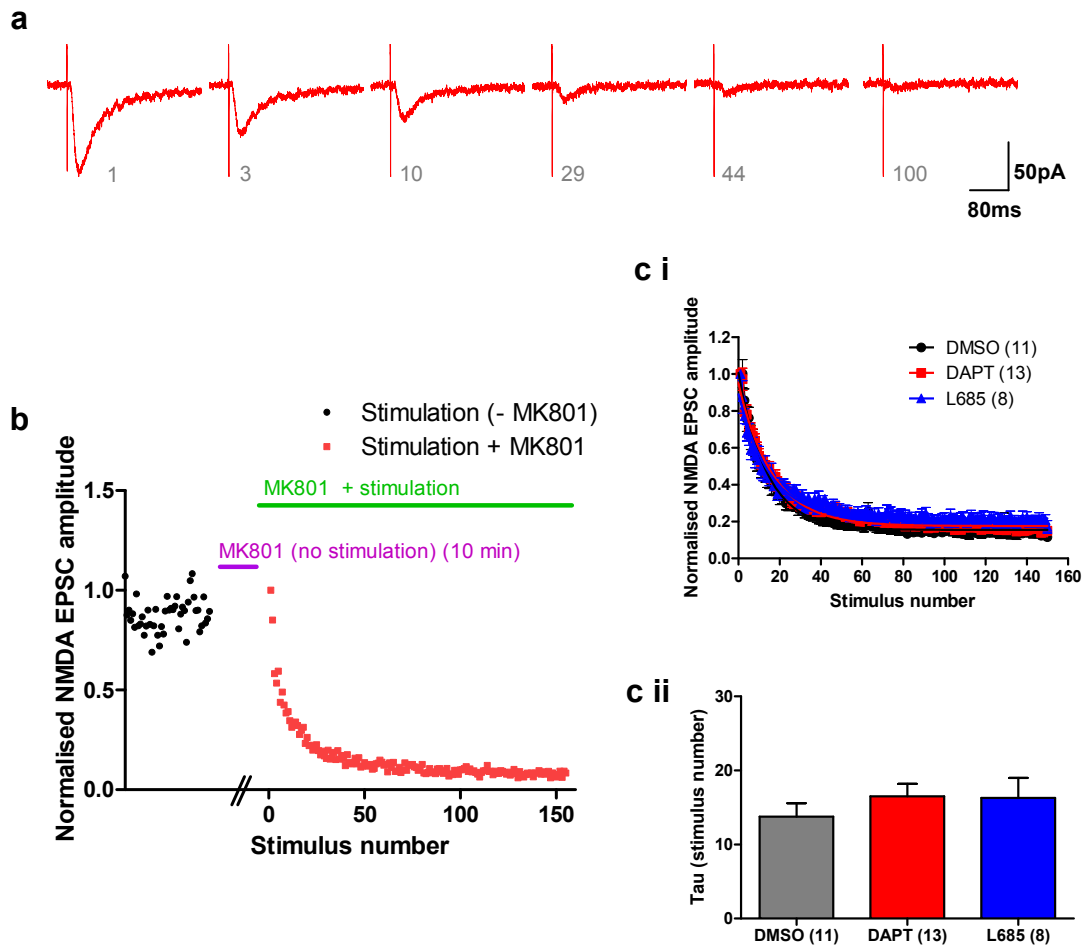


Figure 4.7 – Examining the effect of γ -secretase inhibition on rate of MK801 NMDA receptor block.

(a) Sample traces showing the gradual decrease in NMDA receptor current amplitude with continuous application of MK801 and extracellular stimulation at 0.125 Hz. Grey numbers represent trace number. (b) Graph shows evoked NMDA current response in the absence (black points) and presence of MK801 (red points). Points were normalised to the amplitude of the first evoked NMDA current obtained in the presence of MK801. (c) Quantification of rate of MK801 block. Timecourse of averaged responses to MK801 block (c i) and quantification of decay time constant (c ii) for DMSO (grey), DAPT (red) and L-685,458 (blue). There was no significant difference in the rate of MK801 block between γ -secretase inhibitor treated slices and DMSO control (Figure cii, DMSO: $n = 11$, τ : 13.76 ± 1.83 ; DAPT: $n = 13$, $\tau = 16.51 \pm 1.68$; L-685,458: $n = 8$, τ : 16.30 ± 2.69 . Student's t-test, DMSO versus DAPT, $p = 0.28$; DMSO versus L-685,458, $p = 0.43$). This results indicates that γ -secretase activity inhibition does not affect rate of MK801 block, suggesting that γ -secretase activity is not required for the regulation of release probability.

4.4 Discussion

As discussed in chapter 3, this and other studies have provided evidence that presenilin and γ -secretase activity is implicated in modulating mEPSC frequency. This chapter set out to examine whether presenilin and γ -secretase activity is implicated in regulating Pr at hippocampal synapses and to determine if a change in Pr is associated with the change in mEPSC frequency. The role of presenilin and γ -secretase activity in modulating release probability has not been extensively studied. This study showed using FM styryl dye imaging at single synapses of PS1 $-/-$ mice and γ -secretase inhibitors treated cells that release probability is not altered upon presenilin manipulation in dissociated hippocampal cultures. Estimating the rate of MK801 block and PPR in organotypic slices treated with γ -secretase inhibitors, corroborated our results obtained from optical methods and revealed no alteration in release probability when compared to control conditions. Together these findings suggest that presenilin associated γ -secretase activity is not required for the regulation of Pr.

Despite the lack of effect on measures of Pr, the effectiveness of γ -secretase inhibitors in modulating mEPSC frequency is robust. However, in order to confirm that γ -secretase inhibitors are active and modulating APP processing, our collaborators from the University of Chicago led by Professor Sangram Sisodia performed western blot analysis on rat dissociated cultures treated with the same batches of γ -secretase inhibitors as used in this chapter. Full length APP and APP C-terminal fragments (CTF) expression was probed using an antibody recognising the C-terminal fragments of APP. The results showed that treatment of rat cultures with γ -secretase inhibitors DAPT and L-685,458, led to a strong accumulation of APP CTFs in the lysate, which was expected from previous reports (see for example, Parent et al., 2005) and strongly implied that γ -secretase inhibitors were effective at blocking γ -secretase proteolysis of endogenous APP (see Appendix I). This result provides further evidence that the lack of effect on release probability is not due to a lack of γ -secretase activity inhibition using DAPT and L-685,458.

A recent study suggests a role for neprilysin, one of several enzymes implicated in the degradation of endogenous A β , in regulating presynaptic release (Abramov et al., 2009). Abramov and colleagues found that acute block of neprilysin activity using a selective inhibitor, thiorphan, and an antibody that neutralises neprilysin activity, increased FM dye uptake into presynaptic terminals and proposed that neprilysin activity negatively modulated basal presynaptic vesicle endocytosis. The thiorphan induced increase in vesicle endocytosis was abolished by treatment with γ -secretase inhibitor, L-685,458, suggesting that γ -secretase activity inhibitor prevents the thiorphan induced increase in release probability. However, it was also shown that treatment with L-685,458, did not lead to a change in synaptic vesicle endocytosis, with the amount of FM dye taken up into synaptic vesicles in γ -secretase treated cells and control cells being comparable. This result suggests that γ -secretase activity does not regulate vesicle endocytosis under basal conditions and by extension; loss of γ -secretase activity does not seem to alter release probability relative to control cells. This conclusion is consistent with the findings presented in this chapter. The authors also provide evidence that A β acts as a positive regulator of release probability, as the thiorphan induced elevation of release probability was abolished by other manipulations which decreased A β production including treatment with β -secretase, antibodies that sequester extracellular A β and upon loss of APP in knock-out cells.

However, another study that was published during the course of this work showed that PPR and neurotransmitter release was altered in a conditional double knock-out of presenilin 1 and 2 (Zhang et al., 2009). Using acute slices obtained from a mouse model where both presenilin genes were specifically eliminated from presynaptic neurons (double knockout in CA3 pyramidal neurons and recording from wild type postsynaptic CA1 neurons of the hippocampus), Zhang and colleagues showed a decrease in PPR and a slower rate of MK801 block. This effect on decreasing release probability upon presenilin elimination was seen in low (0.5-2.6 mM) calcium but not high (5-7.5 mM) calcium concentrations and not observed when presenilin was eliminated from the postsynaptic cell in acute slices. In the same study, PPR was also examined in hippocampal dissociated cultures prepared from presenilin double knock-out. In this preparation, knock-out of presenilin was induced by infection of Cre-GFP lentivirus for 72 hrs and western blot analysis

confirmed the complete absence of PS1 CTF in mature neuronal cultures, presumably from both pre and postsynaptic sites. Examination of PPR was also found to be reduced in these neuronal cultures. The general conclusions from this study suggest that presenilins is implicated in regulating Pr. The reason for the discrepancy between the study by Zhang et al., (2009) and the data presented in this chapter and Abramov et al., (2009) is unclear. The double presenilin knock-out strategy used by Zhang et al., (2009) is potentially different to pharmacological inhibition of γ -secretase activity used in this chapter. One key point that is not clear from the double presenilin knockout animals is whether the effect is dependent or independent of γ -secretase activity of presenilins as both are effectively eliminated upon deletion of the gene. If the effect on Pr is operating through a γ -secretase independent manner then pharmacological inhibition of γ -secretase activity (as presented in this chapter) may not lead to a decrease in release probability. Examining release probability in nicastrin knock-out mice (Tabuchi et al., 2009) which should lack functional γ -secretase complexes but should express presenilin would provide further insight into whether γ -secretase activity is specifically required for regulation of presynaptic function.

4.5 Conclusion

This chapter showed that expression or γ -secretase activity of presenilin (1) dispensable for regulation of release probability. This result suggest that the elevation in mEPSC frequency observed in PS1 knock-out and γ -secretase inhibitor treated cells is not associated with alterations in presynaptic release properties.

Chapter 5: The role of presenilin in modulating synapse number in hippocampal neurons

5.1 Introduction

As discussed in chapter 3, a robust increase in mEPSC frequency was observed upon pharmacological inhibition of γ -secretase activity or elimination of PS1^{-/-} gene. Release probability was thoroughly explored in chapter 4 and no significant differences between presenilin manipulated and control cells were observed, suggesting a change in Pr is not responsible for the change in mEPSC frequency. In this current chapter, the number of synaptic contacts was extensively examined to determine if presenilin may play a role in modulating synapse structure and function of hippocampal neurons.

Synapse number was assessed using either immunocytochemical methods which involved antibody labelling of pre and postsynaptically localised proteins in primary dissociated cultures or estimations of spine number from neurons of organotypic slices by filling cells with Alexa 488 hydrazide (made up in internal solution) to enable visualisation. A previous report from Parent et al (2005) showed that wild type PS1 cortical neurons treated with γ -secretase inhibitors showed an increase in the number of postsynaptic spines when compared to untreated PS1 wild type cells in cortical cultures (Parent et al., 2005). Additionally, PS1 knock-out neurons and PS1 wild type cells treated with γ -secretase inhibitors showed an increase in postsynaptic density marker PSD-95 that overlapped with presynaptic active zone marker bassoon when compared to untreated wild type cells. Analysis of individual PSD-95 and bassoon clusters revealed that the increase in colocalised PSD-95 and bassoon clusters may be due to a postsynaptic increase in PSD-95 signal following γ -secretase activity inhibition or PS1 elimination without an alteration in bassoon signal. One drawback of this study was that the synapse density or number was not

specifically investigated; purely the percentage difference in PSD-95 and bassoon clusters between cells with and without presenilin manipulations was examined. Despite this limited method of analysis, the results suggested that PS1 associated γ -secretase activity could play a role in regulating synapse formation in cortical cultures. In this chapter, I set out to examine the association of synaptic proteins and spine number in greater detail in hippocampal dissociated cultures and slice cultures.

5.2 Examination of synapse number in rat dissociated neurons treated with γ -secretase inhibitors

Synapses are defined as the functional connection between a presynaptic and a postsynaptic cell. Whilst immunofluorescence labelling does not directly assess functionality (only inferred), past studies have suggested that pre and postsynaptic colocalised clusters can display elements of synaptic function such as synaptic vesicle release (see for example: Branco et al., 2008; Darcy et al., 2006). For this reason, synapses were identified as puncta/ regions which contained colocalised presynaptic and postsynaptic markers. To be extra careful that only neuronal markers were analysed, only puncta that co-localised with neuronal marker, MAP2 were assessed. Additionally, the number of pre and postsynaptic puncta were separately examined to determine if there were any differences in the non-colocalised population, which may potentially correspond to extrasynaptic receptors (see for review, Triller and Choquet, 2005) or presynaptic orphan synapses (Krueger et al., 2003; Staras et al., 2010). Antibodies recognising presynaptic vesicle proteins synapsin and synaptophysin were used to identify presynaptic compartments (Lu et al., 1992; Lu et al., 1996; Tarsa and Goda, 2002) that associate with synaptic vesicles at both excitatory and inhibitory terminals. To specifically target excitatory connections, antibodies recognising two postsynaptic excitatory synapse markers were used. Homer is an excitatory postsynaptic density scaffold protein (see Sheng and Hoogenraad, 2007) and GluA1 is an AMPA receptor subunit found predominately at excitatory synapses (see Scannevin and Huganir, 2000). For

GluA1 labelling, antibodies were applied to live cells to aid labelling of the surface population of receptors, as opposed to the internal pool (Cingolani et al., 2008; Passafaro et al., 2001). For most experiments, images were acquired by placing the neuron of interest into the centre of the field of view which essentially enabled an estimate of the majority of synaptic markers to be analysed. However the total synapse number could not be readily assessed as some dendritic branches often extended beyond the boundaries of the image acquisition window and hence could not be analysed.

Firstly, co-localisation of presynaptic vesicle marker synapsin and excitatory postsynaptic density scaffold protein Homer was examined (Figure 5.1). Analysis showed that there was an increase in co-localised Homer and synapsin puncta following γ -secretase inhibitor treatment with DAPT and L-685,458 (Figure 5.1 b i; DMSO: $n = 55$, 1.07 ± 0.40 co-localised puncta per $10 \mu\text{m}$; DAPT: $n = 50$, 1.51 ± 0.07 co-localised puncta per $10 \mu\text{m}$; L-685,458: $n = 51$, 1.35 ± 0.08 co-localised puncta per $10 \mu\text{m}$. Student's t-test: DMSO versus DAPT, $p = < 0.0001$ ***; DMSO versus L-685,458, $p = 0.0038$ **). This result was complimented by a significant increase in both presynaptic synapsin density (Figure 5.1 b iii) and postsynaptic Homer density (Figure 5.1 b iii). Together these results implicate a role for γ -secretase activity inhibition in increasing excitatory synapse density. However, further analysis of synapsin and GluA1 co-localised puncta did not reveal a significant difference following γ -secretase inhibitor treatment (Figure 5.2 b; DMSO: $n = 56$, 1.29 ± 0.06 co-localised puncta per $10 \mu\text{m}$; DAPT: $n = 57$, 1.47 ± 0.07 co-localised puncta per $10 \mu\text{m}$; L-685,458: $n = 40$, 1.36 ± 0.07 co-localised puncta per $10 \mu\text{m}$. Student's t-test: DMSO versus DAPT, $p = 0.053$; DMSO versus L-685,458, $p = 0.486$). In the same cells, analysis of synapsin puncta revealed a modest yet significant increase in density following L-685,458 treatment but only a small but non significant increase in synapsin density was observed in DAPT treated cells when compared to DMSO mock control cells (Figure 5.2 b ii). Analysis of GluA1 density alone showed an increase in both DAPT and L-685,458 treated cells with respect to DMSO mock controls, potentially indicating an increase in extrasynaptic rather than synaptic surface GluA1 (Figure 5.2 b iii). The reasons for the observed differences in the densities of Homer and synapsin co-localised puncta and GluA1 and synapsin co-localised puncta are currently not fully understood.

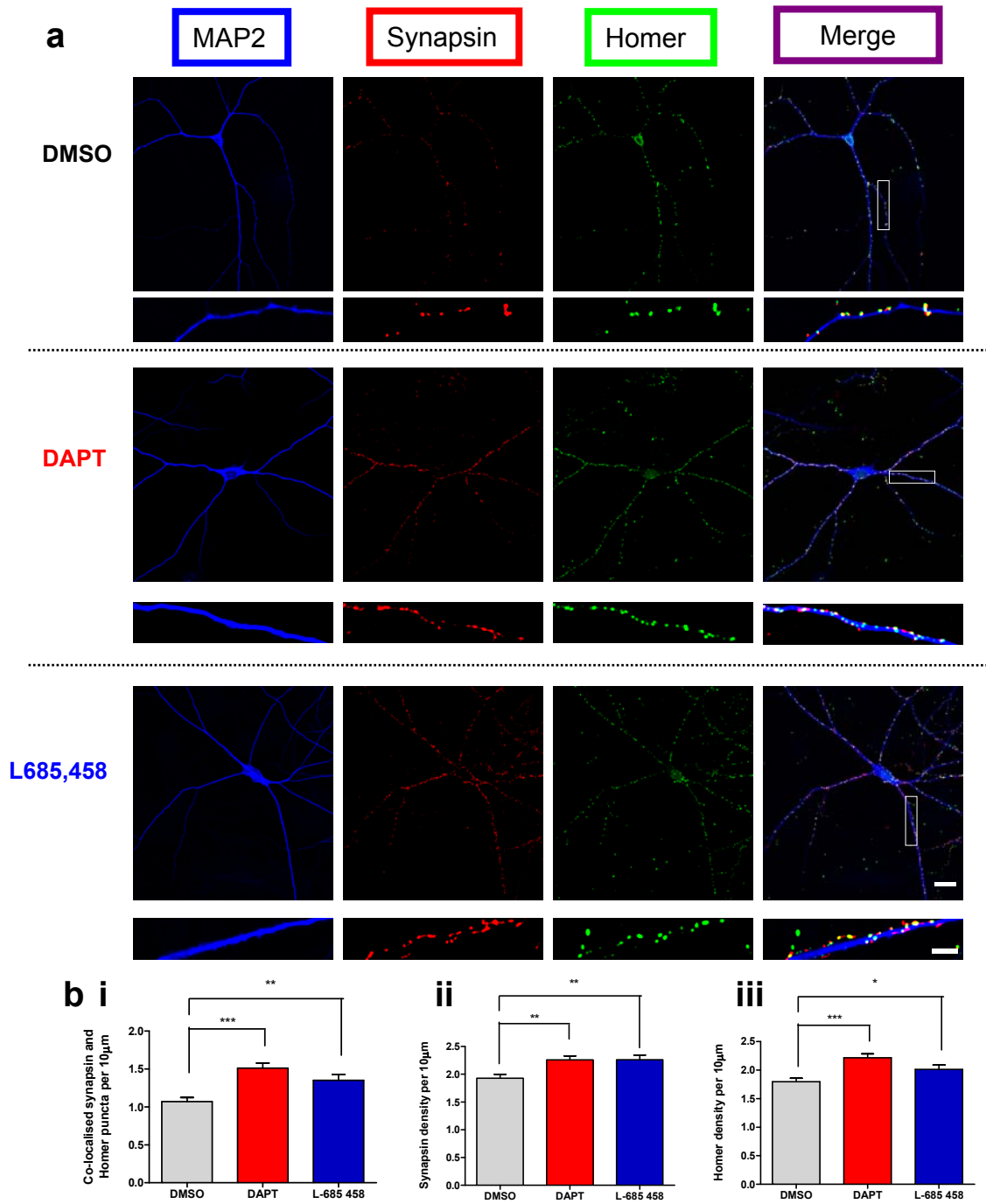


Figure 5.1 – Immunofluorescence analysis of presynaptic synapsin and postsynaptic Homer markers of cells treated with γ -secretase inhibitors, DAPT or L-685,458.

(a) Sample images of neurons treated for 48 hrs with DMSO mock (top, grey) or γ -secretase inhibitor, DAPT (middle, red) or L-685,458 (bottom, blue). Antibody labelling was performed against MAP2 (neuronal marker, blue), Homer (postsynaptic marker, green) and synapsin (presynaptic marker, red). Scale bar: low magnification images 20 μ m, inset images 6 μ m. (b) Summary of immunofluorescence quantification of co-localised Homer and synapsin puncta (i), synapsin puncta (ii) and Homer puncta (iii) of cells treated with DMSO (grey), DAPT (red) or L-685,458 (blue). All puncta were expressed as density per 10 μ m. A significant increase in colocalised synapsin and Homer puncta density (i) was observed in DAPT treated cells and L-685,458 treated cells when compared to DMSO control (student's t-test: DMSO versus DAPT, $p < 0.0001$ ***; DMSO versus L-685,458, $p = 0.004$ **). There was also a significant difference in synapsin puncta density (ii) between DMSO and DAPT (t-test: $p = 0.001$ **) and DMSO and L-685,458 (t-test: $p = 0.003$ **). Analysis of Homer density also revealed a significant increase following γ -secretase inhibitor treatment when compared to DMSO control (t-test: DMSO versus DAPT, $p = 0.0001$ ***; DMSO versus L-685,458, $p = 0.03$ *). $n = 55$ cells were analysed for DMSO mock, $n = 50$ for DAPT and $n = 51$ for L-685,458, pooled from 3 separate cultures. Analysis to compare statistical significant between γ -secretase inhibitor treated and DMSO mock treated cells was performed using student's t-test

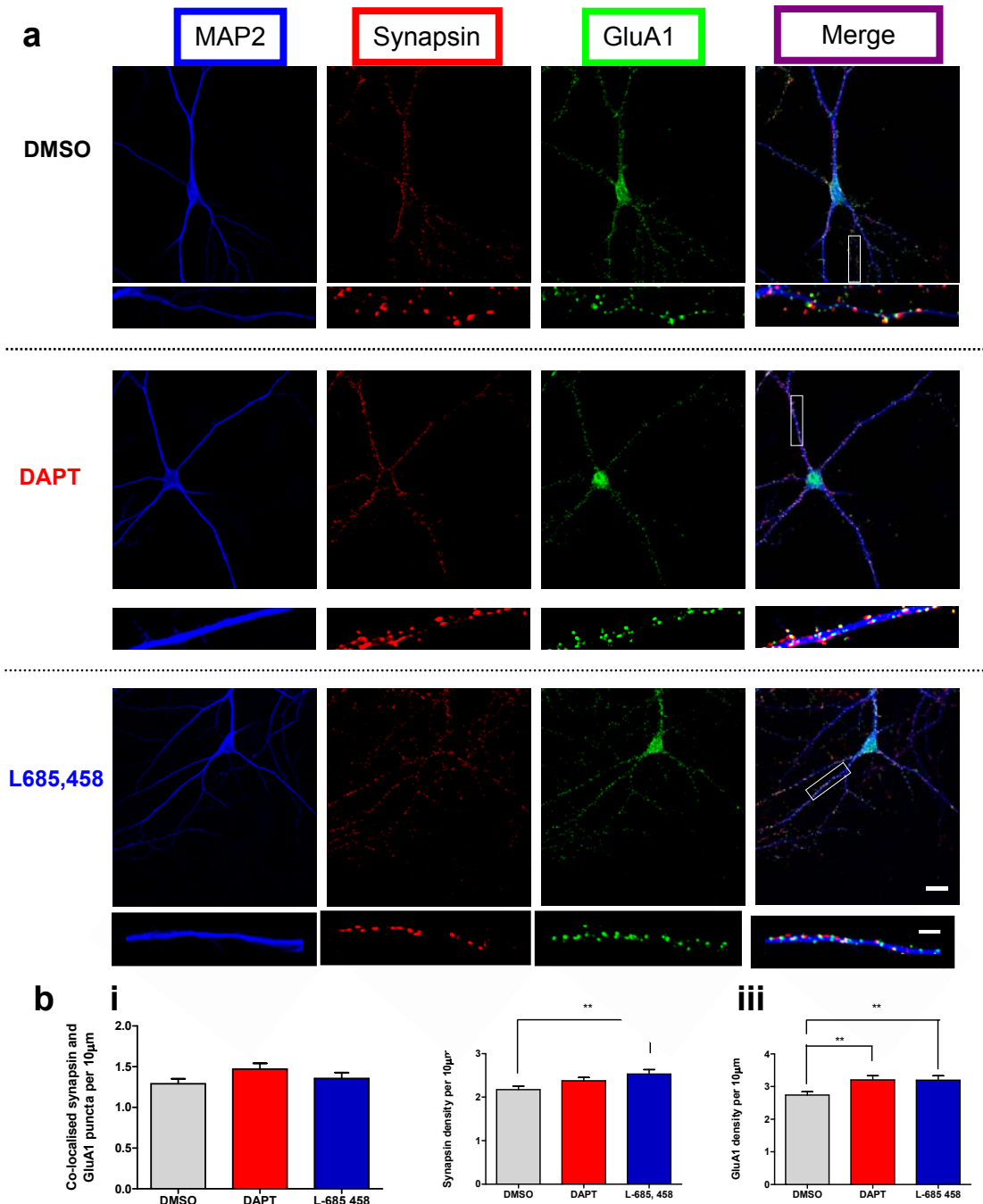


Figure 5.2 – Immunofluorescence analysis of presynaptic synapsin and postsynaptic GluA1 of cells treated with γ -secretase inhibitors, DAPT or L-685,458.

(a) Sample images of neurons treated for 48 hrs with DMSO mock (top, grey) or γ -secretase inhibitor, DAPT (middle, red) or L-685,458 (bottom, blue). Antibody labelling was performed against MAP2 (neuronal marker, blue), GluA1 (postsynaptic marker, green) and synapsin (presynaptic marker, red). Scale bar: low magnification images 20 μ m, inset images 6 μ m. (b) Summary of immunofluorescence quantification of co-localised Homer and synapsin puncta (i), synapsin puncta (ii) and Homer puncta (iii) of cells treated with DMSO (grey), DAPT (red) or L-685,458 (blue). All puncta were expressed as density per 10 μ m. No significant increase in colocalised synapsin and Homer puncta density (i) was observed in DAPT treated cells and L-685,458 treated cells when compared to DMSO control. There was a small but significant increase in synapsin puncta density (ii) between DMSO and L-685,458 treated cells (t-test: $p = 0.005$ **). No significant difference in synapsin density was observed between DMSO and DAPT. Analysis of GluA1 density revealed a significant increase following γ -secretase inhibitor treatment when compared to DMSO control (t-test: DMSO versus DAPT, $p = 0.005$ **; DMSO versus L-685,458, $p = 0.008$ **). $n = 56$ cells were analysed for DMSO mock, $n = 57$ for DAPT and $n = 40$ for L-685,458, pooled from 3 separate cultures. Analysis to compare statistical significant between γ -secretase inhibitor treated and DMSO mock treated cells was performed using student's t-test.

5.3 Examination of synapse number in PS1^{+/+} and PS1^{-/-} mice neurons

To further examine whether presenilin is involved in regulation of synapse number, immunofluorescence labelling was performed on PS1^{+/+} and PS1^{-/-} mice cultures. The effect of γ -secretase inhibition on mEPSC frequency was mimicked by PS1^{-/-} phenotype, and thus the similarities in mEPSC properties could reflect a shared mechanism in regulating synapse number. To test this, both PS1^{+/+} and PS1^{-/-} littermate cultures were labelled in parallel with presynaptic vesicle marker, synaptophysin. Experiments and analysis was performed using the same procedures as that used for rat cultures (see above and methods). Quantification showed that the mean density of synaptophysin puncta in PS1^{-/-} neurons was higher than PS1^{+/+} neurons but not at a statistically significant level (Figure: 5.3, Student's t-test; $p = 0.09$).

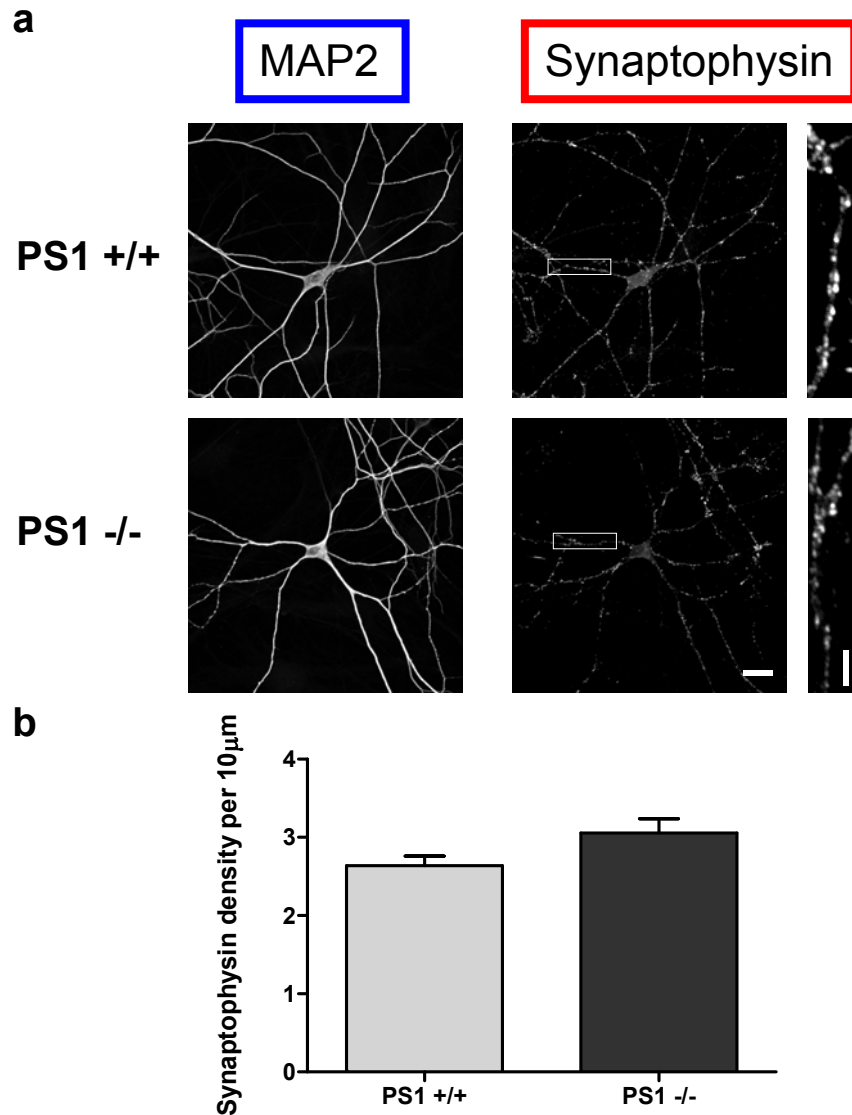


Figure 5.3 – Immunofluorescence analysis of synaptophysin in PS1 +/+ and PS1 -/- cells

(a) Sample images of PS1 +/+ (top) and PS1 -/- (bottom) neurons. Antibody labelling was performed against MAP2 (neuronal marker, left) and synaptophysin (presynaptic marker, right). Scale bars: low magnification images 20 μm, inset images 6 μm.

(b) Summary of immunofluorescence quantification of synaptophysin density in PS1 +/+ and PS1 -/- cells. Synaptophysin puncta were expressed as density per 10 μm. Analysis of synaptophysin puncta showed no significant difference between PS1 +/+ and PS1 -/- cells. n = 19 cells were analysed for PS1 +/+ cells and n = 27 cells were analysed for PS1 -/- cells, pooled from 2 separate cultures. Statistical analysis was performed using student's t-test (bar graphs; p = 0.09).

5.4 Examination of spine number in rat organotypic slice cultures treated with γ -secretase inhibitors

Antibody labelling experiments in rat dissociated cultures suggest that γ -secretase activity may play a role in regulating colocalised Homer and synapsin positive puncta number and thus may provide an explanation for the increase in mEPSC frequency. As with rat dissociated cultures, an increase in mEPSC frequency was also observed in the more intact organotypic slice system upon treatment with γ -secretase inhibitor DAPT and L-685,458. To determine if an increase in synapse number is also observed in organotypic neurons and to test if γ -secretase activity is able to regulate synapse number across different experimental systems, further analysis was performed on CA1 pyramidal cells. Earlier studies have shown that most spines of CA1 pyramidal cell receive one excitatory synaptic input *in vivo* and hence spine number could be assumed to be a fairly good measure of glutamatergic synapse number in slices (Harris and Stevens, 1989; Megias et al., 2001; Schikorski and Stevens, 1997). In order to visualise CA1 pyramidal neurons in organotypic slices, cells were filled with Alexa 488 hydrazide through the patch pipette, fixed and imaged using confocal microscopy. High magnification sections of apical and basal dendrites from secondary proximal branches were used for analysis.

Low magnification images of filled cells showed that there were no gross morphological changes in cells chronically treated with γ -secretase inhibitors DAPT or L-685,458 and DMSO mock controls (Figure 5.4). Analysis of apical and basal dendritic processes also did not show any statistically significant changes in mean spine density (Figure 5.4 b). This result suggests that γ -secretase activity inhibition does not lead to changes in the number of postsynaptic spines in organotypic slice cultures.

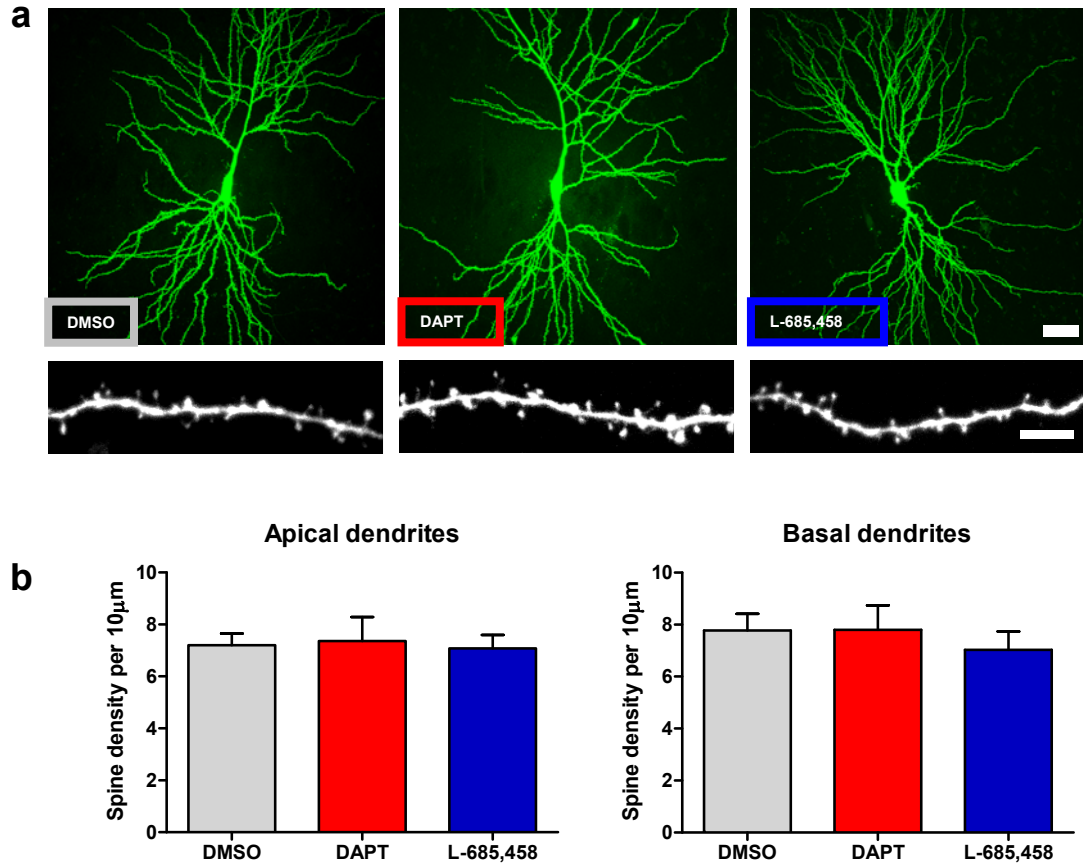


Figure 5.4 – Spine analysis of organotypic slices treated with γ -secretase inhibitors

(a) Sample image a neuron treated for 48 hrs with DMSO mock (left), DAPT (middle) and L-685,458 (right) at low magnification (top) Scale bar, 30 μ m. High magnification images of typical neurons from slices treated with DMSO (left, bottom), DAPT (middle, bottom) and L-685,458 (right, bottom). Scale bar, 5 μ m. **(b)** Quantification of spine density of apical dendrites (left) and basal dendrites (right). No significant differences were observed in either apical or basal spine density in cells treated with DMSO mock (n: 7 cells), DAPT (n: 6 cells), or L-685,458 (n: 6 cells).

5.5 Discussion

The aim of the experiments outlined in this chapter was to investigate whether disruption of γ -secretase activity leads to any changes in synapse number in dissociated and organotypic hippocampal cultures. The results show that cells treated with DAPT and L-685,458 displayed a tendency for an increase in synapsin, Homer and GluA1 density, suggesting γ -secretase activity inhibition modulates both pre and postsynaptic marker density. Moreover, a significant increase in synapsin and Homer co-localised puncta was observed, in accordance with a previous study by Parent et al., (2005) where an increase in synaptic marker co-localisation was also found. Overall the data from these two studies suggests that γ -secretase activity acts as a negative regulator of synapse number and the increase in synapse number may provide a structural correlate to the functional increase in mEPSC frequency following presenilin manipulations. This is in line with previous studies which show that increases in synapse density are correlated with changes in mEPSC frequency (see for example, El-Husseini et al., 2000; Flavell et al., 2006; Levinson et al., 2005).

However, analysis of the density of co-localised GluA1 and synapsin did not reveal any significant differences between γ -secretase inhibitor treated and DMSO mock control neurons. This result suggests that an increase in synapse number (observed as an increase in synapsin and Homer co-localisation) does not necessarily accompany an increase in synaptically located GluA1 receptors. This is not totally unexpected as a study on cultured spinal neurons found that GluA1 AMPA subunits are not always expressed at all excitatory synapses (O'Brien et al., 1997). This result suggests that the increase in mEPSC frequency observed in PS1^{-/-} neurons and in γ -secretase inhibitor treated cells is potentially not due to unsilencing of postsynaptic silent synapses as no change in synaptic GluA1 receptors was observed. This is in agreement with the lack of change in postsynaptic mEPSC amplitude. However, it is currently unclear from this study whether there is any change in the synaptic surface expression of other glutamate receptor subtypes, such as GluA-2, and further experiments will be required to examine this question in more detail. The increase in total GluA1 density (presumably extrasynaptic receptors) however may suggest that

more GluA1 receptors are in a mobile state which may potentially be implicated in synapse formation.

5.5.1 Limitations and points of further investigation

An assessment of synapse number in PS1^{-/-} cells was made. Analysis of PS1^{-/-} neurons did not reveal a significant increase in presynaptic synaptophysin density relative to PS1^{+/+} neurons. Postsynaptic Homer or GluA1 marker labeling was not performed for mice neurons as these cells were also used for PS1 antibody labeling (data not shown, see chapter 8: overall summary). As Homer, GluA1 and PS1 antibodies were all derived from rabbit, this meant only one antibody could be used for a given experiment. As PS1 was always used, this meant that only presynaptic labeling was assessed. One limitation of sole pre or postsynaptic labeling is that the signal may not always correlate with the expression of a functional synapse. This was emphasised by a recent study that showed individual assessment of pre or postsynaptic markers may not reflect the analysis of pre and postsynaptic co-localised synaptic labelling. Parent et al., (2006) showed that PS1^{-/-} cells exhibit an increase in synaptic PSD-95 and bassoon co-localised signal when compared to wild type cells, suggestive of an increase in synapse number. This result was in line with the observed increase of PSD-95 signal in PS1^{-/-} cells. However separate analysis of bassoon labeling did not reveal an increase in signal in PS1^{-/-} cells when compared to control cells. This study highlights a case where the co-localised synaptic labeling should be used for assessment of synapse number. Thus, future experiments examining co-staining between pre and postsynaptic markers may provide a more accurate estimate of synapse number in PS1^{-/-} and PS1^{+/+} cells.

A recent study by Zhang et al., (2009) also showed no changes in synaptophysin labelling in conditional presenilin double knockout mice suggesting that synaptophysin levels are not altered upon complete elimination of presenilins (Zhang et al., 2009). However, postsynaptic markers were also not assessed in this study. Additionally, as synaptophysin is a universal presynaptic vesicle protein found at both inhibitory and excitatory synapses, the effect on excitatory synapses may

potentially be masked if there is a particularly high ratio of inhibitory to excitatory synapses in the regions being analysed. To test this possibility, excitatory (Homer, PSD-95, GluA1 or GluA2) and inhibitory (GABA_A or gephyrin) postsynaptic markers should be examined for co-localisation with presynaptic markers. Additionally, presynaptic excitatory (VGluT) and inhibitory (VGAD) markers can be analysed for co-localisation with postsynaptic markers.

Morphological changes and spine loss have been reported in different AD mice models (see for example, Moolman et al., 2004). In line with this, studies have shown that A β peptides can cause reversible spine loss (Calabrese et al., 2007; Shankar et al., 2007; Shrestha et al., 2006). However, it was not clear if loss of γ -secretase activity could lead to changes in postsynaptic spine density in intact slice preparations. Analysis of postsynaptic spine number also did not reveal any significant differences between γ -secretase inhibitor treated and DMSO mock control cells. The lack of spine changes observed in organotypic slices is contrary to the observations by Parent et al., (2005) which report an increase in spine number following γ -secretase inhibitor treatment (and also in PS1^{-/-} cells) in dissociated cortical cultures. The lack of change in spine number also diverges from the synaptic (Homer and synapsin colocalised puncta) marker results obtained from γ -secretase treated dissociated cultures (Figure 5.1). Potentially the differences may be due to the differences in the preparation (such as drug penetration) but this is unlikely as mEPSC recordings showed an increase in frequency in both dissociated cultures and organotypic slice cultures following γ -secretase inhibitor treatment.

A couple of recent studies investigating the density of spines within different regions of the dendritic tree of hippocampal CA1 pyramidal cells reported that spines are not homogeneously distributed. Extensive electron microscopy analysis on 3-D reconstructed dendritic branches revealed that spines were denser at regions closer to the dendritic branch points and also spine density was higher in distal compared to more proximal regions of the dendritic tree (Katz et al., 2009, but also see Megias et al., 2001). For the organotypic CA1 spine analysis experiments described in this chapter, only a small section of the secondary dendrites was assessed, which represents a minor proportion of the total dendritic spine population. Additionally, a change in synapse number can arise not just from a change in synapse density but

also an increase in dendritic length and increased complexity of dendritic branching. To gain more information on synapse distribution, Sholl analysis can also be used to assess dendritic branching and complexity. In light of the reports by Katz et al., (2009), assessment of spine number should be revisited and a more in depth analysis covering a greater proportion of dendritic spines should be performed (ideally along the total dendritic length) in order to get a more reliable assessment of the synapse number in organotypic slices in the presence or absence of γ -secretase inhibitors. Notably, a study investigating the morphological and functional differences between acute and organotypic slices concluded that cells from organotypic slices displayed a much greater level of complexity and variability than cells from acute slices at an equivalent stage in development (De Simoni et al., 2003). This study indicates that analysis of a greater number of cells is warranted to ensure a more accurate assessment of spine number in organotypic slices. Separation of spines into different classes may also provide information about whether γ -secretase activity of presenilins is involved in regulating spine morphology and maturation. However, this method ultimately relies on being able to completely fill the spine head with dye and being able to accurately resolve the spine shape with no loss of signal (photobleaching) during image capture. The limitations of this approach have been extensively debated in reports by De Simoni et al., (2004) and Svoboda (2004).

Two recent studies have also investigated the impact of γ -secretase inhibitor treatment on postsynaptic changes. One study by Inoue et al., (2009) reported that treatment of mature rat hippocampal dissociated cultures with γ -secretase inhibitor, compound E for 1 week led to a modest but significant decrease in GluA1 receptor staining when compared to DMSO control (Inoue et al., 2009). This result is potentially in disagreement with the results of GluA1 receptor staining presented in this chapter. However, differences in methodology may explain the divergent results. In the study by Inoue et al., (2009), primary antibodies were applied after cell fixation and permeabilisation which would effectively sample the total population (surface and internal pools) of GluA1. This is different to the live labeling procedure used in this chapter, which identifies predominantly the surface population. This means the results from the two studies are not necessarily comparable as different GluA1 populations are examined. Additionally, Inoue et al., (2009) reported no significant changes in presynaptic synaptophysin or postsynaptic

PSD-95 density following γ -secretase inhibitor treatment. Surprisingly, the co-localisation between pre and postsynaptic markers was not reported in this study, despite the double labelling of presynaptic (synaptophysin) and postsynaptic (PSD-95) markers. Intriguingly, Inoue and colleagues report a decrease in spine density in the absence of a change in PSD-95 puncta (Inoue et al., 2009). The lack of effect on PSD-95 labelling is also inconsistent with reports by Parent et al., (2005) which showed that PSD-95 marker staining increases following γ -secretase inhibitor treatment with compound E. The reason for the difference is not entirely clear but differences in drug incubation time may be a possibility, as Inoue et al., (2009) treat for 7 days whilst Parent et al., (2005) treat for a maximum of 24 hrs. If these studies are correct, together the results proposes a model where synapse number is temporally altered depending on the duration of γ -secretase inhibitor exposure with synapse number initially increasing (approximately 4-48 hrs preincubation) followed by a subsequent decrease in synaptic components (after 7 days). Prolonged time lapse imaging would provide a valuable way to examine this case.

The long term effect of γ -secretase inhibition *in vivo* has recently been studied by Bittner et al., (2009). Using live two photon imaging of wild type mice neocortical neurons, this study reported a decrease in dendritic spine density *in vivo* following systemic administration of γ -secretase inhibitor DAPT (100 mg/ kg) (Bittner et al., 2009). Timelapse imaging revealed a significant decrease in mature (persistent) spines, 8 days after the administration of DAPT. The density became progressively lower with extended periods of imaging. No significant changes in spine density were observed after 48 hrs treatment, which suggests that the decrease in spine density requires long γ -secretase treatment periods *in vivo*. Additionally, no effect was observed on the number of transient spines suggesting that γ -secretase specifically targets a specific population of spines. Interestingly, when spine morphology was examined, no differences between the proportion of thin, stubby and mushroom shaped spines was observed following γ -secretase inhibition, suggesting block of γ -secretase activity affects all spine types equally. Presynaptic changes were not examined. The *in vivo* results obtained by Bittner and colleagues are generally in agreement with the spine density results reported by Inoue et al., (2009) in dissociated cultures, but in disagreement with the study by Parent et al., (2005) where an increase in spine density is observed following 24 hr treatment with

γ -secretase inhibitors and the results obtained in γ -secretase treated organotypic slices where no change was observed (Figure 5.4). Further examination of synapse number is warranted to investigate the reasons underlying the reported differential effects.

Due to limitations in time and resources further analysis could not be undertaken during the course of this project. Immunofluorescence analysis of synaptic markers has provided much useful information with regards to understanding relative changes in synaptic proteins. However this technique does not exclude labelling of immature/ nascent synapses in addition to mature synapses. For this, electron microscopy examination should also be pursued to clarify the change in synapse number using ultrastructural methods. Electron microscopy may potentially provide more accurate estimates of synapse number than immunofluorescence methods as the resolution is greater. For example, electron microscopy may reveal two closely associated synapses which may potentially appear as one using immunofluorescence labeling techniques. However one potential drawback with this approach is that only a sub section of synapses can be assessed in practice which precludes the assessment of total synapse number. As synapse distribution on neurons is not homogeneously distributed, there is potential for some bias introduced by synapse selection. Furthermore an estimate of functional synapse number should also be examined to enable better correlations to be made between mEPSC frequency and synapse number. This could be achieved through a combination of paired recordings, quantal analysis and identification of synapses by filling the cells with horseradish peroxidase or biocytin as proposed by Branco and Staras, (2009) amongst many others. Co-immunolabelling for voltage gated calcium channels required for neurotransmitter release and synapsin, a synaptic vesicle protein associated with synapse maturation can also aid identification of functionally mature synapses (Cocot et al., 1998; Lu et al., 1992; Scholz and Miller, 1995).

One aim of this experiment was to determine if γ -secretase inhibition alters synapse number as a possible explanation for the elevated mEPSC frequency observed in chapter 3. Ideally function and synapse number should be assessed in the same cell to determine if there is direct correlation. However this was not possible due to technical difficulties in re-identifying neurons that had been previously used for

recordings after immunofluorescence labeling. This meant that estimates of synapse number were performed on neurons that were separate to the neurons that were used for spontaneous recordings. As the effect of γ -secretase inhibition on spontaneous currents seemed to be restricted to excitatory synapses, immunofluorescence labeling was only performed on excitatory synapse markers; Homer and GluA1. The effect of γ -secretase treatment on inhibitory synapse number was not investigated during these experiments but future studies should examine if there is any alterations in inhibitory synapse number.

5.5.2 Potential mechanisms for γ -secretase associated regulation of synapse number

Currently, the mechanisms that modulate changes in synapse number are poorly understood. Conceivably, there are possibly many different mechanisms that a neuron can use to dynamically and homeostatically regulate synapse formation and elimination throughout its lifetime (see Garner et al., 2002; Goda and Davis, 2003; Ziv and Garner, 2004). Investigating how γ -secretase activity is involved in regulating signaling pathways implicated in synapse formation and elimination will be important to aid our understanding of the role of presenilin in regulating synapse number. As different reports have indicated differential effects of γ -secretase inhibition on synapse density, there is a possibility that more than one mechanism is involved in regulating synapse number.

Parent and colleagues (2005) reported that elimination of PS1^{-/-} gene or inhibition of γ -secretase activity in cortical neurons led to an increase in neurite outgrowth and synaptogenesis. Loss of presenilin expression/activity was also strongly associated with the accumulation of membrane-bound DCC C-terminal fragments and enhanced cAMP/ PKA signaling and phosphorylation of PKA substrates. Previous studies have shown that cAMP/ PKA signaling is involved in regulation of synaptic plasticity including LTP (see Malenka and Nicoll, 1999; Malinow and Malenka, 2002). In line with this observation, studies have also shown that enhanced cAMP signaling can increase mEPSC frequency (see for example, Bie and Pan, 2005;

Bouron, 1999). cAMP/ PKA signaling has also been linked with regulation of synapse morphology (see for example, Ma et al., 1999). Therefore inhibition of γ -secretase processing of DCC can cause accumulation of DCC CTF and enhanced cAMP/ PKA signaling which could lead to an increase in synapse number and mEPSC frequency. This provides evidence that γ -secretase inhibition or knock-out of presenilin can alter structure and function of cortical synapses. It remains to be determined whether changes in cAMP/PKA signaling also occur in hippocampal neurons following inhibition of γ -secretase activity.

Inoue and colleagues showed that γ -secretase activity could enhance formation and maintenance of dendritic spines through an EphA4 dependent mechanism (Inoue et al., 2009). The authors proposed that γ -secretase processing of EphA4 can generate EphA4 intracellular domain fragments which could activate Rac signaling. Rac signaling is implicated in the regulation of the actin cytoskeleton and provides a mechanism for the up-regulation of dendritic spines. Pharmacological block of γ -secretase activity was shown to have the opposite effect, with a decrease in dendritic spines and total GluA1 expression, possibly due to down-regulation of Rac signalling. The authors report that γ -secretase processing of EphA4 can be blocked by NMDA and AMPA receptor antagonists, AP5 and CNQX, suggesting that γ -secretase associated regulation of synapse number is dependent on synaptic activity.

These examples highlight separate mechanisms by which γ -secretase activity is potentially involved in modulating synapse number. There are possibly other γ -secretase modulated signaling pathways which could play a role in regulating synapse number that are yet to be determined. Other γ -secretase substrates or cleavage products such as cadherins (Baki et al., 2001; Marambaud et al., 2002), ErbB4 (Garcia et al., 2000), and A β (Kamenetz et al., 2003) may potentially play a role in synapse regulation in the hippocampus. Determining how, when and where γ -secretase may process potential substrates involved in synaptogenesis and synapse maintenance will be important to further our understanding of the role of presenilin in regulating synapse number.

Another important point to note is that different γ -secretase dependent signaling pathways may be temporally activated/ regulated depending on the developmental expression of the substrates. As mentioned above, γ -secretase activity inhibition was

shown to cause an increase in synapse number with treatment times of 24-48 hrs (Parent et al., 2005 and current chapter) whilst longer treatments (e.g. a week, see Inoue et al., 2009), could cause a decrease in synapse number. The reason for the difference in synapse number at different time points is not known but we can speculate that different signalling pathways may be engaged at different time points which may be associated with the temporally differential effects on synapse number. Interestingly other transgenic mice studies have revealed that synapse number may be bidirectionally altered. In certain AD transgenic mice models, cholinergic synapse density was shown to be initially elevated in younger animals, but with age a progressive decrease in synapse number was observed (see for review: Bell and Cuello, 2006). Developmental differences in synapse number were also identified in presenilin double knock-out animals which showed an increase in synapse number during juvenile-early adult ages (Aoki et al., 2009) and then a decrease in synapse number in later adult ages (Saura et al., 2004). Understanding how these different variables and factors are incorporated may eventually provide an explanation for the difference in synapse number observed with different treatment times.

5.6 Conclusion

This chapter showed that γ -secretase activity of presenilin (1) is involved in regulation of synapse density in hippocampal dissociated neurons. This result suggests that presenilin is potentially involved in modulating pre and postsynaptic structure. Together with the results reported in chapter 3, these findings indicate a role for presenilin in regulating hippocampal synapse structure and function.

Chapter 6: The role of presenilin in modulating intracellular calcium in hippocampal neurons

6.1 Introduction

As discussed in chapter 3, inhibition of γ -secretase activity in neurons was shown to increase mEPSC frequency in both hippocampal dissociated cultures and organotypic slice cultures. Results from chapters 4 and 5 indicate that the increase in mEPSC frequency may be associated more closely with an increase in synapse number, rather an alteration in release probability. The rate of FM-dye destaining, PPR and rate of NMDA current block by MK801 was not significantly altered between γ -secretase inhibitor treated and control groups suggesting release probability is not impaired. However, another possible factor that may influence mEPSC frequency is changes in basal intracellular calcium and release of calcium from presynaptic calcium stores (see Bardo et al., 2006; Collin et al., 2005).

6.1.1 Evidence for calcium regulation of miniature frequency

The view that action potentials can cause depolarisation of the nerve terminal that leads to opening of presynaptic voltage gated calcium channels and subsequent neurotransmitter release is well established (Cowan et al., 2001). However, the involvement of calcium in mediating release of spontaneous miniature currents has been debated. Initial studies at the NMJ showed that miniature end-plate potentials can occur in the absence of action potentials suggesting that these spontaneous fusion events can occur independently of calcium influx (Fatt and Katz, 1952).

Additionally, studies by Scanziani et al., (1992) showed that cadmium; a non-selective calcium channel antagonist can reduce the amplitude of evoked responses but does not alter the amplitude or frequency of excitatory or inhibitory miniature postsynaptic currents in hippocampal organotypic slices suggesting that voltage gated calcium channels are not involved in modulating spontaneous release (Scanziani et al., 1992). However there are several studies that report that spontaneous postsynaptic currents are modulated by calcium in the presynaptic terminals. Whole-cell recordings from dissociated cortical neurons showed that the frequency of miniature inhibitory postsynaptic currents was reduced when immersed in a solution containing 0 mM calcium in the extracellular solution, and further decreases in frequency were observed upon addition of BAPTA-AM, a high affinity calcium chelator (Xu et al., 2009). Together these findings suggest that mIPSCs are sensitive to global changes in basal calcium levels. Furthermore, it has been shown that changing extracellular calcium concentration can influence both mIPSC and mEPSC frequency suggesting that spontaneous currents are sensitive to changes in extracellular calcium (Xu et al., 2009).

Several studies have shown that internal ER calcium stores may be involved in modulating calcium at presynaptic boutons. Reports published several years ago provided evidence that presynaptic terminals exhibited spontaneous calcium signals in both hippocampal CA3 pyramidal cells (Emptage et al., 2001) and cerebellar interneurons (Llano et al., 2000). Additionally it was found that intracellular calcium may modulate the frequency of miniature currents in the cerebellum (Bardo et al., 2002; Llano et al., 2000), hippocampus (Emptage et al., 2001) and cortex (Simkus and Stricker, 2002), via RyR to regulate calcium release from intracellular ER stores.

Exogenous application of the plant alkaloid ryanodine is often used to affect RyR calcium release from ER stores. Interestingly, ryanodine can alter the channel properties of RyR in a concentration dependent manner with concentrations under 10 μM causing channels to be held in a sub-conductive state and enabling calcium release, whilst concentrations above 10 μM led to blockade of the channel and inhibition of calcium release from ER stores (Bardo et al., 2006; Bouchard et al., 2003). Indeed, reports have shown that ryanodine application at 10 μM lead to an increase in the frequency of miniature events (Llano et al., 2000) whilst 20 – 100 μM

concentrations decrease miniature current frequency (Emptage et al., 2001; Llano et al., 2000). Together this data suggests that intracellular calcium stores play an important role in regulating miniature events.

Finally, some miniature currents (~5%) still remain in 0 mM calcium solution supplemented with calcium chelator BAPTA-AM and thapsigargin, an inhibitor of calcium uptake into the ER, indicating that a small population of miniature postsynaptic currents are generated in the absence of a calcium related trigger (Xu et al., 2009).

6.1.2 The role of presenilins in regulating intracellular calcium

A recent study proposes a role for presenilins in regulating neurotransmitter release at CA3-CA1 synapses in the hippocampus (Zhang et al., 2009). PS1 and 2 homozygous floxed mice were crossed with either α -CaMKII-Cre or Grik4-Cre mice to generate CA1 region (postsynaptic) or CA3 region (presynaptic) specific conditional presenilin double knockout mice respectively. Interestingly, this study reports that CA3 region-specific conditional presenilin double knock-out animals show a multitude of different synaptic changes including impairment in long term potentiation, a decrease in paired-pulse facilitation and a decrease in the rate of MK801 block. These parameters were not affected in CA1 region-specific knock-outs. The authors provide evidence that the synaptic changes observed in CA3 presenilin double knock-out mice were linked to impairments in intracellular ER calcium signalling in CA3 neurons.

ER calcium release can occur from two separate ER resident channels, the RyR or the IP₃R. The mechanisms underlying release from these channels differ. IP₃Rs are stimulated by IP₃ which is a product of an intracellular second messenger cascade. Activation of G-protein coupled receptors on the plasma membrane leads to stimulation of a G-protein and subsequent induction of phospholipase C (PLC)-dependent cleavage of phosphatidylinositol-4, 5,-bisphosphate to produce IP₃. In contrast, RyR are activated by agonist induced elevations in intracellular calcium, for

example through voltage-gated calcium channels (VGCC), by a process known as calcium induced calcium release (CICR). Activation of RyR located on the ER membrane occurs when calcium ions bind to the cytoplasmic domain of RyR, which then open to allow release of calcium from the ER (Mattson, 2010).

In the study by Zhang et al., (1999), cellular depolarisation was achieved using acute extracellular application (5 or 30 sec bath application) of high KCl (80 mM) solution to cells. Fura-2 imaging showed that KCl-stimulated CICR from intracellular stores is decreased upon treatment of control neurons with 100 μ M ryanodine in control neurons. This reduction in calcium release was mimicked and occluded in PS double knock-out cultured cells, suggesting presenilins can modulate presynaptic facilitation by regulating CICR. A role for IP₃Rs was discounted as block of IP₃Rs using Xestospongin C did not produce a decrease in KCl-stimulated CICR response.

Interestingly, the reported differences in facilitation and PPR were only observed in conditional double presenilin knockouts of presynaptic neurons and analysis of either PS1 or PS2 single knock-outs showed normal synaptic responses (Yu et al., 2001; Zhang et al., 2009). This intriguing result suggests that there is a difference to knocking out both PS as opposed to eliminating either one and there may be processes in place to compensate when only one is eliminated to maintain synaptic plasticity. However there is no change in PS2 protein expression in the PS1 conditional knockout mice as shown by western blot analysis suggesting that if compensation is present, it is likely to be associated with a change in functionality rather than changes in protein levels (Yu et al., 2001).

One potential limitation of this presynaptic presenilin double knock-out model is that it is not clear how presenilin is modulating calcium release through the ryanodine receptors. It is not known whether the attenuation in synaptic facilitation, short-term plasticity and intracellular calcium is directly due to eliminating presenilin proteins or just the loss of the γ -secretase activity of presenilins. Essentially, this study does not distinguish between γ -secretase dependent presenilin activities from the γ -secretase independent effects of presenilin, as both are abolished. It is also not clear how presenilins may modulate ER release through RyR.

Recent findings have shown that presenilins can act in a γ -secretase independent manner to regulate intracellular calcium dynamics. A study performed in planer lipid bilayer membranes and murine embryonic fibroblasts (MEFs) has shown that presenilin in its holoprotein form can act as a passive calcium leak channel (Tu et al., 2006). This effect does not require γ -secretase activity as the PS1-D257A mutant which lacks γ -secretase activity is also capable of forming calcium leak channels. Furthermore, overexpression of this presenilin mutant can rescue the decrease in calcium signalling in presenilin double knock-out MEFs indicating that γ -secretase activity of presenilins is dispensable for its function as a passive calcium leak channel. At present, it is not known whether presenilin holoproteins also form leak channels in neurons. But if they do, then this would provide another explanation for the reduced intracellular calcium signalling observed in the presenilin double knock-out mice. The decrease in synaptic transmitter release reported by Zhang et al., (2009), therefore may be due to a lack of presenilin holoprotein and/ or reduced activation of the ryanodine receptor which then causes a decrease in intracellular calcium by minimising release from ER stores. If this hypothesis is true then γ -secretase activity of presenilins is not necessarily required.

The first aim of this section was to investigate whether pharmacological inhibition of γ -secretase activity leads to any changes in basal intracellular calcium concentration which may contribute to the changes in hippocampal mEPSC frequency, through live calcium imaging of Fura-2. The second part of this chapter will address whether γ -secretase activity blockade alters intracellular calcium concentrations during calcium induced calcium release (CICR). In order to test the potential involvement of γ -secretase activity in modulating KCl-induced CICR from stores, pharmacological inhibition using γ -secretase inhibitors DAPT and L-685, 458 was used. This approach enables blockade of total γ -secretase (PS1 and PS2 complexes) enzymatic activity, whilst presumably leaving other γ -secretase independent functions of presenilins intact (Li et al., 2000).

6.2 Investigating the effect of γ -secretase inhibition on basal intracellular calcium levels

Fura-2 is a widely used and well characterised ratiometric dye which enables the quantitative measurement of intracellular calcium concentration whilst eliminating experimental inconsistencies including variations in dye loading, excitation intensity, detector deficiency and optical pathlength (Grynkiewicz et al., 1985; Maravall et al., 2000). Rat hippocampal dissociated cultures chronically treated (48 hr) with either DMSO (mock control) or γ -secretase inhibitors, DAPT or L-685,458 were loaded with Fura-2 calcium dye by adding Fura-2 AM, a non-fluorescent membrane permeable form of Fura-2 (1 μ M) to the culture medium and incubating at 37°C for 25 mins. Upon entering cells endogenous cellular esterases cleave the ester groups of Fura-2 AM to generate fluorescent Fura-2 which remains intracellular. Healthy hippocampal cells loaded with Fura-2 were excited using 340 and 380 nm UV wavelengths. To measure basal calcium concentration, paired 340 and 380 nm images were captured in the presence of TTX (1 μ M) and picrotoxin (10 μ M), to parallel conditions used for mEPSC recordings. A ratio value for each frame was obtained by dividing fluorescence values excited by 340 nm and 380 nm wavelengths. In addition to the direct comparison of ratio values, these values were also used to estimate intracellular calcium concentrations according to standard procedures first described by Grynkiewicz et al., (1985) (see methods). Figure 6.1 shows a representative region of a coverslip taken under DIC optics (Figure 6.1.a) and with 340 nm (Figure 6.1.b i) and 380 nm wavelength excitation (Figure 6.1.b ii).

Cells treated with DAPT or L-685,458 showed no significant differences in 340/380 nm ratio values when compared with DMSO mock control cells under basal conditions (Figure 6.1.c.i, DMSO, n = 12, mean: 1.00 ± 0.03 ; DAPT, n = 12, mean: 1.04 ± 0.03 ; L-685,458, n = 14, mean: 1.023 ± 0.03 . Mann-Whitney test, DMSO versus DAPT: p = 0.54; DMSO versus L-685,458: p = 0.82). Calcium concentration measurements for DMSO, DAPT or L-685,458 cells were also not significantly different under basal conditions (Figure 6.1.c.ii, DMSO, mean: 25.76 ± 2.29 nM;

DAPT, mean: 28.56 ± 2.64 nM; L-685,458, mean: 27.44 ± 2.50 nM. Mann-Whitney test, DMSO versus DAPT, $p = 0.54$; DMSO versus L-685,458, $p = 0.82$). These resting calcium concentration values are in good agreement with an earlier study conducted on hippocampal CA1 pyramidal cells where Fura-2 was administered into the cell through the patch pipette and calcium concentration was estimated to be between 25 - 50 nM (Lancaster and Batchelor, 2000). This experiment suggests that γ -secretase inhibition does not alter basal calcium concentration, and that the increase in mEPSC frequency observed following γ -secretase inhibitor treatment may not be linked to a change in intracellular calcium concentration.

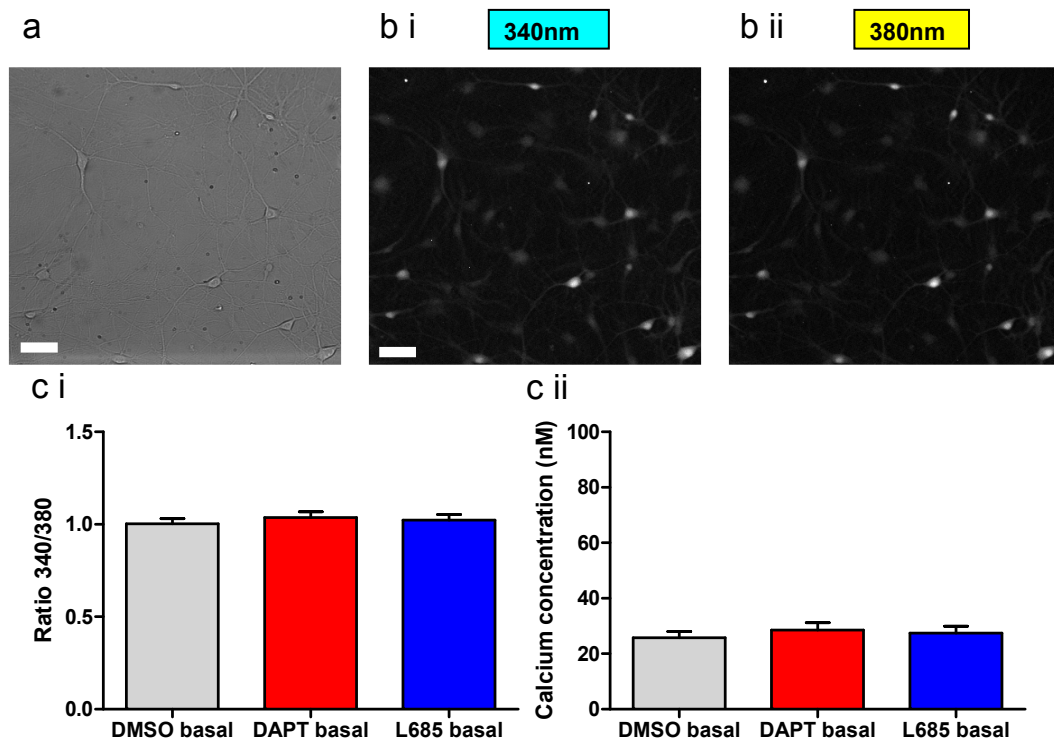


Figure 6.1 - Measurement of basal calcium in hippocampal neurons

Low magnification image of dissociated hippocampal rat neurons viewed with DIC optics (a). The same cells loaded with Fura-2 can be examined using excitation wavelengths of 340 nm (b i) and 380 nm (b ii). Cells were imaged during basal conditions (i.e. in the absence of exogenous stimulation). Scale bar is 50 μ m. (c) Quantification of basal Fura fluorescence signal ratio of 340/380 nm (c i) and respective basal calcium concentration estimates (c ii) for cells treated with DMSO mock (grey) or γ -secretase inhibitors DAPT (red) and L-685,458 (blue). There was no significant differences in the 340/380 nm ratio between γ -secretase inhibitor treated cells and DMSO controls during basal conditions (DMSO, $n = 12$, mean: 1.00 ± 0.03 ; DAPT, $n = 12$, mean: 1.04 ± 0.03 ; L-685,458, $n = 14$, mean: 1.023 ± 0.03 . Mann-Whitney test, DMSO versus DAPT, $p = 0.54$; DMSO versus L-685,458, $p = 0.82$). Analysis of calcium concentration also revealed no significant differences between DMSO and DAPT or L-685,458 treated cells (DMSO, mean: 25.76 ± 2.29 nM; DAPT, mean: 28.56 ± 2.64 nM; L-685,458, mean: 27.44 ± 2.50 nM. Mann-Whitney test, DMSO versus DAPT, $p = 0.54$; DMSO versus L-685,458, $p = 0.82$). n corresponds to the number of coverslips used.

6.3 Investigating the effect of γ -secretase inhibition on intracellular calcium levels during KCl-induced CICR

The same approach as that used to image intracellular calcium concentrations during basal conditions (Figure 6.1) was applied to KCl-induced CICR. Somatic regions were examined in a way that was closely related to the methodology applied by Zhang et al., (2009) but with some slight modifications. The KCl concentration used to stimulate CICR was dropped from 80 mM to 60 mM, images were acquired using a 10x objective rather than a 40x lens and Fura-2-AM was applied at a concentration of 1 μ M for 25 min at 37°C rather than 5 μ M for 45 min at 37°C. The high KCl extracellular solution used to stimulate CICR was a modified version of normal dissociated extracellular solution where NaCl was partly replaced by 60 mM KCl and osmotic balance was maintained at around 290 mOsm. Experiments were performed sequentially, switching between DMSO mock control, DAPT and L-685,458. All results were presented as 340/380 nm ratio values and calcium concentrations (see methods).

Fura-2 fluorescence is dynamically altered upon bath application (30 sec) of high KCl extracellular solution. Representative images of a cell loaded with Fura-2 are shown in Figure 6.2 a. Acute application of KCl (green bar) causes an increase in 340 nm wavelength fluorescence (Figure 6.2 a, top row and i) and a decrease in 380 nm wavelength fluorescence (Figure 6.2 a, bottom row and ii). Ratio values were obtained by dividing 340 by 380 nm fluorescent values and an increase in ratio values temporally coincided with KCl application (Figure 6.2 b), indicating an elevation of intracellular calcium, presumably from both calcium influx from extracellular regions and release from internal calcium stores during CICR. Calcium signal from glial cells was also assessed and judged to have a minimal effect on calcium measurements from the soma of neurons (Figure 6.2 c)

Analysis of 340/380 nm wavelength ratio values did not reveal any significant differences between mock DMSO and γ -secretase inhibitors DAPT or L-685,458

during KCl stimulated CICR (Figure 6.3.b.i, peak ratio: DMSO, n = 12, 6.94 ± 0.32 ; DAPT, n = 12, 6.44 ± 0.24 ; L-685,458, n = 14, 6.90 ± 0.38 . Student's t-test: DMSO versus DAPT, p = 0.232; DMSO versus L-685,458, p = 0.94). Analysis of peak calcium concentration during KCl-stimulated CICR also showed no differences between control and γ -secretase inhibitor treated cells (Figure 6.3.b.i, peak calcium concentration: DMSO, n = 12, 958.5 ± 87 nM; DAPT, n = 12, 808.1 ± 59 nM; L-685,458, n = 14, 999.4 ± 140.9 nM. Student's t-test: DMSO versus DAPT, p = 0.17; DMSO versus L-685,458, p = 0.82). This result suggests that γ -secretase activity is dispensable for calcium release from internal stores during KCl-stimulated CICR and the reduced calcium signals seen in presenilin double knock-out mice (Zhang et al., 2009) may be a result of loss of γ -secretase-independent activity, rather than loss of γ -secretase-dependent activity.

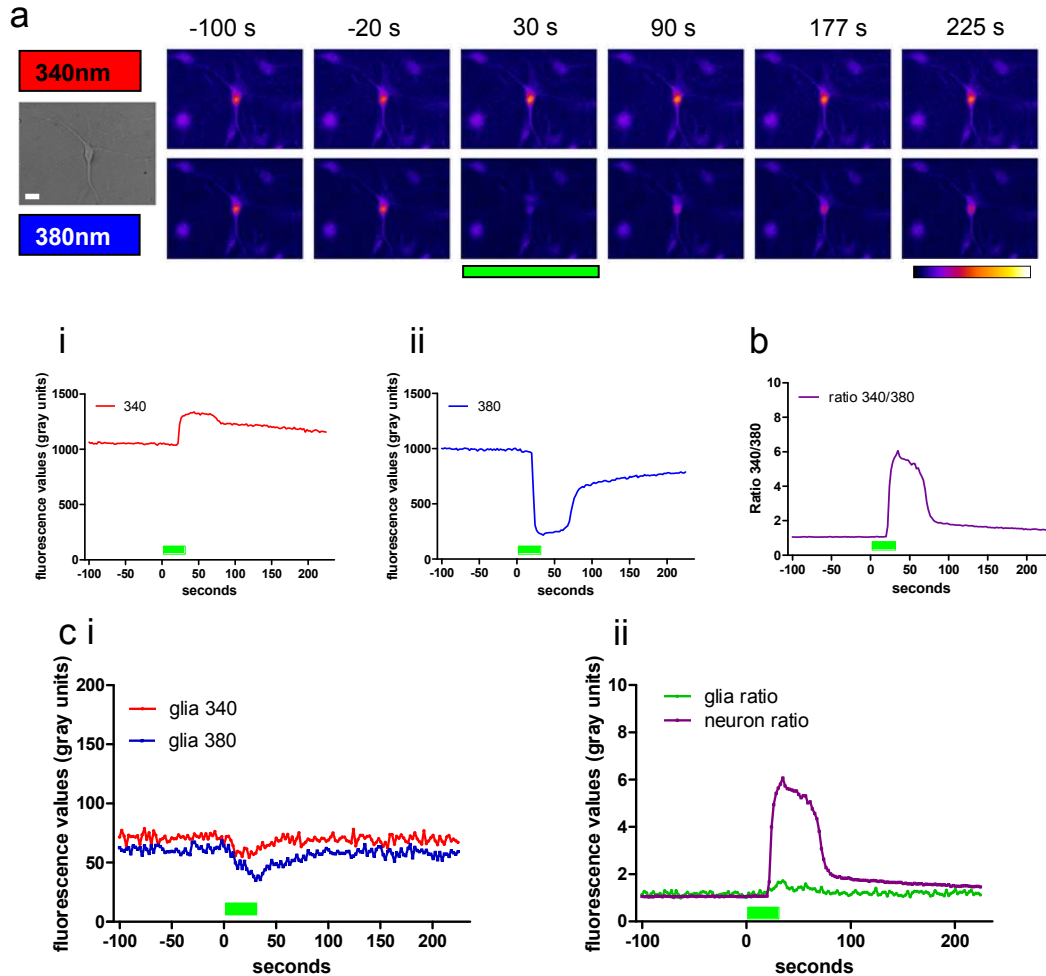


Figure 6.2 - Characterisation of KCl-stimulated calcium induced calcium release (CICR) in rat hippocampal dissociated neurons.

(a) Sample images of a neuron loaded with fura-2 and excited with 340 nm wavelength (top row and i) and 380 nm wavelength (bottom row and ii). The time 0 corresponds to the time when 60 mM KCl was applied to the bath (30 sec duration). KCl application is represented by the green bar. Note, how the (somatic) fluorescence intensity decreases in 380 nm wavelength images and (modestly) increases in 340 nm wavelength images during KCl application to indicate KCl-stimulated CICR, presumably from internal stores. The ratio of 340 and 380 nm wavelength responses is shown in (b). Astrocytes surrounding and beneath neurons can also take up Fura-2. To investigate the contribution of KCl-stimulated CICR from glia, a region of interest was drawn around an astrocyte devoid of neurons. The 340 nm and 380 nm wavelength responses from an astrocyte is shown in (c i). Note the small effect on 340 and 380 nm fluorescence during KCl application, suggesting a minor KCl-induced CICR event in glial cells. (c ii) shows the 340/380 nm Fura fluorescence ratio from the glial cell (green line) superimposed onto the neuronal ratio obtained from (b). This result suggests that the change in fluorescence values observed during KCl application is mainly attributed to calcium changes from neuronal rather than glial cells.

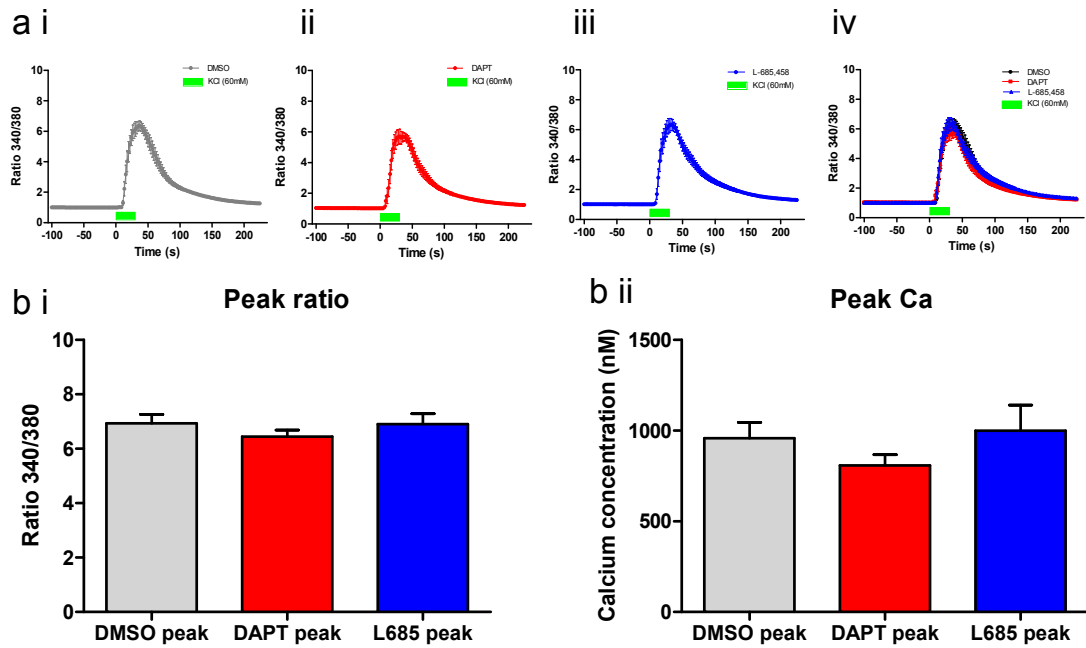


Figure 6.3 - Measurement of peak calcium during KCl-stimulated CICR in hippocampal neurons.

(a) Graphs showing the averaged timecourse of KCl-stimulated CICR for DMSO (i, grey, $n = 12$), DAPT (ii, red, $n = 12$) and L-685,458 (iii, blue, $n = 14$). An overlay of the three treatments is shown in (iv). Green bar represents KCl bath application (60 mM, 30 s)

(b) Summary of peak 340/380 nm wavelength fluorescence ratio (i) and peak calcium concentration (ii) of cells shown in (a). Peak responses correspond to maximum measured calcium increase during KCl-stimulated CICR. There was no significant differences in the peak ratio measured between DMSO mock control and γ -secretase inhibitor treated cells (DMSO, $n = 12$, 6.94 ± 0.32 ; DAPT, $n = 12$, 6.44 ± 0.24 ; L-685,458, $n = 14$, 6.90 ± 0.38 . Student's t-test: DMSO versus DAPT, $p = 0.232$; DMSO versus L-685,458, $p = 0.94$). There was also no significant change in peak calcium concentration (DMSO, $n = 12$, 958.5 ± 87 nM; DAPT, $n = 12$, 808.1 ± 59 nM; L-685,458, $n = 14$, 999.4 ± 140.9 nM. Student's t-test: DMSO versus DAPT, $p = 0.17$; DMSO versus L-685,458, $p = 0.82$). Together this result indicates that γ -secretase activity block does not alter somatic peak calcium responses during KCl-stimulated CICR.

6.4 Investigating the effects of ryanodine receptor and SERCA blockade in γ -secretase inhibitor treated hippocampal neurons

In separate experiments to test the involvement of calcium stores in regulating intracellular calcium, cells were pre-incubated with ryanodine (20-30 μ M (Emptage et al., 2001) for 1 hr at 37 °C) or Thapsigargin (3.8 μ M (Emptage et al., 2001) for 1 hr at 37 °C) to reduce calcium release from intracellular stores. Cells were maintained in solutions reflecting the respective treatments (e.g for ryanodine samples, cells were pre-treated and maintained in ryanodine) for the duration of calcium imaging experiments.

Firstly, hippocampal neurons pre-treated with ryanodine to block RyRs were examined for any differences in basal calcium and peak calcium responses during KCl-stimulated CICR in γ -secretase treated cells and DMSO mock cells. Ryanodine did not have a significant effect on the calcium concentration estimates under basal conditions in control or γ -secretase treated cells (Figure 6.4). This result is consistent with a previous study which showed that ryanodine (30 μ M) does not influence basal calcium levels in presynaptic terminals (Emptage et al., 2001) though the results presented in this chapter examines calcium levels in the soma rather than axonal boutons. Additionally, the peak response to KCl-stimulated CICR in ryanodine pre-treated cells was also not significantly altered (Figure 6.5). Two conclusions can be made from our result. Firstly, block of RyR does not reduce the peak calcium response during KCl-stimulated CICR in cells. Secondly, there is no significant difference between the peak calcium concentrations between cells treated with γ -secretase inhibitors and control cells with or without ryanodine receptor blockade. However this latter result deviates from observations reported by Zhang et al., (2009) who have shown that ryanodine could reduce KCl-stimulated CICR in control neurons. Currently, the reasons for this difference are not entirely clear.

Next, Thapsigargin, an irreversible inhibitor of the SERCA pump was tested. The SERCA pump is located on the ER membrane and is responsible for maintaining the intracellular calcium homeostasis by actively transporting calcium ions from the cytoplasm into the ER lumen. The hypothesis is that inhibition of the SERCA pump by thapsigargin leads to a reduction of calcium in the ER and therefore decreases the amount of intracellular calcium rise during KCl-induced CICR. Hence, this experiment should effectively act as a control for KCl-induced CICR, whereby depletion of the ER calcium store by thapsigargin would lead to a decrease in intracellular calcium levels upon cell depolarisation.

Assessment of basal calcium concentrations in DMSO mock and γ -secretase treated cells, with or without thapsigargin application, revealed no significant differences between any groups (Figure 6.6). This result suggests that depletion of ER stores by thapsigargin does not significantly influence measurements of basal somatic calcium concentration. However, examination of peak calcium responses during KCl-stimulated CICR did reveal a difference following thapsigargin treatment in DMSO mock and also γ -secretase treated cells (Figure 6.7). A significant decrease in KCl stimulated CICR peak 340/ 380 nm wavelength ratio values and calcium concentration measurements was observed in DMSO mock and γ -secretase inhibitor, DAPT and L-685,458 treated cells following thapsigargin treatment (Figure 6.7). However the magnitude of the reduction between control cells and γ -secretase treated cells was not significantly different. These results highlight several points. Firstly, calcium release from ER stores makes a strong contribution to intracellular calcium levels during KCl-stimulated CICR as depletion of stores by thapsigargin leads to a decrease in peak calcium responses. Secondly, γ -secretase activity block does not significantly alter the cellular response to thapsigargin, suggesting that the decrease in peak calcium levels following thapsigargin treatment is independent of γ -secretase activity. This finding provides evidence that γ -secretase activity is not required for modulation of intracellular calcium during KCl-stimulated CICR.

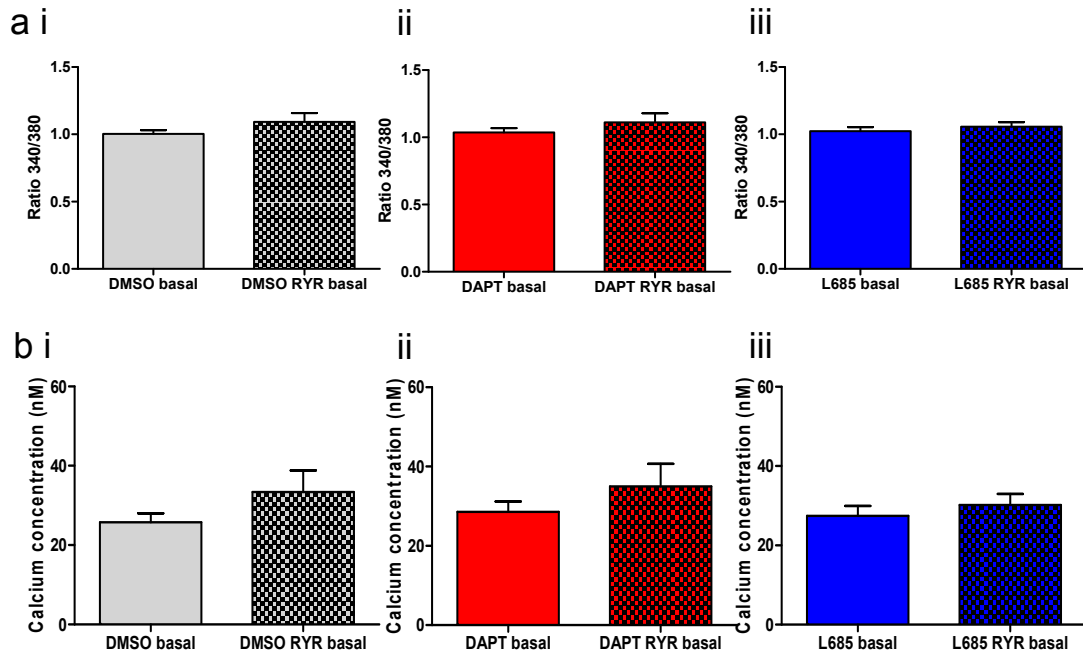


Figure 6.4 - The effects of ryanodine receptor inhibition on basal calcium levels in hippocampal neurons.

(a) Graphs showing 340/380 nm wavelength fluorescence ratio values for DMSO (i), DAPT (ii) and L-685,458 (iii) treated cells, in the absence (plain columns) or presence (checked columns) of ryanodine (20-30 μ M) during basal conditions. There was no significant differences in basal calcium ratio values between cells with or without ryanodine treatment in DMSO (Fig 6.4 a i, without ryanodine: $n = 12$, mean: 1.00 ± 0.03 ; with ryanodine: $n = 9$, mean: 1.09 ± 0.06 . Student's *t*-test, DMSO with ryanodine versus without ryanodine, $p = 0.18$), DAPT (Fig 6.4 a ii, without ryanodine: $n = 12$, mean: 1.04 ± 0.03 ; with ryanodine: $n = 10$, mean: 1.11 ± 0.06 . Student's *t*-test, DAPT with ryanodine versus without ryanodine, $p = 0.30$), or L-685,458 (Fig 6.4 a iii, without ryanodine: $n = 14$, mean: 1.02 ± 0.03 ; with ryanodine: $n = 9$, mean: 1.06 ± 0.03 . Student's *t*-test, L-685,458 with ryanodine versus without ryanodine, $p = 0.48$) groups.

(b) Summary of basal calcium concentration estimates from cells shown in (a). As with ratio measurements, no significant differences were observed in calcium concentration measurements between cells treated or untreated with ryanodine in DMSO (Fig 6.4 b i, without ryanodine: $n = 12$, mean: 25.76 ± 2.29 nM; with ryanodine: $n = 9$, mean: 33.39 ± 5.44 nM. Student's *t*-test, DMSO with ryanodine versus without ryanodine, $p = 0.17$), DAPT (Fig 6.4 b ii, without ryanodine: $n = 12$, mean: 28.56 ± 2.64 ; with ryanodine: $n = 10$, mean: 34.96 ± 5.71 . Student's *t*-test, DAPT with ryanodine versus without ryanodine, $p = 0.29$), or L-685,458 (Fig 6.4 b iii, without ryanodine: $n = 14$, mean: 27.44 ± 2.50 ; with ryanodine: $n = 9$, mean: 30.17 ± 2.82 . Student's *t*-test, L-685, 458 with ryanodine versus without ryanodine, $p = 0.49$) groups.

This data suggests that ryanodine does not significantly alter intracellular calcium concentration during basal conditions. Additionally there were no differences in basal calcium concentration in DMSO mock cells or in cells treated with γ -secretase inhibitors DAPT and L-685,458, implying that γ -secretase activity is not required for regulating basal calcium in the presence or absence of ryanodine.

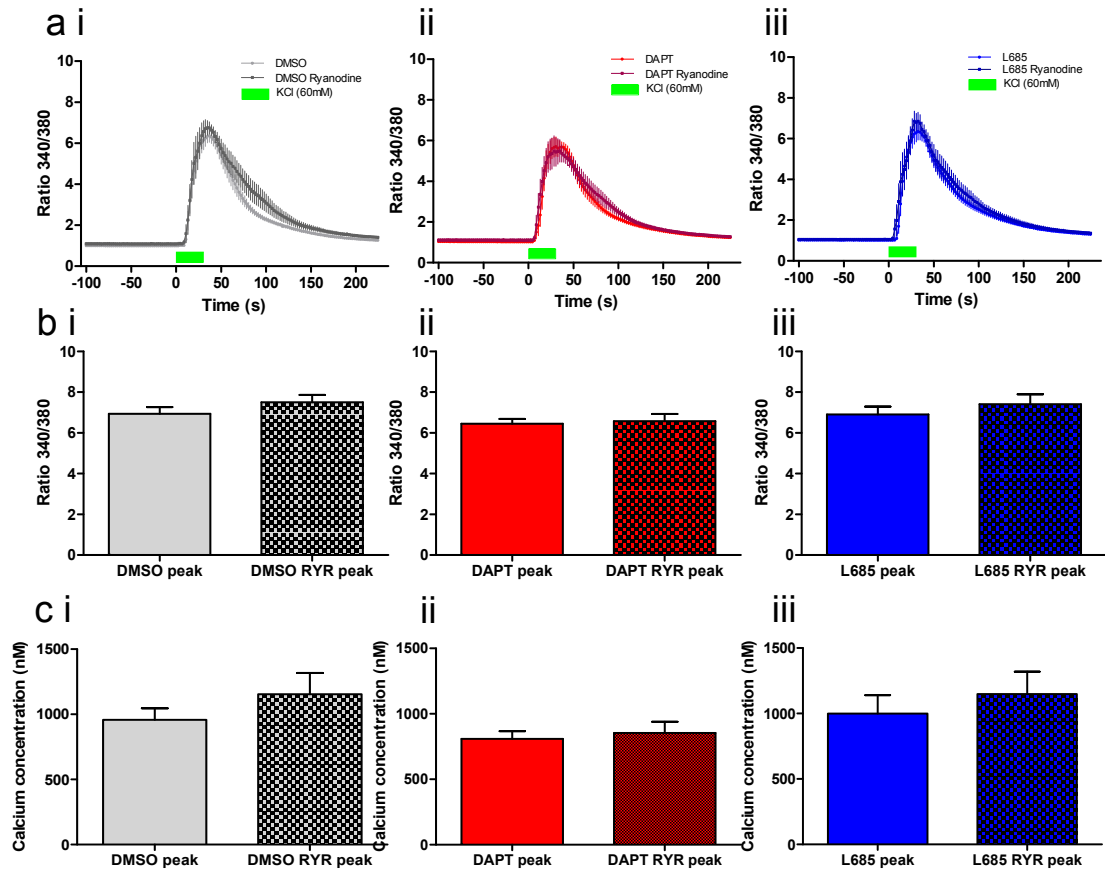


Figure 6.5 - The effects of ryanodine receptor inhibition on peak calcium during KCl-stimulated CICR in hippocampal neurons.

(a) Graphs showing the averaged timecourse of Fura-2 ratio measurements during KCl-stimulated CICR in cells treated with DMSO (grey (i)), DAPT (red (ii)) or L-685,458 (blue (iii)) in the absence (light lines) or presence (dark lines) of ryanodine. Green bar represents KCl bath application (60 mM).

(b) Graphs showing 340/380 nm wavelength Fura-2 fluorescence ratio values for DMSO (i), DAPT (ii) and L-685,458 (iii) treated cells, in the absence (plain columns) or presence (checked columns) of ryanodine (20-30 μ M) during KCl-stimulated CICR. There was no significant differences in peak calcium ratio values between cells with or without ryanodine treatment in DMSO (Fig 6.5 b i, without ryanodine: $n = 12$, mean: 6.94 ± 0.32 ; with ryanodine: $n = 9$, mean: 7.50 ± 0.36 . Student's t-test, DMSO with ryanodine versus without ryanodine, $p = 0.27$), DAPT (Fig 6.5 b a ii, without ryanodine: $n = 12$, mean: 6.44 ± 0.24 ; with ryanodine: $n = 10$, mean: 6.57 ± 0.36 . Student's t-test, DAPT with ryanodine versus without ryanodine, $p = 0.77$), or L-685,458 (Fig 6.5 b iii, without ryanodine: $n = 14$, mean: 6.90 ± 0.38 ; with ryanodine: $n = 9$, mean: 7.40 ± 0.49 . Student's t-test, L-685,458 with ryanodine versus without ryanodine, $p = 0.42$) groups.

(b) Summary of peak calcium concentration estimates from cells shown in (b). As with ratio measurements, no significant differences were observed in calcium concentration measurements between cells treated or untreated with ryanodine in DMSO (Fig 6.5 c i, without ryanodine: $n = 12$, mean: 958.5 ± 86.88 nM; with ryanodine: $n = 9$, mean: 1154 ± 163.6 nM. Student's t-test, DMSO with ryanodine versus without ryanodine, $p = 0.27$), DAPT (Fig 6.5 c ii, without ryanodine: $n = 12$, mean: 808.1 ± 58.66 ; with ryanodine: $n = 10$, mean: 854.8 ± 84.02 . Student's t-test, DAPT with ryanodine versus without ryanodine, $p = 0.65$), or L-685,458 (Fig 6.5 c iii, without ryanodine: $n = 14$, mean: 999.4 ± 140.9 ; with ryanodine: $n = 9$, mean: 1149 ± 170.7 . Student's t-test, L-685,458 with ryanodine versus without ryanodine, $p = 0.51$) groups.

This data suggests that ryanodine does not significantly alter intracellular calcium concentration during KCl-stimulated CICR. Additionally there is no differences in basal calcium concentration in DMSO mock cells or in cells treated with γ -secretase inhibitors DAPT and L-685,458, implying that γ -secretase activity is not required for regulating peak calcium in the presence or absence of ryanodine.

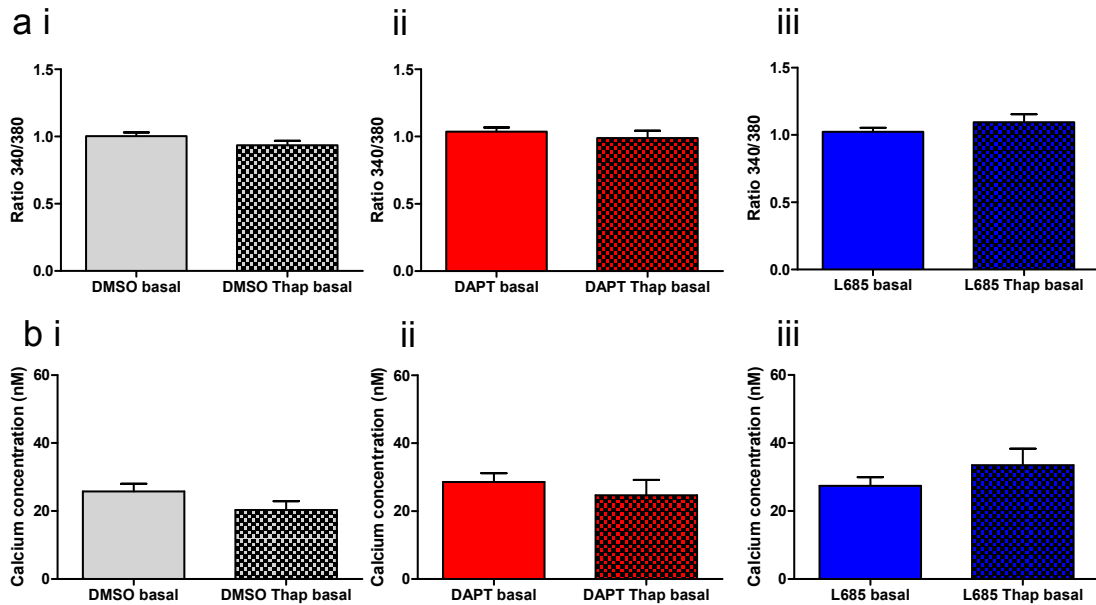


Figure 6.6 - The effects of thapsigargin on basal calcium levels in hippocampal neurons

(a) Graphs showing 340/380 nm wavelength ratio values for DMSO (i, grey), DAPT (ii, red) and L-685,458 (iii, blue) treated cells, in the absence (plain columns) or presence (checked columns) of thapsigargin (3.8 μ M) during basal conditions. There was no significant differences in basal calcium ratio values between cells treated or untreated with thapsigargin in DMSO (Fig 6.6 a i, without thapsigargin: n = 12, mean: 1.00 ± 0.03 ; with thapsigargin: n = 5, mean: 0.94 ± 0.03 . Student's t-test, DMSO with thapsigargin versus without thapsigargin, p = 0.19), DAPT (Fig 6.6 a ii, without thapsigargin: n = 12, mean: 1.04 ± 0.03 ; with thapsigargin: n = 5, mean: 0.99 ± 0.05 . Student's t-test, DAPT with thapsigargin versus without thapsigargin, p = 0.44), or L-685,458 (Fig 6.6 a iii, without thapsigargin: n = 14, mean: 1.02 ± 0.03 ; with thapsigargin: n = 5, mean: 1.096 ± 0.06 . Student's t-test, L-685,458 with thapsigargin versus without thapsigargin, p = 0.25) groups.

(b) Summary of basal calcium concentration estimates from cells shown in (a). As with ratio measurements, no significant differences were observed in calcium concentration measurements between cells treated or untreated with thapsigargin in DMSO (Fig 6.6 b i, without thapsigargin: n = 12, mean: 25.76 ± 2.29 nM; with thapsigargin: n = 5, mean: 20.31 ± 2.62 nM. Student's t-test, DMSO with thapsigargin versus without thapsigargin, p = 0.19), DAPT (Fig 6.6 b ii, without thapsigargin: n = 12, mean: 28.56 ± 2.64 ; with thapsigargin: n = 5, mean: 24.66 ± 4.51 . Student's t-test, DAPT with thapsigargin versus without thapsigargin, p = 0.45), or L-685,458 (Fig 6.6 b iii, without thapsigargin: n = 14, mean: 27.44 ± 2.50 ; with thapsigargin: n = 5, mean: 33.45 ± 4.86 . Student's t-test, L-685,458 with thapsigargin versus without thapsigargin, p = 0.25) groups.

This data indicate that thapsigargin does not significantly alter intracellular calcium concentration during basal conditions. Additionally there is no difference in basal calcium concentration in DMSO mock cells or in cells treated with γ -secretase inhibitors DAPT and L-685,458, implying that γ -secretase activity is not required for regulating basal calcium in the presence or absence of thapsigargin.

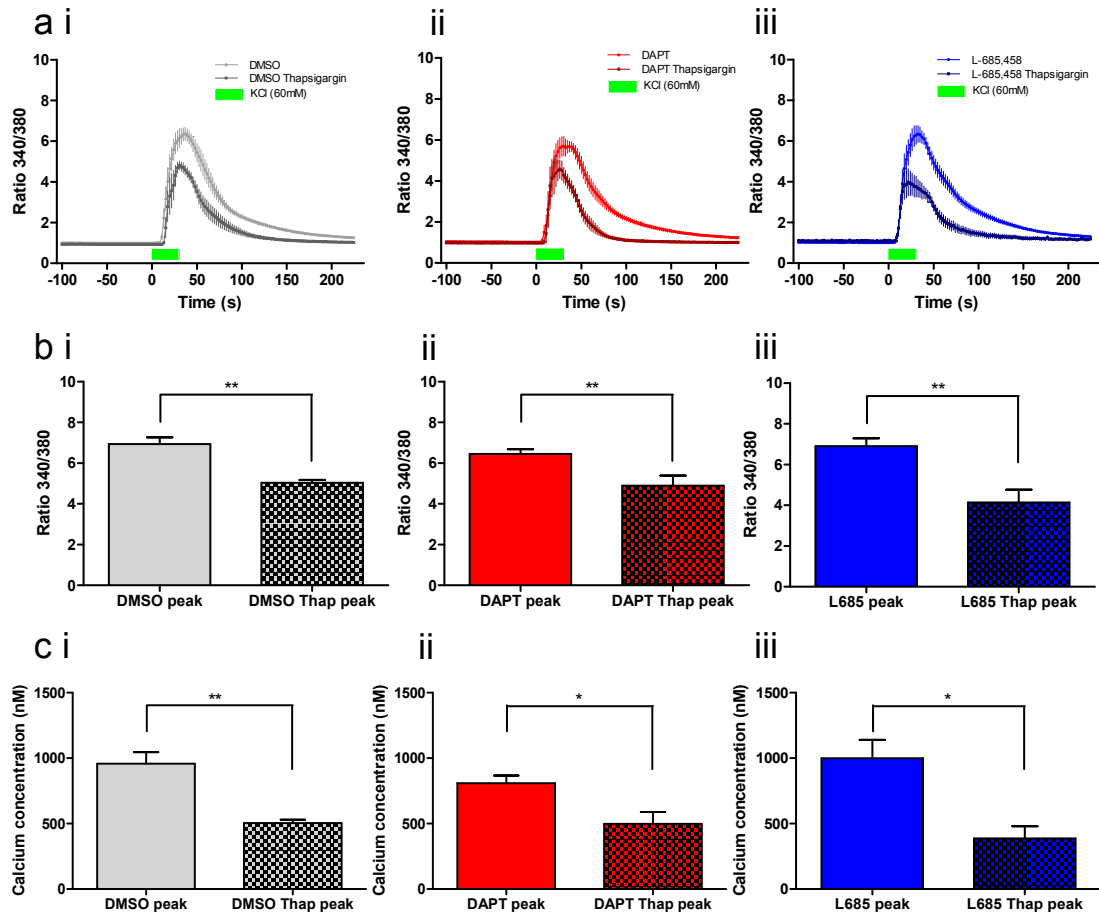


Figure 6.7 - The effects of thapsigargin receptor inhibition on peak calcium during KCl-stimulated CICR in hippocampal neurons

(a) Graphs showing the averaged timecourse of Fura-2 ratio measurements during KCl-stimulated CICR in cells treated with DMSO (grey (i)), DAPT (red (ii)) or L-685,458 (blue (iii)) in the absence (light lines) or presence (dark lines) of thapsigargin. Green bar represents KCl bath application (60 mM).

(b) Graphs showing 340/380 nm wavelength fluorescence ratio values for DMSO (i), DAPT (ii) and L-685,458 (iii) treated cells, in the absence (plain columns) or presence (checked columns) of thapsigargin (3.8 μ M) during KCl-stimulated CICR. There was a significant difference in peak calcium ratio values between cells with or without thapsigargin treatment in DMSO (Fig 6.7 b i, without thapsigargin: n = 12, mean: 6.94 ± 0.32 ; with thapsigargin: n = 5, mean: 5.04 ± 0.14 . Student's t-test, DMSO with thapsigargin versus without thapsigargin, p = 0.002**), DAPT (Fig 6.7 a ii, without thapsigargin: n = 12, mean: 6.44 ± 0.24 ; with thapsigargin: n = 5, mean: 4.89 ± 0.49 . Student's t-test, DAPT with thapsigargin versus without thapsigargin, p = 0.006**), or L-685,458 (Fig 6.7 b iii, without thapsigargin: n = 14, mean: 6.90 ± 0.38 ; with thapsigargin: n = 5, mean: 4.14 ± 0.63 . Student's t-test, L-685,458 with thapsigargin versus without thapsigargin, p = 0.002**) groups.

(c) Summary of peak calcium concentration estimates from cells shown in (b). As with ratio measurements, a significant difference was observed in calcium concentration measurements between cells treated or untreated with thapsigargin in DMSO (Fig 6.7 c i, without thapsigargin: n = 12, mean: 958.5 ± 86.88 nM; with thapsigargin: n = 5, mean: 504.4 ± 24.62 nM. Student's t-test, DMSO with thapsigargin versus without thapsigargin, p = 0.005**), DAPT (Fig 6.7 c ii, without thapsigargin: n = 12, mean: 808.1 ± 58.66 ; with thapsigargin: n = 5, mean: 497.8 ± 90.87 . Student's t-test, DAPT with thapsigargin versus without thapsigargin, p = 0.012*), or L-685,458 (Fig 6.7 c iii, without thapsigargin: n = 14, mean: 999.4 ± 140.9 ; with thapsigargin: n = 5, mean: 386.3 ± 93.00 . Student's t-test, L-685,458 with thapsigargin versus without thapsigargin, p = 0.023*) groups.

This data provides evidence that thapsigargin reduces intracellular calcium concentration during KCl-stimulated CICR, presumably by depleting ER calcium stores. However, there was no differences in the response between DMSO, DAPT or L-685,458 treated cells suggesting that γ -secretase activity is not required for the thapsigargin action on ER serca pump and internal calcium stores.

6.5 Discussion

Previous studies have shown that the frequency of miniature currents is sensitive to changes in intracellular and extracellular calcium (Emptage et al., 2001; Llano et al., 2000; Xu et al., 2009). To determine if alterations in intracellular calcium could contribute to the increase in mEPSC frequency observed in cells treated with γ -secretase inhibitors, Fura-2 fluorescence was imaged and calcium measurements were obtained during basal conditions in the presence of TTX. The results outlined in this chapter, show that there are no major changes in basal neuronal calcium concentrations between DMSO mock and γ -secretase inhibitor treated cells, suggesting that the increase in mEPSC frequency is potentially not associated with a change in intracellular calcium concentration. However, only somatic calcium concentration has been assessed and a more focused examination of axonal boutons is warranted to get a better estimate of synaptic calcium in presynaptic terminals under basal conditions. Additionally further experiments will be required to directly examine whether the increase in mEPSC frequency observed in γ -secretase inhibitor treated cells is due to alterations in ER calcium release. One approach would be to treat γ -secretase inhibitor treated cells with ryanodine or thapsigargin and determine if there is any reduction in mEPSC frequency.

Calcium imaging techniques were also used to probe the involvement of γ -secretase activity in the modulation of KCl-stimulated CICR from internal ER stores. As discussed above, one study showed that presenilin double knock-out cells exhibited a reduced elevation in intracellular calcium during KCl-stimulated CICR compared to control cells (Zhang et al., 2009). This reduction was mimicked by control cells treated with ryanodine, whereas it was occluded in knockout cells treated with ryanodine. The presynaptic knockout of presenilins also led to changes in synaptic plasticity including an impairment of LTP, a decrease in PPF and a slower rate of MK801 block. Zhang and colleagues (2009) propose that the changes in presynaptic function are associated with a reduction in intracellular calcium concentration due to defective calcium signalling involving RyRs located on the ER membrane. However, one key question remains: is the decrease in intracellular calcium

concentration observed during KCl-stimulated CICR in presenilin double knock-out cells due to γ -secretase dependent or γ -secretase independent mechanisms?

To test this, KCl-stimulated CICR was induced in wild type rat hippocampal cells where γ -secretase activity was pharmacologically blocked with specific inhibitors, DAPT and L-685,458. Estimations of peak calcium during KCl-stimulated CICR were not altered between DMSO mock and γ -secretase inhibitor treated cells. This result argues against a role for γ -secretase activity in the modulation of calcium release from stores during KCl-stimulated CICR. This result implies that the reduced calcium responses observed during KCl-stimulated CICR in conditional presenilin double knock-out neurons is potentially due to γ -secretase-independent modulation of ER stores rather than a mechanism that is dependent on γ -secretase activity.

This result parallels findings from human salivary gland epithelial (HSG) cells where potent γ -secretase inhibitors, DAPT (10 μ M, 18-20 hrs pretreatment) or compound E (25 μ M, 4 hrs pretreatment) do not alter agonist (carbachol) mediated calcium release from internal stores (Oh and Turner, 2006). In this previous study, an additional check to show that γ -secretase activity was inhibited following DAPT treatment was carried out by western blot analysis for APP-CTF. Oh and Turner (2006) found a band which corresponded to APP-CTF in cells treated with DAPT, which strongly indicated that DAPT could block γ -secretase activity and inhibited processing of APP-CTF. Furthermore, this band was absent in control HSG cells indicating γ -secretase activity was present in untreated cells. This indicated that the lack of effect on agonist-mediated intracellular calcium release was not due to a lack of γ -secretase inhibition.

However, other studies have suggested otherwise, and that γ -secretase activity may be required for regulation of intracellular calcium release. Leissring et al., (2002) showed using N2a neuroblastoma cells that application of peptide aldehydes YIL and CIL, compounds that were previously thought to act as γ -secretase inhibitors could lead to a reduction in agonist (bradykinin)-induced calcium release from intracellular stores. These aldehyde peptides have a fairly low potency and have been used prior to the discovery of small molecule inhibitors such as DAPT (Dovey

et al., 2001), which are now more commonly used. Leissring and colleagues propose that the decrease in calcium release from stores is associated with AICD nuclear signalling and transcription with the reduction in calcium being mimicked by APP knock-out and presenilin double knock-out fibroblasts (Leissring et al., 2002). However further experiments by Oh and Turner (2006) revealed that YIL may be reducing calcium release from stores through a secondary mechanism independently of γ -secretase activity. Application of YIL was found to elevate basal IP_3 levels (two-fold higher than control cells), which led to a reduced sensitivity of IP_3R to IP_3 and caused a subsequent reduction in agonist-induced calcium release from ER stores. Oh and Turner (2006) also provided evidence that AICD does not modulate intracellular calcium release in HSG cells. When AICD production was blocked by APP siRNA knock-down, calcium release from stores was not decreased, contrary to the findings made by Leissring et al., (2002). The reason for the discrepancy between these two studies is not clear. One possibility may be cell type specific differences in calcium store proteins and regulatory mechanisms, but further studies are warranted to understand the nature of these differences. Hence the results presented in this chapter, where γ -secretase activity blockade is found to have no effect on KCl-stimulated CICR in hippocampal neurons is in agreement with the observations presented by Oh and Turner (2006) in HSG cells.

In this chapter, I also found that inhibition of SERCA pump activity by thapsigargin but not RyR by ryanodine leads to a decrease in intracellular calcium concentration during KCl-stimulated CICR in hippocampal neurons. This result suggests that calcium load in the ER plays a larger role in regulating intracellular calcium concentration during KCl-stimulated CICR than calcium release through the RyR. However, comparing γ -secretase inhibitor treated cells to control cells revealed no differences in calcium responses following preincubation with thapsigargin or ryanodine under basal conditions or during KCl-stimulated CICR. This result provides further evidence that γ -secretase activity is not involved in the modulation of intracellular calcium.

The lack of effect of ryanodine treatment on peak calcium responses during KCl-stimulated CICR was surprising as the study by Zhang et al., (2009) showed that block of RyR in wild type cells led to a decrease in intracellular calcium presumably

due to a decrease in calcium release through RyR from ER stores. It is currently unclear why there is a difference in the results. Past studies have indicated that ryanodine receptor composition may differ between culture systems or cell types (Collin et al., 2005). Alternatively, the result may be due to a difference in the ryanodine concentrations used. Low concentrations of ryanodine (less than 10 μM) can maintain the RyR in a sub-conductance state which enables calcium release from ER stores, however ryanodine at high concentrations will block RyR and decreases calcium release through RyR (Bardo et al., 2006; Bouchard et al., 2003; Collin et al., 2005). The ryanodine concentration used by Zhang et al., (2009) was 100 μM whilst a concentration of 20-30 μM was used for the experiments in this chapter. Importantly, ryanodine concentration of 20-30 μM was used in previous studies and shown to inhibit RyR and decrease mEPSC frequency in cultured slice preparations (Emptage et al., 2001). In line with this observation, an earlier study showed that 4 μM ryanodine could block reconstituted RyR in lipid bilayers (McPherson et al., 1991). Therefore, 20-30 μM ryanodine (like 100 μM ryanodine) should be a sufficient concentration that can block RyR in dissociated neurons. Further investigations will be required to determine the reason for the difference between the results of this chapter and Zhang et al., (2009).

A recent study proposes another mechanism for presenilins to regulate intracellular calcium. Green et al., (2008) showed that presenilins could interact directly with the SERCA pump in the ER. Experiments performed on presenilin double knock-out fibroblasts demonstrated that SERCA pump function was reduced (despite an increased expression of SERCA) leading to an elevation in cytoplasmic calcium and reduction in ER calcium concentration suggesting that presenilin was important for cellular calcium homeostasis (Green et al., 2008). Interestingly the authors found that a decrease in SERCA activity led to a diminished $\text{A}\beta$ production and vice versa suggesting that the SERCA pump could regulate APP processing presumably through γ -secretase activity. However this study using presenilin double knock-out animals did not examine whether direct inhibition of γ -secretase activity could alter SERCA pump activity, so whether calcium homeostasis was regulated by γ -secretase dependent or independent mechanisms remained unclear.

In summary the results in this chapter show that inhibition of γ -secretase activity of presenilins does not alter basal somatic calcium or calcium changes in response to KCl-stimulated CICR. This indicates that the reduced intracellular calcium observed in presenilin double knock-out neurons may arise as a result of loss of γ -secretase independent actions of presenilins rather than loss of γ -secretase dependent actions of presenilins. An alternative method to show that γ -secretase activity is dispensable for the reduction in KCl-stimulated CICR is to transfect a γ -secretase inactive mutant presenilin construct (e.g. D257A) into presenilin double knock-out neurons. This construct lacks γ -secretase activity but should enable the study of γ -secretase independent functions of presenilin. If γ -secretase activity is not required (i.e. a γ -secretase independent action of presenilin is involved) then expression of this mutant construct should be sufficient to rescue the deficit in intracellular calcium seen in presenilin double knock-out cells. An alternative strategy would be to perform calcium imaging experiments in a nicastrin knock-out mouse (Tabuchi et al., 2009) which is also deficient in γ -secretase activity but should exhibit some degree of γ -secretase independent actions of presenilin. However one possible drawback with the nicastrin knock-out animals is that PS1 (NTF and CTF) expression was also reduced when compared to wild type control animals suggesting that nicastrin may regulate the expression of presenilin to a certain degree. However not all components of the γ -secretase complex were equally affected in nicastrin knock-out cells. Whilst PEN-2, like PS1 also showed a decreased expression, APH-1 was not reduced (Tabuchi et al., 2009) suggesting that different mechanisms are implicated in the regulation of different components of the γ -secretase complex in nicastrin knock-out animals. This suggests that nicastrin knock-out animals may not generate the same phenotype as wild type neurons treated with γ -secretase inhibitors.

One technical point to note is that intracellular calcium concentrations have been estimated using an AM ester form of Fura-2. This dye is well characterised and commonly used for intracellular calcium concentration measurements. However, as it can readily pass through the cell membrane the possibility of the dye entering intracellular organelles and even the ER cannot be excluded (Scott and Rusakov, 2008). However as the experiments presented here were designed to reflect the conditions used in an early study by Zhang and colleagues (2009), the studies should still be comparable to each other.

6.5.1 Calcium regulation and Familial Alzheimer's disease

In addition to the amyloid cascade and tau neuropathology hypotheses, many reports suggest that dysregulation of intracellular calcium homeostasis is a leading cause of AD pathology (See for review: Mattson, 2004). Studies from FAD patients (Etcheberrigaray et al., 1998; Hirashima et al., 1996; Ito et al., 1994), cell culture experiments (Cedazo-Minguez et al., 2002; Guo et al., 1996; Smith et al., 2002) and transgenic animals expressing mutant presenilins (Stutzmann et al., 2004; Stutzmann et al., 2006) show that many of the presenilin mutations associated with FAD lead to aberrant intracellular ER calcium release due to overload of calcium in ER stores. However, several studies report an opposite effect where FAD presenilin mutations lead to decreased ER calcium levels (Giacomello et al., 2005; Zatti et al., 2004; Zatti et al., 2006) which suggest different FAD mutations may lead to dysregulation of calcium through different molecular mechanisms. Overall, greater research efforts will be required to understand how calcium homeostasis is altered in FAD patients.

6.6 Conclusion

This chapter showed that γ -secretase activity of presenilin (1) is not required for modulation of intracellular calcium concentration in hippocampal dissociated neurons. By extension this finding proposes that changes in mEPSC frequency upon elimination of presenilin activity or expression cannot be explained by changes in somatic calcium.

Chapter 7: The role of β -secretase in modulating synapse function in hippocampal neurons.

7.1: Introduction

The data presented in previous chapters have shown that presenilin and associated γ -secretase activity is implicated in regulating aspects of synapse function in hippocampal dissociated and organotypic slice cultures. The results outlined in chapters 3 and 5 provide evidence for a role for γ -secretase activity in modulating spontaneous synaptic transmission and synapse number. However experiments discussed in chapters 4 and 6 suggest that γ -secretase activity is potentially not involved in the regulation of release probability or intracellular calcium concentration. The next question to address is the mechanisms underlying this phenomenon: how does pharmacological blockade of γ -secretase increase synapse density and mEPSC frequency?

γ -secretase is a promiscuous enzyme complex capable of cleaving many transmembrane proteins (see Table 1.1) that are implicated in a wide range of cellular functions from cell-cell adhesion and intracellular signalling pathways to gene transcription. It is conceivable that inhibiting its activity and thereby decreasing proteolysis of its targets may have some lasting impact on neuronal function. One way to approach this question is to identify which substrate or cleavage product(s) of γ -secretase is implicated in the modulation of mEPSC frequency. A suitable candidate is APP. Several studies over the past few years

have investigated the role of APP and its cleavage products, most notably $A\beta$, in modulating synaptic function using a variety of different methods and manipulations.

One breakthrough study performed on organotypic slice cultures showed that mEPSC frequency was significantly decreased whilst mEPSC amplitude was not changed upon overexpressing wild type APP in CA1 pyramidal cells using a sindbis viral vector (Kamenetz et al., 2003). AMPA and NMDA evoked responses were also decreased in cells infected with APP when compared to uninfected controls. Transfection of β -CTF, the membrane fragment that is generated from β -secretase cleavage of APP, also reduced evoked responses (Kamenetz et al., 2003). This suggests that soluble APP- β fragment is not required for EPSC amplitude depression. However β -CTF and APP overexpressing cells chronically treated with γ -secretase inhibitor, L-685,458 (1 μ M for 24 hrs) did not exhibit any changes in AMPA and NMDA evoked currents when compared to untreated cells, suggesting γ -secretase activity is necessary for the decrease in current amplitude. Additionally, a mutant APP construct which was unable to undergo β -secretase cleavage, and accumulated α -CTF (the membrane fragment made after α -secretase cleavage of APP), did not exhibit changes in synaptic transmission, indicating that α -CTF and AICD (intracellular fragment generated after γ -secretase cleavage of α -CTF) were not likely involved (Kamenetz et al., 2003). Taken together these observations suggest that γ -secretase processing of APP and possibly $A\beta$ is required and sufficient for the electrophysiological changes in synaptic transmission. Evidence for a direct involvement of $A\beta$ in modulating evoked AMPA responses was provided by application of exogenous $A\beta_{40}$ and $A\beta_{42}$ peptides which led to a dose-dependent decrease in field potential responses in control non-infected slices. Altogether this study provides convincing evidence that increases in $A\beta$ peptide causes depression of postsynaptic current amplitude in organotypic slices. Interestingly no alteration in PPR was observed in cells overexpressing WT APP suggesting, that elevated $A\beta$ production is not involved in regulating presynaptic release probability (Kamenetz et al., 2003). A follow up study showed that the decreased evoked amplitude response seen in APP overexpressing cells was due to AMPA receptor removal from spines and a decrease in spine density (Hsieh et al., 2006). Exogenous application of $A\beta_{42}$ also induced spine loss in APP overexpressing cells. However, overexpression of a point mutant of APP which prevents β -secretase cleavage and hence prevents $A\beta$

generation prevented the loss of spines (Hsieh et al., 2006). A recent study also indicated that $A\beta$ released from axons and dendrites of neurons can reduce spine density at nearby dendritic processes (Wei et al., 2010). Timelapse imaging also revealed that pre and postsynaptic changes can simultaneously occur upon treatment with $A\beta$ to cause synapse uncoupling and loss (Calabrese et al., 2007). This suggests that $A\beta$ may be released from both pre and postsynaptic compartments to influence both structure and function of the synapse in hippocampal neurons.

Another study using semliki forest virus to overexpress human WT APP (APP695) in hippocampal autaptic cultures corroborated the observations seen in organotypic slice cultures. This study showed that upon APP overexpression mEPSC amplitude was not affected but mEPSC frequency was decreased compared to uninfected control cells (Ting et al., 2007). The authors also demonstrated that overexpression of APP decreased evoked EPSC size whilst a mutant version of APP (M596V), which was defective in BACE-mediated APP processing and (could not generate $A\beta$) did not exhibit changes in current amplitude. There were no significant differences in PPR, rate of refilling of the RRP or RRP size in control, WT APP and BACE mutant infected cells, suggesting that $A\beta$ was not required for regulation of these specific presynaptic parameters. However a small decrease in the rate of stimulated FM vesicle destaining in WT APP overexpressing neurons was observed. This suggests that $A\beta$ may be involved in modulating vesicle exocytosis (Ting et al., 2007). Overall these reports provide strong evidence that APP overexpression and elevated $A\beta$ production that could potentially result from it can cause a reduction in synaptic responses in hippocampal dissociated cultures.

A study using a converse approach showed that mEPSC frequency is increased whilst mEPSC amplitude is not altered in APP knock-out animals compared to wild type controls (Priller et al., 2006). When release properties were examined, APP knock-out cells revealed no significant differences in the rate of NMDA current block during MK801 application or in the rate of readily releasable pool (RRP) refilling. An alternative protocol to assess RRP size was also used. Repetitive stimulation at 10 Hz and 50 Hz, where cumulative amplitude response is correlated to pool size (Schneggenburger et al., 1999), was used to show that there were no significant differences in presynaptic vesicle pool size between wild type and APP

knock-out neurons. Immunostaining of APP knock-out autaptic cultures revealed both an increase in dendritic length and the number of synaptophysin positive puncta. Furthermore, immunolabelling of hippocampal sections from juvenile knock-out animals showed an increase in synaptophysin staining in the stratum radiatum and moleculare layers when compared to wild type control sections (Priller et al., 2006). This data suggests that loss of APP leads to both functional and structural changes at hippocampal synapses and in the opposite direction to that observed with APP overexpression studies. It is thus tempting to speculate that A β may play a role in balancing and maintaining the number of synaptic contacts under normal physiological conditions.

The results from APP knock-out animals share many similarities with the data obtained from hippocampal neurons after γ -secretase inhibitor treatment or from PS1^{-/-} mice (Chapters 3-5). Hence the effects may potentially arise from a common mechanism. As both APP and γ -secretase activity are required for the generation of A β , there is a possibility that the similarities in alterations of synapse structure and function observed in APP knock-out and PS1 knock-out cells may arise from a decrease in A β . This suggests that loss of A β generation may have a positive effect in regulating synapses. To examine this possibility, Priller et al., (2006) sought to rescue the wild type phenotype in APP knock-out cells by preincubating hippocampal cells with exogenous A β_{42} or with culture media obtained from cell lines that secrete A β peptides. Recordings showed that chronic treatment with A β peptides resulted in a reduced mEPSC frequency that did not quite reach the frequency observed in wild type neurons. Reasons why a full rescue has not been observed are not known but there could be a variety of explanations including problems with getting A β to synaptic sites. However, the identity of the specific form of A β peptide that is involved in regulating synapse function under physiological conditions is currently unknown. It is also unknown if extracellular A β or intracellular A β is involved in modulating this effect on synapse function. Together, these studies provide evidence that A β may act as a bidirectional regulator of mEPSC frequency in the hippocampus by influencing the number of functional synapses rather than changes in presynaptic release properties.

As outlined in the introduction, A β production arises from the sequential cleavage of APP by two enzymatic processes. The latter step which involves γ -secretase and its unique ability to intramembraneously cleave β -CTF fragments to generate AICD and A β has already been extensively explored in this thesis. However the contribution of the initial cleavage of APP to generate β -CTF (and soluble APP- β) by β -secretase has not been addressed.

The aim of this chapter was to determine if β -secretase inhibition has any effects on hippocampal synapse function. This would also indirectly test whether A β may act as a bidirectional regulator of synapse structure and function in hippocampal neurons.

7.2: Investigating the effects of β -secretase activity inhibition on mEPSC properties

To pharmacologically block β -secretase activity in neurons, a selective β -secretase inhibitor IV was used (1 μ M (Wen et al., 2008)). Experiments using β -secretase inhibitor IV were performed in the same way as γ -secretase inhibitor treated cells. mEPSC recordings from rat dissociated cells treated with β -secretase inhibitor IV exhibited a significant increase in mean mEPSC frequency when compared to DMSO mock treated cells (Figure 7.1 b left, DMSO: n = 8, mean: 1.84 ± 0.65 Hz; β -secretase inhibitor IV: n = 17, mean 5.59 ± 0.86 Hz. Student's t-test: p = 0.01*). Analysis of mEPSC amplitude showed no significant changes between β -secretase treated and control cells (Figure 7.1 b right, DMSO: mean: 21.0 ± 3.30 pA; β -secretase inhibitor IV: mean: 26.04 ± 2.57 pA. Student's t-test: p = 0.26).

mEPSC recordings were also performed on organotypic slices treated with β -secretase inhibitor IV. As observed in dissociated cells, slices treated with β -secretase inhibitors also exhibited an increase in mean mEPSC frequency when compared to DMSO mock treated cells, however the difference was not statistically significant (Figure 7.2 b left, DMSO: n = 7, mean: 0.36 ± 0.06 Hz; β -secretase

inhibitor IV: $n = 9$, mean: 0.65 ± 0.16 Hz. Student's t-test: $p = 0.14$). No significant effects were observed in mean mEPSC amplitude between β -secretase inhibitor IV treated and mock control slices (DMSO: mean: 18.30 ± 1.29 pA; β -secretase inhibitor IV: mean: 20.81 ± 1.15 pA. Student's t-test: $p = 0.17$). These results indicate that neurons from dissociated and organotypic hippocampal cultures exhibit a tendency towards an increase in mEPSC frequency upon chronic β -secretase inhibitor treatment. This finding partially mimics the effects of γ -secretase inhibitor treatment. Whilst the overall effect of β -secretase inhibition on mEPSC properties is similar to that observed with γ -secretase inhibition, the magnitude of the effect is generally lower in β -secretase inhibitor treated cells than γ -secretase treated cells when compared to matched DMSO controls. The reasons for this are not entirely clear, but suggest that β -secretase and γ -secretase modulation of mEPSC frequency likely occur through the same pathway, potentially involving an alteration in APP processing and/ or decreased $A\beta$ production.

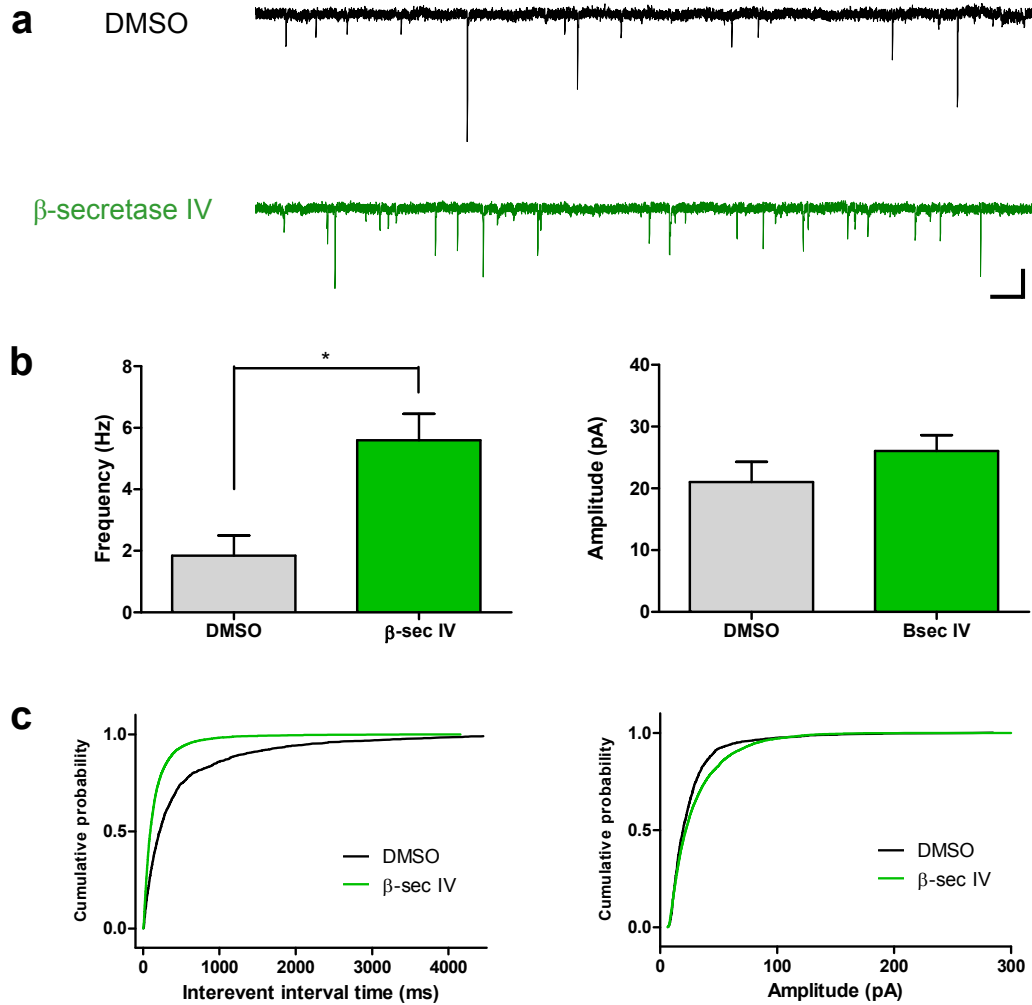


Figure 7.1 – mEPSC frequency is modulated by chronic treatment with β -secretase inhibitor in rat dissociated hippocampal neurons.

(a) Sample traces of mEPSC recordings from rat hippocampal dissociated neurons chronically treated for 48 hr with mock DMSO control (black) or β -secretase inhibitor (green). Scale bar, 25 pA, 200 ms. (b) Summary of mEPSC frequency (left) and amplitude (right) for DMSO (grey, $n = 8$, frequency mean: 1.84 ± 0.65 Hz, amplitude mean: 21.0 ± 3.30 pA) and β -secretase inhibitor (green, $n = 17$, frequency mean 5.59 ± 0.86 Hz, amplitude mean: 26.04 ± 2.57 pA). Statistical analysis was performed using student's t-test ($p = 0.01^*$). Chronic treatment with β -secretase inhibitor significantly increased mean mEPSC frequency compared to mock DMSO control but did not change mEPSC amplitude. (c) Cumulative distribution plots of mEPSC inter-event interval (left) and mEPSC amplitude (right) for data shown in (b).

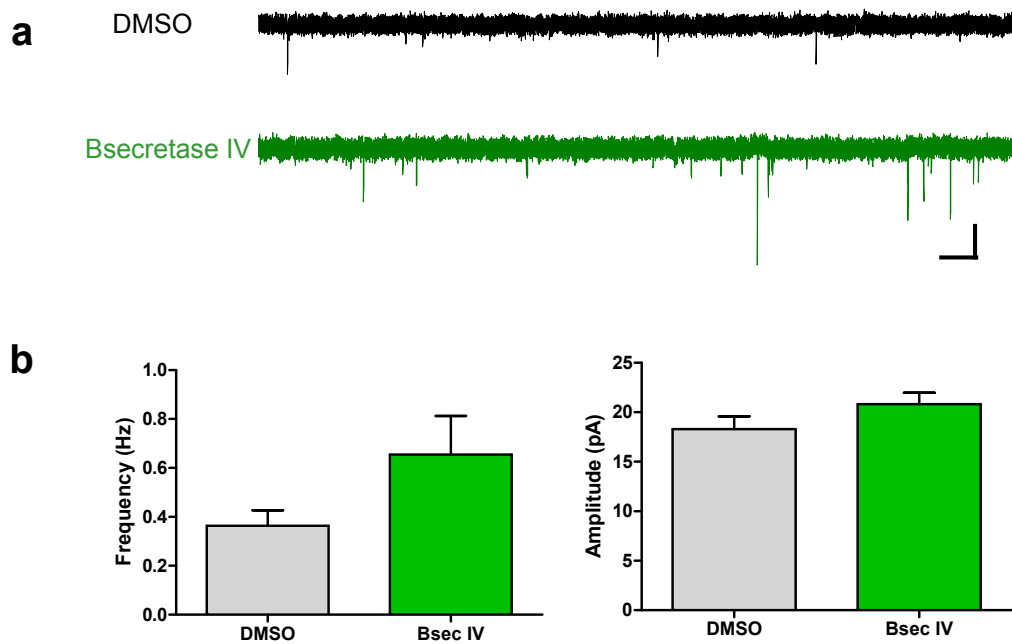


Figure 7.2 – mEPSC recordings of rat hippocampal organotypic slice cultures chronically treated with β -secretase inhibitor.

(a) Sample traces of mEPSC recordings from hippocampal rat organotypic slices treated for 48 hr with mock DMSO control (black) or β -secretase inhibitor IV (green). Scale bar, 20pA, 1 sec. (b) Summary of mEPSC frequency (left) and amplitude (right) for DMSO (grey, $n = 7$, frequency mean: 0.36 ± 0.06 Hz, amplitude mean: 18.30 ± 1.29 pA) and β -secretase inhibitor (green, $n = 9$, frequency mean: 0.65 ± 0.16 Hz, amplitude mean: 20.81 ± 1.15 pA) recordings. Statistical analysis was performed using student's t-test. When compared to DMSO control cells, chronic treatment with β -secretase inhibitor elevated mEPSC frequency but this effect did not reach statistical significance ($p = 0.14$). Differences in mEPSC amplitude between cells treated with mock DMSO and β -secretase inhibitor were not statistically different ($p = 0.17$).

7.3: Estimating release probability with styryl dyes in rat dissociated cells treated with β -secretase inhibitor

To investigate whether β -secretase inhibition had any effect on release probability, FM-dye destaining from synaptic vesicles was examined in hippocampal dissociated cultures. The same protocol as that used for γ -secretase inhibitors was applied to cells treated with β -secretase inhibitors. Destaining of synaptic vesicles was performed in low (1 mM), normal (2.2 mM) and high (5 mM) extracellular calcium concentrations (Figure 7.3). The decay time constant of DMSO control cells and β -secretase treated cells were compared to determine if there are any relative differences in release probability estimates. Analysis showed that there were no significant differences in the rate of fluorescence loss from presynaptic terminals during evoked vesicle exocytosis between β -secretase inhibitor IV treated and DMSO treated cells at any calcium concentration suggesting block of β -secretase activity does not lead to a significant change in the rate of vesicle destaining (Figure 7.3). Overall this experiment shows that blocking β -secretase activity does not influence release probability at single synapses. Together with the lack of effect of γ -secretase treatment on release probability, our data suggests that lack of A β generation/ decreased APP processing is not a necessary factor involved in the regulation of presynaptic release.

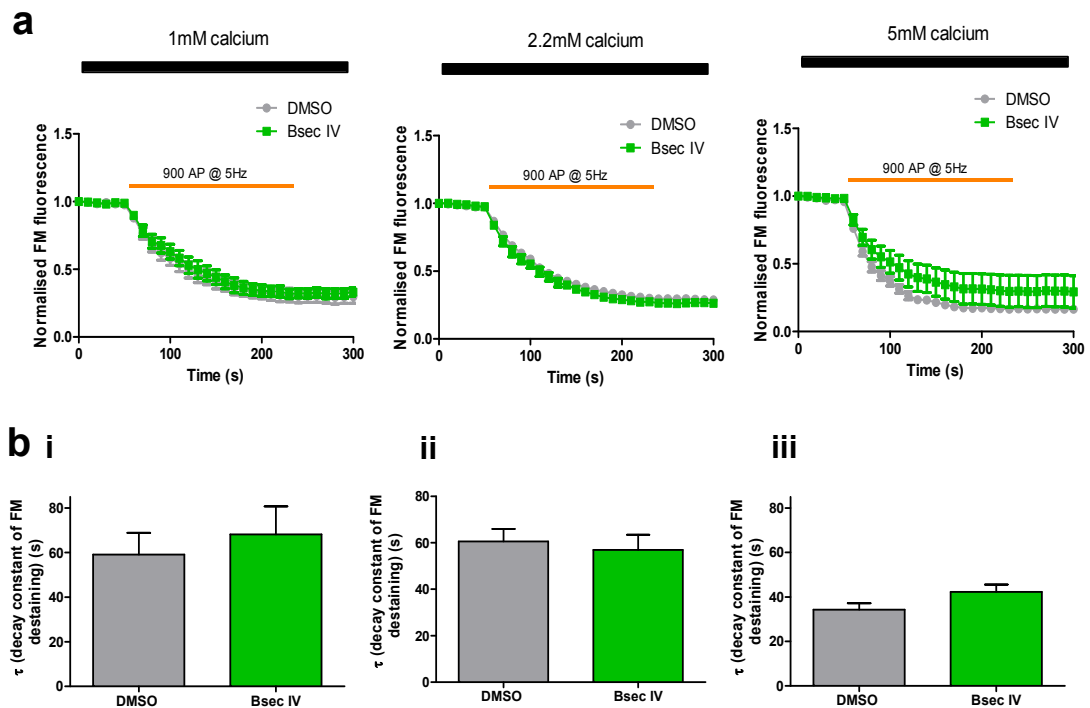


Figure 7.3 – Destaining kinetics of β -secretase treated rat dissociated cultured neurons in different concentrations of extracellular calcium.

(a) Average destaining timecourse of mock DMSO cells (grey circle) and β -secretase inhibitor IV treated cells (green square) in 1 mM calcium (left), 2.2 mM calcium (middle) and 5 mM calcium (right) in extracellular bath solution. Orange bar shows timecourse of field stimulation (900 stimuli at 5 Hz) used to elicit FM dye destaining from neuronal boutons. (b) Summary of decay time constants (τ) obtained from experiments shown in (a). DMSO (grey) and β -secretase inhibitor IV (green) treated cells respond similarly at a given extracellular calcium concentration. (b)(i) Mean response to 1 mM extracellular calcium shows DMSO ($\tau = 59.13 \pm 9.76$, $n = 6$) and β -secretase inhibitor IV cells ($\tau = 68.16 \pm 12.56$, $n = 6$) are similar. (b)(ii) The same lack of significant difference is observed in 2.2 mM extracellular solution (DMSO, $\tau = 60.63 \pm 5.33$, $n = 19$; β -secretase inhibitor IV, $\tau = 56.96 \pm 6.55$, $n = 11$). (b)(iii) Also at 5 mM extracellular calcium the decay time constant between DMSO ($\tau = 34.30 \pm 2.86$, $n = 7$) and β -secretase inhibitor IV ($\tau = 42.27 \pm 3.32$, $n = 5$) is not significantly altered. Note the increase in the rate of destaining from 2.2 mM to 5 mM extracellular calcium.

7.4: Investigating synapse number of rat dissociated cells treated with β -secretase inhibitor

Rat dissociated cells treated with β -secretase inhibitor IV was imaged and analysed in the same way as cells treated with γ -secretase inhibitors. Estimates of synapse number were obtained by analysing the density of Homer and synapsin co-localised puncta and was found to be not significantly different between DMSO control and β -secretase inhibitor IV treated cells (Figure 7.4). Analysis of individual signals revealed that β -secretase inhibitor treatment did not alter the density of Homer puncta; however, analysis of synapsin density in the same cells did reveal a significant increase in density when compared to DMSO control cells (Figure 7.4 b). In separate hippocampal cultures, the density of co-localised synapsin and GluA1 puncta was also analysed. No significant differences was observed in synapsin and GluA1 co-localised puncta between cells treated with β -secretase inhibitor IV and DMSO control cells (Figure 7.5). Intriguingly, examination of synapsin density did not reveal any differences between drug treated and mock control treated cells, which is different to the results observed in Figure 7.4. Additional analysis of GluA1 puncta showed that cells treated with β -secretase inhibitor IV had a significantly greater number of GluA1 positive puncta than DMSO mock control cells (Figure 7.5 b iii)

Due to the differences in the results obtained from these two sets of immunofluorescent labelling experiments, it is currently not possible to make strong conclusions with regards to the role of β -secretase in modulating synapse number. In general, the results suggest that β -secretase inhibition does not greatly alter the density of presynaptic synapsin and postsynaptic Homer and GluA1 puncta. This result is different to the observations made with γ -secretase inhibitor treatment, where a fairly robust effect on synapse formation was seen. Taken together, the greater number of synapses in APP knock-out mice (Priller et al., 2006) and γ -secretase inhibitor treated cells (Parent et al., 2005 and chapter 5), potentially arises

from a mechanism that does not involve loss of $A\beta$ production as inhibition of β -secretase does not lead to a strong change in synapse number.

Analysis of dendritic spines in organotypic slices treated with either DMSO (mock control) or β -secretase inhibitor IV also revealed no significant differences in spine density in apical or basal dendritic branches (Figure 7.6). This result indicates that blockade of β -secretase activity does not alter spine density.

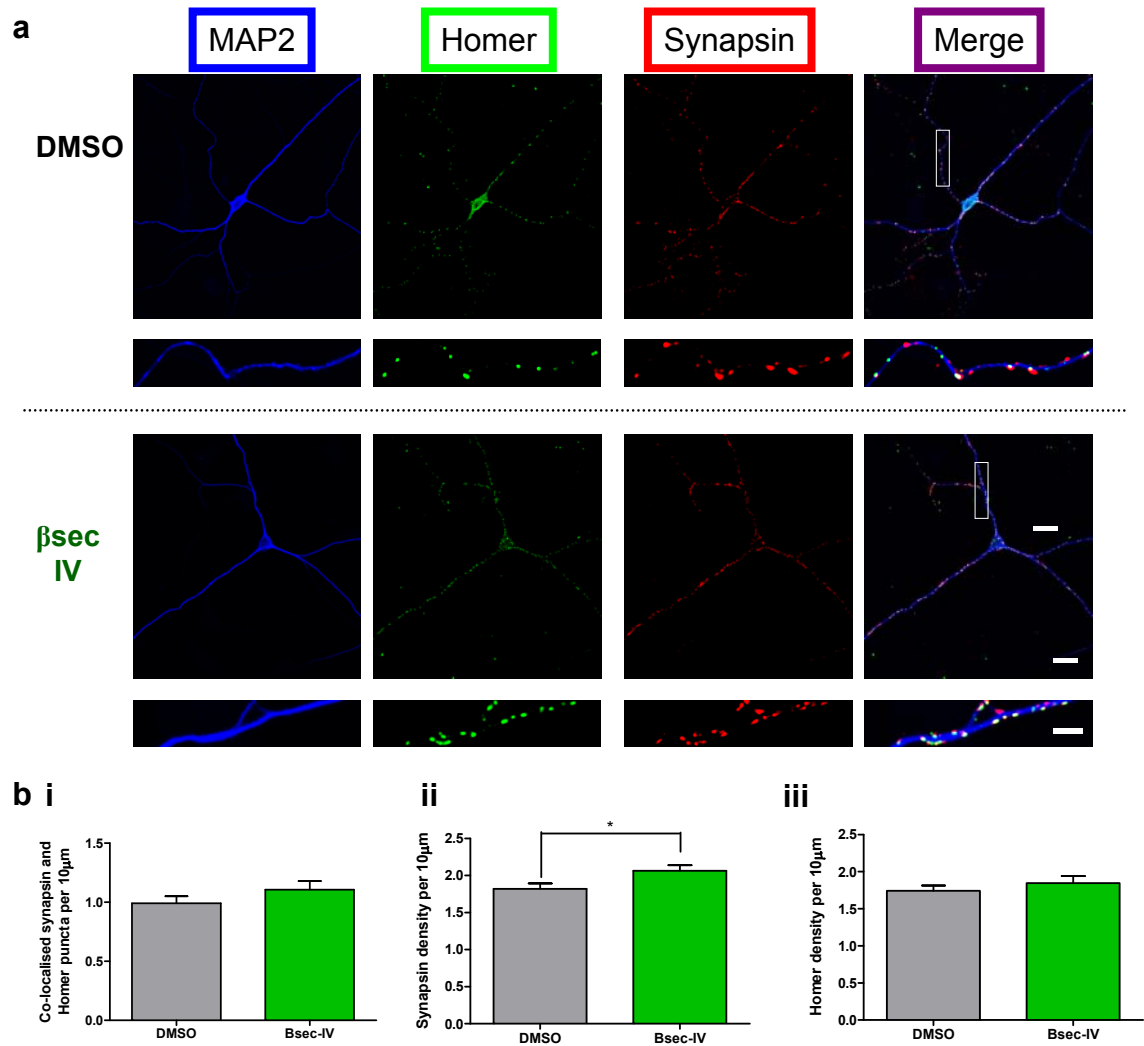


Figure 7.4 – Immunofluorescence analysis of presynaptic synapsin and postsynaptic Homer markers of cells treated with β -secretase inhibitor IV

(a) Sample images of neurons treated for 48 hrs with DMSO (top) or β -secretase inhibitor IV (bottom). Antibody labelling was performed against MAP2 (neuronal marker, blue), Homer (postsynaptic marker, green) and synapsin (presynaptic marker, red). Scale bar: low magnification images 20 μ m, inset images 6 μ m.

(b) Summary of co-localised Homer and synapsin puncta (i), synapsin puncta (ii) and Homer puncta (iii) of cells treated with DMSO (grey) or β -secretase inhibitor IV (green). All puncta were expressed as density per 10 μ m. Analysis of synapsin and Homer colocalised puncta showed no significant differences between DMSO control (density mean: 0.922 ± 0.06 Hz) and β -secretase inhibitor IV treated cells (density mean: 1.106 ± 0.07 Hz). There was also no significant difference in Homer puncta density between DMSO (density mean: 1.742 ± 0.07 Hz) and β -secretase treatment (density mean: 1.846 ± 0.09 Hz). However, a small but significant increase in synapsin density was observed upon treatment with β -secretase inhibitor IV (density mean: 2.064 ± 0.08 Hz) when compared to DMSO control (density mean: 1.819 ± 0.07 Hz) (DMSO versus β -secretase inhibitor, $p = 0.02$ *). $n = 39$ cells were analysed for mock DMSO and $n = 33$ for β -secretase IV, pooled from 2 separate cultures. Statistical analysis was performed using student's t-test (bar graphs; $p < 0.05$ *).

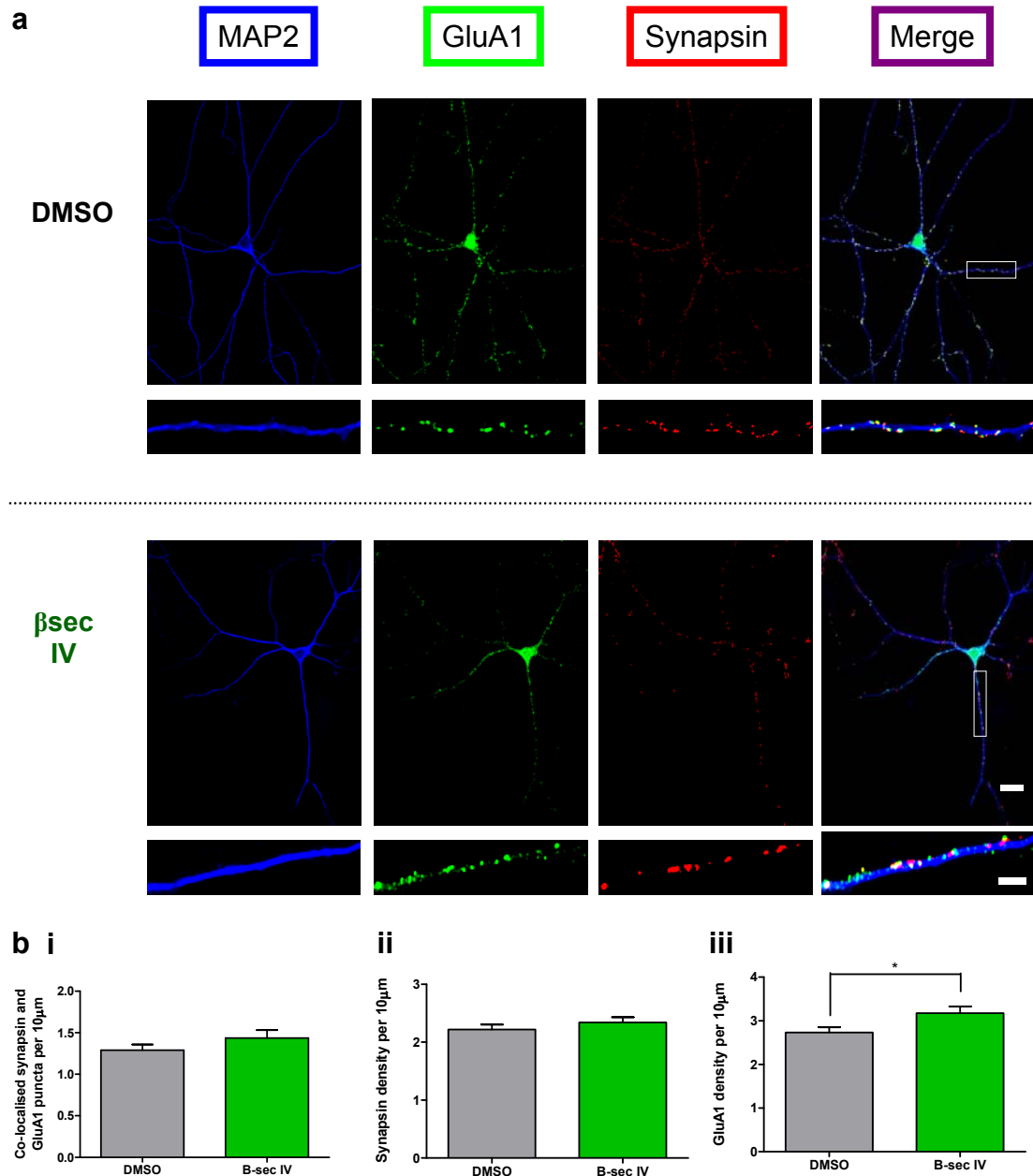


Figure 7.5 – Immunofluorescence analysis of presynaptic synapsin and postsynaptic GluA1 markers of cells treated with β -secretase inhibitor IV

(a) Sample images of neurons treated for 48 hrs with DMSO (top) or β -secretase inhibitor IV (bottom). Antibody labelling was performed against MAP2 (neuronal marker, blue), GluA1 (postsynaptic marker, green) and synapsin (presynaptic marker, red). Scale bar: low magnification images 20 μ m, inset images 6 μ m. (b) Summary of immunofluorescence quantification of co-localised Homer and GluA1 puncta (i), synapsin puncta (ii) and GluA1 puncta (iii) of cells treated with DMSO (grey) or β -secretase inhibitor (green). All puncta were expressed as density per 10 μ m. Analysis of synapsin and Homer colocalised puncta showed no significant differences between DMSO mock control (density mean: 1.289 ± 0.07 Hz) and β -secretase inhibitor IV treated cells (density mean: 1.436 ± 0.09 Hz). There was also no significant difference in synapsin puncta density between DMSO (density mean: 2.218 ± 0.09 Hz) and β -secretase treatment (density mean: 2.340 ± 0.09 Hz). However, a small but significant increase in GluA1 density was observed upon treatment with β -secretase inhibitor IV (density mean: 3.174 ± 0.15 Hz) when compared to DMSO control (density mean: 2.73 ± 0.12 Hz) (DMSO versus β -secretase inhibitor, $p = 0.02$ *). $n = 46$ cells were analysed for DMSO mock and $n = 42$ for β -secretase inhibitor IV, pooled from 2 separate cultures. Statistical analysis was performed using student's t-test (bar graphs; $p < 0.05$ *).

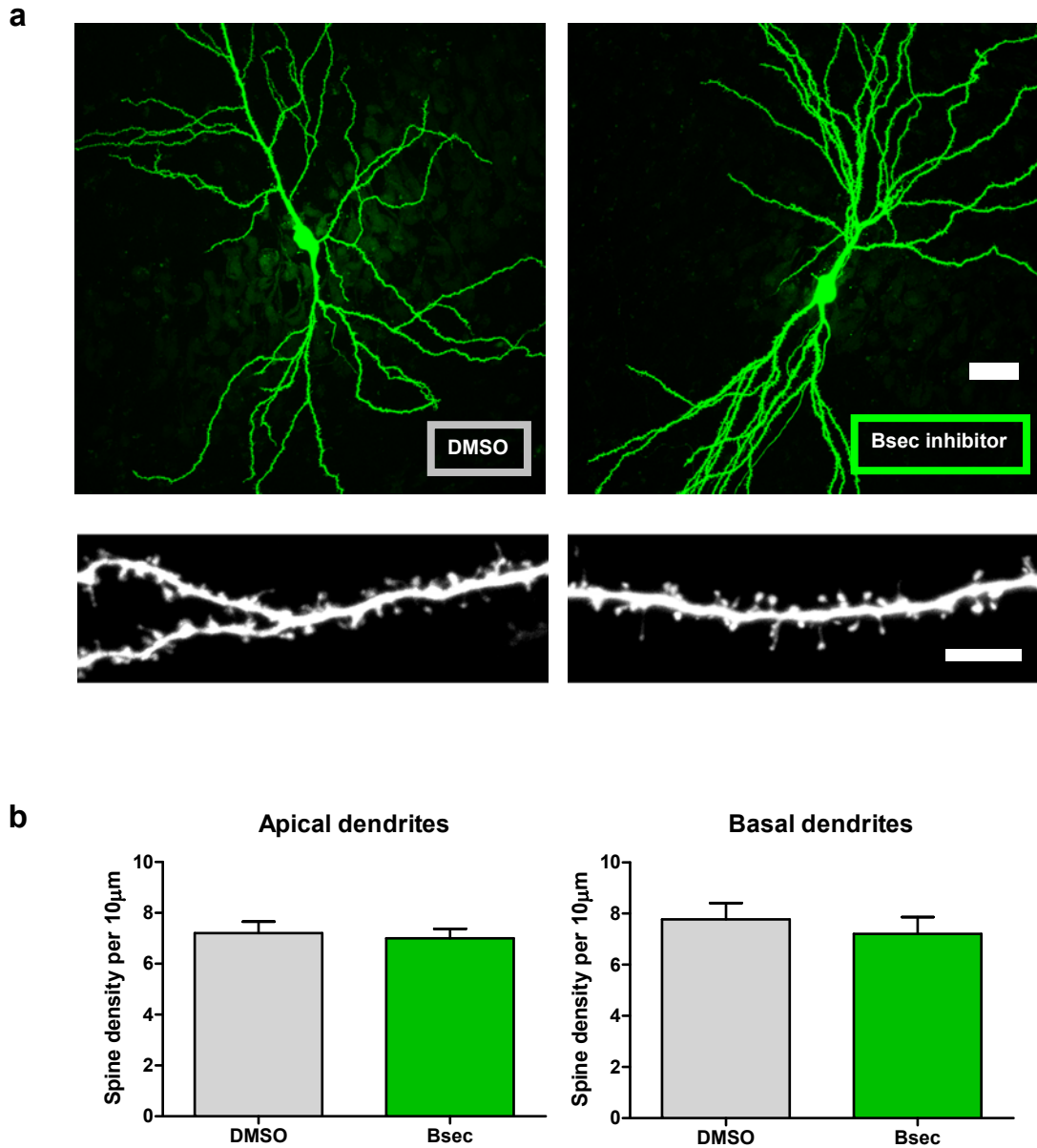


Figure 7.6 – Spine analysis of organotypic slices treated with β -secretase inhibitor IV

(a) Sample image a neuron treated for 48hrs with DMSO (left) or β -secretase inhibitor IV (right) at low magnification (top) Scale bar, 30 μ m. High magnification images of typical neurons from DMSO treated slice (left, bottom) and β -secretase inhibitor IV treated slice (right, bottom). Scale bar, 5 μ m. (b) Quantification of spine density of apical dendrites (left) and basal dendrites (right). No significant differences were observed in either apical or basal spine density in cells treated with DMSO (n: 7 cells) or β -secretase inhibitor IV (n: 5 cells).

7.5: Discussion

The experiments presented in this chapter examined the effects of pharmacological inhibition of β -secretase activity on mEPSC properties, release probability and synapse number. In previous chapters, it was shown that blockade of γ -secretase activity by specific inhibitors or elimination of PS1 gene led to an increase in mEPSC frequency and synapse number but not in release probability. Intriguingly, an earlier study by Priller et al., (2006) showed very similar observations in synaptic properties in APP knock-out mice. Putting these two sets of results together, where both APP knock-out and γ -secretase inhibitor treated cells exhibited an increase in mEPSC frequency and synapse number, I wanted to test the hypothesis that loss of APP processing, or more specifically, loss of A β generation could have a positive effect on regulating synapse function. This was achieved by pharmacologically targeting β -secretase activity to prevent A β generation.

Initial experiments implicated β -secretase activity in regulating mEPSC properties as chronic treatment with inhibitor IV led to an increase in mEPSC frequency when compared to DMSO control cells. A statistically significant increase in mEPSC frequency was observed upon prolonged treatment with β -secretase inhibitor IV in dissociated hippocampal neurons (Figure 7.1). However, when the same treatment was applied to organotypic slice cultures, a large but statistically insignificant result was obtained (Figure 7.2). Power analysis predicts that a sample size of 16-18 may provide a statistically significant result suggesting that further experiments are required to improve the current sample size (DMSO, $n = 7$; β -secretase inhibitor IV, $n = 9$).

Next, FM dye destaining experiments were performed to examine the role of β -secretase in regulating release probability. No significant effects were observed in vesicle destaining kinetics between β -secretase treated and DMSO control cells suggesting that block of β -secretase activity does not alter release probability. These results are in line with observations made with γ -secretase inhibitor treated cells (Parent et al., 2005, chapters 3 and 4) and APP knock-out cells (Priller et al., 2006), which potentially suggests that elimination of A β production could modulate

mEPSC frequency but not release probability. However, β -secretase inhibition had no significant effect on synapse density when compared to DMSO controls. This result suggests that lack of $A\beta$ production is potentially not associated with the increase in synapse number observed in APP knock-out and γ -secretase inhibitor treated cells. The differential effects of γ -secretase inhibition and β -secretase inhibition on synaptic marker expression suggests that the cellular effects of these two pharmacological manipulations may be separable and occur independently of loss of $A\beta$ production.

This result also indicates that the increase in mEPSC frequency in cells treated with β -secretase inhibitor IV is potentially not correlated with a change in synapse number. However, further morphological analysis is warranted to determine if other synaptic markers are altered upon treatment with β -secretase inhibitors. Ideally a measure of functional synapses should also be investigated as immunofluorescence labelling does not distinguish between functional and non functional synapses e.g. orphan synapses.

BACE-1 knock-out mice

Another approach to test the involvement of β -secretase action on synapse function is to examine BACE-1 knock-out mice. As expected, studies have shown that BACE-1 knock-out mice do not produce $A\beta$ peptides or plaques (Cai et al., 2001; Luo et al., 2001; Roberds et al., 2001). BACE-1 knock-out animals are viable, fertile and do not exhibit any major developmental defects. However, past reports have revealed that certain aspects of synapse function and memory are impaired in BACE-1 knock-out mice (Laird et al., 2005; Ohno et al., 2004). BACE-1 knock-out mice of 16 months of age (but not at 3 months) exhibit impaired performance in spatial reference memory tests, such as the hidden platform and probe trial tests of the Morris water maze when compared to non-transgenic control animals (Laird et al., 2005). BACE-1 animals also show impaired performance on the radial water maze and Y-maze task, tests of spatial working memory (Laird et al., 2005). Overall, these behavioural tests demonstrate that hippocampal spatial memory is impaired in

BACE-1 knock-out mice. Examination of synaptic responses through input-output curves for AMPA and NMDA field potentials do not reveal any differences between BACE-1 knock-out and control mice. Intriguingly, a significant difference in PPR between BACE-1 knock-out and control mice is observed with an inter-stimulus interval of 50ms but not at lower (~30 ms) or higher (~100 ms, 300 ms, 500 ms) inter stimulus intervals. This suggests that under certain conditions BACE-1 may modulate presynaptic function. This effect on PPR is potentially in conflict with the lack of change in presynaptic function measured through synaptic vesicle exocytosis upon treatment with β -secretase inhibitors (Figure 7.3). However the two experiments are not entirely comparable as the former measures the short term plasticity changes in population responses from brain slices, whilst the latter measures presynaptic vesicle dynamics from single synapses in cultured neurons. Due to time constraints, PPR was not examined in β -secretase inhibitor treated organotypic slices in this present study but future investigations may help determine whether the effect on PPR persists across different β -secretase manipulations.

BACE-1 knock-out mice also exhibited no differences in the induction or maintenance of LTP or long term depression (LTD) when compared to wild type animals. However applying theta burst stimulation to slices that have already undergone LTD to induce de-depression revealed that BACE-1 cells underwent greater de-depression than wild type cells. These slice experiments indicate that BACE-1 may be important in regulating certain aspects of synaptic plasticity (Laird et al., 2005). Currently there are no studies on BACE-1 knock-out mice that have examined either excitatory or inhibitory spontaneous synaptic currents. Analysis of synapse number in the hippocampus also remains to be performed in BACE-1 knock-out animals. Altogether, further experiments are required to obtain a greater understanding of the potential pre and postsynaptic roles of β -secretase / BACE-1 at hippocampal synapses.

Differences between γ -secretase and β -secretase inhibition on synapse function

The potential differential effects of β -secretase and γ -secretase inhibitors on the regulation of synapse number suggest that A β may not act as a negative regulator of synapse number. Parent et al., (2005) provide some evidence for an alternative mechanism that regulates the increase in synapse number observed in γ -secretase inhibitor treated cells and PS1 knock-out cells. They propose that the increase in neurite outgrowth and synapse formation in γ -secretase inhibitor treated cells and PS1 knock-out cortical neurons may arise as a result of enhanced PKA/cAMP signalling through accumulation of unprocessed DCC fragments. It is conceivable that this mechanism may also be implicated in hippocampal neurons, though this has not been directly tested during the course of this project.

The results presented in this thesis suggest that blocking γ -secretase and β -secretase share some common outcomes but also some divergent results. The increase in mEPSC frequency observed upon treatment with either inhibitor suggests a common, but as yet undefined mechanism in regulating spontaneous currents. However from the approach taken in this current study, it is not possible to determine if the two inhibitors act along the same pathway or if separate pathways that both generate an increase in mEPSC frequency are implicated. One possible experiment to examine this would be to apply both γ -secretase and β -secretase inhibitors to the same cell and determine if there is a greater/lesser change in frequency compared to treatment with either inhibitor alone. Ideally such an experiment should be performed with acute pharmacological application so that the effects of drug application could be compared to a control time period in the same cell. However this approach was not possible with the γ -secretase inhibitors as the increase in mEPSC frequency occurred progressively over time (Figure 3.1 and 3.2). A time course for β -secretase action was not performed for this study so the minimum treatment time required to elicit an effect on mEPSC frequency is yet to be determined. Notably other studies where β -secretase inhibitor IV was used also adopted a fairly chronic application (Abramov et al., 2009; Wen et al., 2008).

In addition, the results from chapter 3 and 5 indicate that γ -secretase inhibitor treatment leads to an increase in synapse number and mEPSC frequency. Studies of quantal parameters (see for review, Kerchner and Nicoll, 2008) suggest that synapse number and mEPSC frequency are correlated and that an increase in mEPSC frequency may arise from an increase in the number of functional synaptic sites.

However the results in this chapter do not fully examine this association and further studies will be required to determine if this is the case. For example, if both mEPSC frequency and synapse number of PS1 knock-out neurons drop to the same level as wild type animals following re-introduction of active γ -secretase complexes (i.e. through transfection/ infection), then this would provide greater evidence that synapse number and mEPSC frequency are highly associated. However, there may be technical problems associated with this approach. Whilst γ -secretase has been reconstituted by transfection of all 4 components of γ -secretase into certain cell types such as yeast and CHO cells (Edbauer et al., 2003; Kimberly et al., 2003), there are currently no published reports showing reconstituted γ -secretase activity in PS1 knock-out neurons.

However if mEPSC frequency and synapse number are not correlated and act through separate mechanisms, then this may affect our interpretation of the β -secretase inhibitor experiments. In APP overexpression studies (Kamenetz et al., 2003), it was shown that both mEPSC frequency and synapse number were decreased and no change in PPR was observed. This suggests that overproduction of A β may lead to a decrease in synapse number and mEPSC frequency. In APP knock-out animals (and PS1 knock-out mice) the opposite was observed, with an increase in synapse number and mEPSC frequency, indicating a positive regulation of synapse function by a lack of A β . However β -secretase inhibitor application which should also diminish A β generation, only leads to an increase in mEPSC frequency with no significant change in synapse density. If mEPSC frequency and synapse number are linked then this would suggest that A β does not regulate these two synaptic parameters. However if mEPSC frequency and synapse number are dissociable then A β may be involved in regulating mEPSC frequency but not in regulating synapse number. Indeed, from the experiments performed so far, we cannot rule out that a loss of A β may still be a possible mechanism that causes the elevation of excitatory synaptic transmission following γ -secretase and β -secretase

inhibition. In line with this notion, other studies have shown that soluble A β oligomers predominantly bind to glutamatergic synapses (Calabrese et al., 2007; Koffie et al., 2009; Renner et al., 2010). However the role of A β was not directly tested in this project. To examine this possibility a rescue experiment where application of A β to γ -secretase or β -secretase treated cells could be attempted. However, this experiment is not trivial for two main reasons; the A β species potentially involved in regulating mEPSC frequency is still currently unknown and the mechanism by which A β may be potentially regulating mEPSC properties remains undetermined. A previous study (Priller et al., 2006) had attempted this rescue experiment with A β_{42} peptides (on APP knock-out mice) and found only a partial rescue of the mEPSC frequency rate when compared to control cells. One possibility for the lack of a full rescue is that the A β isoform endogenously released from neurons under normal physiological conditions is more likely to be A β_{40} rather than A β_{42} (Hoey et al., 2009). Therefore a more successful rescue may be achieved with application of A β_{40} peptides. Further studies are required to discriminate between these possibilities.

In studies where A β production was either elevated (through APP overexpression – see Kamenetz et al., 2003; Ting et al., 2007) or eliminated (in APP knock-out mice – see Priller et al., 2006), PS1 knock-out mice (Chapter 4), γ -secretase inhibitor treatment (Chapter 4) and β -secretase inhibitor treatment (current chapter), no change in PPR, rate of MK801 block or the rate of synaptic vesicle destaining was observed when compared to control cells. These results indicate that A β is potentially not involved in regulating release probability.

However a recent paper suggests that A β may act as a positive regulator of release probability (Abramov et al., 2009). Abramov and colleagues made use of thiorphan, a neutral endopeptidase (NEP) inhibitor. Thiorphan can inhibit the activity of neprilysin, a member of the M13 zinc-dependent metallopeptidase family and one of the enzymes implicated in degrading A β from the synapse. They showed that application of thiorphan to neuronal cultures led to an elevation in endogenous A β_{40} and A β_{42} levels, in line with previous *in vivo* studies (Newell et al., 2003). They also found that application of thiorphan led to an increase in FM dye uptake into presynaptic vesicles during endocytosis, suggestive of an increase in release

probability. It was also shown that thiorphan could also increase the rate of vesicle exocytosis. AF1126, an antibody that neutralises neprilysin activity also led to an increase in FM dye uptake into presynaptic terminals. Together this data indicates that neprilysin activity negatively modulates basal presynaptic vesicle endocytosis and exocytosis to regulate release probability. The effect of neprilysin inhibition on elevating release probability was shown to be mediated by $A\beta$, as HJ5.1 and 4G8, antibodies that chelate extracellular $A\beta$ peptides prevented the thiorphan-induced elevation of presynaptic activity. γ -secretase and β -secretase inhibitors also blocked the effect of thiorphan on endocytosis. APP knock-out cells also did not exhibit the thiorphan-induced enhancement of presynaptic endocytosis whilst transfection of APP into APP knock-out cells could rescue the thiorphan associated presynaptic enhancement. This suggested that APP processing / $A\beta$ production was required for the thiorphan associated effect. Together this data presents a convincing argument that elevations in endogenous $A\beta$ may regulate the thiorphan induced in presynaptic enhancement of release probability.

However block of extracellular $A\beta$ using HJ5.1 and 4G8 antibodies or blocking $A\beta$ production using chronic γ -secretase and β -secretase inhibitor treatment did not show any differences in synaptic vesicle endocytosis when compared to control neurons. This result suggests that eliminating $A\beta$ alone does not have any impact on release probability and in line with experiments presented in chapter 4 (PS1 knock-out mice and γ -secretase inhibitor treatment), this current chapter (β -secretase inhibitor treatment) and the study by Priller and colleagues (APP knock-out mice)(Priller et al., 2006). These results suggest that $A\beta$ does not regulate release probability in a bidirectional manner. Whilst elevating endogenous $A\beta$ may enhance synaptic vesicle endocytosis (Abramov et al., 2009), blocking $A\beta$ production has no positive or negative effect on vesicle recycling. This result is potentially in disagreement with a recent study using presenilin double knock-out mice. Zhang and colleagues (2009) showed that the rate of MK801-mediated NMDA current block and PPR was decreased in presenilin double knock-out cells relative to control cells suggesting that loss of $A\beta$ generation leads to a decrease in release probability (Zhang et al., 2009). Further studies are required to determine the differences between these studies.

Intriguingly, inhibition of A β degradation by thiorphan also led to an increase in mEPSC frequency, suggesting that elevating A β may increase the rate of spontaneous currents. This is potentially in conflict with previous studies where APP overexpression (and enhanced A β production) (Kamenetz et al., 2003; Ting et al., 2007) led to a decrease in mEPSC frequency. The reason for the discrepancy is not clear but may be explained by differences in the methods used to generate excess A β . For example, the studies by Kamenetz et al., (2003) and Ting et al., (2007) examined the effects of overproduction of exogenous human A β (Kamenetz et al., 2003; Ting et al., 2007) whilst Abramov et al., (2009) investigated the effects of elevated levels of endogenous rat A β by inhibition of its degradation (Abramov et al., 2009). Additionally synapse associated side effects of thiorphan treatment cannot be excluded as this compound has also been shown to act on other cellular neutral endopeptidases including enkephalinase.

Understanding the role of A β in modulating different aspects of synapse function not only requires an idea of the mechanisms involved but also an understanding of the amount of A β required to cause these effects. The concentration of A β in samples is often not known in most overexpression or neprilysin inhibition studies. Potentially the amount of A β produced by neurons can also vary as several studies have indicated that A β release can be regulated by synaptic activity (Cirrito et al., 2005; Cirrito et al., 2008; Kamenetz et al., 2003). One recent study examines this question in greater detail using exogenous application of defined amounts of A β peptides. Recordings of spontaneous currents revealed that only 50 nM of A β was required for a significant decrease in mEPSC frequency, whilst no significant effect on mEPSC amplitude was observed until application of 1 μ M of A β peptides, suggesting that different concentrations of A β have differential effects on mEPSC frequency and amplitude (Parodi et al., 2010). It is therefore possible that A β within the concentration range of 50 - 500 nM may correspond to the amount of A β produced in APP overexpressing cells which were previously shown to have similar decreases in mEPSC frequency with no changes in mEPSC amplitude (Kamenetz et al., 2003; Ting et al., 2007). Both mEPSC frequency and amplitude progressively decreased upon treatment with increasing concentrations of A β .

Furthermore, it was shown that both monomeric and fibrillar forms of A β did not alter mEPSC properties suggesting that dimers or oligomers of A β may be involved.

Examination of mIPSCs following treatment with A β (500 nM, 24 hr) revealed no differences in mIPSC frequency or amplitude indicating that A β acts selectively at glutamatergic synapses (Parodi et al., 2010). Interestingly, exogenous A β treatment (500 nM, 24 hrs) also influenced synaptic vesicle release; where a decrease in the rate of exocytosis was observed, suggesting that release probability was decreased. This is potentially the opposite effect to the observations of Abramov and colleagues who have reported that elevating A β levels using inhibitors that block A β degradation increases the rate of vesicle exocytosis. The reason for the discrepancy is currently unknown. In the Parodi study, electron microscopy also revealed a decrease in the presynaptic vesicle pool size suggesting that the decrease in mEPSC frequency could be correlated with a structural change in preynaptic vesicle pool. Interestingly A β was also shown to alter mEPSC frequency in a temporally defined manner, with significant decreases in mEPSC frequency being observed following 12-24 hrs treatment whereas treatment for 0.5–2 hrs caused a significant increase in mEPSC frequency. Furthermore it was shown that this transient increase in mEPSC frequency was associated with an elevation in intracellular calcium. Interestingly, this elevation in intracellular calcium could not be blocked by a cocktail of calcium channel antagonists including ω -conotoxin, agatoxinVI or nifedipine or glutamate receptor antagonists D-AP5 and CNQX, excluding the likely involvement of voltage gated calcium channels and postsynaptic glutamate receptors. Intriguingly, treatment with Na7, a small peptide that has been shown to block ion flux through channels formed by A β , could block the increase in mEPSC frequency and intracellular calcium, suggesting that A β forms pores in the neuronal membrane which allows influx of calcium into the cell (see Arispe et al., 1993a; Arispe et al., 1993b). This study proposes that the decrease in mEPSC frequency observed following 24 hr treatment with A β arises as a consequence of enhanced synaptic vesicle release causing vesicle pool depletion during the first two hours of A β treatment.

7.6 Conclusion

This chapter showed that β -secretase inhibition, like γ -secretase inhibition can cause changes in mEPSC frequency but not release probability, suggesting BACE1 may regulate spontaneous synaptic currents but not presynaptic release. However a difference in synaptic function was observed following treatment with β -secretase inhibition or γ -secretase treatment, with no significant up or down regulation in synapse number being observed with the former and an increase being observed with the latter. This finding implies that β -secretase is not required for regulation of synapse density and highlights disparate roles for β -secretase and γ -secretase in modulation of synapse function in hippocampal neurons.

Chapter 8: Overall summary and general discussions

8.1 Research summary

Genetic and biochemical studies have emphasised the key role of PS1 in the pathogenesis of AD. However, more recent studies have also shown that PS1 is able to interact and process a wide range of cellular proteins (see Table 1.1). Whilst the functional significance of these reported interactions remain to be fully examined, they indicate that presenilin could affect a range of signalling pathways also in neurons. Understanding the biology of PS1 may provide insights into the possible physiological functions that are disrupted in neurons during AD. The aim of this current project has been to gain a better understanding of the role of presenilin (1) at hippocampal synapses. My findings implicate presenilin in modulating certain aspects of hippocampal synapse function.

Whole-cell recordings have revealed that presenilin is involved in regulating spontaneous synaptic transmission at excitatory but not inhibitory synapses in dissociated and organotypic cultures (Chapter 3). These results are consistent with previous studies that have indicated a role for presenilin in regulating glutamatergic synaptic currents (Kamenetz et al., 2003; Parent et al., 2005; Priller et al., 2006). Further experiments provide evidence that alterations in miniature frequency are associated with changes in synapse number rather than release probability. Specifically, live imaging and electrophysiological experiments indicate that presenilin activity and expression is dispensable for the regulation of release probability (Chapter 4). In contrast, immunocytochemical analysis reveals an increase in the number of co-apposed pre and postsynaptic markers of excitatory synapses (Chapter 5). One interpretation of this outcome is that γ -secretase activity may play a role in regulating structural components of synapses and hence act as a

modulator of synapse number. This increase in excitatory synapse number may potentially provide an explanation for the increase in mEPSC frequency and implicates presenilin in regulating both structural and functional properties of hippocampal synapses.

The role of γ -secretase activity of presenilin in regulating intracellular calcium levels has also been examined in the soma of hippocampal neurons. Inhibition of γ -secretase activity does not alter measurements of intracellular calcium under basal conditions or following KCl-stimulated CICR (Chapter 6). This result indicates that γ -secretase activity is not involved in modulating intracellular somatic calcium levels at rest or after cell depolarisation. This finding also suggests that the reported reduction in intracellular calcium in PS1 and PS2 double knock-out neurons upon KCl stimulated CICR (Zhang et al., 2009) occurs through a mechanism involving a γ -secretase independent activity of presenilin rather than a γ -secretase dependent action of presenilin. However, the underlying mechanism remains to be fully understood. My result also proposes that the elevation in mEPSC frequency observed in PS1 knock-out and γ -secretase inhibitor treated cells is potentially not associated with alterations in intracellular calcium. However only somatic calcium has been examined in this present study and further calcium imaging of axonal boutons will provide a more accurate insight into the role of presenilin in modulating intracellular calcium at the synapse.

The last part of this study has addressed the role of β -secretase activity in the regulation of synapse function (Chapter 7). The aim has been to gain insights into the mechanisms underlying the synaptic effects observed in presenilin 1 knock-out and γ -secretase inhibitor treated hippocampal neurons. The observed synaptic changes could occur through a direct loss of presenilin activity or an indirect effect of the loss of a γ -secretase cleavage product. One possible candidate cleavage product that is greatly reduced with both presenilin manipulations is A β . APP overexpression studies (Hsieh et al., 2006; Kamenetz et al., 2003; Ting et al., 2007; Wei et al., 2010) and APP knock out studies (Priller et al., 2006) provide evidence that A β may play a bidirectional role in modulating synapse structure and function. Interestingly, the synaptic characteristics of APP knock-out animals are very similar to the synaptic properties observed in PS1 knock-out animals (Chapter 3, 4 and 5,

Parent et al., 2005; Priller et al., 2006). As both APP and PS1 are required for APP processing and A β generation, it is possible that the alterations in synaptic parameters that are observed in both knock-out studies may arise from the common loss of A β production. To this end, I have examined whether blocking A β generation using β -secretase inhibitors would lead to any changes in synapse function.

Similarly to γ -secretase inhibitor treatment, chronic treatment of hippocampal neurons with β -secretase inhibitor increases mEPSC frequency but does not alter synaptic vesicle exocytosis, suggesting that β -secretase activity is required for regulation of synaptic transmission but not for regulation of release probability (Chapter 7). However, β -secretase inhibition has no significant effect on synapse number, as estimated through a lack of change in Homer and synapsin co-localised synaptic puncta (Chapter 7). This result diverges from the observations made from neurons treated with γ -secretase inhibitors where an increase in co-localised synaptic puncta is seen. The simplest interpretation of these results is that A β does not act as a bidirectional regulator of synaptic transmission and synapse number. However such a conclusion assumes that the effects on spontaneous synaptic currents and synapse number are correlated. If synaptic currents and synapse number are independently regulated, then the increase in mEPSC frequency observed in PS1 knock-out animals, APP knock-out animals and γ -secretase and β -secretase inhibitor treated cells may potentially still be regulated by A β , whilst the change in synapse number probably not requiring A β .

PS1 overexpression studies have also been attempted during the course of this project as an alternative way to analyse presenilin associated regulation of synaptic function. The utility of this approach was illustrated in an earlier study from Kaether et al., (2002), where PS1-EGFP constructs were expressed in stably transfected HEK cells and found to traffic to different subcellular compartments including the ER and the plasma membrane (Kaether et al., 2002). The study found that exogenously expressed constructs could replace endogenous PS1 and PS2 despite the limited level of overexpression due to tight regulation of cellular γ -secretase levels (Thinakaran et al., 1997). Functionality of wild type PS1 constructs was confirmed through the production of A β peptides. The expression of the PS1 D385N-EGFP mutant

construct which did not possess γ -secretase activity, however, led to accumulation of APP CTF in cell lysate preparations (Kaether et al., 2002).

My aim was to overexpress either wild type PS1-EGFP or PS1 D385N-EGFP mutant constructs in mature dissociated cultured neurons and evaluate the effects on different synaptic and neuronal properties. With regards to mEPSC recordings, the plan was to determine if transfection of these constructs could rescue synaptic alterations observed in PS1 knock-out cells. Transfection of wild type PS1 back into PS1 knock-out cells is expected to rescue the wild type control phenotype. Conversely, if γ -secretase is required for modulation of mEPSC frequency, transfection of catalytically inactive PS1 D385N-EGFP mutant constructs into PS1 knock-out cells should not rescue the wild type phenotype. Potentially, this approach also enables the pre and postsynaptic effects of presenilin overexpression to be assessed with targeted transfection in either pre or postsynaptic neurons.

Unfortunately, I found that transient transfection of cDNA using calcium phosphate method did not generate successful expression. At best, weak intracellular (possibly ER) EGFP signal was observed following post-hoc staining and signal amplification with an EGFP antibody (data not shown). No significant EGFP fluorescence was observed in live cells. The reasons for this are not entirely clear. One possibility is that the half-life of γ -secretase complex is long. Past studies have shown that exogenous full length PS is rapidly degraded with a half life of several hours. However, catalytically active N and C terminal PS fragments are more stable and have a half life of at least 24 hours in cultured cells (and possibly up to several days – personal correspondence from C. Kaether) (Dries and Yu, 2008; Kim et al., 1997; Podlisny et al., 1997; Ratovitski et al., 1997; Steiner et al., 1998; Thinakaran et al., 1997). This relatively long time frame poses problems for integration of exogenous PS protein into endogenous γ -secretase complexes in neurons with transient overexpression methods. As the cellular levels of γ -secretase are tightly controlled and depend on the availability of co-factors; APH-1, PEN-2 and nicastrin (Thinakaran et al., 1997), it is understood that transient overexpression of unincorporated presenilin will remain within the ER and then get degraded by proteasome, caspase or cysteine protease activity (Steiner et al., 1998). Potentially, a way around the long half life of endogenous γ -secretase is to overexpress the

construct for longer duration so that exogenous presenilin will have sufficient time to replace endogenous presenilin within the cellular γ -secretase complex. However, the calcium phosphate transfection method can often render cells unhealthy, making long-lasting expression difficult, and so an alternative DNA delivery system such as the use of lentiviral vectors which enables prolonged expression of exogenous proteins should be investigated (see Pratt et al., 2009). Another possibility for the lack of expression is that presenilin may be misfolded, or improperly inserted into membrane compartments such as the ER in neurons with transient transfection (Haass and De Strooper, 1999).

Several attempts were also made to clarify the subcellular location of presenilin 1 in my hippocampal neuronal culture system using immunocytochemical techniques. As already mentioned several groups had investigated the expression of presenilin in neurons using in situ hybridisation and mRNA probes and found PS1 in the hippocampus, cerebellum and other tissues of humans and mice (Berezovska et al., 1997; Kovacs et al., 1996; Lee et al., 1996). Immunoblot analysis also found that PS1 and PS2 were expressed in cultured neurons and astrocytes (Lee et al., 1996). However, the subcellular localisation of endogenous PS1 in hippocampal neurons is still under debate. One of the first studies to examine the subcellular localisation of PS1 using overexpression of exogenous Flag tagged PS1 and PS2 constructs in non neuronal cells showed that PS1 and 2 primarily localised in ER and Golgi regions (Kovacs et al., 1996). However it was not shown whether these constructs incorporated into γ -secretase complexes. A later report using a functional GFP tagged PS construct, which was able to incorporate into the γ -secretase complex, was found to be localised to the ER, Golgi, endosomes, lysosomes and plasma membrane (Kaether et al., 2002). Other studies have also tried to investigate the localisation of endogenous PS1 in neuronal cultures. Annaert et al., (1999) performed analysis of PS1 wild type neurons and showed that the uncleaved presenilin holoprotein was associated with the nuclear envelope whilst PS NTF and CTF fragments were associated with post ER membranes and the intermediate compartment but not in regions downstream of the cis-Golgi. A recent immunofluorescence study showed that PS1 co-localised with synaptic markers, Homer and Bassoon suggesting that presenilin was present at pre and postsynaptic compartments of mature synapses

(Inoue et al., 2009). One major drawback to most reports investigating the localisation of endogenous PS1 is the lack of a negative control, such as a PS1 knockout. One study of cortical neuronal cultures showed that endogenous PS1 staining was associated with the soma and neuritic processes in wild type neurons and only diffuse somatic signal was seen with PS1 knock-out neurons (Parent et al., 2005). However, in my hands, the use of several anti-PS1 antibodies did not lead to clear-cut results regarding the subcellular localisation of PS1 in hippocampal neurons. The main problem I experienced was the highly similar PS1 antibody associated signal in both wild type and PS1 knock-out cultured neurons, suggesting a high degree of non-specific staining with the antibodies I was using (data not shown). Further examination with different PS1 antibodies in PS1 knock-out and wild type neurons will be necessary to fully determine the subcellular localisation of endogenous PS1 in hippocampal neurons.

Studies have demonstrated that axon transport defects are also observed during early stages of AD pathogenesis (Morfini et al., 2002; Stokin et al., 2005; Stokin and Goldstein, 2006). Early observations examining the role of APP in neurons found that APP could be transported along axonal processes (Buxbaum et al., 1998c; Koo et al., 1990). One study showed that APP could act as a receptor for kinesin-1, an axonal motor protein important for fast axonal transport of synaptic cargo (Kamal et al., 2000). The same group also found that the three components required for A β generation: PS1, BACE1 and APP were closely associated within axonal vesicles, promoting the idea that A β generation and release could occur within axonal processes (Kamal et al., 2001). However, a later report could not confirm these findings. Lazarov and colleagues found that not only did APP and kinesin-1 not co-fractionate or co-precipitate, transport of kinesin-1 in axons was not altered in APP knock-out mice suggesting that APP was not a necessary component of kinesin-1 associated axonal transport (Lazarov et al., 2005). Biochemical and immunolabelling analysis also showed that PS1, BACE1 and APP co-localisation was not observed in the axons of the sciatic nerve, suggesting that the proteolytic machinery for A β generation could not be cotransported with APP (Lazarov et al., 2005). The reasons for the discrepancies between these studies are currently unclear. Whilst the results of Lazarov and colleagues question whether APP is involved in kinesin-1 associated axonal transport, it remains to be determined whether APP and

PS1 are implicated in synaptic vesicle transport. Reports have indicated that PS1 can co-localise with presynaptic vesicle proteins and that other γ -secretase components can also be found in synaptic vesicle membrane fractions (Behr et al., 1999; Frykman et al., 2010; Smith et al., 2000; Thinakaran and Parent, 2004). However the functional relevance of this link remains to be determined. The anterograde and retrograde axonal trafficking of synaptic vesicles between presynaptic boutons in mature cultures was previously characterised in the lab (Darcy et al., 2006; Staras et al., 2010). The reason for inter-bouton movement of vesicles remains to be fully understood but may play a role in synaptogenesis, synapse refinement or synaptic plasticity (Darcy et al., 2006; Krueger et al., 2003). As γ -secretase activity of presenilins may be implicated in regulation of synapse number (Chapter 5), I sought to investigate whether γ -secretase activity may also alter synaptic vesicle trafficking as a possible mechanism for regulation of synapse formation. To address this question, timelapse imaging was used to estimate the rate of FM-labelled synaptic vesicle movement back into a bouton using a Fluorescence Recovery after Photobleaching (FRAP) assay. Whilst this protocol mainly examines the recovery of FM labelled recycled synaptic vesicles into pre-existing synapses rather than being a direct measure of synaptogenesis, the rate of recovery of fluorescently labelled vesicles into a synapse may provide an insight into synaptic vesicle movement associated with formation of new synapses (Darcy et al., 2006; Krueger and Fitzsimonds, 2006; Krueger et al., 2003). Due to the low number of cells, it is currently not possible to make strong conclusions about the role of presenilins in synaptic vesicle trafficking. However, initial experiments suggest that there are no significant differences in the rate of fluorescence recovery between control and γ -secretase inhibitor treated cells (data not shown). This preliminary finding suggests that presenilin activity is potentially not implicated in the axonal transport of synaptic vesicles between presynaptic boutons and in agreement with the findings observed by Lazarov et al., (2005) who find that presenilin is not involved in axon transport. Further studies will be required to determine if this initial finding holds.

A recent Society for Neuroscience abstract also reported similar findings to the observations presented in this current project (Pratt et al., 2009). Recordings from hippocampal dissociated autaptic cultures from constitutive PS1 knock-out mice revealed a dramatic increase in mEPSC frequency (Pratt et al., 2009). The authors

also reported that evoked AMPA or NMDA current amplitude or paired-pulse ratio was not altered in PS1 knock-out mice suggesting that loss of PS1 gene had a selective effect on spontaneous currents. Additionally, the increase in mEPSC frequency could be blocked by intracellular application of calcium buffer, EGTA or rescued by exogenous expression of wild type PS1. This study suggests that PS1 gene elimination may cause an increase in mEPSC through an elevation of intracellular calcium. Whilst our calcium imaging experiments from the soma of hippocampal neurons do not indicate a change in somatic calcium concentrations during basal or CICR, our data do not rule out an alteration in calcium homeostasis in axonal terminals and hence further studies will be required to address this question. One possible experiment is to image calcium in functional axonal boutons identified by loading with FM dyes. KCl application can then be used to do two things: induce FM dye destaining to confirm synaptic vesicle exocytosis and to simulate CICR in active synapses to examine calcium release from intracellular stores (Evans and Cousin, 2007). This approach will enable calcium within functional boutons to be measured in response to KCl-stimulated CICR.

Overall this project has provided further insights into the role of presenilin in modulating different aspects of synapse function in hippocampal neurons. The data presented also shows that presenilin may have presynaptic and postsynaptic functions. Whilst an increase in mEPSC frequency is often associated with a change in presynaptic function, the alteration in synapse number indicates that pre and /or postsynaptic changes can occur to enable formation of new synaptic puncta. This is in line with studies which show that changes can occur to pre and postsynaptic sides of the synapse during A β peptide application to simulate pathological synaptic events associated with AD, in vitro (Calabrese et al., 2007; Wei et al., 2010).

However, further investigations are necessary to establish the molecular mechanisms that underlie the synaptic changes observed following presenilin manipulations. Whilst different synaptic studies have proposed that loss of γ -secretase activity can alter the processing of different substrates of γ -secretase (see for example: APP (Kamenetz et al., 2003; Priller et al., 2006), DCC (Parent et al., 2005), Eph4 receptor (Inoue et al., 2009 but see Table 1.1) it is currently unclear how signalling pathways downstream of γ -secretase could modify synaptic function. It is currently not known

if the synaptic effects reported in this thesis arise from disruption of one signalling pathway or if the changes are the result of the collective disruption of multiple γ -secretase modulated pathways. These questions will need to be addressed in future studies.

8.2 Possible γ -secretase dependent and γ -secretase independent action of presenilin at hippocampal synapses

Many previous studies have used presenilin knock-out mice to investigate the cellular role of presenilin. However, as discussed, one major drawback with this approach is the loss of both γ -secretase dependent and γ -secretase independent actions of presenilin. Early studies indicated that presenilin is predominantly involved in γ -secretase dependent processes, as the catalytically inactive holoprotein form of presenilin has been believed to be rapidly degraded (Annaert et al., 1999; Podlisny et al., 1997; Xia et al., 1997). However, more recent studies have shown that presenilin can modulate some cellular processes in a γ -secretase independent manner, including regulation of intracellular calcium by forming an ER calcium leak channel and regulating cellular β -catenin levels (Kang et al., 1999; Koo and Kopan, 2004; Tu et al., 2006). The exact percentage of presenilin which functions in a γ -secretase dependent and a γ -secretase independent context is not currently known.

Previously, it has been shown that γ -secretase independent action of presenilin is potentially involved in modulating intracellular calcium concentration. A study conducted using presenilin double knock-out animals showed that intracellular calcium was decreased compared to wild type control cells upon KCl-induced CICR (Zhang et al., 2009). However, in this thesis work, as γ -secretase inhibitors did not

alter intracellular calcium in hippocampal neurons under basal conditions or during KCl-induced CICR (chapter 6), it was concluded that γ -secretase activity was dispensable for presenilin associated regulation of intracellular calcium. These experiments highlight the value of using a combinational approach of knock-out mice models and pharmacological inhibitors of presenilin catalytic activity to distinguish between γ -secretase dependent and γ -secretase independent actions of presenilin. However, to clarify γ -secretase independent functions of presenilin, a rescue experiment should also be performed as suggested above, making use of the wild type and the catalytically inactive mutant presenilin, PS1 D385N. Being able to determine which synaptic functions are regulated by γ -secretase dependent actions and which synaptic effects involve γ -secretase independent action of presenilin may provide further insights into the possible cellular mechanisms modulated by presenilin at hippocampal synapses.

8.3 Neuronal activity, A β peptides and synaptic transmission

As already mentioned, chronic β -secretase and γ -secretase treatment were both shown to increase mEPSC frequency. One interpretation of this data is that loss of A β can elevate spontaneous synaptic transmission. Several studies have shown that A β generation from neurons can occur in an activity dependent manner (Cirrito et al., 2005; Cirrito et al., 2008; Kamenetz et al., 2003). Decreasing neuronal activity by application of tetrodotoxin (TTX), led to a decrease in A β generation, whereas application of picrotoxin, which blocked inhibitory GABA_A receptors leading to an elevation of neuronal activity, was associated with an increase in A β ; moreover, an increase in A β generation was associated with a decrease in evoked current amplitude and mEPSC frequency (Kamenetz et al., 2003). This led to the proposal that A β was involved in a negative feedback mechanism, where increased neuronal activity enhanced A β production which subsequently decreased synaptic transmission to prevent excessive neuronal activity. The same study also showed the opposite configuration where blocking endogenous A β production via chronic

treatment with γ -secretase inhibitor, L-685,458, could lead to an increase in synaptic activity (in line with results presented in chapter 3). These findings suggest that a potential physiological role of A β is to bidirectionally regulate neuronal activity depending on the amount of A β secreted/produced.

However, it is not entirely clear how neuronal activity could alter A β production. Kamenetz et al., (2003) present evidence that A β associated depression of synaptic currents is linked with an elevation of β -secretase activity caused by enhanced neuronal activity, as evidenced by elevated β -CTF generation under conditions that increased neuronal activity. However, it was not shown whether β -secretase inhibitors could prevent this elevation in β -CTF generation. Additionally, this experiment does not rule out the possibility that neuronal activity can also regulate (elevate) γ -secretase activity. Indeed, if the negative feedback model proposed by Kamenetz is dependent on enhanced A β generation, then it is reasonable to assume that neuronal activity should enhance both β -secretase and γ -secretase activity. The effects of β -secretase and γ -secretase inhibitors on the activity dependent production/secretion of A β remain to be determined.

8.4 Evaluating γ -secretase inhibitors as a possible therapeutic strategy for AD

Early findings showing a crucial role for presenilin in A β generation also raised the possibility of γ -secretase as a therapeutic target for treatment of AD. It was proposed that application of γ -secretase inhibitors may limit the speed and extent of A β plaque deposition and associated neuronal pathology, such as dystrophic neurites, calcium homeostasis dysregulation and spine loss and therefore slowing down the rate of disease progression (Dickson and Vickers, 2001; Hsieh et al., 2006; Knowles et al., 1999; Kuchibhotla et al., 2008; Spires-Jones et al., 2007; Wei et al., 2010; Wu et al., 2010). Indeed several rodent studies have shown that certain γ -secretase inhibitors can limit the deposition of A β *in vivo* (Dovey et al., 2001; Schenk et al., 1999, but see Garcia-Alloza et al., 2009). Clinical trials in humans

have also commenced with certain γ -secretase inhibitors. One specific inhibitor, LY450139 showed a reduction in A β biosynthesis in a dose-dependent manner indicating that γ -secretase inhibitor treatment could also alter A β levels in humans (Bateman et al., 2009).

However, studies have proposed that A β has other physiological functions at synapses, therefore blocking synthesis completely may lead to a disruption of these other putative functions of A β (see for review: Marcello et al., 2008). This notion is also applicable to presenilin which is implicated in the cleavage of a wide range of cellular type 1 transmembrane proteins and regulating many different signalling pathways (see Table 1.1). Whilst different inhibitors may have differential effects on γ -secretase processing of different substrates, the use of γ -secretase inhibitors for therapeutic purposes should be considered with caution, especially until the molecular mechanisms underlying the synaptic changes following chronic γ -secretase treatment are better understood. It is currently unclear how 48 hr treatment with γ -secretase inhibitors may alter functional and structural properties of hippocampal synapses. As DAPT and L-685,458 are both cell permeable inhibitors, it is suspected that inhibition of γ -secretase enzymatic activity should be fairly rapid. However, acute treatment did not generate a change in electrophysiological properties (see chapter 3) and suggests that synaptic changes associated with prolonged inhibition of γ -secretase activity may be a result of more long term cellular adaptations. As γ -secretase is implicated in many different intracellular signalling pathways (see Table 1.1), it is conceivable that inhibition of γ -secretase activity or function could alter nuclear signalling, gene transcription and protein synthesis which may take hours – days to be fully revealed in neurons. Alternatively, the synaptic changes following 48 hr γ -secretase inhibitor treatment may occur as a result of protein degradation. It is possible that γ -secretase negatively regulates synapse number through an intermediate player e.g. a protein or cue that inhibits synapse formation and therefore when γ -secretase activity is blocked the interaction and function of this player is lost. However the synaptic effects may only be observed once this protein/ cue has degraded. Again this possible sequence of events may occur over longer time frames. Further studies are required to evaluate these possibilities experimentally and also to determine likely mechanisms and candidate players. Additionally, the results of the power

calculations suggest that further studies should be conducted to clarify the cellular effects of acute γ -secretase inhibition.

As shown in chapter 3 and other studies (Kamenetz et al., 2003; Parent et al., 2005; Priller et al., 2006), γ -secretase inhibitor treatment was associated with an increase in the rate of spontaneous excitatory currents and synapse number. While an increase in synapse number may seem advantageous when it comes to treating the synapse and neuronal loss that accompanies AD progression, an increase in mEPSC frequency in the absence of a change in mIPSC frequency may cause an overall shift in the excitatory and inhibitory network balance towards a more excited state. The long term implications of this potential change in network activity are not clear. It is also not known whether γ -secretase treatment could eventually cause changes in the intrinsic excitability of neurons. However, elevated neuronal activity has previously been linked to excitotoxicity (Barten and Albright, 2008; Zoghbi et al., 2000). Whilst not directly examined, changes in neuronal activity and firing may potentially cause excitotoxicity and provide an alternative explanation for the reported temporal difference in synapse number following γ -secretase treatment. Whilst 4-48 hr treatments typically led to an increase in synapse number (Chapter 5, Parent et al., 2005), longer treatment was associated with a loss of postsynaptic spines (Bittner et al., 2009; Inoue et al., 2009). These temporal changes in synapse number were also reflected by presenilin double knock-out studies where an increase in synapse number was seen in young animals and a decrease in synapse number (and eventually neurodegeneration) was observed in older animals when compared to control animals (Aoki et al., 2009; Saura et al., 2004). Therefore acute or short term treatment with γ -secretase inhibitors may promote synaptogenesis whilst chronic or long term use may cause the opposite and enhance synapse loss. It is possible that the enhanced synaptic transmission or neuronal activity associated with shorter term γ -secretase treatment could eventually lead to excitotoxicity in neurons which may then cause synapse loss. Understanding the mechanisms relating to this temporal effect on synapse number will hopefully provide insights into how the balance between synapse loss and synapse gain could be tipped towards the latter for treatment of AD. Identifying a therapeutic window for γ -secretase treatment may be sufficient to enhance synapse number and counteract synapse loss.

The use of γ -secretase modulators rather than inhibitors may prove to be a better therapeutic strategy. Such modulators are designed to alter γ -secretase processing of specific substrates whilst leaving the processing of other substrates intact. Currently, γ -secretase modulators are being developed which specifically target γ -secretase processing of APP whilst sparing Notch processing (Wolfe, 2009). Studies have also identified that non-steroidal anti-inflammatory drugs (NSAIDs) alter PS1 conformation and shift γ -secretase cleavage of APP to selectively reduce $A\beta_{42}$ production whilst enhancing $A\beta_{40}$ production (Eriksen et al., 2003; Lleo et al., 2004; Weggen et al., 2001; Weggen et al., 2003). NSAIDs treatment was also associated with a reduction in microglia activation (and inflammation) and amyloid plaque pathology in a mouse model of AD (Lim et al., 2000). Crucially Notch signalling was not impaired following treatment which makes NSAIDs an attractive therapeutic possibility (Weggen et al., 2001). However, clinical trials have indicated that long term treatment with NSAID could inhibit cyclo-oxygenase (COX1) activity which could promote gastrointestinal dysregulation (see Bergmans and De Strooper, 2010). Recent developments of newer NSAID derivatives which can reduce $A\beta$ deposition whilst bypassing gastrointestinal side-effects are promising options and further studies will determine whether they will be clinically useful (Imbimbo et al., 2009).

8.5 Relation of current findings to AD

This study mainly focuses on the role of presenilin under basal physiological conditions. This and other studies have provided insights into the biology of presenilin at the synapse and also the role of γ -secretase activity in hippocampal neurons. However, the experiments presented in this thesis, do not provide direct information about the effects of clinical mutations in presenilins on synapse function. Indeed, (conditional) presenilin knock-out animals are not strictly a model for AD as these animals lack $A\beta$ plaques (Saura et al., 2004). Though, these animals have been used to demonstrate that presenilin is important for cell survival, and is therefore regarded as a good model for neurodegenerative studies associated with AD (Saura et al., 2004). However some observations outlined in this thesis are also observed in certain AD transgenic mouse models. With regards to synapse number, studies from

mice models which give rise to amyloid pathology have revealed that estimates of alterations in synapse number can be variable between different AD models. For example, Vesicular Acetyl Choline Transporter (VACht) labelling revealed that cholinergic presynaptic bouton number was increased in APP (K670N, M671L) single mutant mice but not altered in PS1 (M146L) single mutant mice (Hu et al., 2003; Wong et al., 1999). Intriguingly, APP (K670N, M671L) and PS1 (M146L) double transgenic mice showed a reduction in VACht labelling but an increase in synaptophysin positive puncta, suggesting that different synaptic proteins can be differentially affected even in the same mouse model (Hu et al., 2003; Wong et al., 1999). Interestingly, the extent of plaque deposition was also associated with differential observations in synapse number as an increase in presynaptic marker labelling was seen in the absence of plaques whilst a decrease in synapses was observed with the onset and development of plaques (Bell and Cuello, 2006). However, a study of young (4 months old) TgCRND8 mice, which expresses human APP695 gene with the K680M/N671L and V717F mutations and is a model of early onset AD, showed that VGLUT (presynaptic glutamate transporter) and VGAD (presynaptic GABA transporter) positive bouton number was increased in amyloid plaque free areas as well as in areas next to plaques when compared to non transgenic controls (Bell and Cuello, 2006). Overall the temporal changes in synapse number in these AD mouse models reflected observations in γ -secretase treated cells and presenilin double knock-out cells. However, it remains unclear if the signalling pathways involved in synaptic regulation in knock-out studies are the same as in AD mouse models. It also remains to be fully determined whether different AD mice models exhibit the same defects in cell signalling which ultimately lead to neurodegeneration and amyloid accumulation in these animals.

Studies of human PS1 (A246E) mutant transgenic mice revealed some differences in synaptic properties when compared to PS1 knock-out and γ -secretase treated cultures. Priller et al., (2007) reported that PS1 (A246E) mutant mice autaptic cultures showed a reduction in evoked NMDA and AMPA EPSC amplitude, mEPSC frequency and synapse density, essentially the opposite effects to that observed in PS1 knock-out mice (Priller et al., 2007). However, a separate study performed in acute slices showed that NMDA field responses and NR1 and NR2B subunit expression was elevated in the same PS1 mutant mice (Dewachter et al., 2008). It is

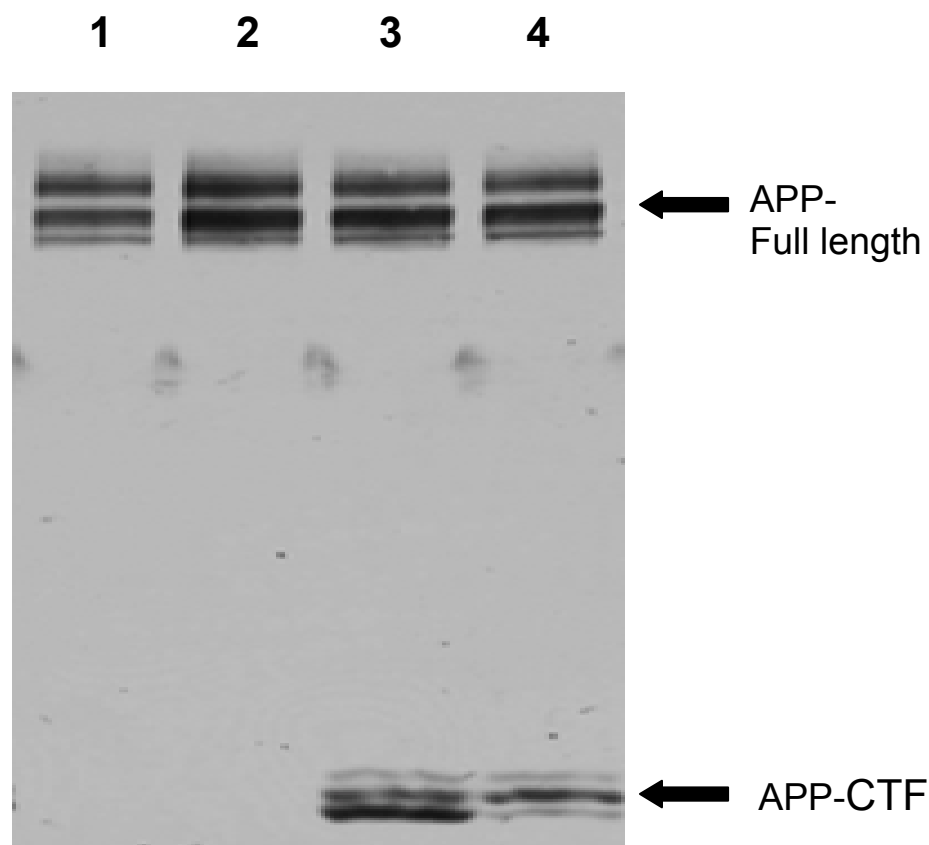
unclear why there is a difference in NMDA receptor responses between these two studies. Consistent with the increase in NMDA receptor responses, Dewachter et al., (2008) also showed that LTP and activated nuclear c-fos expression was increased in PS1 (A246E) mutant animals (see also Parent et al., 1999). Analysis of a transgenic mouse overexpressing an aggressive FAD PS1 (L286V) mutation showed some similar properties to PS1 (A246E) mutant mice (Auffret et al., 2009). In young 4-5 month animals, NMDA receptor field responses, LTP and spine density was increased, however this facilitation in synapse function disappears in older animals, as 13-14 month mice showed a decrease in the magnitude of LTP and NMDA receptor response, indicating an age-dependent effect on synapse function (Auffret et al., 2009). However, similarly to PS1 knock-out mice, paired-pulse ratio and mEPSC amplitude were not altered in PS1 (A246E) or PS1 (L286V) mutant mice (Auffret et al., 2009; Dewachter et al., 2008; Priller et al., 2007), suggesting that most perturbations in presenilin function in general do not alter these synaptic parameters (but see Zhang et al., 2009). Further studies of other presenilin mutant mice will be useful to help determine if there are further differences in synaptic properties between different FAD clinical mutations and also determine if there are further similarities between presenilin knock-out animals and FAD mutant mice.

8.7 Final remarks

The cellular and molecular mechanisms underlying AD are still poorly understood. The role of presenilin in regulating different cellular processes during pathological conditions has received much attention in recent years. The importance of presenilin in AD pathogenesis is exemplified by the findings that mutations in *PSEN1* gene are strongly associated with the onset of the more aggressive FAD. Presenilin is also implicated in AD pathology as it the enzyme complex that gives rise to A β peptides, the major constituents of A β plaques. However, the role of presenilin in regulating different cellular processes under physiological conditions is relatively poorly defined. The aim of this study was to gain a better insight into the potential role that presenilins play in regulating synapse function at hippocampal synapses. The results presented in this thesis indicate that presenilin is important for modulating excitatory synapse structure and function and are in agreement with other PS1 knock-out and γ -secretase pharmacological studies (Kamenetz et al., 2003; Parent et al., 2005; Priller et al., 2006). The experiments performed during the course of this work also tried to examine the role of presenilin in some unexplored aspects of synapse function. The results provide evidence that presenilin is not implicated in regulation of release probability and γ -secretase activity of presenilin is not involved in regulating somatic intracellular calcium. Additionally, the findings suggest that β -secretase and γ -secretase may have some differential synaptic functions and provide some insight into targeting β -secretase and γ -secretase inhibition as possible therapeutic options. Further studies are required to fully understand the molecular mechanism underlying these synaptic changes and determine whether similar observations are present *in vivo*. Ultimately it will be important to extensively investigate whether these synaptic changes may be linked to the synapse dysfunction observed during the early stages of AD, with the aim that better alternative therapeutic strategies may be designed.

Appendix

Appendix I: Western blot of APP from rat dissociated neuronal cultures

**Key:**

1. Mock DMSO control
2. β -secretase inhibitor IV
3. γ -secretase inhibitor DAPT
4. γ -secretase inhibitor L-685,458

Western blot analysis of rat dissociated neurons treated with mock DMSO control (1), β -secretase inhibitor IV (2), γ -secretase inhibitor DAPT (3) or γ -secretase inhibitor L-685,458 (4). Full length APP and APP C-terminal fragments (CTFs) were probed with an antibody (O443) recognizing the C-terminal fragments of APP. Bands corresponding to APP-CTFs accumulated in cells treated with γ -secretase inhibitors DAPT (3) and L-685,458 (4) but not in β -secretase inhibitor IV (2) or mock DMSO control cells. This result indicates that γ -secretase inhibitors can efficiently prevent presenilin mediated intramembranous proteolysis of APP-CTF in rat dissociated neurons, suggesting that DAPT and L-685,458 are active and can inhibit γ -secretase activity of presenilin. Based on bicinchoninic acid protein quantification, 60 μ g of protein was loaded in each lane. Immunoblots were performed blind to treatment and repeated on 3 separate cultures. Western blot experiments were performed by Dr Xulun Zhang from the laboratory of Professor Sangram Sisodia at the University of Chicago, USA.

Bibliography

Abramov,E., Dolev,I., Fogel,H., Ciccotosto,G.D., Ruff,E., and Slutsky,I. (2009). Amyloid-beta as a positive endogenous regulator of release probability at hippocampal synapses. *Nat. Neurosci.* *12*, 1567-1576.

Adesnik,H., Nicoll,R.A., and England,P.M. (2005). Photoinactivation of native AMPA receptors reveals their real-time trafficking. *Neuron* *48*, 977-985.

Akbari,Y., Hitt,B.D., Murphy,M.P., Dagher,N.N., Tseng,B.P., Green,K.N., Golde,T.E., and LaFerla,F.M. (2004). Presenilin regulates capacitative calcium entry dependently and independently of gamma-secretase activity. *Biochem. Biophys. Res. Commun.* *322*, 1145-1152.

Allen,C., and Stevens,C.F. (1994). An evaluation of causes for unreliability of synaptic transmission. *Proc. Natl. Acad. Sci. U. S. A* *91*, 10380-10383.

Allinson,T.M., Parkin,E.T., Turner,A.J., and Hooper,N.M. (2003). ADAMs family members as amyloid precursor protein alpha-secretases. *J. Neurosci. Res.* *74*, 342-352.

Allsop,D., Landon,M., and Kidd,M. (1983). The isolation and amino acid composition of senile plaque core protein. *Brain Res.* *259*, 348-352.

Almkvist,O. (1996). Neuropsychological features of early Alzheimer's disease: preclinical and clinical stages. *Acta Neurol. Scand. Suppl* *165*, 63-71.

Andersen,P., Morris,R., Amaral,D., Bliss,T.V., and O'Keefe,J. (2007). *The Hippocampus Book* (Oxford: Oxford University Press).

Anderson,J.P., Esch,F.S., Keim,P.S., Sambamurti,K., Lieberburg,I., and Robakis,N.K. (1991). Exact cleavage site of Alzheimer amyloid precursor in neuronal PC-12 cells. *Neurosci. Lett.* *128*, 126-128.

Annaert,W., and De Strooper,B. (2002). A cell biological perspective on Alzheimer's disease. *Annu. Rev. Cell Dev. Biol.* *18*, 25-51.

Annaert,W.G., Esselens,C., Baert,V., Boeve,C., Snellings,G., Cupers,P., Craessaerts,K., and De Strooper,B. (2001). Interaction with telencephalin and the amyloid precursor protein predicts a ring structure for presenilins. *Neuron* *32*, 579-589.

Annaert,W.G., Levesque,L., Craessaerts,K., Dierinck,I., Snellings,G., Westaway,D., George-Hyslop,P.S., Cordell,B., Fraser,P., and De Strooper,B. (1999). Presenilin 1 controls gamma-secretase processing of amyloid precursor protein in pre-golgi compartments of hippocampal neurons. *J. Cell Biol* *147*, 277-294.

Aoki,C., Lee,J., Nedelescu,H., Ahmed,T., Ho,A., and Shen,J. (2009). Increased levels of NMDA receptor NR2A subunits at pre- and postsynaptic sites of the

- hippocampal CA1: an early response to conditional double knockout of presenilin 1 and 2. *J. Comp Neurol.* *517*, 512-523.
- Arispe,N., Pollard,H.B., and Rojas,E. (1993a). Giant multilevel cation channels formed by Alzheimer disease amyloid beta-protein [A beta P-(1-40)] in bilayer membranes. *Proc. Natl. Acad. Sci. U. S. A* *90*, 10573-10577.
- Arispe,N., Rojas,E., and Pollard,H.B. (1993b). Alzheimer disease amyloid beta protein forms calcium channels in bilayer membranes: blockade by tromethamine and aluminum. *Proc. Natl. Acad. Sci. U. S. A* *90*, 567-571.
- Arriagada,P.V., Marzloff,K., and Hyman,B.T. (1992). Distribution of Alzheimer-type pathologic changes in nondemented elderly individuals matches the pattern in Alzheimer's disease. *Neurology* *42*, 1681-1688.
- Asai,M., Hattori,C., Szabo,B., Sasagawa,N., Maruyama,K., Tanuma,S., and Ishiura,S. (2003). Putative function of ADAM9, ADAM10, and ADAM17 as APP alpha-secretase. *Biochem. Biophys. Res. Commun.* *301*, 231-235.
- Auffret,A., Gautheron,V., Repici,M., Kraftsik,R., Mount,H.T., Mariani,J., and Rovira,C. (2009). Age-dependent impairment of spine morphology and synaptic plasticity in hippocampal CA1 neurons of a presenilin 1 transgenic mouse model of Alzheimer's disease. *J. Neurosci.* *29*, 10144-10152.
- Auger,C., and Marty,A. (2000). Quantal currents at single-site central synapses. *J. Physiol* *526 Pt 1*, 3-11.
- Azad,N.A., Al,B.M., and Loy-English,I. (2007). Gender differences in dementia risk factors. *Gend. Med.* *4*, 120-129.
- Baimbridge,K.G., Celio,M.R., and Rogers,J.H. (1992). Calcium-binding proteins in the nervous system. *Trends Neurosci.* *15*, 303-308.
- Baki,L., Marambaud,P., Efthimiopoulos,S., Georgakopoulos,A., Wen,P., Cui,W., Shioi,J., Koo,E., Ozawa,M., Friedrich,V.L., Jr., and Robakis,N.K. (2001). Presenilin-1 binds cytoplasmic epithelial cadherin, inhibits cadherin/p120 association, and regulates stability and function of the cadherin/catenin adhesion complex. *Proc. Natl. Acad. Sci. U. S. A* *98*, 2381-2386.
- Bardo,S., Cavazzini,M.G., and Emptage,N. (2006). The role of the endoplasmic reticulum Ca²⁺ store in the plasticity of central neurons. *Trends Pharmacol. Sci.* *27*, 78-84.
- Bardo,S., Robertson,B., and Stephens,G.J. (2002). Presynaptic internal Ca²⁺ stores contribute to inhibitory neurotransmitter release onto mouse cerebellar Purkinje cells. *Br. J. Pharmacol.* *137*, 529-537.
- Barnes,C.A., Jung,M.W., McNaughton,B.L., Korol,D.L., Andreasson,K., and Worley,P.F. (1994). LTP saturation and spatial learning disruption: effects of task variables and saturation levels. *J. Neurosci.* *14*, 5793-5806.

- Barria,A., and Malinow,R. (2005). NMDA receptor subunit composition controls synaptic plasticity by regulating binding to CaMKII. *Neuron* 48, 289-301.
- Barten,D.M., and Albright,C.F. (2008). Therapeutic strategies for Alzheimer's disease. *Mol. Neurobiol.* 37, 171-186.
- Basarsky,T.A., Parpura,V., and Haydon,P.G. (1994). Hippocampal synaptogenesis in cell culture: developmental time course of synapse formation, calcium influx, and synaptic protein distribution. *J. Neurosci.* 14, 6402-6411.
- Bashir,Z.I., and Collingridge,G.L. (1992). Synaptic plasticity: long-term potentiation in the hippocampus. *Curr. Opin. Neurobiol.* 2, 328-335.
- Batchelor,A.M., and Garthwaite,J. (1997). Frequency detection and temporally dispersed synaptic signal association through a metabotropic glutamate receptor pathway. *Nature* 385, 74-77.
- Bateman,R.J., Siemers,E.R., Mawuenyega,K.G., Wen,G., Browning,K.R., Sigurdson,W.C., Yarasheski,K.E., Friedrich,S.W., Demattos,R.B., May,P.C., Paul,S.M., and Holtzman,D.M. (2009). A gamma-secretase inhibitor decreases amyloid-beta production in the central nervous system. *Ann. Neurol.* 66, 48-54.
- Baude,A., Nusser,Z., Roberts,J.D., Mulvihill,E., McIlhinney,R.A., and Somogyi,P. (1993). The metabotropic glutamate receptor (mGluR1 alpha) is concentrated at perisynaptic membrane of neuronal subpopulations as detected by immunogold reaction. *Neuron* 11, 771-787.
- Beel,A.J., and Sanders,C.R. (2008). Substrate specificity of gamma-secretase and other intramembrane proteases. *Cell Mol. Life Sci.* 65, 1311-1334.
- Behr,D., Elle,C., Underwood,J., Davis,J.B., Ward,R., Karran,E., Masters,C.L., Beyreuther,K., and Multhaup,G. (1999). Proteolytic fragments of Alzheimer's disease-associated presenilin 1 are present in synaptic organelles and growth cone membranes of rat brain. *J. Neurochem.* 72, 1564-1573.
- Bejar,R., Yasuda,R., Krugers,H., Hood,K., and Mayford,M. (2002). Transgenic calmodulin-dependent protein kinase II activation: dose-dependent effects on synaptic plasticity, learning, and memory. *J. Neurosci.* 22, 5719-5726.
- Bell,K.F., and Cuello,A.C. (2006). Altered synaptic function in Alzheimer's disease. *European Journal of Pharmacology* 545, 11-21.
- Bennett,B.D., Babu-Khan,S., Loeloff,R., Louis,J.C., Curran,E., Citron,M., and Vassar,R. (2000). Expression analysis of BACE2 in brain and peripheral tissues. *J. Biol. Chem.* 275, 20647-20651.
- Bentahir,M., Nyabi,O., Verhamme,J., Tolia,A., Horre,K., Wiltfang,J., Esselmann,H., and De Strooper,B. (2006). Presenilin clinical mutations can affect gamma-secretase activity by different mechanisms. *J. Neurochem.* 96, 732-742.

- Berezovska,O., Xia,M.Q., Page,K., Wasco,W., Tanzi,R.E., and Hyman,B.T. (1997). Developmental regulation of presenilin mRNA expression parallels notch expression. *J. Neuropathol. Exp. Neurol.* *56*, 40-44.
- Bergmans,B.A., and De Strooper,B. (2010). gamma-secretases: from cell biology to therapeutic strategies. *Lancet Neurol.* *9*, 215-226.
- Berridge,M., Lipp,P., and Bootman,M. (1999). Calcium signalling. *Curr. Biol.* *9*, R157-R159.
- Berridge,M.J., Bootman,M.D., and Roderick,H.L. (2003). Calcium signalling: dynamics, homeostasis and remodelling. *Nat. Rev. Mol. Cell Biol.* *4*, 517-529.
- Berridge,M.J., Lipp,P., and Bootman,M.D. (2000). The versatility and universality of calcium signalling. *Nat. Rev. Mol. Cell Biol.* *1*, 11-21.
- Bertram,L., and Tanzi,R.E. (2004). The current status of Alzheimer's disease genetics: what do we tell the patients? *Pharmacol. Res.* *50*, 385-396.
- Bezprozvanny,I., and Mattson,M.P. (2008). Neuronal calcium mishandling and the pathogenesis of Alzheimer's disease. *Trends Neurosci.* *31*, 454-463.
- Bie,B., and Pan,Z.Z. (2005). Increased glutamate synaptic transmission in the nucleus raphe magnus neurons from morphine-tolerant rats. *Mol. Pain* *1*, 7.
- Bitan,G., Kirkitadze,M.D., Lomakin,A., Vollers,S.S., Benedek,G.B., and Teplow,D.B. (2003). Amyloid beta -protein (Abeta) assembly: Abeta 40 and Abeta 42 oligomerize through distinct pathways. *Proc. Natl. Acad. Sci. U. S. A* *100*, 330-335.
- Bittner,T., Fuhrmann,M., Burgold,S., Jung,C.K., Volbracht,C., Steiner,H., Mitteregger,G., Kretschmar,H.A., Haass,C., and Herms,J. (2009). Gamma-secretase inhibition reduces spine density in vivo via an amyloid precursor protein-dependent pathway. *J. Neurosci.* *29*, 10405-10409.
- Blennow,K., de Leon,M.J., and Zetterberg,H. (2006). Alzheimer's disease. *Lancet* *368*, 387-403.
- Bliss,T.V., and Collingridge,G.L. (1993). A synaptic model of memory: long-term potentiation in the hippocampus. *Nature* *361*, 31-39.
- Bliss,T.V., Douglas,R.M., Errington,M.L., and Lynch,M.A. (1986). Correlation between long-term potentiation and release of endogenous amino acids from dentate gyrus of anaesthetized rats. *J. Physiol* *377*, 391-408.
- Bliss,T.V., and Lomo,T. (1973). Long-lasting potentiation of synaptic transmission in the dentate area of the anaesthetized rabbit following stimulation of the perforant path. *J. Physiol* *232*, 331-356.
- Bojarski,L., Herms,J., and Kuznicki,J. (2008). Calcium dysregulation in Alzheimer's disease. *Neurochem. Int.* *52*, 621-633.

- Borchelt,D.R., Thinakaran,G., Eckman,C.B., Lee,M.K., Davenport,F., Ratovitsky,T., Prada,C.M., Kim,G., Seekins,S., Yager,D., Slunt,H.H., Wang,R., Seeger,M., Levey,A.I., Gandy,S.E., Copeland,N.G., Jenkins,N.A., Price,D.L., Younkin,S.G., and Sisodia,S.S. (1996). Familial Alzheimer's disease-linked presenilin 1 variants elevate Abeta1-42/1-40 ratio in vitro and in vivo. *Neuron* 17, 1005-1013.
- Bouchard,R., Pattarini,R., and Geiger,J.D. (2003). Presence and functional significance of presynaptic ryanodine receptors. *Prog. Neurobiol.* 69, 391-418.
- Bouron,A. (1999). Adenosine suppresses protein kinase A- and C-induced enhancement of glutamate release in the hippocampus. *Eur. J. Neurosci.* 11, 4446-4450.
- Braak,H., and Braak,E. (1991a). Demonstration of amyloid deposits and neurofibrillary changes in whole brain sections. *Brain Pathol.* 1, 213-216.
- Braak,H., and Braak,E. (1991b). Neuropathological staging of Alzheimer-related changes. *Acta Neuropathol.* 82, 239-259.
- Braak,H., and Braak,E. (1997). Frequency of stages of Alzheimer-related lesions in different age categories. *Neurobiol. Aging* 18, 351-357.
- Branco,T., Marra,V., and Staras,K. (2009). Examining size-strength relationships at hippocampal synapses using an ultrastructural measurement of synaptic release probability. *J. Struct. Biol.*
- Branco,T., and Staras,K. (2009). The probability of neurotransmitter release: variability and feedback control at single synapses. *Nat. Rev. Neurosci.* 10, 373-383.
- Branco,T., Staras,K., Darcy,K.J., and Goda,Y. (2008). Local dendritic activity sets release probability at hippocampal synapses. *Neuron* 59, 475-485.
- Bray,S.J. (2006). Notch signalling: a simple pathway becomes complex. *Nat. Rev. Mol. Cell Biol.* 7, 678-689.
- Brenowitz,S.D., and Regehr,W.G. (2003). Calcium dependence of retrograde inhibition by endocannabinoids at synapses onto Purkinje cells. *J. Neurosci.* 23, 6373-6384.
- Brouwers,N., Sleegers,K., and Van Broeckhoven,C. (2008). Molecular genetics of Alzheimer's disease: an update. *Ann. Med.* 40, 562-583.
- Buee,L., Bussiere,T., Buee-Scherrer,V., Delacourte,A., and Hof,P.R. (2000). Tau protein isoforms, phosphorylation and role in neurodegenerative disorders. *Brain Res. Brain Res. Rev.* 33, 95-130.
- Burns,A., and Iliffe,S. (2009). Alzheimer's disease. *BMJ* 338, b158.
- Busche,M.A., Eichhoff,G., Adelsberger,H., Abramowski,D., Wiederhold,K.H., Haass,C., Staufenbiel,M., Konnerth,A., and Garaschuk,O. (2008). Clusters of hyperactive neurons near amyloid plaques in a mouse model of Alzheimer's disease. *Science* 321, 1686-1689.

- Buxbaum, J.D., Choi, E.K., Luo, Y., Lilliehook, C., Crowley, A.C., Merriam, D.E., and Wasco, W. (1998a). Calsenilin: a calcium-binding protein that interacts with the presenilins and regulates the levels of a presenilin fragment. *Nat. Med.* 4, 1177-1181.
- Buxbaum, J.D., Gandy, S.E., Cicchetti, P., Ehrlich, M.E., Czernik, A.J., Fracasso, R.P., Ramabhadran, T.V., Unterbeck, A.J., and Greengard, P. (1990). Processing of Alzheimer beta/A4 amyloid precursor protein: modulation by agents that regulate protein phosphorylation. *Proc. Natl. Acad. Sci. U. S. A* 87, 6003-6006.
- Buxbaum, J.D., Liu, K.N., Luo, Y., Slack, J.L., Stocking, K.L., Peschon, J.J., Johnson, R.S., Castner, B.J., Cerretti, D.P., and Black, R.A. (1998b). Evidence that tumor necrosis factor alpha converting enzyme is involved in regulated alpha-secretase cleavage of the Alzheimer amyloid protein precursor. *J. Biol. Chem.* 273, 27765-27767.
- Buxbaum, J.D., Thinakaran, G., Koliatsos, V., O'Callahan, J., Slunt, H.H., Price, D.L., and Sisodia, S.S. (1998c). Alzheimer amyloid protein precursor in the rat hippocampus: transport and processing through the perforant path. *J. Neurosci.* 18, 9629-9637.
- Cai, H., Wang, Y., McCarthy, D., Wen, H., Borchelt, D.R., Price, D.L., and Wong, P.C. (2001). BACE1 is the major beta-secretase for generation of Abeta peptides by neurons. *Nat. Neurosci.* 4, 233-234.
- Calabrese, B., Shaked, G.M., Tabarean, I.V., Braga, J., Koo, E.H., and Halpain, S. (2007). Rapid, concurrent alterations in pre- and postsynaptic structure induced by naturally-secreted amyloid-beta protein. *Mol. Cell Neurosci.* 35, 183-193.
- Campbell, W.A., Reed, M.L., Strahle, J., Wolfe, M.S., and Xia, W. (2003). Presenilin endoproteolysis mediated by an aspartyl protease activity pharmacologically distinct from gamma-secretase. *J. Neurochem.* 85, 1563-1574.
- Cao, X., and Sudhof, T.C. (2001). A transcriptionally [correction of transriptively] active complex of APP with Fe65 and histone acetyltransferase Tip60. *Science* 293, 115-120.
- Cao, X., and Sudhof, T.C. (2004). Dissection of amyloid-beta precursor protein-dependent transcriptional transactivation. *J. Biol. Chem.* 279, 24601-24611.
- Capell, A., Grunberg, J., Pesold, B., Diehlmann, A., Citron, M., Nixon, R., Beyreuther, K., Selkoe, D.J., and Haass, C. (1998). The proteolytic fragments of the Alzheimer's disease-associated presenilin-1 form heterodimers and occur as a 100-150-kDa molecular mass complex. *J. Biol. Chem.* 273, 3205-3211.
- Capell, A., Kaether, C., Edbauer, D., Shirotani, K., Merkl, S., Steiner, H., and Haass, C. (2003). Nicastrin interacts with gamma-secretase complex components via the N-terminal part of its transmembrane domain. *J. Biol. Chem.* 278, 52519-52523.
- Castro, C.A., Silbert, L.H., McNaughton, B.L., and Barnes, C.A. (1989). Recovery of spatial learning deficits after decay of electrically induced synaptic enhancement in the hippocampus. *Nature* 342, 545-548.

Caughey,B., and Lansbury,P.T. (2003). Protofibrils, pores, fibrils, and neurodegeneration: separating the responsible protein aggregates from the innocent bystanders. *Annu. Rev. Neurosci.* 26, 267-298.

Cedazo-Minguez,A., Popescu,B.O., Ankarcrona,M., Nishimura,T., and Cowburn,R.F. (2002). The presenilin 1 deltaE9 mutation gives enhanced basal phospholipase C activity and a resultant increase in intracellular calcium concentrations. *J. Biol. Chem.* 277, 36646-36655.

Chakroborty,S., Goussakov,I., Miller,M.B., and Stutzmann,G.E. (2009). Deviant ryanodine receptor-mediated calcium release resets synaptic homeostasis in presymptomatic 3xTg-AD mice. *J. Neurosci.* 29, 9458-9470.

Chan,S.L., Mayne,M., Holden,C.P., Geiger,J.D., and Mattson,M.P. (2000). Presenilin-1 mutations increase levels of ryanodine receptors and calcium release in PC12 cells and cortical neurons. *J. Biol. Chem.* 275, 18195-18200.

Chan,Y.M., and Jan,Y.N. (1999). Presenilins, processing of beta-amyloid precursor protein, and notch signaling. *Neuron* 23, 201-204.

Chavez-Gutierrez,L., Tolia,A., Maes,E., Li,T., Wong,P.C., and De,S.B. (2008). Glu(332) in the Nicastrin ectodomain is essential for gamma-secretase complex maturation but not for its activity. *J. Biol. Chem.* 283, 20096-20105.

Chen,F., Hasegawa,H., Schmitt-Ulms,G., Kawarai,T., Bohm,C., Katayama,T., Gu,Y., Sanjo,N., Glista,M., Rogaeva,E., Wakutani,Y., Pardossi-Piquard,R., Ruan,X., Tandon,A., Checler,F., Marambaud,P., Hansen,K., Westaway,D., George-Hyslop,P., and Fraser,P. (2006). TMP21 is a presenilin complex component that modulates gamma-secretase but not epsilon-secretase activity. *Nature* 440, 1208-1212.

Chen,F., Yang,D.S., Petanceska,S., Yang,A., Tandon,A., Yu,G., Rozmahel,R., Ghiso,J., Nishimura,M., Zhang,D.M., Kawarai,T., Levesque,G., Mills,J., Levesque,L., Song,Y.Q., Rogaeva,E., Westaway,D., Mount,H., Gandy,S., St George-Hyslop,P., and Fraser,P.E. (2000). Carboxyl-terminal fragments of Alzheimer beta-amyloid precursor protein accumulate in restricted and unpredicted intracellular compartments in presenilin 1-deficient cells. *J. Biol. Chem.* 275, 36794-36802.

Cheung,K.H., Mei,L., Mak,D.O., Hayashi,I., Iwatsubo,T., Kang,D.E., and Foskett,J.K. (2010). Gain-of-function enhancement of IP3 receptor modal gating by familial Alzheimer's disease-linked presenilin mutants in human cells and mouse neurons. *Sci. Signal.* 3, ra22.

Cheung,K.H., Shineman,D., Muller,M., Cardenas,C., Mei,L., Yang,J., Tomita,T., Iwatsubo,T., Lee,V.M., and Foskett,J.K. (2008). Mechanism of Ca²⁺ disruption in Alzheimer's disease by presenilin regulation of InsP3 receptor channel gating. *Neuron* 58, 871-883.

Chua,J.J., Kindler,S., Boyken,J., and Jahn,R. (2010). The architecture of an excitatory synapse. *J. Cell Sci.* 123, 819-823.

- Chyung,J.H., Raper,D.M., and Selkoe,D.J. (2005). Gamma-secretase exists on the plasma membrane as an intact complex that accepts substrates and effects intramembrane cleavage. *J. Biol Chem.* *280*, 4383-4392.
- Cingolani,L.A., Thalhammer,A., Yu,L.M., Catalano,M., Ramos,T., Colicos,M.A., and Goda,Y. (2008). Activity-dependent regulation of synaptic AMPA receptor composition and abundance by beta3 integrins. *Neuron* *58*, 749-762.
- Cirrito,J.R., Kang,J.E., Lee,J., Stewart,F.R., Verges,D.K., Silverio,L.M., Bu,G., Mennerick,S., and Holtzman,D.M. (2008). Endocytosis is required for synaptic activity-dependent release of amyloid-beta in vivo. *Neuron* *58*, 42-51.
- Cirrito,J.R., Yamada,K.A., Finn,M.B., Sloviter,R.S., Bales,K.R., May,P.C., Schoepp,D.D., Paul,S.M., Mennerick,S., and Holtzman,D.M. (2005). Synaptic activity regulates interstitial fluid amyloid-beta levels in vivo. *Neuron* *48*, 913-922.
- Citron,M., Oltersdorf,T., Haass,C., McConlogue,L., Hung,A.Y., Seubert,P., Vigo-Pelfrey,C., Lieberburg,I., and Selkoe,D.J. (1992). Mutation of the beta-amyloid precursor protein in familial Alzheimer's disease increases beta-protein production. *Nature* *360*, 672-674.
- Citron,M., Westaway,D., Xia,W., Carlson,G., Diehl,T., Levesque,G., Johnson-Wood,K., Lee,M., Seubert,P., Davis,A., Kholodenko,D., Motter,R., Sherrington,R., Perry,B., Yao,H., Strome,R., Lieberburg,I., Rommens,J., Kim,S., Schenk,D., Fraser,P., St George,H.P., and Selkoe,D.J. (1997). Mutant presenilins of Alzheimer's disease increase production of 42-residue amyloid beta-protein in both transfected cells and transgenic mice. *Nat. Med.* *3*, 67-72.
- Coco,S., Verderio,C., De,C.P., and Matteoli,M. (1998). Calcium dependence of synaptic vesicle recycling before and after synaptogenesis. *J. Neurochem.* *71*, 1987-1992.
- Collin,T., Marty,A., and Llano,I. (2005). Presynaptic calcium stores and synaptic transmission. *Curr. Opin. Neurobiol.* *15*, 275-281.
- Collingridge,G.L., Kehl,S.J., and McLennan,H. (1983). Excitatory amino acids in synaptic transmission in the Schaffer collateral-commissural pathway of the rat hippocampus. *J. Physiol* *334*, 33-46.
- Conlon,R.A., Reaume,A.G., and Rossant,J. (1995). Notch1 is required for the coordinate segmentation of somites. *Development* *121*, 1533-1545.
- Cook,D.G., Sung,J.C., Golde,T.E., Felsenstein,K.M., Wojczyk,B.S., Tanzi,R.E., Trojanowski,J.Q., Lee,V.M., and Doms,R.W. (1996). Expression and analysis of presenilin 1 in a human neuronal system: localization in cell bodies and dendrites. *Proc. Natl. Acad. Sci. U. S. A* *93*, 9223-9228.
- Corder,E.H., Saunders,A.M., Pericak-Vance,M.A., and Roses,A.D. (1995). There is a pathologic relationship between ApoE-epsilon 4 and Alzheimer's disease. *Arch. Neurol.* *52*, 650-651.

- Corder,E.H., Saunders,A.M., Risch,N.J., Strittmatter,W.J., Schmechel,D.E., Gaskell,P.C., Jr., Rimmler,J.B., Locke,P.A., Conneally,P.M., Schmechel,K.E., and . (1994). Protective effect of apolipoprotein E type 2 allele for late onset Alzheimer disease. *Nat. Genet.* 7, 180-184.
- Corder,E.H., Saunders,A.M., Strittmatter,W.J., Schmechel,D.E., Gaskell,P.C., Small,G.W., Roses,A.D., Haines,J.L., and Pericak-Vance,M.A. (1993). Gene dose of apolipoprotein E type 4 allele and the risk of Alzheimer's disease in late onset families. *Science* 261, 921-923.
- Cowan,W.M., Sudhof,T.C., and Stevens,C.F. (2001). *Synapses* (Baltimore: John Hopkins University Press).
- Crystal,A.S., Morais,V.A., Pierson,T.C., Pijak,D.S., Carlin,D., Lee,V.M., and Doms,R.W. (2003). Membrane topology of gamma-secretase component PEN-2. *J. Biol. Chem.* 278, 20117-20123.
- Cull-Candy,S., Brickley,S., and Farrant,M. (2001). NMDA receptor subunits: diversity, development and disease. *Curr. Opin. Neurobiol.* 11, 327-335.
- Cupers,P., Bentahir,M., Craessaerts,K., Orlans,I., Vanderstichele,H., Saftig,P., De,S.B., and Annaert,W. (2001). The discrepancy between presenilin subcellular localization and gamma-secretase processing of amyloid precursor protein. *J. Cell Biol.* 154, 731-740.
- Daigle,I., and Li,C. (1993). *apl-1*, a *Caenorhabditis elegans* gene encoding a protein related to the human beta-amyloid protein precursor. *Proc. Natl. Acad. Sci. U. S. A* 90, 12045-12049.
- Darcy,K.J., Staras,K., Collinson,L.M., and Goda,Y. (2006). Constitutive sharing of recycling synaptic vesicles between presynaptic boutons. *Nat. Neurosci.* 9, 315-321.
- Dash,P.K., Moore,A.N., and Orsi,S.A. (2005). Blockade of gamma-secretase activity within the hippocampus enhances long-term memory. *Biochem. Biophys. Res. Commun.* 338, 777-782.
- Dawson,G.R., Seabrook,G.R., Zheng,H., Smith,D.W., Graham,S., O'Dowd,G., Bowery,B.J., Boyce,S., Trumbauer,M.E., Chen,H.Y., van der Ploeg,L.H., and Sirinathsinghji,D.J. (1999). Age-related cognitive deficits, impaired long-term potentiation and reduction in synaptic marker density in mice lacking the beta-amyloid precursor protein. *Neuroscience* 90, 1-13.
- De Ferrari,G.V., and Inestrosa,N.C. (2000). Wnt signaling function in Alzheimer's disease. *Brain Res. Brain Res. Rev.* 33, 1-12.
- De Robertis,E.D., and Bennett,H.S. (1955). Some features of the submicroscopic morphology of synapses in frog and earthworm. *J. Biophys Biochem Cytol* 1, 47-58.
- De Simoni,A., Fernandes,F., and Edwards,F.A. (2004). Spines and dendrites cannot be assumed to distribute dye evenly. *Trends Neurosci.* 27, 15-16.

- De Simoni,A., Griesinger,C.B., and Edwards,F.A. (2003). Development of rat CA1 neurones in acute versus organotypic slices: role of experience in synaptic morphology and activity. *J. Physiol* 550, 135-147.
- De Simoni,A., and Yu,L.M. (2006). Preparation of organotypic hippocampal slice cultures: interface method. *Nat. Protoc.* 1, 1439-1445.
- De Strooper, B. (2007). Loss-of-function presenilin mutations in Alzheimer disease. Talking Point on the role of presenilin mutations in Alzheimer disease. *EMBO Rep.* 8, 141-146.
- De Strooper,B., and Annaert,W. (2000). Proteolytic processing and cell biological functions of the amyloid precursor protein. *J. Cell Sci.* 113 (Pt 11), 1857-1870.
- De Strooper,B., and Annaert,W. (2001). Presenilins and the intramembrane proteolysis of proteins: facts and fiction. *Nat Cell Biol* 3, E221-E225.
- De Strooper,B., Vassar,R., and Golde,T. (2010). The secretases: enzymes with therapeutic potential in Alzheimer disease. *Nat. Rev. Neurol.* 6, 99-107.
- De Strooper,B. (2003). Aph-1, Pen-2, and Nicastrin with Presenilin generate an active gamma-Secretase complex. *Neuron* 38, 9-12.
- De Strooper,B., Annaert,W., Cupers,P., Saftig,P., Craessaerts,K., Mumm,J.S., Schroeter,E.H., Schrijvers,V., Wolfe,M.S., Ray,W.J., Goate,A., and Kopan,R. (1999). A presenilin-1-dependent gamma-secretase-like protease mediates release of Notch intracellular domain. *Nature* 398, 518-522.
- De Strooper,B., Beullens,M., Contreras,B., Levesque,L., Craessaerts,K., Cordell,B., Moechars,D., Bollen,M., Fraser,P., George-Hyslop,P.S., and Van Leuven,F. (1997). Phosphorylation, subcellular localization, and membrane orientation of the Alzheimer's disease-associated presenilins. *J. Biol Chem.* 272, 3590-3598.
- De Strooper,B., Saftig,P., Craessaerts,K., Vanderstichele,H., Guhde,G., Annaert,W., Von Figura,K., and Van Leuven,F. (1998). Deficiency of presenilin-1 inhibits the normal cleavage of amyloid precursor protein. *Nature* 391, 387-390.
- Dekosky,S.T., and Scheff,S.W. (1990). Synapse loss in frontal cortex biopsies in Alzheimer's disease: correlation with cognitive severity. *Ann. Neurol.* 27, 457-464.
- Del Castillo,J., and Katz,B. (1954a). Action, and spontaneous release, of acetylcholine at an inexcitable nerve-muscle junction. *J. Physiol* 126, 27P.
- Del Castillo,J., and Katz,B. (1954b). Quantal components of the end-plate potential. *J. Physiol* 124, 560-573.
- Delaere,P., Duyckaerts,C., Masters,C., Beyreuther,K., Piette,F., and Hauw,J.J. (1990). Large amounts of neocortical beta A4 deposits without neuritic plaques nor tangles in a psychometrically assessed, non-demented person. *Neurosci. Lett.* 116, 87-93.

- Demuro,A., Mina,E., Kayed,R., Milton,S.C., Parker,I., and Glabe,C.G. (2005). Calcium dysregulation and membrane disruption as a ubiquitous neurotoxic mechanism of soluble amyloid oligomers. *J. Biol. Chem.* *280*, 17294-17300.
- Dewachter,I., Ris,L., Croes,S., Borghgraef,P., Devijver,H., Voets,T., Nilius,B., Godaux,E., and Van,L.F. (2008). Modulation of synaptic plasticity and Tau phosphorylation by wild-type and mutant presenilin1. *Neurobiol. Aging* *29*, 639-652.
- Dickson,T.C., and Vickers,J.C. (2001). The morphological phenotype of beta-amyloid plaques and associated neuritic changes in Alzheimer's disease. *Neuroscience* *105*, 99-107.
- Dobrunz,L.E. (2002). Release probability is regulated by the size of the readily releasable vesicle pool at excitatory synapses in hippocampus. *Int. J. Dev. Neurosci.* *20*, 225-236.
- Dobrunz,L.E., and Stevens,C.F. (1997). Heterogeneity of release probability, facilitation, and depletion at central synapses. *Neuron* *18*, 995-1008.
- Dodge,F.A., Jr., and Rahamimoff,R. (1967). Co-operative action a calcium ions in transmitter release at the neuromuscular junction. *J. Physiol* *193*, 419-432.
- Dominguez,D.I., Hartmann,D., and De,S.B. (2004). BACE1 and presenilin: two unusual aspartyl proteases involved in Alzheimer's disease. *Neurodegener. Dis.* *1*, 168-174.
- Donoviel,D.B., Hadjantonakis,A.K., Ikeda,M., Zheng,H., Hyslop,P.S., and Bernstein,A. (1999). Mice lacking both presenilin genes exhibit early embryonic patterning defects. *Genes & Development* *13*, 2801-2810.
- Dovey,H.F., John,V., Anderson,J.P., Chen,L.Z., de Saint,A.P., Fang,L.Y., Freedman,S.B., Folmer,B., Goldbach,E., Holsztynska,E.J., Hu,K.L., Johnson-Wood,K.L., Kennedy,S.L., Kholodenko,D., Knops,J.E., Latimer,L.H., Lee,M., Liao,Z., Lieberburg,I.M., Motter,R.N., Mutter,L.C., Nietz,J., Quinn,K.P., Sacchi,K.L., Seubert,P.A., Shopp,G.M., Thorsett,E.D., Tung,J.S., Wu,J., Yang,S., Yin,C.T., Schenk,D.B., May,P.C., Altstiel,L.D., Bender,M.H., Boggs,L.N., Britton,T.C., Clemens,J.C., Czilli,D.L., Dieckman-McGinty,D.K., Droste,J.J., Fuson,K.S., Gitter,B.D., Hyslop,P.A., Johnstone,E.M., Li,W.Y., Little,S.P., Mabry,T.E., Miller,F.D., and Audia,J.E. (2001). Functional gamma-secretase inhibitors reduce beta-amyloid peptide levels in brain. *J. Neurochem.* *76*, 173-181.
- Dries,D.R., and Yu,G. (2008). Assembly, maturation, and trafficking of the gamma-secretase complex in Alzheimer's disease. *Curr. Alzheimer Res.* *5*, 132-146.
- Duff,K., Eckman,C., Zehr,C., Yu,X., Prada,C.M., Perez-tur,J., Hutton,M., Buee,L., Harigaya,Y., Yager,D., Morgan,D., Gordon,M.N., Holcomb,L., Refolo,L., Zenk,B., Hardy,J., and Younkin,S. (1996). Increased amyloid-[beta]42(43) in brains of mice expressing mutant presenilin 1. *Nature* *383*, 710-713.
- Ebinu,J.O., and Yankner,B.A. (2002). A RIP tide in neuronal signal transduction. *Neuron* *34*, 499-502.

- Edbauer,D., Winkler,E., Haass,C., and Steiner,H. (2002). Presenilin and nicastrin regulate each other and determine amyloid beta-peptide production via complex formation. *Proc. Natl. Acad. Sci. U. S. A* *99*, 8666-8671.
- Edbauer,D., Winkler,E., Regula,J.T., Pesold,B., Steiner,H., and Haass,C. (2003). Reconstitution of gamma-secretase activity. *Nat Cell Biol* *5*, 486-488.
- Edwards,F.A., Konnerth,A., Sakmann,B., and Takahashi,T. (1989). A thin slice preparation for patch clamp recordings from neurones of the mammalian central nervous system. *Pflugers Arch.* *414*, 600-612.
- Efthimiopoulos,S., Floor,E., Georgakopoulos,A., Shioi,J., Cui,W., Yasothornsrikul,S., Hook,V.Y., Wisniewski,T., Buee,L., and Robakis,N.K. (1998). Enrichment of presenilin 1 peptides in neuronal large dense-core and somatodendritic clathrin-coated vesicles. *J. Neurochem.* *71*, 2365-2372.
- Eichenbaum,H. (2000). Hippocampus: mapping or memory? *Curr. Biol.* *10*, R785-R787.
- El-Husseini,A.E., Schnell,E., Chetkovich,D.M., Nicoll,R.A., and Brecht,D.S. (2000). PSD-95 involvement in maturation of excitatory synapses. *Science* *290*, 1364-1368.
- Emptage,N.J., Reid,C.A., and Fine,A. (2001). Calcium stores in hippocampal synaptic boutons mediate short-term plasticity, store-operated Ca²⁺ entry, and spontaneous transmitter release. *Neuron* *29*, 197-208.
- Endres,K., and Fahrenholz,F. (2010). Upregulation of the alpha-secretase ADAM10 -risk or reason for hope? *FEBS J.* *277*, 1585-1596.
- Engert,F., and Bonhoeffer,T. (1997). Synapse specificity of long-term potentiation breaks down at short distances. *Nature* *388*, 279-284.
- Engert,F., and Bonhoeffer,T. (1999). Dendritic spine changes associated with hippocampal long-term synaptic plasticity. *Nature* *399*, 66-70.
- Erdahl,W.L., Chapman,C.J., Taylor,R.W., and Pfeiffer,D.R. (1995). Effects of pH conditions on Ca²⁺ transport catalyzed by ionophores A23187, 4-BrA23187, and ionomycin suggest problems with common applications of these compounds in biological systems. *Biophys J.* *69*, 2350-2363.
- Eriksen,J.L., Sagi,S.A., Smith,T.E., Weggen,S., Das,P., McLendon,D.C., Ozols,V.V., Jessing,K.W., Zavitz,K.H., Koo,E.H., and Golde,T.E. (2003). NSAIDs and enantiomers of flurbiprofen target gamma-secretase and lower A β 42 in vivo. *J. Clin. Invest* *112*, 440-449.
- Esch,F.S., Keim,P.S., Beattie,E.C., Blacher,R.W., Culwell,A.R., Oltersdorf,T., McClure,D., and Ward,P.J. (1990). Cleavage of amyloid beta peptide during constitutive processing of its precursor. *Science* *248*, 1122-1124.
- Esler,W.P., Kimberly,W.T., Ostaszewski,B.L., Diehl,T.S., Moore,C.L., Tsai,J.Y., Rahmati,T., Xia,W., Selkoe,D.J., and Wolfe,M.S. (2000). Transition-state analogue inhibitors of gamma-secretase bind directly to presenilin-1. *Nat Cell Biol* *2*, 428-434.

Etcheberrigaray,R., Hirashima,N., Nee,L., Prince,J., Govoni,S., Racchi,M., Tanzi,R.E., and Alkon,D.L. (1998). Calcium responses in fibroblasts from asymptomatic members of Alzheimer's disease families. *Neurobiol. Dis.* 5, 37-45.

Evans,G.J., and Cousin,M.A. (2007). Simultaneous monitoring of three key neuronal functions in primary neuronal cultures. *J. Neurosci. Methods* 160, 197-205.

Fassler,M., Zocher,M., Klare,S., de la Fuente,A.G., Scheuermann,J., Capell,A., Haass,C., Valkova,C., Veerappan,A., Schneider,D., and Kaether,C. (2010). Masking of transmembrane-based retention signals controls ER export of gamma-secretase. *Traffic* 11, 250-258.

Fatt,P., and Katz,B. (1952). Spontaneous subthreshold activity at motor nerve endings. *J. Physiol* 117, 109-128.

Feng,R., Rampon,C., Tang,Y.P., Shrom,D., Jin,J., Kyin,M., Sopher,B., Miller,M.W., Ware,C.B., Martin,G.M., Kim,S.H., Langdon,R.B., Sisodia,S.S., and Tsien,J.Z. (2001). Deficient neurogenesis in forebrain-specific presenilin-1 knockout mice is associated with reduced clearance of hippocampal memory traces. *Neuron* 32, 911-926.

Flavell,S.W., Cowan,C.W., Kim,T.K., Greer,P.L., Lin,Y., Paradis,S., Griffith,E.C., Hu,L.S., Chen,C., and Greenberg,M.E. (2006). Activity-dependent regulation of MEF2 transcription factors suppresses excitatory synapse number. *Science* 311, 1008-1012.

Fortini,M.E. (2002). gamma-secretase mediated proteolysis in cell surface receptor signalling. *Nat Rev Mol Cell Biol* 3, 673-684.

Fortini,M.E. (2003). Neurobiology Double trouble for neurons. *Nature* 425, 565-566.

Fraering,P.C., LaVoie,M.J., Ye,W., Ostaszewski,B.L., Kimberly,W.T., Selkoe,D.J., and Wolfe,M.S. (2004a). Detergent-dependent dissociation of active gamma-secretase reveals an interaction between Pen-2 and PS1-NTF and offers a model for subunit organization within the complex. *Biochemistry* 43, 323-333.

Fraering,P.C., Ye,W., Strub,J.M., Dolios,G., LaVoie,M.J., Ostaszewski,B.L., van,D.A., Wang,R., Selkoe,D.J., and Wolfe,M.S. (2004b). Purification and characterization of the human gamma-secretase complex. *Biochemistry* 43, 9774-9789.

Francis,R., McGrath,G., Zhang,J., Ruddy,D.A., Sym,M., Apfeld,J., Nicoll,M., Maxwell,M., Hai,B., Ellis,M.C., Parks,A.L., Xu,W., Li,J., Gurney,M., Myers,R.L., Himes,C.S., Hiebsch,R., Ruble,C., Nye,J.S., and Curtis,D. (2002). aph-1 and pen-2 are required for Notch pathway signaling, gamma-secretase cleavage of betaAPP, and presenilin protein accumulation. *Dev. Cell* 3, 85-97.

Fraser,P.E., Yang,D.S., Yu,G., Levesque,L., Nishimura,M., Arawaka,S., Serpell,L.C., Rogaeva,E., and George-Hyslop,P. (2000). Presenilin structure, function and role in Alzheimer disease. *Biochim. Biophys. Acta* 1502, 1-15.

- Frerking, M., Borges, S., and Wilson, M. (1997). Are some minis multiquantal? *J. Neurophysiol.* *78*, 1293-1304.
- Friedmann, E., Lemberg, M.K., Weihofen, A., Dev, K.K., Dengler, U., Rovelli, G., and Martoglio, B. (2004). Consensus analysis of signal peptide peptidase and homologous human aspartic proteases reveals opposite topology of catalytic domains compared with presenilins. *J. Biol. Chem.* *279*, 50790-50798.
- Frykman, S., Hur, J.Y., Franberg, J., Aoki, M., Winblad, B., Nahalkova, J., Behbahani, H., and Tjernberg, L.O. (2010). Synaptic and endosomal localization of active gamma-secretase in rat brain. *PLoS. One.* *5*, e8948.
- Futai, K., Kim, M.J., Hashikawa, T., Scheiffele, P., Sheng, M., and Hayashi, Y. (2007). Retrograde modulation of presynaptic release probability through signaling mediated by PSD-95-neurologin. *Nat. Neurosci.* *10*, 186-195.
- Garcia, R.A., Vasudevan, K., and Buonanno, A. (2000). The neuregulin receptor ErbB-4 interacts with PDZ-containing proteins at neuronal synapses. *Proc. Natl. Acad. Sci. U. S. A* *97*, 3596-3601.
- Garcia-Alloza, M., Subramanian, M., Thyssen, D., Borrelli, L.A., Fauq, A., Das, P., Golde, T.E., Hyman, B.T., and Bacskai, B.J. (2009). Existing plaques and neuritic abnormalities in APP:PS1 mice are not affected by administration of the gamma-secretase inhibitor LY-411575. *Mol. Neurodegener.* *4*, 19.
- Garner, C.C., Zhai, R.G., Gundelfinger, E.D., and Ziv, N.E. (2002). Molecular mechanisms of CNS synaptogenesis. *Trends Neurosci.* *25*, 243-251.
- Georgakopoulos, A., Marambaud, P., Efthimiopoulos, S., Shioi, J., Cui, W., Li, H.C., Schutte, M., Gordon, R., Holstein, G.R., Martinelli, G., Mehta, P., Friedrich, V.L., Jr., and Robakis, N.K. (1999). Presenilin-1 forms complexes with the cadherin/catenin cell-cell adhesion system and is recruited to intercellular and synaptic contacts. *Mol Cell* *4*, 893-902.
- Georgopoulou, N., McLaughlin, M., McFarlane, I., and Breen, K.C. (2001). The role of post-translational modification in beta-amyloid precursor protein processing. *Biochem. Soc. Symp.* 23-36.
- Geppert, M., Goda, Y., Hammer, R.E., Li, C., Rosahl, T.W., Stevens, C.F., and Sudhof, T.C. (1994). Synaptotagmin I: a major Ca²⁺ sensor for transmitter release at a central synapse. *Cell* *79*, 717-727.
- Giacomello, M., Barbiero, L., Zatti, G., Squitti, R., Binetti, G., Pozzan, T., Fasolato, C., Ghidoni, R., and Pizzo, P. (2005). Reduction of Ca²⁺ stores and capacitative Ca²⁺ entry is associated with the familial Alzheimer's disease presenilin-2 T122R mutation and anticipates the onset of dementia. *Neurobiol. Dis.* *18*, 638-648.
- Giese, K.P., Fedorov, N.B., Filipkowski, R.K., and Silva, A.J. (1998). Autophosphorylation at Thr286 of the alpha calcium-calmodulin kinase II in LTP and learning. *Science* *279*, 870-873.

Glenner,G.G., and Wong,C.W. (1984a). Alzheimer's disease and Down's syndrome: sharing of a unique cerebrovascular amyloid fibril protein. *Biochem. Biophys. Res. Commun.* *122*, 1131-1135.

Glenner,G.G., and Wong,C.W. (1984b). Alzheimer's disease: initial report of the purification and characterization of a novel cerebrovascular amyloid protein. *Biochem. Biophys. Res. Commun.* *120*, 885-890.

Glenner,G.G., Wong,C.W., Quaranta,V., and Eanes,E.D. (1984). The amyloid deposits in Alzheimer's disease: their nature and pathogenesis. *Appl. Pathol.* *2*, 357-369.

Goate,A., Chartier-Harlin,M.C., Mullan,M., Brown,J., Crawford,F., Fidani,L., Giuffra,L., Haynes,A., Irving,N., James,L., and . (1991). Segregation of a missense mutation in the amyloid precursor protein gene with familial Alzheimer's disease. *Nature* *349*, 704-706.

Goda,Y. (2002). Cadherins communicate structural plasticity of presynaptic and postsynaptic terminals. *Neuron* *35*, 1-3.

Goda,Y., and Davis,G.W. (2003). Mechanisms of Synapse Assembly and Disassembly. *Neuron* *40*, 243-264.

Goedert,M., and Spillantini,M.G. (2006). A century of Alzheimer's disease. *Science* *314*, 777-781.

Gomez-Isla,T., Price,J.L., McKeel,D.W., Jr., Morris,J.C., Growdon,J.H., and Hyman,B.T. (1996). Profound loss of layer II entorhinal cortex neurons occurs in very mild Alzheimer's disease. *J. Neurosci.* *16*, 4491-4500.

Gotz,J., Chen,F., van,D.J., and Nitsch,R.M. (2001). Formation of neurofibrillary tangles in P3011 tau transgenic mice induced by Abeta 42 fibrils. *Science* *293*, 1491-1495.

Goutte,C., Tsunozaki,M., Hale,V.A., and Priess,J.R. (2002). APH-1 is a multipass membrane protein essential for the Notch signaling pathway in *Caenorhabditis elegans* embryos. *Proc. Natl. Acad. Sci. U. S. A* *99*, 775-779.

Green,K.N., Demuro,A., Akbari,Y., Hitt,B.D., Smith,I.F., Parker,I., and LaFerla,F.M. (2008). SERCA pump activity is physiologically regulated by presenilin and regulates amyloid beta production. *J. Cell Biol.* *181*, 1107-1116.

Green,K.N., and LaFerla,F.M. (2008). Linking calcium to Abeta and Alzheimer's disease. *Neuron* *59*, 190-194.

Grundke-Iqbal,I., Iqbal,K., Quinlan,M., Tung,Y.C., Zaidi,M.S., and Wisniewski,H.M. (1986a). Microtubule-associated protein tau. A component of Alzheimer paired helical filaments. *J. Biol. Chem.* *261*, 6084-6089.

Grundke-Iqbal,I., Iqbal,K., Tung,Y.C., Quinlan,M., Wisniewski,H.M., and Binder,L.I. (1986b). Abnormal phosphorylation of the microtubule-associated

protein tau (tau) in Alzheimer cytoskeletal pathology. *Proc. Natl. Acad. Sci. U. S. A* 83, 4913-4917.

Grynkiewicz,G., Poenie,M., and Tsien,R.Y. (1985). A new generation of Ca²⁺ indicators with greatly improved fluorescence properties. *J. Biol. Chem.* 260, 3440-3450.

Gu,Y., Misonou,H., Sato,T., Dohmae,N., Takio,K., and Ihara,Y. (2001). Distinct intramembrane cleavage of the beta-amyloid precursor protein family resembling gamma-secretase-like cleavage of Notch. *J. Biol Chem.* 276, 35235-35238.

Gu,Y., Sanjo,N., Chen,F., Hasegawa,H., Petit,A., Ruan,X., Li,W., Shier,C., Kawarai,T., Schmitt-Ulms,G., Westaway,D., George-Hyslop,P., and Fraser,P.E. (2004). The presenilin proteins are components of multiple membrane-bound complexes that have different biological activities. *J. Biol Chem.* 279, 31329-31336.

Guo,Q., Fu,W., Sopher,B.L., Miller,M.W., Ware,C.B., Martin,G.M., and Mattson,M.P. (1999). Increased vulnerability of hippocampal neurons to excitotoxic necrosis in presenilin-1 mutant knock-in mice. *Nat. Med.* 5, 101-106.

Guo,Q., Furukawa,K., Sopher,B.L., Pham,D.G., Xie,J., Robinson,N., Martin,G.M., and Mattson,M.P. (1996). Alzheimer's PS-1 mutation perturbs calcium homeostasis and sensitizes PC12 cells to death induced by amyloid beta-peptide. *Neuroreport* 8, 379-383.

Haass,C., and De Strooper,B. (1999). The presenilins in Alzheimer's disease--proteolysis holds the key. *Science* 286, 916-919.

Haass,C., Hung,A.Y., Selkoe,D.J., and Teplow,D.B. (1994). Mutations associated with a locus for familial Alzheimer's disease result in alternative processing of amyloid beta-protein precursor. *J. Biol. Chem.* 269, 17741-17748.

Haass,C., Schlossmacher,M.G., Hung,A.Y., Vigo-Pelfrey,C., Mellon,A., Ostaszewski,B.L., Lieberburg,I., Koo,E.H., Schenk,D., Teplow,D.B., and . (1992). Amyloid beta-peptide is produced by cultured cells during normal metabolism. *Nature* 359, 322-325.

Haass,C., and Selkoe,D.J. (2007). Soluble protein oligomers in neurodegeneration: lessons from the Alzheimer's amyloid beta-peptide. *Nat Rev Mol Cell Biol* 8, 101-112.

Haass,C., and Steiner,H. (2002). Alzheimer disease gamma-secretase: a complex story of GxGD-type presenilin proteases. *Trends Cell Biol.* 12, 556-562.

Hansson,E.M., Stromberg,K., Bergstedt,S., Yu,G., Naslund,J., Lundkvist,J., and Lendahl,U. (2005). Aph-1 interacts at the cell surface with proteins in the active gamma-secretase complex and membrane-tethered Notch. *J. Neurochem.* 92, 1010-1020.

Hardy,J. (1997). Amyloid, the presenilins and Alzheimer's disease. *Trends Neurosci* 20, 154-159.

Hardy,J., and Mullan,M. (1992). Alzheimer's disease. In search of the soluble. *Nature* 359, 268-269.

Hardy,J., and Selkoe,D.J. (2002). The amyloid hypothesis of Alzheimer's disease: progress and problems on the road to therapeutics. *Science* 297, 353-356.

Harris,K.M., Jensen,F.E., and Tsao,B. (1992). Three-dimensional structure of dendritic spines and synapses in rat hippocampus (CA1) at postnatal day 15 and adult ages: implications for the maturation of synaptic physiology and long-term potentiation. *J. Neurosci.* 12, 2685-2705.

Harris,K.M., and Stevens,J.K. (1989). Dendritic spines of CA 1 pyramidal cells in the rat hippocampus: serial electron microscopy with reference to their biophysical characteristics. *J. Neurosci.* 9, 2982-2997.

Harris,K.M., and Sultan,P. (1995). Variation in the number, location and size of synaptic vesicles provides an anatomical basis for the nonuniform probability of release at hippocampal CA1 synapses. *Neuropharmacology* 34, 1387-1395.

Hass,M.R., Sato,C., Kopan,R., and Zhao,G. (2009). Presenilin: RIP and beyond. *Semin. Cell Dev. Biol.* 20, 201-210.

Hebert,S.S., Serneels,L., Dejaegere,T., Horre,K., Dabrowski,M., Baert,V., Annaert,W., Hartmann,D., and De,S.B. (2004). Coordinated and widespread expression of gamma-secretase in vivo: evidence for size and molecular heterogeneity. *Neurobiol. Dis.* 17, 260-272.

Herms,J., Schneider,I., Dewachter,I., Caluwaerts,N., Kretschmar,H., and Van,L.F. (2003). Capacitive calcium entry is directly attenuated by mutant presenilin-1, independent of the expression of the amyloid precursor protein. *J. Biol. Chem.* 278, 2484-2489.

Herreman,A., Hartmann,D., Annaert,W., Saftig,P., Craessaerts,K., Serneels,L., Umans,L., Schrijvers,V., Checler,F., Vanderstichele,H., Baekelandt,V., Dressel,R., Cupers,P., Huylebroeck,D., Zwijsen,A., Van,L.F., and De,S.B. (1999). Presenilin 2 deficiency causes a mild pulmonary phenotype and no changes in amyloid precursor protein processing but enhances the embryonic lethal phenotype of presenilin 1 deficiency. *Proc. Natl. Acad. Sci. U. S. A* 96, 11872-11877.

Herreman,A., Serneels,L., Annaert,W., Collen,D., Schoonjans,L., and De,S.B. (2000). Total inactivation of gamma-secretase activity in presenilin-deficient embryonic stem cells. *Nat. Cell Biol.* 2, 461-462.

Hessler,N.A., Shirke,A.M., and Malinow,R. (1993). The probability of transmitter release at a mammalian central synapse. *Nature* 366, 569-572.

Hirashima,N., Etcheberrigaray,R., Bergamaschi,S., Racchi,M., Battaini,F., Binetti,G., Govoni,S., and Alkon,D.L. (1996). Calcium responses in human fibroblasts: a diagnostic molecular profile for Alzheimer's disease. *Neurobiol. Aging* 17, 549-555.

- Hoey,S.E., Williams,R.J., and Perkinson,M.S. (2009). Synaptic NMDA receptor activation stimulates alpha-secretase amyloid precursor protein processing and inhibits amyloid-beta production. *J. Neurosci.* *29*, 4442-4460.
- Hollmann,M., and Heinemann,S. (1994). Cloned glutamate receptors. *Annu. Rev. Neurosci.* *17*, 31-108.
- Hollmann,M., O'Shea-Greenfield,A., Rogers,S.W., and Heinemann,S. (1989). Cloning by functional expression of a member of the glutamate receptor family. *Nature* *342*, 643-648.
- Holtzman,D.M. (2001). Role of apoe/Abeta interactions in the pathogenesis of Alzheimer's disease and cerebral amyloid angiopathy. *J. Mol. Neurosci.* *17*, 147-155.
- Holtzman,D.M., Bales,K.R., Tenkova,T., Fagan,A.M., Parsadanian,M., Sartorius,L.J., Mackey,B., Olney,J., McKeel,D., Wozniak,D., and Paul,S.M. (2000a). Apolipoprotein E isoform-dependent amyloid deposition and neuritic degeneration in a mouse model of Alzheimer's disease. *Proc. Natl. Acad. Sci. U. S. A* *97*, 2892-2897.
- Holtzman,D.M., Fagan,A.M., Mackey,B., Tenkova,T., Sartorius,L., Paul,S.M., Bales,K., Ashe,K.H., Irizarry,M.C., and Hyman,B.T. (2000b). Apolipoprotein E facilitates neuritic and cerebrovascular plaque formation in an Alzheimer's disease model. *Ann. Neurol.* *47*, 739-747.
- Hsieh,H., Boehm,J., Sato,C., Iwatsubo,T., Tomita,T., Sisodia,S., and Malinow,R. (2006). AMPAR removal underlies Abeta-induced synaptic depression and dendritic spine loss. *Neuron* *52*, 831-843.
- Hu,L., Wong,T.P., Cote,S.L., Bell,K.F., and Cuello,A.C. (2003). The impact of Abeta-plaques on cortical cholinergic and non-cholinergic presynaptic boutons in alzheimer's disease-like transgenic mice. *Neuroscience* *121*, 421-432.
- Huang,E.P., and Stevens,C.F. (1997). Estimating the distribution of synaptic reliabilities. *J. Neurophysiol.* *78*, 2870-2880.
- Hussain,I., Powell,D., Howlett,D.R., Tew,D.G., Meek,T.D., Chapman,C., Gloger,I.S., Murphy,K.E., Southan,C.D., Ryan,D.M., Smith,T.S., Simmons,D.L., Walsh,F.S., Dingwall,C., and Christie,G. (1999). Identification of a novel aspartic protease (Asp 2) as beta-secretase. *Mol Cell Neurosci* *14*, 419-427.
- Imbimbo,B.P., Hutter-Paier,B., Villetti,G., Facchinetti,F., Cenacchi,V., Volta,R., Lanzillotta,A., Pizzi,M., and Windisch,M. (2009). CHF5074, a novel gamma-secretase modulator, attenuates brain beta-amyloid pathology and learning deficit in a mouse model of Alzheimer's disease. *Br. J. Pharmacol.* *156*, 982-993.
- Inoue,E., Deguchi-Tawarada,M., Togawa,A., Matsui,C., Arita,K., Katahira-Tayama,S., Sato,T., Yamauchi,E., Oda,Y., and Takai,Y. (2009). Synaptic activity prompts gamma-secretase-mediated cleavage of EphA4 and dendritic spine formation. *J. Cell Biol.* *185*, 551-564.
- Ito,E., Oka,K., Etcheberrigaray,R., Nelson,T.J., McPhie,D.L., Tofel-Grehl,B., Gibson,G.E., and Alkon,D.L. (1994). Internal Ca²⁺ mobilization is altered in

fibroblasts from patients with Alzheimer disease. *Proc. Natl. Acad. Sci. U. S. A* *91*, 534-538.

Iwatsubo,T., Odaka,A., Suzuki,N., Mizusawa,H., Nukina,N., and Ihara,Y. (1994). Visualization of A beta 42(43) and A beta 40 in senile plaques with end-specific A beta monoclonals: evidence that an initially deposited species is A beta 42(43). *Neuron* *13*, 45-53.

Jarrett,J.T., Berger,E.P., and Lansbury,P.T., Jr. (1993). The carboxy terminus of the beta amyloid protein is critical for the seeding of amyloid formation: implications for the pathogenesis of Alzheimer's disease. *Biochemistry* *32*, 4693-4697.

Jarriault,S., and Greenwald,I. (2002). Suppressors of the egg-laying defective phenotype of sel-12 presenilin mutants implicate the CoREST corepressor complex in LIN-12/Notch signaling in *C. elegans*. *Genes Dev.* *16*, 2713-2728.

Jiang,Q., Lee,C.Y., Mandrekar,S., Wilkinson,B., Cramer,P., Zelcer,N., Mann,K., Lamb,B., Willson,T.M., Collins,J.L., Richardson,J.C., Smith,J.D., Comery,T.A., Riddell,D., Holtzman,D.M., Tontonoz,P., and Landreth,G.E. (2008). ApoE promotes the proteolytic degradation of A beta. *Neuron* *58*, 681-693.

Jones,M.W., Errington,M.L., French,P.J., Fine,A., Bliss,T.V., Garel,S., Charnay,P., Bozon,B., Laroche,S., and Davis,S. (2001a). A requirement for the immediate early gene *Zif268* in the expression of late LTP and long-term memories. *Nat. Neurosci.* *4*, 289-296.

Jones,M.W., Peckham,H.M., Errington,M.L., Bliss,T.V., and Routtenberg,A. (2001b). Synaptic plasticity in the hippocampus of awake C57BL/6 and DBA/2 mice: interstrain differences and parallels with behavior. *Hippocampus* *11*, 391-396.

Kaether,C., Capell,A., Edbauer,D., Winkler,E., Novak,B., Steiner,H., and Haass,C. (2004). The presenilin C-terminus is required for ER-retention, nicastrin-binding and gamma-secretase activity. *EMBO J.* *23*, 4738-4748.

Kaether,C., Haass,C., and Steiner,H. (2006a). Assembly, trafficking and function of gamma-secretase. *Neurodegener. Dis.* *3*, 275-283.

Kaether,C., Lammich,S., Edbauer,D., Ertl,M., Rietdorf,J., Capell,A., Steiner,H., and Haass,C. (2002). Presenilin-1 affects trafficking and processing of betaAPP and is targeted in a complex with nicastrin to the plasma membrane. *J. Cell Biol* *158*, 551-561.

Kaether,C., Scheuermann,J., Fassler,M., Zilow,S., Shirotani,K., Valkova,C., Novak,B., Kacmar,S., Steiner,H., and Haass,C. (2007). Endoplasmic reticulum retention of the gamma-secretase complex component Pen2 by Rer1. *EMBO Rep.* *8*, 743-748.

Kaether,C., Schmitt,S., Willem,M., and Haass,C. (2006b). Amyloid precursor protein and Notch intracellular domains are generated after transport of their precursors to the cell surface. *Traffic.* *7*, 408-415.

- Kamal,A., Almenar-Queralt,A., LeBlanc,J.F., Roberts,E.A., and Goldstein,L.S. (2001). Kinesin-mediated axonal transport of a membrane compartment containing beta-secretase and presenilin-1 requires APP. *Nature* 414, 643-648.
- Kamal,A., Stokin,G.B., Yang,Z., Xia,C.H., and Goldstein,L.S. (2000). Axonal transport of amyloid precursor protein is mediated by direct binding to the kinesin light chain subunit of kinesin-I. *Neuron* 28, 449-459.
- Kamenetz,F., Tomita,T., Hsieh,H., Seabrook,G., Borchelt,D., Iwatsubo,T., Sisodia,S., and Malinow,R. (2003). APP processing and synaptic function. *Neuron* 37, 925-937.
- Kang,D.E., Soriano,S., Frosch,M.P., Collins,T., Naruse,S., Sisodia,S.S., Leibowitz,G., Levine,F., and Koo,E.H. (1999). Presenilin 1 facilitates the constitutive turnover of beta-catenin: differential activity of Alzheimer's disease-linked PS1 mutants in the beta-catenin-signaling pathway. *J. Neurosci* 19, 4229-4237.
- Kang,J., Lemaire,H.G., Unterbeck,A., Salbaum,J.M., Masters,C.L., Grzeschik,K.H., Multhaup,G., Beyreuther,K., and Muller-Hill,B. (1987). The precursor of Alzheimer's disease amyloid A4 protein resembles a cell-surface receptor. *Nature* 325, 733-736.
- Katz,B., and Miledi,R. (1968). The role of calcium in neuromuscular facilitation. *J. Physiol* 195, 481-492.
- Katz,Y., Menon,V., Nicholson,D.A., Geinisman,Y., Kath,W.L., and Spruston,N. (2009). Synapse distribution suggests a two-stage model of dendritic integration in CA1 pyramidal neurons. *Neuron* 63, 171-177.
- Kazee,A.M., and Johnson,E.M. (1998). Alzheimer's Disease Pathology in Non-Demented Elderly. *J. Alzheimers. Dis.* 1, 81-89.
- Kerchner,G.A., and Nicoll,R.A. (2008). Silent synapses and the emergence of a postsynaptic mechanism for LTP. *Nat. Rev. Neurosci.* 9, 813-825.
- Khachaturian,Z.S. (1989). The role of calcium regulation in brain aging: reexamination of a hypothesis. *Aging (Milano.)* 1, 17-34.
- Kidd,M. (1963). Paired helical filaments in electron microscopy of Alzheimer's disease. *Nature* 197, 192-193.
- Kim,D.Y., Ingano,L.A., Carey,B.W., Pettingell,W.H., and Kovacs,D.M. (2005). Presenilin/gamma-secretase-mediated cleavage of the voltage-gated sodium channel beta2-subunit regulates cell adhesion and migration. *J. Biol. Chem.* 280, 23251-23261.
- Kim,J., Basak,J.M., and Holtzman,D.M. (2009a). The role of apolipoprotein E in Alzheimer's disease. *Neuron* 63, 287-303.
- Kim,J., Castellano,J.M., Jiang,H., Basak,J.M., Parsadanian,M., Pham,V., Mason,S.M., Paul,S.M., and Holtzman,D.M. (2009b). Overexpression of low-density

lipoprotein receptor in the brain markedly inhibits amyloid deposition and increases extracellular A beta clearance. *Neuron* 64, 632-644.

Kim,S.H., Lah,J.J., Thinakaran,G., Levey,A., and Sisodia,S.S. (2000). Subcellular localization of presenilins: association with a unique membrane pool in cultured cells. *Neurobiol. Dis.* 7, 99-117.

Kim,S.H., and Sisodia,S.S. (2005). Evidence that the "NF" motif in transmembrane domain 4 of presenilin 1 is critical for binding with PEN-2. *J. Biol. Chem.* 280, 41953-41966.

Kim,T.W., Pettingell,W.H., Hallmark,O.G., Moir,R.D., Wasco,W., and Tanzi,R.E. (1997). Endoproteolytic cleavage and proteasomal degradation of presenilin 2 in transfected cells. *J. Biol. Chem.* 272, 11006-11010.

Kimberly,W.T., LaVoie,M.J., Ostaszewski,B.L., Ye,W., Wolfe,M.S., and Selkoe,D.J. (2003). Gamma-secretase is a membrane protein complex comprised of presenilin, nicastrin, Aph-1, and Pen-2. *Proc. Natl. Acad. Sci. U. S. A* 100, 6382-6387.

Kimberly,W.T., Xia,W., Rahmati,T., Wolfe,M.S., and Selkoe,D.J. (2000). The transmembrane aspartates in presenilin 1 and 2 are obligatory for gamma-secretase activity and amyloid beta-protein generation. *J. Biol. Chem.* 275, 3173-3178.

Kirschenbaum,F., Hsu,S.C., Cordell,B., and McCarthy,J.V. (2001). Substitution of a glycogen synthase kinase-3beta phosphorylation site in presenilin 1 separates presenilin function from beta-catenin signaling. *J. Biol. Chem.* 276, 7366-7375.

Klunk,W.E., Engler,H., Nordberg,A., Wang,Y., Blomqvist,G., Holt,D.P., Bergstrom,M., Savitcheva,I., Huang,G.F., Estrada,S., Ausen,B., Debnath,M.L., Barletta,J., Price,J.C., Sandell,J., Lopresti,B.J., Wall,A., Koivisto,P., Antoni,G., Mathis,C.A., and Langstrom,B. (2004). Imaging brain amyloid in Alzheimer's disease with Pittsburgh Compound-B. *Ann. Neurol.* 55, 306-319.

Knowles,R.B., Wyart,C., Buldyrev,S.V., Cruz,L., Urbanc,B., Hasselmo,M.E., Stanley,H.E., and Hyman,B.T. (1999). Plaque-induced neurite abnormalities: implications for disruption of neural networks in Alzheimer's disease. *Proc. Natl. Acad. Sci. U. S. A* 96, 5274-5279.

Koch,R.A., and Barish,M.E. (1994). Perturbation of intracellular calcium and hydrogen ion regulation in cultured mouse hippocampal neurons by reduction of the sodium ion concentration gradient. *J. Neurosci.* 14, 2585-2593.

Koffie,R.M., Meyer-Luehmann,M., Hashimoto,T., Adams,K.W., Mielke,M.L., Garcia-Alloza,M., Micheva,K.D., Smith,S.J., Kim,M.L., Lee,V.M., Hyman,B.T., and Spires-Jones,T.L. (2009). Oligomeric amyloid beta associates with postsynaptic densities and correlates with excitatory synapse loss near senile plaques. *Proc. Natl. Acad. Sci. U. S. A* 106, 4012-4017.

Kojro,E., and Fahrenholz,F. (2005). The non-amyloidogenic pathway: structure and function of alpha-secretases. *Subcell. Biochem.* 38, 105-127.

- Koo,E.H., and Kopan,R. (2004). Potential role of presenilin-regulated signaling pathways in sporadic neurodegeneration. *Nat Med.* *10 Suppl*, S26-S33.
- Koo,E.H., Sisodia,S.S., Archer,D.R., Martin,L.J., Weidemann,A., Beyreuther,K., Fischer,P., Masters,C.L., and Price,D.L. (1990). Precursor of amyloid protein in Alzheimer disease undergoes fast anterograde axonal transport. *Proc. Natl. Acad. Sci. U. S. A* *87*, 1561-1565.
- Koo,E.H., and Squazzo,S.L. (1994). Evidence that production and release of amyloid beta-protein involves the endocytic pathway. *J. Biol. Chem.* *269*, 17386-17389.
- Koo,E.H., Squazzo,S.L., Selkoe,D.J., and Koo,C.H. (1996). Trafficking of cell-surface amyloid beta-protein precursor. I. Secretion, endocytosis and recycling as detected by labeled monoclonal antibody. *J. Cell Sci.* *109 (Pt 5)*, 991-998.
- Kopan,R., and Ilagan,M.X. (2004). Gamma-secretase: proteasome of the membrane? *Nat Rev Mol Cell Biol* *5*, 499-504.
- Kornilova,A.Y., Bihel,F., Das,C., and Wolfe,M.S. (2005). The initial substrate-binding site of gamma-secretase is located on presenilin near the active site. *Proc. Natl. Acad. Sci. U. S. A* *102*, 3230-3235.
- Kovacs,D.M., Fausett,H.J., Page,K.J., Kim,T.W., Moir,R.D., Merriam,D.E., Hollister,R.D., Hallmark,O.G., Mancini,R., Felsenstein,K.M., Hyman,B.T., Tanzi,R.E., and Wasco,W. (1996). Alzheimer-associated presenilins 1 and 2: neuronal expression in brain and localization to intracellular membranes in mammalian cells. *Nat Med.* *2*, 224-229.
- Krueger,S., and Fitzsimonds,R.M. (2006). Remodeling the plasticity debate: the presynaptic locus revisited. *Physiology. (Bethesda.)* *21*, 346-351.
- Krueger,S.R., Kolar,A., and Fitzsimonds,R.M. (2003). The presynaptic release apparatus is functional in the absence of dendritic contact and highly mobile within isolated axons. *Neuron* *40*, 945-957.
- Kuchibhotla,K.V., Goldman,S.T., Lattarulo,C.R., Wu,H.Y., Hyman,B.T., and Bacsikai,B.J. (2008). Abeta plaques lead to aberrant regulation of calcium homeostasis in vivo resulting in structural and functional disruption of neuronal networks. *Neuron* *59*, 214-225.
- Kullmann,D.M., and Asztely,F. (1998). Extrasynaptic glutamate spillover in the hippocampus: evidence and implications. *Trends Neurosci.* *21*, 8-14.
- Kumar-Singh,S., Theuns,J., Van,B.B., Pirici,D., Vennekens,K., Corsmit,E., Cruts,M., Dermaut,B., Wang,R., and Van,B.C. (2006). Mean age-of-onset of familial alzheimer disease caused by presenilin mutations correlates with both increased Abeta42 and decreased Abeta40. *Hum. Mutat.* *27*, 686-695.
- LaFerla,F.M. (2002). Calcium dyshomeostasis and intracellular signalling in Alzheimer's disease. *Nat. Rev. Neurosci.* *3*, 862-872.

- LaFerla, F.M., and Oddo, S. (2005). Alzheimer's disease: Abeta, tau and synaptic dysfunction. *Trends Mol. Med.* *11*, 170-176.
- Lah, J.J., Heilman, C.J., Nash, N.R., Rees, H.D., Yi, H., Counts, S.E., and Levey, A.I. (1997). Light and electron microscopic localization of presenilin-1 in primate brain. *J. Neurosci.* *17*, 1971-1980.
- Lah, J.J., and Levey, A.I. (2000). Endogenous presenilin-1 targets to endocytic rather than biosynthetic compartments. *Mol. Cell Neurosci.* *16*, 111-126.
- Lai, M.T., Chen, E., Crouthamel, M.C., DiMuzio-Mower, J., Xu, M., Huang, Q., Price, E., Register, R.B., Shi, X.P., Donoviel, D.B., Bernstein, A., Hazuda, D., Gardell, S.J., and Li, Y.M. (2003). Presenilin-1 and presenilin-2 exhibit distinct yet overlapping gamma-secretase activities. *J. Biol. Chem.* *278*, 22475-22481.
- Laird, F.M., Cai, H., Savonenko, A.V., Farah, M.H., He, K., Melnikova, T., Wen, H., Chiang, H.C., Xu, G., Koliatsos, V.E., Borchelt, D.R., Price, D.L., Lee, H.K., and Wong, P.C. (2005). BACE1, a major determinant of selective vulnerability of the brain to amyloid-beta amyloidogenesis, is essential for cognitive, emotional, and synaptic functions. *J. Neurosci.* *25*, 11693-11709.
- Lammich, S., Kojro, E., Postina, R., Gilbert, S., Pfeiffer, R., Jasionowski, M., Haass, C., and Fahrenholz, F. (1999). Constitutive and regulated alpha-secretase cleavage of Alzheimer's amyloid precursor protein by a disintegrin metalloprotease. *Proc. Natl. Acad. Sci. U. S. A* *96*, 3922-3927.
- Lancaster, B., and Batchelor, A.M. (2000). Novel action of BAPTA series chelators on intrinsic K⁺ currents in rat hippocampal neurones. *J. Physiol* *522 Pt 2*, 231-246.
- Lantos, P.L., Luthert, P.J., Hanger, D., Anderton, B.H., Mullan, M., and Rossor, M. (1992). Familial Alzheimer's disease with the amyloid precursor protein position 717 mutation and sporadic Alzheimer's disease have the same cytoskeletal pathology. *Neurosci. Lett.* *137*, 221-224.
- Laudon, H., Hansson, E.M., Melen, K., Bergman, A., Farmery, M.R., Winblad, B., Lendahl, U., von, H.G., and Naslund, J. (2005). A nine-transmembrane domain topology for presenilin 1. *J. Biol. Chem.* *280*, 35352-35360.
- LaVoie, M.J., Fraering, P.C., Ostaszewski, B.L., Ye, W., Kimberly, W.T., Wolfe, M.S., and Selkoe, D.J. (2003). Assembly of the gamma-secretase complex involves early formation of an intermediate subcomplex of Aph-1 and nicastrin. *J. Biol. Chem.* *278*, 37213-37222.
- Lazarov, O., Morfini, G.A., Lee, E.B., Farah, M.H., Szodorai, A., DeBoer, S.R., Koliatsos, V.E., Kins, S., Lee, V.M., Wong, P.C., Price, D.L., Brady, S.T., and Sisodia, S.S. (2005). Axonal transport, amyloid precursor protein, kinesin-1, and the processing apparatus: revisited. *J. Neurosci* *25*, 2386-2395.
- Lazarov, V.K., Fraering, P.C., Ye, W., Wolfe, M.S., Selkoe, D.J., and Li, H. (2006). Electron microscopic structure of purified, active gamma-secretase reveals an aqueous intramembrane chamber and two pores. *Proc. Natl. Acad. Sci. U. S. A* *103*, 6889-6894.

- Lee, M.K., Slunt, H.H., Martin, L.J., Thinakaran, G., Kim, G., Gandy, S.E., Seeger, M., Koo, E., Price, D.L., and Sisodia, S.S. (1996). Expression of presenilin 1 and 2 (PS1 and PS2) in human and murine tissues. *J. Neurosci* 16, 7513-7525.
- Lee, M.S., Kao, S.C., Lemere, C.A., Xia, W., Tseng, H.C., Zhou, Y., Neve, R., Ahljianian, M.K., and Tsai, L.H. (2003). APP processing is regulated by cytoplasmic phosphorylation. *J. Cell Biol.* 163, 83-95.
- Lee, S.F., Shah, S., Li, H., Yu, C., Han, W., and Yu, G. (2002). Mammalian APH-1 interacts with presenilin and nicastrin and is required for intramembrane proteolysis of amyloid-beta precursor protein and Notch. *J. Biol. Chem.* 277, 45013-45019.
- Lee, S.M., Lee, J.W., Song, Y.S., Hwang, D.Y., Kim, Y.K., Nam, S.Y., Kim, D.J., Yun, Y.W., Yoon, D.Y., and Hong, J.T. (2005). Ryanodine receptor-mediated interference of neuronal cell differentiation by presenilin 2 mutation. *J. Neurosci. Res.* 82, 542-550.
- Lee, V.M., Goedert, M., and Trojanowski, J.Q. (2001). Neurodegenerative tauopathies. *Annu. Rev. Neurosci.* 24, 1121-1159.
- Leissring, M.A., Murphy, M.P., Mead, T.R., Akbari, Y., Sugarman, M.C., Jannatipour, M., Anliker, B., Muller, U., Saftig, P., De Strooper, B., Wolfe, M.S., Golde, T.E., and LaFerla, F.M. (2002). A physiologic signaling role for the gamma-secretase-derived intracellular fragment of APP. *Proc. Natl. Acad. Sci. U. S. A* 99, 4697-4702.
- Leissring, M.A., Yamasaki, T.R., Wasco, W., Buxbaum, J.D., Parker, I., and LaFerla, F.M. (2000). Calsenilin reverses presenilin-mediated enhancement of calcium signaling. *Proc. Natl. Acad. Sci. U. S. A* 97, 8590-8593.
- Levesque, G., Yu, G., Nishimura, M., Zhang, D.M., Levesque, L., Yu, H., Xu, D., Liang, Y., Rogaeva, E., Ikeda, M., Duthie, M., Murgolo, N., Wang, L., VanderVere, P., Bayne, M.L., Strader, C.D., Rommens, J.M., Fraser, P.E., and St George-Hyslop, P. (1999). Presenilins interact with armadillo proteins including neural-specific plakophilin-related protein and beta-catenin. *J. Neurochem.* 72, 999-1008.
- Levinson, J.N., Chery, N., Huang, K., Wong, T.P., Gerrow, K., Kang, R., Prange, O., Wang, Y.T., and El-Husseini, A. (2005). Neuroligins mediate excitatory and inhibitory synapse formation: involvement of PSD-95 and neurexin-1beta in neuroligin-induced synaptic specificity. *J. Biol. Chem.* 280, 17312-17319.
- Levitan, D., Lee, J., Song, L., Manning, R., Wong, G., Parker, E., and Zhang, L. (2001). PS1 N- and C-terminal fragments form a complex that functions in APP processing and Notch signalling. *Proc. Natl. Acad. Sci. U. S. A* 98, 12186-12190.
- Levy-Lahad, E., Wijsman, E.M., Nemens, E., Anderson, L., Goddard, K.A., Weber, J.L., Bird, T.D., and Schellenberg, G.D. (1995). A familial Alzheimer's disease locus on chromosome 1. *Science* 269, 970-973.
- Li, H., Wolfe, M.S., and Selkoe, D.J. (2009). Toward structural elucidation of the gamma-secretase complex. *Structure.* 17, 326-334.

- Li, Y.M., Xu, M., Lai, M.T., Huang, Q., Castro, J.L., DiMuzio-Mower, J., Harrison, T., Lellis, C., Nadin, A., Neduvilil, J.G., Register, R.B., Sardana, M.K., Shearman, M.S., Smith, A.L., Shi, X.P., Yin, K.C., Shafer, J.A., and Gardell, S.J. (2000). Photoactivated gamma-secretase inhibitors directed to the active site covalently label presenilin 1. *Nature* *405*, 689-694.
- Lim, G.P., Yang, F., Chu, T., Chen, P., Beech, W., Teter, B., Tran, T., Ubeda, O., Ashe, K.H., Frautschy, S.A., and Cole, G.M. (2000). Ibuprofen suppresses plaque pathology and inflammation in a mouse model for Alzheimer's disease. *J. Neurosci.* *20*, 5709-5714.
- Lin, X., Koelsch, G., Wu, S., Downs, D., Dashti, A., and Tang, J. (2000). Human aspartic protease memapsin 2 cleaves the beta-secretase site of beta-amyloid precursor protein. *Proc. Natl. Acad. Sci. U. S. A* *97*, 1456-1460.
- Lisman, J.E., Raghavachari, S., and Tsien, R.W. (2007). The sequence of events that underlie quantal transmission at central glutamatergic synapses. *Nat. Rev. Neurosci.* *8*, 597-609.
- Llano, I., Gonzalez, J., Caputo, C., Lai, F.A., Blayney, L.M., Tan, Y.P., and Marty, A. (2000). Presynaptic calcium stores underlie large-amplitude miniature IPSCs and spontaneous calcium transients. *Nat. Neurosci.* *3*, 1256-1265.
- Lleo, A., Berezovska, O., Herl, L., Raju, S., Deng, A., Bacsikai, B.J., Frosch, M.P., Irizarry, M., and Hyman, B.T. (2004). Nonsteroidal anti-inflammatory drugs lower Abeta42 and change presenilin 1 conformation. *Nat. Med.* *10*, 1065-1066.
- Louvi, A., and Artavanis-Tsakonas, S. (2006). Notch signalling in vertebrate neural development. *Nat. Rev. Neurosci.* *7*, 93-102.
- Lu, B., Czernik, A.J., Popov, S., Wang, T., Poo, M.M., and Greengard, P. (1996). Expression of synapsin I correlates with maturation of the neuromuscular synapse. *Neuroscience* *74*, 1087-1097.
- Lu, B., Greengard, P., and Poo, M.M. (1992). Exogenous synapsin I promotes functional maturation of developing neuromuscular synapses. *Neuron* *8*, 521-529.
- Lucic, V., Yang, T., Schweikert, G., Forster, F., and Baumeister, W. (2005). Morphological characterization of molecular complexes present in the synaptic cleft. *Structure.* *13*, 423-434.
- Luo, W.J., Wang, H., Li, H., Kim, B.S., Shah, S., Lee, H.J., Thinakaran, G., Kim, T.W., Yu, G., and Xu, H. (2003). PEN-2 and APH-1 coordinately regulate proteolytic processing of presenilin 1. *J. Biol Chem.* *278*, 7850-7854.
- Luo, Y., Bolon, B., Kahn, S., Bennett, B.D., Babu-Khan, S., Denis, P., Fan, W., Kha, H., Zhang, J., Gong, Y., Martin, L., Louis, J.C., Yan, Q., Richards, W.G., Citron, M., and Vassar, R. (2001). Mice deficient in BACE1, the Alzheimer's beta-secretase, have normal phenotype and abolished beta-amyloid generation. *Nat. Neurosci.* *4*, 231-232.
- Lynch, M.A. (2004). Long-term potentiation and memory. *Physiol Rev.* *84*, 87-136.

- Ma,L., Zablow,L., Kandel,E.R., and Siegelbaum,S.A. (1999). Cyclic AMP induces functional presynaptic boutons in hippocampal CA3-CA1 neuronal cultures. *Nat. Neurosci.* 2, 24-30.
- Madden,D.R. (2002). The structure and function of glutamate receptor ion channels. *Nat. Rev. Neurosci.* 3, 91-101.
- Maguire,E.A., Frackowiak,R.S., and Frith,C.D. (1997). Recalling routes around london: activation of the right hippocampus in taxi drivers. *J. Neurosci.* 17, 7103-7110.
- Malenka,R.C., and Nicoll,R.A. (1998). Excitatory synapses. Is bigger better? *Nature* 396, 414-415.
- Malenka,R.C., and Nicoll,R.A. (1999). Long-term potentiation--a decade of progress? *Science* 285, 1870-1874.
- Malinow,R., and Malenka,R.C. (2002). AMPA receptor trafficking and synaptic plasticity. *Annu. Rev Neurosci* 25, 103-126.
- Marambaud,P., and Robakis,N.K. (2005). Genetic and molecular aspects of Alzheimer's disease shed light on new mechanisms of transcriptional regulation. *Genes, Brain and Behavior* 4, 134-146.
- Marambaud,P., Shioi,J., Serban,G., Georgakopoulos,A., Sarnier,S., Nagy,V., Baki,L., Wen,P., Efthimiopoulos,S., Shao,Z., Wisniewski,T., and Robakis,N.K. (2002). A presenilin-1/gamma-secretase cleavage releases the E-cadherin intracellular domain and regulates disassembly of adherens junctions. *EMBO J.* 21, 1948-1956.
- Marambaud,P., Wen,P.H., Dutt,A., Shioi,J., Takashima,A., Siman,R., and Robakis,N.K. (2003). A CBP Binding Transcriptional Repressor Produced by the PS1/[epsilon]-Cleavage of N-Cadherin Is Inhibited by PS1 FAD Mutations. *Cell* 114, 635-645.
- Maravall,M., Mainen,Z.F., Sabatini,B.L., and Svoboda,K. (2000). Estimating intracellular calcium concentrations and buffering without wavelength ratioing. *Biophys. J.* 78, 2655-2667.
- Marcello,E., Epis,R., and Di Luca,M. (2008). Amyloid flirting with synaptic failure: towards a comprehensive view of Alzheimer's disease pathogenesis. *Eur. J. Pharmacol.* 585, 109-118.
- Martin,S.J., and Morris,R.G. (2002). New life in an old idea: the synaptic plasticity and memory hypothesis revisited. *Hippocampus* 12, 609-636.
- Masliah,E., Hansen,L., Albright,T., Mallory,M., and Terry,R.D. (1991). Immunoelectron microscopic study of synaptic pathology in Alzheimer's disease. *Acta Neuropathol.* 81, 428-433.
- Mastrangelo,P., Mathews,P.M., Chishti,M.A., Schmidt,S.D., Gu,Y., Yang,J., Mazzella,M.J., Coomaraswamy,J., Horne,P., Strome,B., Pelly,H., Levesque,G., Ebeling,C., Jiang,Y., Nixon,R.A., Rozmahel,R., Fraser,P.E., George-Hyslop,P.,

- Carlson,G.A., and Westaway,D. (2005). Dissociated phenotypes in presenilin transgenic mice define functionally distinct gamma-secretases. *Proc. Natl. Acad. Sci. U. S. A* *102*, 8972-8977.
- Mattson,M.P. (1992). Calcium as sculptor and destroyer of neural circuitry. *Exp. Gerontol.* *27*, 29-49.
- Mattson,M.P. (1997). Cellular actions of beta-amyloid precursor protein and its soluble and fibrillogenic derivatives. *Physiol Rev.* *77*, 1081-1132.
- Mattson,M.P. (2004). Pathways towards and away from Alzheimer's disease. *Nature* *430*, 631-639.
- Mattson,M.P. (2010). ER calcium and Alzheimer's disease: in a state of flux. *Sci. Signal.* *3*, e10.
- Mattson,M.P., Barger,S.W., Cheng,B., Lieberburg,I., Smith-Swintosky,V.L., and Rydel,R.E. (1993). beta-Amyloid precursor protein metabolites and loss of neuronal Ca²⁺ homeostasis in Alzheimer's disease. *Trends Neurosci.* *16*, 409-414.
- McBain,C.J., and Mayer,M.L. (1994). N-methyl-D-aspartic acid receptor structure and function. *Physiol Rev.* *74*, 723-760.
- McCarthy,J.V., Twomey,C., and Wujek,P. (2009). Presenilin-dependent regulated intramembrane proteolysis and gamma-secretase activity. *Cell Mol. Life Sci.* *66*, 1534-1555.
- McGowan,E., Eriksen,J., and Hutton,M. (2006). A decade of modeling Alzheimer's disease in transgenic mice. *Trends Genet.* *22*, 281-289.
- McNaughton,B.L., Barnes,C.A., Rao,G., Baldwin,J., and Rasmussen,M. (1986). Long-term enhancement of hippocampal synaptic transmission and the acquisition of spatial information. *J. Neurosci.* *6*, 563-571.
- McPherson,P.S., Kim,Y.K., Valdivia,H., Knudson,C.M., Takekura,H., Franzini-Armstrong,C., Coronado,R., and Campbell,K.P. (1991). The brain ryanodine receptor: a caffeine-sensitive calcium release channel. *Neuron* *7*, 17-25.
- Megias,M., Emri,Z., Freund,T.F., and Gulyas,A.I. (2001). Total number and distribution of inhibitory and excitatory synapses on hippocampal CA1 pyramidal cells. *Neuroscience* *102*, 527-540.
- Meijering,E., Jacob,M., Sarria,J.C., Steiner,P., Hirling,H., and Unser,M. (2004). Design and validation of a tool for neurite tracing and analysis in fluorescence microscopy images. *Cytometry A* *58*, 167-176.
- Meyer-Luehmann,M., Spires-Jones,T.L., Prada,C., Garcia-Alloza,M., de,C.A., Rozkalne,A., Koenigsnecht-Talboo,J., Holtzman,D.M., Bacskai,B.J., and Hyman,B.T. (2008). Rapid appearance and local toxicity of amyloid-beta plaques in a mouse model of Alzheimer's disease. *Nature* *451*, 720-724.

- Mohler,H., Fritschy,J.M., Vogt,K., Crestani,F., and Rudolph,U. (2005). Pathophysiology and pharmacology of GABA(A) receptors. *Handb. Exp. Pharmacol.* 225-247.
- Moolman,D.L., Vitolo,O.V., Vonsattel,J.P., and Shelanski,M.L. (2004). Dendrite and dendritic spine alterations in Alzheimer models. *J. Neurocytol.* 33, 377-387.
- Morais,V.A., Crystal,A.S., Pijak,D.S., Carlin,D., Costa,J., Lee,V.M., and Doms,R.W. (2003). The transmembrane domain region of nicastrin mediates direct interactions with APH-1 and the gamma-secretase complex. *J. Biol. Chem.* 278, 43284-43291.
- Morfini,G., Pigino,G., Beffert,U., Busciglio,J., and Brady,S.T. (2002). Fast axonal transport misregulation and Alzheimer's disease. *Neuromolecular. Med.* 2, 89-99.
- Mori,H., Takio,K., Ogawara,M., and Selkoe,D.J. (1992). Mass spectrometry of purified amyloid beta protein in Alzheimer's disease. *J. Biol. Chem.* 267, 17082-17086.
- Morohashi,Y., Kan,T., Tominari,Y., Fuwa,H., Okamura,Y., Watanabe,N., Sato,C., Natsugari,H., Fukuyama,T., Iwatsubo,T., and Tomita,T. (2006). C-terminal fragment of presenilin is the molecular target of a dipeptidic gamma-secretase-specific inhibitor DAPT (N-[N-(3,5-difluorophenacetyl)-L-alanyl]-S-phenylglycine t-butyl ester). *J. Biol. Chem.* 281, 14670-14676.
- Morris,R.G., Anderson,E., Lynch,G.S., and Baudry,M. (1986). Selective impairment of learning and blockade of long-term potentiation by an N-methyl-D-aspartate receptor antagonist, AP5. *Nature* 319, 774-776.
- Morris,R.G., Garrud,P., Rawlins,J.N., and O'Keefe,J. (1982). Place navigation impaired in rats with hippocampal lesions. *Nature* 297, 681-683.
- Morris,R.G., Moser,E.I., Riedel,G., Martin,S.J., Sandin,J., Day,M., and O'Carroll,C. (2003). Elements of a neurobiological theory of the hippocampus: the role of activity-dependent synaptic plasticity in memory. *Philos. Trans. R. Soc. Lond B Biol. Sci.* 358, 773-786.
- Moser,E.I., Krobot,K.A., Moser,M.B., and Morris,R.G. (1998). Impaired spatial learning after saturation of long-term potentiation. *Science* 281, 2038-2042.
- Mumm,J.S., and Kopan,R. (2000). Notch signaling: from the outside in. *Dev. Biol.* 228, 151-165.
- Mumm,J.S., Schroeter,E.H., Saxena,M.T., Griesemer,A., Tian,X., Pan,D.J., Ray,W.J., and Kopan,R. (2000). A ligand-induced extracellular cleavage regulates gamma-secretase-like proteolytic activation of Notch1. *Mol. Cell* 5, 197-206.
- Murayama,M., Tanaka,S., Palacino,J., Murayama,O., Honda,T., Sun,X., Yasutake,K., Nihonmatsu,N., Wolozin,B., and Takashima,A. (1998). Direct association of presenilin-1 with beta-catenin. *FEBS Lett.* 433, 73-77.

- Murthy, V.N., Sejnowski, T.J., and Stevens, C.F. (1997). Heterogeneous release properties of visualized individual hippocampal synapses. *Neuron* *18*, 599-612.
- Naruse, S., Thinakaran, G., Luo, J.J., Kusiak, J.W., Tomita, T., Iwatsubo, T., Qian, X., Ginty, D.D., Price, D.L., Borchelt, D.R., Wong, P.C., and Sisodia, S.S. (1998). Effects of PS1 deficiency on membrane protein trafficking in neurons. *Neuron* *21*, 1213-1221.
- Nelson, O., Tu, H., Lei, T., Bentahir, M., De, S.B., and Bezprozvanny, I. (2007). Familial Alzheimer disease-linked mutations specifically disrupt Ca²⁺ leak function of presenilin 1. *J. Clin. Invest* *117*, 1230-1239.
- Newell, A.J., Sue, L.I., Scott, S., Rauschkolb, P.K., Walker, D.G., Potter, P.E., and Beach, T.G. (2003). Thiorphan-induced neprilysin inhibition raises amyloid beta levels in rabbit cortex and cerebrospinal fluid. *Neurosci. Lett.* *350*, 178-180.
- Ni, C.Y., Murphy, M.P., Golde, T.E., and Carpenter, G. (2001). gamma -Secretase cleavage and nuclear localization of ErbB-4 receptor tyrosine kinase. *Science* *294*, 2179-2181.
- Niimura, M., Isoo, N., Takasugi, N., Tsuruoka, M., Ui-Tei, K., Saigo, K., Morohashi, Y., Tomita, T., and Iwatsubo, T. (2005). Aph-1 contributes to the stabilization and trafficking of the gamma-secretase complex through mechanisms involving intermolecular and intramolecular interactions. *J. Biol Chem.* *280*, 12967-12975.
- Nishimura, M., Yu, G., Levesque, G., Zhang, D.M., Ruel, L., Chen, F., Milman, P., Holmes, E., Liang, Y., Kawarai, T., Jo, E., Supala, A., Rogaeva, E., Xu, D.M., Janus, C., Levesque, L., Bi, Q., Duthie, M., Rozmahel, R., Mattila, K., Lannfelt, L., Westaway, D., Mount, H.T., Woodgett, J., George-Hyslop, P., and . (1999). Presenilin mutations associated with Alzheimer disease cause defective intracellular trafficking of beta-catenin, a component of the presenilin protein complex. *Nat Med.* *5*, 164-169.
- Nowak, L., Bregestovski, P., Ascher, P., Herbert, A., and Prochiantz, A. (1984). Magnesium gates glutamate-activated channels in mouse central neurones. *Nature* *307*, 462-465.
- Nyabi, O., Bentahir, M., Horre, K., Herreman, A., Gottardi-Littell, N., Van, B.C., Merchiers, P., Spittaels, K., Annaert, W., and De, S.B. (2003). Presenilins mutated at Asp-257 or Asp-385 restore Pen-2 expression and Nicastrin glycosylation but remain catalytically inactive in the absence of wild type Presenilin. *J. Biol. Chem.* *278*, 43430-43436.
- O'Brien, R.J., Mammen, A.L., Blackshaw, S., Ehlers, M.D., Rothstein, J.D., and Huganir, R.L. (1997). The development of excitatory synapses in cultured spinal neurons. *J. Neurosci.* *17*, 7339-7350.
- Oddo, S., Caccamo, A., Kitazawa, M., Tseng, B.P., and LaFerla, F.M. (2003a). Amyloid deposition precedes tangle formation in a triple transgenic model of Alzheimer's disease. *Neurobiol. Aging* *24*, 1063-1070.
- Oddo, S., Caccamo, A., Shepherd, J.D., Murphy, M.P., Golde, T.E., Kaye, R., Metherate, R., Mattson, M.P., Akbari, Y., and LaFerla, F.M. (2003b). Triple-transgenic

model of Alzheimer's disease with plaques and tangles: intracellular Abeta and synaptic dysfunction. *Neuron* *39*, 409-421.

Ogura,T., Mio,K., Hayashi,I., Miyashita,H., Fukuda,R., Kopan,R., Kodama,T., Hamakubo,T., Iwatsubo,T., Tomita,T., and Sato,C. (2006). Three-dimensional structure of the gamma-secretase complex. *Biochem. Biophys. Res. Commun.* *343*, 525-534.

Oh,Y.S., and Turner,R.J. (2005a). Evidence that the COOH terminus of human presenilin 1 is located in extracytoplasmic space. *Am. J. Physiol Cell Physiol* *289*, C576-C581.

Oh,Y.S., and Turner,R.J. (2005b). Topology of the C-terminal fragment of human presenilin 1. *Biochemistry* *44*, 11821-11828.

Oh,Y.S., and Turner,R.J. (2006). Effect of gamma-secretase inhibitors on muscarinic receptor-mediated calcium signaling in human salivary epithelial cells. *Am. J. Physiol Cell Physiol* *291*, C76-C82.

Ohno,M., Sametsky,E.A., Younkin,L.H., Oakley,H., Younkin,S.G., Citron,M., Vassar,R., and Disterhoft,J.F. (2004). BACE1 deficiency rescues memory deficits and cholinergic dysfunction in a mouse model of Alzheimer's disease. *Neuron* *41*, 27-33.

Okabe,S., Miwa,A., and Okado,H. (2001). Spine formation and correlated assembly of presynaptic and postsynaptic molecules. *J. Neurosci* *21*, 6105-6114.

Okuda,T., Yu,L.M., Cingolani,L.A., Kemler,R., and Goda,Y. (2007). beta-Catenin regulates excitatory postsynaptic strength at hippocampal synapses. *Proc. Natl. Acad. Sci. U. S. A* *104*, 13479-13484.

Osenkowski,P., Li,H., Ye,W., Li,D., Aeschbach,L., Fraering,P.C., Wolfe,M.S., Selkoe,D.J., and Li,H. (2009). Cryoelectron microscopy structure of purified gamma-secretase at 12 Å resolution. *Journal of Molecular Biology* *642*-652.

Otmakhov,N., Tao-Cheng,J.H., Carpenter,S., Asrican,B., Dosemeci,A., Reese,T.S., and Lisman,J. (2004). Persistent accumulation of calcium/calmodulin-dependent protein kinase II in dendritic spines after induction of NMDA receptor-dependent chemical long-term potentiation. *J. Neurosci.* *24*, 9324-9331.

Pack-Chung,E., Meyers,M.B., Pettingell,W.P., Moir,R.D., Brownawell,A.M., Cheng,I., Tanzi,R.E., and Kim,T.W. (2000). Presenilin 2 interacts with sorcin, a modulator of the ryanodine receptor. *J. Biol. Chem.* *275*, 14440-14445.

Page,K., Hollister,R., Tanzi,R.E., and Hyman,B.T. (1996). In situ hybridization analysis of presenilin 1 mRNA in Alzheimer disease and in lesioned rat brain. *Proc. Natl. Acad. Sci. U. S. A* *93*, 14020-14024.

Palay,S.L. (1956). Synapses in the central nervous system. *J. Biophys Biochem Cytol* *2*, 193-202.

- Palay,S.L., and Palade,G.E. (1955). The fine structure of neurons. *J. Biophys Biochem Cytol* 69-88.
- Pardossi-Piquard,R., Bohm,C., Chen,F., Kanemoto,S., Checler,F., Schmitt-Ulms,G., St George-Hyslop,P., and Fraser,P.E. (2009). TMP21 transmembrane domain regulates gamma-secretase cleavage. *J. Biol. Chem.* 284, 28634-28641.
- Parent,A.T., Barnes,N.Y., Taniguchi,Y., Thinakaran,G., and Sisodia,S.S. (2005). Presenilin Attenuates Receptor-Mediated Signaling and Synaptic Function. *J. Neurosci.* 25, 1540-1549.
- Parkin,E.T., Turner,A.J., and Hooper,N.M. (2004). Secretase-mediated cell surface shedding of the angiotensin-converting enzyme. *Protein Pept. Lett.* 11, 423-432.
- Parks,A.L., and Curtis,D. (2007). Presenilin diversifies its portfolio. *Trends Genet.* 23, 140-150.
- Parodi,J., Sepulveda,F.J., Roa,J., Opazo,C., Inestrosa,N.C., and Aguayo,L.G. (2010). Beta-amyloid causes depletion of synaptic vesicles leading to neurotransmission failure. *J. Biol. Chem.* 285, 2506-2514.
- Parvathy,S., Hussain,I., Karran,E.H., Turner,A.J., and Hooper,N.M. (1999). Cleavage of Alzheimer's amyloid precursor protein by alpha-secretase occurs at the surface of neuronal cells. *Biochemistry* 38, 9728-9734.
- Parvathy,S., Karran,E.H., Turner,A.J., and Hooper,N.M. (1998). The secretases that cleave angiotensin converting enzyme and the amyloid precursor protein are distinct from tumour necrosis factor-alpha convertase. *FEBS Lett.* 431, 63-65.
- Passafaro,M., Piech,V., and Sheng,M. (2001). Subunit-specific temporal and spatial patterns of AMPA receptor exocytosis in hippocampal neurons. *Nat. Neurosci.* 4, 917-926.
- Paudel,H.K., Lew,J., Ali,Z., and Wang,J.H. (1993). Brain proline-directed protein kinase phosphorylates tau on sites that are abnormally phosphorylated in tau associated with Alzheimer's paired helical filaments. *J. Biol. Chem.* 268, 23512-23518.
- Peters,A., and Kaiserman-Abramof,I.R. (1969). The small pyramidal neuron of the rat cerebral cortex. The synapses upon dendritic spines. *Z. Zellforsch. Mikrosk. Anat.* 100, 487-506.
- Pitas,R.E., Boyles,J.K., Lee,S.H., Hui,D., and Weisgraber,K.H. (1987). Lipoproteins and their receptors in the central nervous system. Characterization of the lipoproteins in cerebrospinal fluid and identification of apolipoprotein B,E(LDL) receptors in the brain. *J. Biol. Chem.* 262, 14352-14360.
- Podlisny,M.B., Citron,M., Amarante,P., Sherrington,R., Xia,W., Zhang,J., Diehl,T., Levesque,G., Fraser,P., Haass,C., Koo,E.H., Seubert,P., George-Hyslop,P., Teplow,D.B., and Selkoe,D.J. (1997). Presenilin proteins undergo heterogeneous endoproteolysis between Thr291 and Ala299 and occur as stable N- and C-terminal fragments in normal and Alzheimer brain tissue. *Neurobiol. Dis.* 3, 325-337.

- Pool,M., Thiemann,J., Bar-Or,A., and Fournier,A.E. (2008). NeuriteTracer: a novel ImageJ plugin for automated quantification of neurite outgrowth. *J. Neurosci. Methods* 168, 134-139.
- Prange,O., and Murphy,T.H. (1999). Correlation of miniature synaptic activity and evoked release probability in cultures of cortical neurons. *J. Neurosci.* 19, 6427-6438.
- Pratt,K.G., Watari,H., Cook,G., and Sullivan,M. Presenilin 1 modulates spontaneous but not evoked release from hippocampal neurons. 523.17/F26 2009 Neuroscience Meeting Planner.Chicago, IL: Society for Neuroscience, 2009.Online. 2009.
Ref Type: Abstract
- Priller,C., Bauer,T., Mitteregger,G., Krebs,B., Kretschmar,H.A., and Herms,J. (2006). Synapse formation and function is modulated by the amyloid precursor protein. *J. Neurosci* 26, 7212-7221.
- Priller,C., Dewachter,I., Vassallo,N., Paluch,S., Pace,C., Kretschmar,H.A., Van Leuven,F., and Herms,J. (2007). Mutant presenilin 1 alters synaptic transmission in cultured hippocampal neurons. *J. Biol Chem.* 282, 1119-1127.
- Prince,M., and Jackson,J. World Alzheimer Report. Alzheimer's Disease International . 2009.
Ref Type: Magazine Article
- Prokop,S., Haass,C., and Steiner,H. (2005). Length and overall sequence of the PEN-2 C-terminal domain determines its function in the stabilization of presenilin fragments. *J. Neurochem.* 94, 57-62.
- Pruessmeyer,J., and Ludwig,A. (2009). The good, the bad and the ugly substrates for ADAM10 and ADAM17 in brain pathology, inflammation and cancer. *Semin. Cell Dev. Biol.* 20, 164-174.
- Querfurth,H.W., and LaFerla,F.M. (2010). Alzheimer's disease. *N. Engl. J. Med.* 362, 329-344.
- Ratovitski,T., Slunt,H.H., Thinakaran,G., Price,D.L., Sisodia,S.S., and Borchelt,D.R. (1997). Endoproteolytic processing and stabilization of wild-type and mutant presenilin. *J. Biol. Chem.* 272, 24536-24541.
- Ray,W.J., Yao,M., Mumm,J., Schroeter,E.H., Saftig,P., Wolfe,M., Selkoe,D.J., Kopan,R., and Goate,A.M. (1999). Cell surface presenilin-1 participates in the gamma-secretase-like proteolysis of Notch. *J. Biol Chem.* 274, 36801-36807.
- Rechards,M., Xia,W., Oorschot,V.M., Selkoe,D.J., and Klumperman,J. (2003). Presenilin-1 exists in both pre- and post-Golgi compartments and recycles via COPI-coated membranes. *Traffic.* 4, 553-565.
- Renner,M., Lacor,P.N., Velasco,P.T., Xu,J., Contractor,A., Klein,W.L., and Triller,A. (2010). Deleterious effects of amyloid beta oligomers acting as an extracellular scaffold for mGluR5. *Neuron* 66, 739-754.

- Ribaut-Barassin,C., Moussaoui,S., Brugg,B., Haeberle,A.M., Huber,G., Imperato,A., Delhaye-Bouchaud,N., Mariani,J., and Bailly,Y.J. (2000). Hemisynaptic distribution patterns of presenilins and beta-APP isoforms in the rodent cerebellum and hippocampus. *Synapse* 35, 96-110.
- Ris,L., Dewachter,I., Reverse,D., Godaux,E., and Van Leuven,F. (2003). Capacitative calcium entry induces hippocampal long term potentiation in the absence of presenilin-1. *J. Biol Chem.* 278, 44393-44399.
- Robakis,N.K., Ramakrishna,N., Wolfe,G., and Wisniewski,H.M. (1987a). Molecular cloning and characterization of a cDNA encoding the cerebrovascular and the neuritic plaque amyloid peptides. *Proc. Natl. Acad. Sci. U. S. A* 84, 4190-4194.
- Robakis,N.K., Wisniewski,H.M., Jenkins,E.C., Devine-Gage,E.A., Houck,G.E., Yao,X.L., Ramakrishna,N., Wolfe,G., Silverman,W.P., and Brown,W.T. (1987b). Chromosome 21q21 sublocalisation of gene encoding beta-amyloid peptide in cerebral vessels and neuritic (senile) plaques of people with Alzheimer disease and Down syndrome. *Lancet* 1, 384-385.
- Roberds,S.L., Anderson,J., Basi,G., Bienkowski,M.J., Branstetter,D.G., Chen,K.S., Freedman,S.B., Frigon,N.L., Games,D., Hu,K., Johnson-Wood,K., Kappenman,K.E., Kawabe,T.T., Kola,I., Kuehn,R., Lee,M., Liu,W., Motter,R., Nichols,N.F., Power,M., Robertson,D.W., Schenk,D., Schoor,M., Shopp,G.M., Shuck,M.E., Sinha,S., Svensson,K.A., Tatsuno,G., Tintrup,H., Wijsman,J., Wright,S., and McConlogue,L. (2001). BACE knockout mice are healthy despite lacking the primary beta-secretase activity in brain: implications for Alzheimer's disease therapeutics. *Hum. Mol. Genet.* 10, 1317-1324.
- Rosen,D.R., Martin-Morris,L., Luo,L.Q., and White,K. (1989). A *Drosophila* gene encoding a protein resembling the human beta-amyloid protein precursor. *Proc. Natl. Acad. Sci. U. S. A* 86, 2478-2482.
- Rosenmund,C., Clements,J.D., and Westbrook,G.L. (1993). Nonuniform probability of glutamate release at a hippocampal synapse. *Science* 262, 754-757.
- Rosenmund,C., and Stevens,C.F. (1996). Definition of the readily releasable pool of vesicles at hippocampal synapses. *Neuron* 16, 1197-1207.
- Rossner,S., Beck,M., Stahl,T., Mendla,K., Schliebs,R., and Bigl,V. (2000). Constitutive overactivation of protein kinase C in guinea pig brain increases alpha-secretory APP processing without decreasing beta-amyloid generation. *Eur. J. Neurosci.* 12, 3191-3200.
- Rowan,M.J., Klyubin,I., Wang,Q., and Anwyl,R. (2005). Synaptic plasticity disruption by amyloid beta protein: modulation by potential Alzheimer's disease modifying therapies. *Biochem. Soc. Trans.* 33, 563-567.
- Rubio,M.E., Curcio,C., Chauvet,N., and Bruses,J.L. (2005). Assembly of the N-cadherin complex during synapse formation involves uncoupling of p120-catenin and association with presenilin 1. *Mol Cell Neurosci* 30, 611-623.

- Sabo,S.L., Ikin,A.F., Buxbaum,J.D., and Greengard,P. (2003). The amyloid precursor protein and its regulatory protein, FE65, in growth cones and synapses in vitro and in vivo. *J. Neurosci.* 23, 5407-5415.
- Sahasrabudhe,S.R., Brown,A.M., Hulmes,J.D., Jacobsen,J.S., Vitek,M.P., Blume,A.J., and Sonnenberg,J.L. (1993). Enzymatic generation of the amino terminus of the beta-amyloid peptide. *J. Biol. Chem.* 268, 16699-16705.
- Saido,T.C., Iwatsubo,T., Mann,D.M., Shimada,H., Ihara,Y., and Kawashima,S. (1995). Dominant and differential deposition of distinct beta-amyloid peptide species, A beta N3(pE), in senile plaques. *Neuron* 14, 457-466.
- Salinas,P.C., and Zou,Y. (2008). Wnt signaling in neural circuit assembly. *Annu. Rev. Neurosci.* 31, 339-358.
- Sato,C., Morohashi,Y., Tomita,T., and Iwatsubo,T. (2006). Structure of the catalytic pore of gamma-secretase probed by the accessibility of substituted cysteines. *J. Neurosci* 26, 12081-12088.
- Sato,T., Diehl,T.S., Narayanan,S., Funamoto,S., Ihara,Y., De Strooper,B., Steiner,H., Haass,C., and Wolfe,M.S. (2007). Active gamma -secretase complexes contain only one of each component. *J. Biol Chem.*
- Saunders,A.M., Strittmatter,W.J., Schmechel,D., George-Hyslop,P.H., Pericak-Vance,M.A., Joo,S.H., Rosi,B.L., Gusella,J.F., Crapper-MacLachlan,D.R., Alberts,M.J., and . (1993). Association of apolipoprotein E allele epsilon 4 with late-onset familial and sporadic Alzheimer's disease. *Neurology* 43, 1467-1472.
- Saura,C.A., Chen,G., Malkani,S., Choi,S.Y., Takahashi,R.H., Zhang,D., Gouras,G.K., Kirkwood,A., Morris,R.G., and Shen,J. (2005). Conditional inactivation of presenilin 1 prevents amyloid accumulation and temporarily rescues contextual and spatial working memory impairments in amyloid precursor protein transgenic mice. *J. Neurosci.* 25, 6755-6764.
- Saura,C.A., Choi,S.Y., Beglopoulos,V., Malkani,S., Zhang,D., Shankaranarayana Rao,B.S., Chattarji,S., Kelleher,R.J., III, Kandel,E.R., Duff,K., Kirkwood,A., and Shen,J. (2004). Loss of presenilin function causes impairments of memory and synaptic plasticity followed by age-dependent neurodegeneration. *Neuron* 42, 23-36.
- Scannevin,R.H., and Huganir,R.L. (2000). Postsynaptic organization and regulation of excitatory synapses. *Nat. Rev. Neurosci.* 1, 133-141.
- Scanziani,M., Capogna,M., Gahwiler,B.H., and Thompson,S.M. (1992). Presynaptic inhibition of miniature excitatory synaptic currents by baclofen and adenosine in the hippocampus. *Neuron* 9, 919-927.
- Scheff,S.W., and Price,D.A. (2003). Synaptic pathology in Alzheimer's disease: a review of ultrastructural studies. *Neurobiol. Aging* 24, 1029-1046.
- Scheiffele,P. (2003). Cell-cell signaling during synapse formation in the CNS. *Annu. Rev. Neurosci.* 26, 485-508.

- Schenk,D., Barbour,R., Dunn,W., Gordon,G., Grajeda,H., Guido,T., Hu,K., Huang,J., Johnson-Wood,K., Khan,K., Kholodenko,D., Lee,M., Liao,Z., Lieberburg,I., Motter,R., Mutter,L., Soriano,F., Shopp,G., Vasquez,N., Vandever,C., Walker,S., Wogulis,M., Yednock,T., Games,D., and Seubert,P. (1999). Immunization with amyloid-beta attenuates Alzheimer-disease-like pathology in the PDAPP mouse. *Nature* 400, 173-177.
- Scheuner,D., Eckman,C., Jensen,M., Song,X., Citron,M., Suzuki,N., Bird,T.D., Hardy,J., Hutton,M., Kukull,W., Larson,E., Levy-Lahad,L., Viitanen,M., Peskind,E., Poorkaj,P., Schellenberg,G., Tanzi,R., Wasco,W., Lannfelt,L., Selkoe,D., and Younkin,S. (1996). Secreted amyloid [beta]-protein similar to that in the senile plaques of Alzheimer's disease is increased in vivo by the presenilin 1 and 2 and APP mutations linked to familial Alzheimer's disease. *Nat Med* 2, 864-870.
- Schikorski,T., and Stevens,C.F. (1997). Quantitative ultrastructural analysis of hippocampal excitatory synapses. *J. Neurosci.* 17, 5858-5867.
- Schneggenburger,R., Meyer,A.C., and Neher,E. (1999). Released fraction and total size of a pool of immediately available transmitter quanta at a calyx synapse. *Neuron* 23, 399-409.
- Scholz,K.P., and Miller,R.J. (1995). Developmental changes in presynaptic calcium channels coupled to glutamate release in cultured rat hippocampal neurons. *J. Neurosci.* 15, 4612-4617.
- Schroeter,E.H., Kisslinger,J.A., and Kopan,R. (1998). Notch-1 signalling requires ligand-induced proteolytic release of intracellular domain. *Nature* 393, 382-386.
- Scott,R., and Rusakov,D.A. (2008). Ca²⁺ stores and use-dependent facilitation of presynaptic Ca²⁺ signaling. *Proc. Natl. Acad. Sci. U. S. A* 105, E80.
- Scoville,W.B., and Milner,B. (1957). Loss of recent memory after bilateral hippocampal lesions. *J. Neurol. Neurosurg. Psychiatry* 20, 11-21.
- Seiffert,D., Bradley,J.D., Rominger,C.M., Rominger,D.H., Yang,F., Meredith,J.E., Jr., Wang,Q., Roach,A.H., Thompson,L.A., Spitz,S.M., Higaki,J.N., Prakash,S.R., Combs,A.P., Copeland,R.A., Arneric,S.P., Hartig,P.R., Robertson,D.W., Cordell,B., Stern,A.M., Olson,R.E., and Zaczek,R. (2000). Presenilin-1 and -2 are molecular targets for gamma-secretase inhibitors. *J. Biol Chem.* 275, 34086-34091.
- Selkoe,D.J. (2000). Notch and presenilins in vertebrates and invertebrates: implications for neuronal development and degeneration. *Curr. Opin. Neurobiol.* 10, 50-57.
- Selkoe,D.J. (2001). Alzheimer's disease: genes, proteins, and therapy. *Physiol Rev.* 81, 741-766.
- Selkoe,D.J. (2002). Alzheimer's disease is a synaptic failure. *Science* 298, 789-791.
- Selkoe,D.J., and Schenk,D. (2003). Alzheimer's disease: molecular understanding predicts amyloid-based therapeutics. *Annu. Rev. Pharmacol. Toxicol.* 43, 545-584.

- Selkoe,D.J., and Wolfe,M.S. (2007). Presenilin: running with scissors in the membrane. *Cell* 131, 215-221.
- Seubert,P., Oltersdorf,T., Lee,M.G., Barbour,R., Blomquist,C., Davis,D.L., Bryant,K., Fritz,L.C., Galasko,D., Thal,L.J., and . (1993). Secretion of beta-amyloid precursor protein cleaved at the amino terminus of the beta-amyloid peptide. *Nature* 361, 260-263.
- Seubert,P., Vigo-Pelfrey,C., Esch,F., Lee,M., Dovey,H., Davis,D., Sinha,S., Schlossmacher,M., Whaley,J., Swindlehurst,C., and . (1992). Isolation and quantification of soluble Alzheimer's beta-peptide from biological fluids. *Nature* 359, 325-327.
- Shah,S., Lee,S.F., Tabuchi,K., Hao,Y.H., Yu,C., LaPlant,Q., Ball,H., Dann,C.E., III, Sudhof,T., and Yu,G. (2005). Nicastrin functions as a gamma-secretase-substrate receptor. *Cell* 122, 435-447.
- Shankar,G.M., Bloodgood,B.L., Townsend,M., Walsh,D.M., Selkoe,D.J., and Sabatini,B.L. (2007). Natural oligomers of the Alzheimer amyloid-beta protein induce reversible synapse loss by modulating an NMDA-type glutamate receptor-dependent signaling pathway. *J. Neurosci.* 27, 2866-2875.
- Shearman,M.S., Beher,D., Clarke,E.E., Lewis,H.D., Harrison,T., Hunt,P., Nadin,A., Smith,A.L., Stevenson,G., and Castro,J.L. (2000). L-685,458, an aspartyl protease transition state mimic, is a potent inhibitor of amyloid beta-protein precursor gamma-secretase activity. *Biochemistry* 39, 8698-8704.
- Shen,J., Bronson,R.T., Chen,D.F., Xia,W., Selkoe,D.J., and Tonegawa,S. (1997). Skeletal and CNS defects in Presenilin-1-deficient mice. *Cell* 89, 629-639.
- Sheng,M., and Hoogenraad,C.C. (2007). The postsynaptic architecture of excitatory synapses: a more quantitative view. *Annu. Rev. Biochem* 76, 823-847.
- Sherrington,CS. (1897). The Central Nervous System. In *A textbook of physiology*, M. Foster, ed. (London: MacMillan).
- Sherrington,R., Rogaev,E.I., Liang,Y., Rogaeva,E.A., Levesque,G., Ikeda,M., Chi,H., Lin,C., Li,G., Holman,K., and . (1995). Cloning of a gene bearing missense mutations in early-onset familial Alzheimer's disease. *Nature* 375, 754-760.
- Shirotani,K., Edbauer,D., Kostka,M., Steiner,H., and Haass,C. (2004a). Immature nicastrin stabilizes APH-1 independent of PEN-2 and presenilin: identification of nicastrin mutants that selectively interact with APH-1. *J. Neurochem.* 89, 1520-1527.
- Shirotani,K., Edbauer,D., Prokop,S., Haass,C., and Steiner,H. (2004b). Identification of distinct gamma-secretase complexes with different APH-1 variants. *J. Biol. Chem.* 279, 41340-41345.
- Shoji,M., Golde,T.E., Ghiso,J., Cheung,T.T., Estus,S., Shaffer,L.M., Cai,X.D., McKay,D.M., Tintner,R., Frangione,B., and . (1992). Production of the Alzheimer amyloid beta protein by normal proteolytic processing. *Science* 258, 126-129.

Shrestha,B.R., Vitolo,O.V., Joshi,P., Lordkipanidze,T., Shelanski,M., and Dunaevsky,A. (2006). Amyloid beta peptide adversely affects spine number and motility in hippocampal neurons. *Mol. Cell Neurosci.* 33, 274-282.

Silva,A.J., Stevens,C.F., Tonegawa,S., and Wang,Y. (1992). Deficient hippocampal long-term potentiation in alpha-calcium-calmodulin kinase II mutant mice. *Science* 257, 201-206.

Simkus,C.R., and Stricker,C. (2002). The contribution of intracellular calcium stores to mEPSCs recorded in layer II neurones of rat barrel cortex. *J. Physiol* 545, 521-535.

Sinha,S., Anderson,J.P., Barbour,R., Basi,G.S., Caccavello,R., Davis,D., Doan,M., Dovey,H.F., Frigon,N., Hong,J., Jacobson-Croak,K., Jewett,N., Keim,P., Knops,J., Lieberburg,I., Power,M., Tan,H., Tatsuno,G., Tung,J., Schenk,D., Seubert,P., Suomensaaari,S.M., Wang,S., Walker,D., Zhao,J., McConlogue,L., and John,V. (1999). Purification and cloning of amyloid precursor protein beta-secretase from human brain. *Nature* 402, 537-540.

Sisodia,S.S. (1992). Beta-amyloid precursor protein cleavage by a membrane-bound protease. *Proc. Natl. Acad. Sci. U. S. A* 89, 6075-6079.

Sisodia,S.S., Annaert,W., Kim,S.H., and De,S.B. (2001). Gamma-secretase: never more enigmatic. *Trends Neurosci.* 24, S2-S6.

Sisodia,S.S., and George-Hyslop,P.H. (2002). gamma-Secretase, Notch, Abeta and Alzheimer's disease: where do the presenilins fit in? *Nat Rev Neurosci* 3, 281-290.

Sisodia,S.S., Koo,E.H., Beyreuther,K., Unterbeck,A., and Price,D.L. (1990). Evidence that beta-amyloid protein in Alzheimer's disease is not derived by normal processing. *Science* 248, 492-495.

Sisodia,S.S., Koo,E.H., Hoffman,P.N., Perry,G., and Price,D.L. (1993). Identification and transport of full-length amyloid precursor proteins in rat peripheral nervous system. *J. Neurosci* 13, 3136-3142.

Skovronsky,D.M., Lee,V.M., and Trojanowski,J.Q. (2006). Neurodegenerative diseases: new concepts of pathogenesis and their therapeutic implications. *Annu. Rev. Pathol.* 1, 151-170.

Skovronsky,D.M., Moore,D.B., Milla,M.E., Doms,R.W., and Lee,V.M. (2000). Protein kinase C-dependent alpha-secretase competes with beta-secretase for cleavage of amyloid-beta precursor protein in the trans-golgi network. *J. Biol. Chem.* 275, 2568-2575.

Smith,I.F., Boyle,J.P., Vaughan,P.F., Pearson,H.A., Cowburn,R.F., and Peers,C.S. (2002). Ca(2+) stores and capacitative Ca(2+) entry in human neuroblastoma (SH-SY5Y) cells expressing a familial Alzheimer's disease presenilin-1 mutation. *Brain Res.* 949, 105-111.

Smith,S.K., Anderson,H.A., Yu,G., Robertson,A.G., Allen,S.J., Tyler,S.J., Naylor,R.L., Mason,G., Wilcock,G.W., Roche,P.A., Fraser,P.E., and Dawbarn,D.

(2000). Identification of syntaxin 1A as a novel binding protein for presenilin-1. *Brain Res. Mol. Brain Res.* 78, 100-107.

Solans,A., Estivill,X., and de La,L.S. (2000). A new aspartyl protease on 21q22.3, BACE2, is highly similar to Alzheimer's amyloid precursor protein beta-secretase. *Cytogenet. Cell Genet.* 89, 177-184.

Spasic,D., and Annaert,W. (2008). Building gamma-secretase: the bits and pieces. *J. Cell Sci.* 121, 413-420.

Spasic,D., Raemaekers,T., Dillen,K., Declerck,I., Baert,V., Serneels,L., Fullekrug,J., and Annaert,W. (2007). Rer1p competes with APH-1 for binding to nicastrin and regulates gamma-secretase complex assembly in the early secretory pathway. *J. Cell Biol.* 176, 629-640.

Spasic,D., Tolia,A., Dillen,K., Baert,V., De,S.B., Vrijens,S., and Annaert,W. (2006). Presenilin-1 maintains a nine-transmembrane topology throughout the secretory pathway. *J. Biol. Chem.* 281, 26569-26577.

Spires,T.L., Meyer-Luehmann,M., Stern,E.A., McLean,P.J., Skoch,J., Nguyen,P.T., Bacskai,B.J., and Hyman,B.T. (2005). Dendritic spine abnormalities in amyloid precursor protein transgenic mice demonstrated by gene transfer and intravital multiphoton microscopy. *J. Neurosci.* 25, 7278-7287.

Spires-Jones,T.L., Meyer-Luehmann,M., Osetek,J.D., Jones,P.B., Stern,E.A., Bacskai,B.J., and Hyman,B.T. (2007). Impaired spine stability underlies plaque-related spine loss in an Alzheimer's disease mouse model. *Am. J. Pathol.* 171, 1304-1311.

Sprengel,R., Suchanek,B., Amico,C., Brusa,R., Burnashev,N., Rozov,A., Hvalby,O., Jensen,V., Paulsen,O., Andersen,P., Kim,J.J., Thompson,R.F., Sun,W., Webster,L.C., Grant,S.G., Eilers,J., Konnerth,A., Li,J., McNamara,J.O., and Seeburg,P.H. (1998). Importance of the intracellular domain of NR2 subunits for NMDA receptor function in vivo. *Cell* 92, 279-289.

Squire,L.R. (1992). Memory and the hippocampus: a synthesis from findings with rats, monkeys, and humans. *Psychol. Rev.* 99, 195-231.

St-Laurent,J., Boulay,M.E., Prince,P., Bissonnette,E., and Boulet,L.P. (2006). Comparison of cell fixation methods of induced sputum specimens: an immunocytochemical analysis. *J. Immunol. Methods* 308, 36-42.

Stachel,S.J., Coburn,C.A., Steele,T.G., Jones,K.G., Loutzenhiser,E.F., Gregro,A.R., Rajapakse,H.A., Lai,M.T., Crouthamel,M.C., Xu,M., Tugusheva,K., Lineberger,J.E., Pietrak,B.L., Espeseth,A.S., Shi,X.P., Chen-Dodson,E., Holloway,M.K., Munshi,S., Simon,A.J., Kuo,L., and Vacca,J.P. (2004). Structure-based design of potent and selective cell-permeable inhibitors of human beta-secretase (BACE-1). *J. Med. Chem.* 47, 6447-6450.

Staras,K., Branco,T., Burden,J.J., Pozo,K., Darcy,K., Marra,V., Ratnayaka,A., and Goda,Y. (2010). A vesicle superpool spans multiple presynaptic terminals in hippocampal neurons. *Neuron* 66, 37-44.

- Steiner,H., Capell,A., Pesold,B., Citron,M., Kloetzel,P.M., Selkoe,D.J., Romig,H., Mendla,K., and Haass,C. (1998). Expression of Alzheimer's disease-associated presenilin-1 is controlled by proteolytic degradation and complex formation. *J. Biol. Chem.* 273, 32322-32331.
- Steiner,H., Duff,K., Capell,A., Romig,H., Grim,M.G., Lincoln,S., Hardy,J., Yu,X., Picciano,M., Fichtler,K., Citron,M., Kopan,R., Pesold,B., Keck,S., Baader,M., Tomita,T., Iwatsubo,T., Baumeister,R., and Haass,C. (1999a). A loss of function mutation of presenilin-2 interferes with amyloid beta-peptide production and notch signaling. *J. Biol. Chem.* 274, 28669-28673.
- Steiner,H., Fluhner,R., and Haass,C. (2008). Intramembrane proteolysis by gamma-secretase. *J. Biol. Chem.* 283, 29627-29631.
- Steiner,H., and Haass,C. (2000). Intramembrane proteolysis by presenilins. *Nat Rev Mol Cell Biol* 1, 217-224.
- Steiner,H., Revesz,T., Neumann,M., Romig,H., Grim,M.G., Pesold,B., Kretschmar,H.A., Hardy,J., Holton,J.L., Baumeister,R., Houlden,H., and Haass,C. (2001). A pathogenic presenilin-1 deletion causes aberrant A β 42 production in the absence of congophilic amyloid plaques. *J. Biol Chem.* 276, 7233-7239.
- Steiner,H., Romig,H., Pesold,B., Philipp,U., Baader,M., Citron,M., Loetscher,H., Jacobsen,H., and Haass,C. (1999b). Amyloidogenic function of the Alzheimer's disease-associated presenilin 1 in the absence of endoproteolysis. *Biochemistry* 38, 14600-14605.
- Steiner,H., Winkler,E., Edbauer,D., Prokop,S., Basset,G., Yamasaki,A., Kostka,M., and Haass,C. (2002). PEN-2 is an integral component of the gamma-secretase complex required for coordinated expression of presenilin and nicastrin. *J. Biol Chem.* 277, 39062-39065.
- Stokin,G.B., and Goldstein,L.S. (2006). Axonal transport and Alzheimer's disease. *Annu. Rev. Biochem.* 75, 607-627.
- Stokin,G.B., Lillo,C., Falzone,T.L., Brusch,R.G., Rockenstein,E., Mount,S.L., Raman,R., Davies,P., Masliah,E., Williams,D.S., and Goldstein,L.S. (2005). Axonopathy and transport deficits early in the pathogenesis of Alzheimer's disease. *Science* 307, 1282-1288.
- Stoppini,L., Buchs,P.A., and Muller,D. (1991). A simple method for organotypic cultures of nervous tissue. *J. Neurosci. Methods* 37, 173-182.
- Strehler,E.E., and Zacharias,D.A. (2001). Role of alternative splicing in generating isoform diversity among plasma membrane calcium pumps. *Physiol Rev.* 81, 21-50.
- Strittmatter,W.J., Weisgraber,K.H., Huang,D.Y., Dong,L.M., Salvesen,G.S., Pericak-Vance,M., Schmechel,D., Saunders,A.M., Goldgaber,D., and Roses,A.D. (1993). Binding of human apolipoprotein E to synthetic amyloid beta peptide: isoform-specific effects and implications for late-onset Alzheimer disease. *Proc. Natl. Acad. Sci. U. S. A* 90, 8098-8102.

- Struhl,G., and Adachi,A. (2000). Requirements for presenilin-dependent cleavage of notch and other transmembrane proteins. *Mol. Cell* 6, 625-636.
- Struhl,G., and Greenwald,I. (1999). Presenilin is required for activity and nuclear access of Notch in *Drosophila*. *Nature* 398, 522-525.
- Stutzmann,G.E., Caccamo,A., LaFerla,F.M., and Parker,I. (2004). Dysregulated IP3 signaling in cortical neurons of knock-in mice expressing an Alzheimer's-linked mutation in presenilin1 results in exaggerated Ca²⁺ signals and altered membrane excitability. *J. Neurosci.* 24, 508-513.
- Stutzmann,G.E., Smith,I., Caccamo,A., Oddo,S., LaFerla,F.M., and Parker,I. (2006). Enhanced ryanodine receptor recruitment contributes to Ca²⁺ disruptions in young, adult, and aged Alzheimer's disease mice. *J. Neurosci.* 26, 5180-5189.
- Stutzmann,G.E., Smith,I., Caccamo,A., Oddo,S., Parker,I., and Laferla,F. (2007). Enhanced ryanodine-mediated calcium release in mutant PS1-expressing Alzheimer's mouse models. *Ann. N. Y. Acad. Sci.* 1097, 265-277.
- Suh,Y.H., and Checler,F. (2002). Amyloid precursor protein, presenilins, and alpha-synuclein: molecular pathogenesis and pharmacological applications in Alzheimer's disease. *Pharmacol. Rev* 54, 469-525.
- Svoboda,K. (2004). Do spines and dendrites distribute dye evenly? *Trends Neurosci.* 27, 445-446.
- Swiatek,P.J., Lindsell,C.E., Del Amo,F.F., Weinmaster,G., and Gridley,T. (1994). Notch1 is essential for postimplantation development in mice. *Genes Dev.* 8, 707-719.
- Sze,C.I., Troncoso,J.C., Kawas,C., Mouton,P., Price,D.L., and Martin,L.J. (1997). Loss of the presynaptic vesicle protein synaptophysin in hippocampus correlates with cognitive decline in Alzheimer disease. *J. Neuropathol. Exp. Neurol.* 56, 933-944.
- Tabuchi,K., Chen,G., Sudhof,T.C., and Shen,J. (2009). Conditional forebrain inactivation of nicastrin causes progressive memory impairment and age-related neurodegeneration. *J. Neurosci.* 29, 7290-7301.
- Takasugi,N., Tomita,T., Hayashi,I., Tsuruoka,M., Niimura,M., Takahashi,Y., Thinakaran,G., and Iwatsubo,T. (2003). The role of presenilin cofactors in the gamma-secretase complex. *Nature* 422, 438-441.
- Tandon,A., and Fraser,P. (2002). The presenilins. *Genome Biol.* 3, reviews3014.
- Tanzi,R.E., and Bertram,L. (2001). New frontiers in Alzheimer's disease genetics. *Neuron* 32, 181-184.
- Tarsa,L., and Goda,Y. (2002). Synaptophysin regulates activity-dependent synapse formation in cultured hippocampal neurons. *Proc. Natl. Acad. Sci. U. S. A* 99, 1012-1016.

- Terry,R.D. (2000). Cell death or synaptic loss in Alzheimer disease. *J. Neuropathol. Exp. Neurol.* *59*, 1118-1119.
- Terry,R.D., Masliah,E., Salmon,D.P., Butters,N., DeTeresa,R., Hill,R., Hansen,L.A., and Katzman,R. (1991). Physical basis of cognitive alterations in Alzheimer's disease: synapse loss is the major correlate of cognitive impairment. *Ann. Neurol.* *30*, 572-580.
- Thinakaran,G., Borchelt,D.R., Lee,M.K., Slunt,H.H., Spitzer,L., Kim,G., Ratovitsky,T., Davenport,F., Nordstedt,C., Seeger,M., Hardy,J., Levey,A.I., Gandy,S.E., Jenkins,N.A., Copeland,N.G., Price,D.L., and Sisodia,S.S. (1996). Endoproteolysis of presenilin 1 and accumulation of processed derivatives in vivo. *Neuron* *17*, 181-190.
- Thinakaran,G., Harris,C.L., Ratovitski,T., Davenport,F., Slunt,H.H., Price,D.L., Borchelt,D.R., and Sisodia,S.S. (1997). Evidence that levels of presenilins (PS1 and PS2) are coordinately regulated by competition for limiting cellular factors. *J. Biol. Chem.* *272*, 28415-28422.
- Thinakaran,G., and Koo,E.H. (2008). Amyloid precursor protein trafficking, processing, and function. *J. Biol. Chem.* *283*, 29615-29619.
- Thinakaran,G., and Parent,A.T. (2004). Identification of the role of presenilins beyond Alzheimer's disease. *Pharmacol. Res.* *50*, 411-418.
- Thinakaran,G., Regard,J.B., Bouton,C.M., Harris,C.L., Price,D.L., Borchelt,D.R., and Sisodia,S.S. (1998). Stable association of presenilin derivatives and absence of presenilin interactions with APP. *Neurobiol. Dis.* *4*, 438-453.
- Ting,J.T., Kelley,B.G., Lambert,T.J., Cook,D.G., and Sullivan,J.M. (2007). Amyloid precursor protein overexpression depresses excitatory transmission through both presynaptic and postsynaptic mechanisms. *Proc. Natl. Acad. Sci. U. S. A* *104*, 353-358.
- Tokuoka,H., and Goda,Y. (2008). Activity-dependent coordination of presynaptic release probability and postsynaptic GluR2 abundance at single synapses. *Proc. Natl. Acad. Sci. U. S. A* *105*, 14656-14661.
- Tolia,A., Chavez-Gutierrez,L., and De,S.B. (2006). Contribution of presenilin transmembrane domains 6 and 7 to a water-containing cavity in the gamma-secretase complex. *J. Biol. Chem.* *281*, 27633-27642.
- Tomita,T., and Iwatsubo,T. (2004). The inhibition of gamma-secretase as a therapeutic approach to Alzheimer's disease. *Drug News Perspect.* *17*, 321-325.
- Triller,A., and Choquet,D. (2005). Surface trafficking of receptors between synaptic and extrasynaptic membranes: and yet they do move! *Trends Neurosci.* *28*, 133-139.
- Tsien,J.Z., Chen,D.F., Gerber,D., Tom,C., Mercer,E.H., Anderson,D.J., Mayford,M., Kandel,E.R., and Tonegawa,S. (1996a). Subregion- and cell type-restricted gene knockout in mouse brain. *Cell* *87*, 1317-1326.

- Tsien, J.Z., Huerta, P.T., and Tonegawa, S. (1996b). The essential role of hippocampal CA1 NMDA receptor-dependent synaptic plasticity in spatial memory. *Cell* 87, 1327-1338.
- Tu, H., Nelson, O., Bezprozvanny, A., Wang, Z., Lee, S.F., Hao, Y.H., Serneels, L., De Strooper, B., Yu, G., and Bezprozvanny, I. (2006). Presenilins form ER Ca²⁺ leak channels, a function disrupted by familial Alzheimer's disease-linked mutations. *Cell* 126, 981-993.
- Turner, P.R., O'Connor, K., Tate, W.P., and Abraham, W.C. (2003). Roles of amyloid precursor protein and its fragments in regulating neural activity, plasticity and memory. *Prog. Neurobiol.* 70, 1-32.
- Uemura, K., Kitagawa, N., Kohno, R., Kuzuya, A., Kageyama, T., Chonabayashi, K., Shibasaki, H., and Shimohama, S. (2003). Presenilin 1 is involved in maturation and trafficking of N-cadherin to the plasma membrane. *J. Neurosci Res.* 74, 184-191.
- Vassar, R. (2004). BACE1: the beta-secretase enzyme in Alzheimer's disease. *J. Mol. Neurosci.* 23, 105-114.
- Vassar, R., Bennett, B.D., Babu-Khan, S., Kahn, S., Mendiaz, E.A., Denis, P., Teplow, D.B., Ross, S., Amarante, P., Loeloff, R., Luo, Y., Fisher, S., Fuller, J., Edenson, S., Lile, J., Jarosinski, M.A., Biere, A.L., Curran, E., Burgess, T., Louis, J.C., Collins, F., Treanor, J., Rogers, G., and Citron, M. (1999). Beta-secretase cleavage of Alzheimer's amyloid precursor protein by the transmembrane aspartic protease BACE. *Science* 286, 735-741.
- Venkitaramani, D.V., Chin, J., Netzer, W.J., Gouras, G.K., Lesne, S., Malinow, R., and Lombroso, P.J. (2007). Beta-amyloid modulation of synaptic transmission and plasticity. *J. Neurosci.* 27, 11832-11837.
- Verkhratsky, A. (2002). The endoplasmic reticulum and neuronal calcium signalling. *Cell Calcium* 32, 393-404.
- Vetrivel, K.S., Cheng, H., Kim, S.H., Chen, Y., Barnes, N.Y., Parent, A.T., Sisodia, S.S., and Thinakaran, G. (2005). Spatial segregation of gamma-secretase and substrates in distinct membrane domains. *J. Biol. Chem.* 280, 25892-25900.
- Vetrivel, K.S., Zhang, Y.W., Xu, H., and Thinakaran, G. (2006). Pathological and physiological functions of presenilins. *Mol Neurodegener.* 1, 4.
- Vetrivel, K.S., Cheng, H., Lin, W., Sakurai, T., Li, T., Nukina, N., Wong, P.C., Xu, H., and Thinakaran, G. (2004). Association of {gamma}-Secretase with Lipid Rafts in Post-Golgi and Endosome Membranes. *J. Biol. Chem.* 279, 44945-44954.
- Wakabayashi, T., and De Strooper, B. (2008). Presenilins: members of the gamma-secretase quartets, but part-time soloists too. *Physiology. (Bethesda.)* 23, 194-204.
- Wall, M.J., and Usowicz, M.M. (1998). Development of the quantal properties of evoked and spontaneous synaptic currents at a brain synapse. *Nat. Neurosci.* 1, 675-682.

- Walsh,D.M., Klyubin,I., Shankar,G.M., Townsend,M., Fadeeva,J.V., Betts,V., Podlisny,M.B., Cleary,J.P., Ashe,K.H., Rowan,M.J., and Selkoe,D.J. (2005). The role of cell-derived oligomers of Abeta in Alzheimer's disease and avenues for therapeutic intervention. *Biochem. Soc. Trans.* *33*, 1087-1090.
- Walsh,D.M., and Selkoe,D.J. (2007). A beta oligomers - a decade of discovery. *J. Neurochem.* *101*, 1172-1184.
- Wang,E., Taylor,R.W., and Pfeiffer,D.R. (1998). Mechanism and specificity of lanthanide series cation transport by ionophores A23187, 4-BrA23187, and ionomycin. *Biophys J.* *75*, 1244-1254.
- Wang,H., Luo,W.J., Zhang,Y.W., Li,Y.M., Thinakaran,G., Greengard,P., and Xu,H. (2004). Presenilins and gamma-secretase inhibitors affect intracellular trafficking and cell surface localization of the gamma-secretase complex components. *J. Biol. Chem.* *279*, 40560-40566.
- Wasco,W., Brook,J.D., and Tanzi,R.E. (1993). The amyloid precursor-like protein (APLP) gene maps to the long arm of human chromosome 19. *Genomics* *15*, 237-239.
- Wasco,W., Bupp,K., Magendantz,M., Gusella,J.F., Tanzi,R.E., and Solomon,F. (1992). Identification of a mouse brain cDNA that encodes a protein related to the Alzheimer disease-associated amyloid beta protein precursor. *Proc. Natl. Acad. Sci. U. S. A* *89*, 10758-10762.
- Watanabe,N., Tomita,T., Sato,C., Kitamura,T., Morohashi,Y., and Iwatsubo,T. (2005). Pen-2 is incorporated into the gamma-secretase complex through binding to transmembrane domain 4 of presenilin 1. *J. Biol. Chem.* *280*, 41967-41975.
- Waters,J., and Smith,S.J. (2000). Phorbol esters potentiate evoked and spontaneous release by different presynaptic mechanisms. *J. Neurosci.* *20*, 7863-7870.
- Weggen,S., Eriksen,J.L., Das,P., Sagi,S.A., Wang,R., Pietrzik,C.U., Findlay,K.A., Smith,T.E., Murphy,M.P., Bulter,T., Kang,D.E., Marquez-Sterling,N., Golde,T.E., and Koo,E.H. (2001). A subset of NSAIDs lower amyloidogenic Abeta42 independently of cyclooxygenase activity. *Nature* *414*, 212-216.
- Weggen,S., Eriksen,J.L., Sagi,S.A., Pietrzik,C.U., Ozols,V., Fauq,A., Golde,T.E., and Koo,E.H. (2003). Evidence that nonsteroidal anti-inflammatory drugs decrease amyloid beta 42 production by direct modulation of gamma-secretase activity. *J. Biol Chem.* *278*, 31831-31837.
- Wei,W., Nguyen,L.N., Kessels,H.W., Hagiwara,H., Sisodia,S., and Malinow,R. (2010). Amyloid beta from axons and dendrites reduces local spine number and plasticity. *Nat. Neurosci.* *13*, 190-196.
- Weidemann,A., Eggert,S., Reinhard,F.B., Vogel,M., Paliga,K., Baier,G., Masters,C.L., Beyreuther,K., and Evin,G. (2002). A novel epsilon-cleavage within the transmembrane domain of the Alzheimer amyloid precursor protein demonstrates homology with Notch processing. *Biochemistry* *41*, 2825-2835.

- Weihofen,A., Binns,K., Lemberg,M.K., Ashman,K., and Martoglio,B. (2002). Identification of signal peptide peptidase, a presenilin-type aspartic protease. *Science* 296, 2215-2218.
- Weihofen,A., and Martoglio,B. (2003). Intramembrane-cleaving proteases: controlled liberation of proteins and bioactive peptides. *Trends Cell Biol* 13, 71-78.
- Wen,Y., Yu,W.H., Maloney,B., Bailey,J., Ma,J., Marie,I., Maurin,T., Wang,L., Figueroa,H., Herman,M., Krishnamurthy,P., Liu,L., Planel,E., Lau,L.F., Lahiri,D.K., and Duff,K. (2008). Transcriptional regulation of beta-secretase by p25/cdk5 leads to enhanced amyloidogenic processing. *Neuron* 57, 680-690.
- Wenthold,R.J., Petralia,R.S., Blahos,J., II, and Niedzielski,A.S. (1996). Evidence for multiple AMPA receptor complexes in hippocampal CA1/CA2 neurons. *J. Neurosci.* 16, 1982-1989.
- Wolfe,M.S. (2009). gamma-Secretase in biology and medicine. *Semin. Cell Dev. Biol.* 20, 219-224.
- Wolfe,M.S., and Guenette,S.Y. (2007). APP at a glance. *J. Cell Sci.* 120, 3157-3161.
- Wolfe,M.S., and Kopan,R. (2004). Intramembrane proteolysis: theme and variations. *Science* 305, 1119-1123.
- Wolfe,M.S., Xia,W., Moore,C.L., Leatherwood,D.D., Ostaszewski,B., Rahmati,T., Donkor,I.O., and Selkoe,D.J. (1999a). Peptidomimetic probes and molecular modeling suggest that Alzheimer's gamma-secretase is an intramembrane-cleaving aspartyl protease. *Biochemistry* 38, 4720-4727.
- Wolfe,M.S., Xia,W., Ostaszewski,B.L., Diehl,T.S., Kimberly,W.T., and Selkoe,D.J. (1999b). Two transmembrane aspartates in presenilin-1 required for presenilin endoproteolysis and gamma-secretase activity. *Nature* 398, 513-517.
- Wong,P.C., Zheng,H., Chen,H., Becher,M.W., Sirinathsinghji,D.J., Trumbauer,M.E., Chen,H.Y., Price,D.L., van der Ploeg,L.H., and Sisodia,S.S. (1997). Presenilin 1 is required for Notch1 and Dll1 expression in the paraxial mesoderm. *Nature* 387, 288-292.
- Wong,T.P., Debeir,T., Duff,K., and Cuellar,A.C. (1999). Reorganization of cholinergic terminals in the cerebral cortex and hippocampus in transgenic mice carrying mutated presenilin-1 and amyloid precursor protein transgenes. *J. Neurosci.* 19, 2706-2716.
- Wu,H.Y., Hudry,E., Hashimoto,T., Kuchibhotla,K., Rozkalne,A., Fan,Z., Spires-Jones,T., Xie,H., Arbel-Ornath,M., Grosskreutz,C.L., Bacskai,B.J., and Hyman,B.T. (2010). Amyloid beta induces the morphological neurodegenerative triad of spine loss, dendritic simplification, and neuritic dystrophies through calcineurin activation. *J. Neurosci.* 30, 2636-2649.
- Wu,L.G., and Saggau,P. (1994). Presynaptic calcium is increased during normal synaptic transmission and paired-pulse facilitation, but not in long-term potentiation in area CA1 of hippocampus. *J. Neurosci.* 14, 645-654.

- Xia,W., Zhang,J., Kholodenko,D., Citron,M., Podlisny,M.B., Teplow,D.B., Haass,C., Seubert,P., Koo,E.H., and Selkoe,D.J. (1997). Enhanced production and oligomerization of the 42-residue amyloid beta-protein by Chinese hamster ovary cells stably expressing mutant presenilins. *J. Biol Chem.* 272, 7977-7982.
- Xu,J., Pang,Z.P., Shin,O.H., and Sudhof,T.C. (2009). Synaptotagmin-1 functions as a Ca²⁺ sensor for spontaneous release. *Nat. Neurosci.* 12, 759-766.
- Yan,R., Bienkowski,M.J., Shuck,M.E., Miao,H., Tory,M.C., Pauley,A.M., Brashier,J.R., Stratman,N.C., Mathews,W.R., Buhl,A.E., Carter,D.B., Tomasselli,A.G., Parodi,L.A., Heinrikson,R.L., and Gurney,M.E. (1999). Membrane-anchored aspartyl protease with Alzheimer's disease beta-secretase activity. *Nature* 402, 533-537.
- Yang,T., Arslanova,D., Gu,Y., Augelli-Szafran,C., and Xia,W. (2008). Quantification of gamma-secretase modulation differentiates inhibitor compound selectivity between two substrates Notch and amyloid precursor protein. *Mol. Brain* 1, 15.
- Ye,Y., Lukinova,N., and Fortini,M.E. (1999). Neurogenic phenotypes and altered Notch processing in *Drosophila* Presenilin mutants. *Nature* 398, 525-529.
- Yoo,A.S., Cheng,I., Chung,S., Grenfell,T.Z., Lee,H., Pack-Chung,E., Handler,M., Shen,J., Xia,W., Tesco,G., Saunders,A.J., Ding,K., Frosch,M.P., Tanzi,R.E., and Kim,T.W. (2000). Presenilin-mediated modulation of capacitative calcium entry. *Neuron* 27, 561-572.
- Yu,G., Chen,F., Levesque,G., Nishimura,M., Zhang,D.M., Levesque,L., Rogaeva,E., Xu,D., Liang,Y., Duthie,M., St George-Hyslop,P.H., and Fraser,P.E. (1998). The presenilin 1 protein is a component of a high molecular weight intracellular complex that contains beta-catenin. *J. Biol. Chem.* 273, 16470-16475.
- Yu,G., Chen,F., Nishimura,M., Steiner,H., Tandon,A., Kawarai,T., Arawaka,S., Supala,A., Song,Y.Q., Rogaeva,E., Holmes,E., Zhang,D.M., Milman,P., Fraser,P.E., Haass,C., and George-Hyslop,P.S. (2000a). Mutation of Conserved Aspartates Affects Maturation of Both Aspartate Mutant and Endogenous Presenilin 1 and Presenilin 2 Complexes. *J. Biol. Chem.* 275, 27348-27353.
- Yu,G., Nishimura,M., Arawaka,S., Levitan,D., Zhang,L., Tandon,A., Song,Y.Q., Rogaeva,E., Chen,F., Kawarai,T., Supala,A., Levesque,L., Yu,H., Yang,D.S., Holmes,E., Milman,P., Liang,Y., Zhang,D.M., Xu,D.H., Sato,C., Rogaeva,E., Smith,M., Janus,C., Zhang,Y., Aebersold,R., Farrer,L., Sorbi,S., Bruni,A., Fraser,P., and George-Hyslop,P. (2000b). Nicastrin modulates presenilin-mediated notch/glp-1 signal transduction and [beta]APP processing. *Nature* 407, 48-54.
- Yu,H., Saura,C.A., Choi,S.Y., Sun,L.D., Yang,X., Handler,M., Kawarabayashi,T., Younkin,L., Fedeles,B., Wilson,M.A., Younkin,S., Kandel,E.R., Kirkwood,A., and Shen,J. (2001). APP processing and synaptic plasticity in presenilin-1 conditional knockout mice. *Neuron* 31, 713-726.

- Zakharenko, S.S., Zablow, L., and Siegelbaum, S.A. (2001). Visualization of changes in presynaptic function during long-term synaptic plasticity. *Nat. Neurosci.* *4*, 711-717.
- Zatti, G., Burgo, A., Giacomello, M., Barbiero, L., Ghidoni, R., Sinigaglia, G., Florean, C., Bagnoli, S., Binetti, G., Sorbi, S., Pizzo, P., and Fasolato, C. (2006). Presenilin mutations linked to familial Alzheimer's disease reduce endoplasmic reticulum and Golgi apparatus calcium levels. *Cell Calcium* *39*, 539-550.
- Zatti, G., Ghidoni, R., Barbiero, L., Binetti, G., Pozzan, T., Fasolato, C., and Pizzo, P. (2004). The presenilin 2 M239I mutation associated with familial Alzheimer's disease reduces Ca²⁺ release from intracellular stores. *Neurobiol. Dis.* *15*, 269-278.
- Zhang, C., Wu, B., Beglopoulos, V., Wines-Samuelson, M., Zhang, D., Dragatsis, I., Sudhof, T.C., and Shen, J. (2009). Presenilins are essential for regulating neurotransmitter release. *Nature* *460*, 632-636.
- Zhang, J., Kang, D.E., Xia, W., Okochi, M., Mori, H., Selkoe, D.J., and Koo, E.H. (1998a). Subcellular distribution and turnover of presenilins in transfected cells. *J. Biol. Chem.* *273*, 12436-12442.
- Zhang, Z., Hartmann, H., Do, V.M., Abramowski, D., Sturchler-Pierrat, C., Staufenbiel, M., Sommer, B., van de, W.M., Clevers, H., Saftig, P., De Strooper, B., He, X., and Yankner, B.A. (1998b). Destabilization of beta-catenin by mutations in presenilin-1 potentiates neuronal apoptosis. *Nature* *395*, 698-702.
- Zhang, Z., Nadeau, P., Song, W., Donoviel, D., Yuan, M., Bernstein, A., and Yankner, B.A. (2000). Presenilins are required for gamma-secretase cleavage of beta-APP and transmembrane cleavage of Notch-1. *Nat. Cell Biol.* *2*, 463-465.
- Zhao, M.G., Toyoda, H., Lee, Y.S., Wu, L.J., Ko, S.W., Zhang, X.H., Jia, Y., Shum, F., Xu, H., Li, B.M., Kaang, B.K., and Zhuo, M. (2005). Roles of NMDA NR2B subtype receptor in prefrontal long-term potentiation and contextual fear memory. *Neuron* *47*, 859-872.
- Zheng, H., Jiang, M., Trumbauer, M.E., Sirinathsinghji, D.J., Hopkins, R., Smith, D.W., Heavens, R.P., Dawson, G.R., Boyce, S., Conner, M.W., Stevens, K.A., Slunt, H.H., Sisodia, S.S., Chen, H.Y., and van der Ploeg, L.H. (1995). beta-Amyloid precursor protein-deficient mice show reactive gliosis and decreased locomotor activity. *Cell* *81*, 525-531.
- Zheng, H., and Koo, E.H. (2006). The amyloid precursor protein: beyond amyloid. *Mol. Neurodegener.* *1*, 5.
- Zheng, W.H., Bastianetto, S., Mennicken, F., Ma, W., and Kar, S. (2002). Amyloid beta peptide induces tau phosphorylation and loss of cholinergic neurons in rat primary septal cultures. *Neuroscience* *115*, 201-211.
- Zhou, J., Liyanage, U., Medina, M., Ho, C., Simmons, A.D., Lovett, M., and Kosik, K.S. (1997). Presenilin 1 interaction in the brain with a novel member of the Armadillo family. *Neuroreport* *8*, 2085-2090.

Zhou,S., Zhou,H., Walian,P.J., and Jap,B.K. (2005). CD147 is a regulatory subunit of the gamma-secretase complex in Alzheimer's disease amyloid beta-peptide production. *Proc. Natl. Acad. Sci. U. S. A* *102*, 7499-7504.

Ziv,N.E., and Garner,C.C. (2004). Cellular and molecular mechanisms of presynaptic assembly. *Nat. Rev. Neurosci.* *5*, 385-399.

Zoghbi,H.Y., Gage,F.H., and Choi,D.W. (2000). Neurobiology of disease. *Curr. Opin. Neurobiol.* *10*, 655-660.

Zuber,B., Nikonenko,I., Klauser,P., Muller,D., and Dubochet,J. (2005). The mammalian central nervous synaptic cleft contains a high density of periodically organized complexes. *Proc. Natl. Acad. Sci. U. S. A* *102*, 19192-19197.

Zucker,R.S., and Regehr,W.G. (2002). Short-term synaptic plasticity. *Annu. Rev. Physiol* *64*, 355-405.